INFORMATION TO USERS

This manuscript has been reproduced from the microfilm master. UMI films the text directly from the original or copy submitted. Thus, some thesis and dissertation copies are in typewriter face, while others may be from any type of computer printer.

The quality of this reproduction is dependent upon the quality of the copy submitted. Broken or indistinct print, colored or poor quality illustrations and photographs, print bleedthrough, substandard margins, and improper alignment can adversely affect reproduction.

In the unlikely event that the author did not send UMI a complete manuscript and there are missing pages, these will be noted. Also, if unauthorized copyright material had to be removed, a note will indicate the deletion.

Oversize materials (e.g., maps, drawings, charts) are reproduced by sectioning the original, beginning at the upper left-hand corner and continuing from left to right in equal sections with small overlaps. Each original is also photographed in one exposure and is included in reduced form at the back of the book.

Photographs included in the original manuscript have been reproduced xerographically in this copy. Higher quality 6" x 9" black and white photographic prints are available for any photographs or illustrations appearing in this copy for an additional charge. Contact UMI directly to order.

UMI

A Bell & Howell Information Company
300 North Zeeb Road, Ann Arbor MI 48106-1346 USA
313/761-4700 800/521-0600

Université d'Ottawa · University of Ottawa

EFFECTS OF THE ALKALI-SILICA REACTION ON UNLOADED , STATICALLY LOADED AND DYNAMICALLY LOADED REINFORCED CONCRETE BEAMS

by

Luc Jean-Guy Monette

A thesis
submitted under the supervision of
Dr. N.J. Gardner

in partial fulfillment of the
requirements for the degree of
Master of Applied Science
in
Civil Engineering

Department of Civil Engineering
University of Ottawa
Ottawa, Ontario
K1N 6N5

To my mother, who is hoping that
one day I will finally graduate

ACKNOWLEDGMENTS

Many thanks to my supervisors Dr. N.J. Gardner of the University of Ottawa and to Dr. P.E. Grattan-Bellew of the National Research Council. Their guidance and expertise were essential to the successful completion of this work.

I am also grateful to B. Kotter, University of Ottawa machine shop, M. Grira, University of Ottawa structures laboratory, G. Mould, G. Chan and T. Hoogeveen of the National Research Council. This research could not have been completed without their skills, expertise and cooperation.

ABSTRACT

The Alkali-Silica Reaction (ASR) affects many concrete structures throughout the world. This reaction occurs between the hydroxyl ions (associated with the Na and K alkalis) in concrete and poorly crystalline or amorphous forms of silica in susceptible aggregates. ASR can cause the expansion and subsequent cracking of the affected concrete. The cracking of the concrete contributes to other durability problems such as freeze thaw of concrete and reinforcing steel corrosion.

Much research has been conducted regarding ASR's effects on plain concrete and on unloaded small scale reinforced concrete beams. The effects of ASR on reinforced concrete beams subjected to flexural load has not been studied..

Small scale, simply supported, singly reinforced concrete beams made of both reactive and non-reactive aggregate have been tested. Reactive and non-reactive concrete cylinders, resonant frequency prisms and CSA expansion prisms were tested with the beams. The reactive and non-reactive specimens, except for the CSA prisms, were tested for the same duration, submerged in a 1N NaOH solution at a temperature of 38 degrees Celsius to accelerate the ASR. The CSA prisms were stored at 38 degrees Celsius at 100% relative humidity. Both the reactive and non-reactive beams were tested under the following loading regimes for the duration of the experiment: unloaded, statically loaded and dynamically loaded to unfactored service load. The experiment was conducted until an amount expansion had occurred in the reactive specimens. Three general aspects of the experiment were of interest:

a) The effect of loading condition on expansions due to the Alkali-Silica Reaction

The severity of ASR in the unloaded, statically and dynamically loaded members were examined. Expansions were monitored in various horizontal locations along the members as well as vertically between the top fiber and the bottom steel location.

b) The effects ASR on the structural behaviour of the beams various beams

The structural behavior of the various reactive beams were compared. Their structural performance compared with the non-reactive controls was also examined. Each of the beams were loaded to failure while observing their ultimate loads and load deflection behavior.

c) The damage rating indices of the beams and of plain concrete

Damage rating indices (DRI is a petrographic method of quantifying internal concrete damage) were performed on the reactive reinforced concrete beams. An attempt was made to correlate measured concrete damage with expansions and the structural behaviour of the various beams.

Flexural loading reduced ASR expansions in the compression zone of the loaded reactive beams. However, the expansions in the loaded reactive beams were still large enough to cause the cracking of the concrete.

The DRI generally corresponded with the expansion results. As expansions increased so did the internal damage of concrete.

The compressive strength of the reactive concrete increased 60% by the end of the experiment from the 28 day compressive strength. The ASR decreased the static modulus of elasticity of the reactive cylinders by 66%. The ASR reduced the flexural strength of the plain reactive concrete.

After measuring the horizontal strains of the non-reactive beams it was determined that non-ASR strains such as creep strains and stiffness degradation strains in the loaded beams were not significant.

The ultimate flexural strength of the non-reactive beams was similar to that of the reactive beams. All of the reactive beams failed in flexure. The non-reactive beams failed in flexure except for two of the beams which failed in shear. This demonstrated the effect of ASR expansions on the shear capacity of reinforced concrete beams.

The ASR did not have a significant effect on the structural behaviour of the simply supported, singly reinforced concrete beams subjected to various loading regimes.

TABLE OF CONTENTS

SECTION	PAGE
ACKNOWLEDGMENTS	i
ABSTRACT	ii
TABLE OF CONTENTS	iv
LIST OF TABLES	x
LIST OF FIGURES	xii
GLOSSARY	xvii
CHAPTER 1 THE ALKALI-SILICA REACTION	1
1.1 INTRODUCTION	1
1.2 HISTORICAL BACKGROUND	2
1.3 THE ALKALI-SILICA REACTION	3
1.3.1 Type of Aggregate	3
1.3.2 Alkalinity of Pore Solution	4
1.3.3 Moisture Content of Concrete	4
1.3.4 Ambient Temperature of Concrete	5
1.3.5 Amount and Distribution of Reinforcement	5
1.3.6 Expansion Mechanisms	5
1.4 SIGNS OF THE REACTION	6
1.4.1 Macro and Microcracks	6
1.4.2 Aggregate Reaction Rims	9
1.4.3 Aggregate Debonding	9
1.4.4 Reactive Gel	10
1.5 IDENTIFICATION OF REACTIVE AGGREGATES	11

1.5.1 Petrographic Examination 12
1.5.2 Accelerated Mortar Bar Test 12
1.5.3 Concrete Prism Test 13
1.5.4 Field Study of Aggregate 14
1.6 EFFECTS OF ASR IN PLAIN CONCRETE 14
1.6.1 Compressive Strength 15
1.6.2 Modulus of Elasticity 15
1.6.3 Tensile Strength 16
1.6.4 Shear Strength 16
1.6.5 Flexural Strength 16
1.7 EFFECTS OF ASR IN REINFORCED CONCRETE 16
1.7.1 Flexural Strength 16
1.7.2 Effect of Restraint 16
1.7.3 Shear Strength 17
1.7.4 Deformations (deflections) 17
1.8 PREVENTION OF ASR 17
1.8.1 Concrete Alkali Content 18
1.8.2 Concrete Moisture Content 18
1.8.3 Supplementary Cementing Materials 18
1.8.4 Chemical Additives 19
1.9 ASSESSMENT OF ASR AFFECTED STRUCTURES 19
1.9.1 Condition of the Structure 19
1.9.2 The State of Expansion 19
1.9.3 Stopping Expansion 20
1.9.4 Method of Repair 20
1.10 STATEMENT OF THE PROBLEM 20
1.10.1 The Effect of Loading Condition on the Alkali-Silica Reaction 21
1.10.2 The Structural Effects of ASR on R/C Beams 21

SECTION PAGE

1.10.3 Comparison of the Damage Rating indices of the Beams 21

CHAPTER 2 LITERATURE REVIEW 25
2.1 MATERIALS 25
2.1.1 Ramachandran, Beaudoin, Sarkar and Aimin 1983 25
2.1.2 Akashi, Amasaki, Takagi and Tomita 1986 26
2.1.3 Swamy and Al-Asali 1988 27
2.1.4 Gunatilaka, Machida and Mutsuyoshi 1990 28
2.1.5 Habita, Brouxel, Prin and Dune 1992 29
2.1.6 Le Roux, Massieu and Godart 1992 30
2.1.7 Guédon and Le Roux 1993 30
2.1.8 Jones and Clark 1996 31
2.1.9 Shayan and Ivanusec 1996 33
2.1.10 Tawfiq, Armaghani and Vysyaraju 1996 34
2.2 STRUCTURAL 35
2.2.1 Koyanagi, Rokugo and Ishida 1986 35
2.2.2 Abe, Kikuta, Masuda and Tomozawa 1989 36
2.2.3 Inoue, Fujii, Kobayashi and Nakano 1989 37
2.2.4 Swamy and Al-Asali 1989 38
2.2.5 Ujike, Nagataki, Sato and Ishikawa 1990 39
2.2.6 Cope and Slade 1992 40
2.2.7 Rigden, Majlesi and Burley 1992 40
2.2.8 Koyanagi, Rokugo, Uchida and Iwase 1996 41
CHAPTER 3 EXPERIMENTAL PROCEDURE 45
3.1 THE EXPERIMENT 45
3.1.1 Beams 46
3.1.2 Cylinders 50
3.1.3 Resonant Frequency Prisms 51

SECTION PAGE

3.1.4 CSA Concrete Prisms 52

3.1.5 Coarse Aggregate 52

3.1.6 Fine Aggregate 53

3.1.7 Mix Design 54

3.1.8 Preparation of Specimens 55

3.2 TESTING PROGRAM 59

3.2.1 Specimen Testing Apparatus 59

3.2.2 Beams 61

3.2.3 Cylinders 62

3.2.4 Resonant Frequency Prisms 63

3.2.5 CSA Concrete Prism Test 64

3.3 DAMAGE RATING INDEX 65

CHAPTER 4 EXPERIMENTAL RESULTS 70

4.1 DESCRIPTION OF RESULTS 70

4.1.1 Beam Expansion Measurement Locations 70

4.1.2 Results 72

4.2 SPECIMEN EXPANSIONS 73

4.2.1 Unloaded Beam Expansions 74

4.2.2 Statically Loaded Beam Expansions 77

4.2.3 Dynamically Loaded Beam Expansions 80

4.2.4 Expansions for Beams Subjected to Various Loading Regimes 83

4.2.5 Expansions of Non-Reactive Control Beams 90

4.2.6 Additional Results 91

4.2.7 Reactive Beam Macrocracking at the End of Loading 92

4.3 DAMAGE RATING INDICES 94

4.3.1 Damage Rating Indices for the Individual Beams 95

4.3.2 Comparison of Damage Rating Indices for the Various Beams 98

4.4 STRUCTURAL BEHAVIOUR OF BEAMS 99

SECTION **PAGE**

4.5 BEHAVIOUR OF CONCRETE CYLINDERS AND PRISMS 104

CHAPTER 5 DISCUSSION 110

5.1 EXPANSIONS 110

5.1.1 Unloaded Beam Expansions 112

5.1.2 Statically Loaded Beam Expansions 113

5.1.3 Dynamically Loaded Beam Expansions 115

5.1.4 Comparison of Various Beam Expansions 117

5.1.5 Expansion of Non-Reactive Control Specimens 122

5.1.6 Cylinder and CSA Prism Expansions and Resonant Frequency Prisms 123

5.1.7 Reactive and Non-Reactive Resonant Frequency Prisms 123

5.1.8 Cracking of Beams 124

5.2 DAMAGE RATING INDICES 124

5.3 STRUCTURAL BEHAVIOUR OF BEAMS 127

5.4 BEHAVIOUR OF CONCRETE CYLINDERS AND PRISMS 129

5.4.1 Cylinders 129

5.4.2 Moduli of Elasticity 130

5.4.3 Concrete Flexural Strength 130

CHAPTER 6 CONCLUSION 132

6.1 EXPANSIONS 132

6.2 DAMAGE RATING INDICES 133

6.3 STRUCTURAL BEHAVIOUR OF THE BEAMS 134

6.4 BEHAVIOUR OF PLAIN CONCRETE SPECIMENS 134

APPENDIX A CHARACTERIZATION OF MATERIALS 135

A.1 AGGREGATE DATA 135

A.1.1 Aggregate Reactivity 135

A.2 SIEVE ANALYSIS AND AGGREGATE BLENDING 137

A.2.1 Coarse Aggregate 137

A.2.2 Fine Aggregates 138

SECTION **PAGE**

A.3 CEMENT 138

A.4 LONGITUDINAL AND TRANSVERSE REINFORCEMENT 139

APPENDIX B EXPERIMENTAL DATA 141

B.1 EXPANSION DATA 141

B.1.1 Unloaded Beam Expansions 143

B.1.2 Statically Loaded Beam Expansions 147

B.1.3 Dynamically Loaded Beam Expansions 151

B.1.4 Expansions of the Beams Subjected to Various Loading regimes 155

B.2 DAMAGE RATING INDEX DATA 165

B.2.1 Unloaded Beam Indices 165

B.2.2 Statically Loaded Beam Indices 166

B.2.3 Dynamically Loaded Beam Indices 167

B.2.4 DRI for the Beams Subjected to Various Loading regimes 168

APPENDIX C ADDITIONAL REFERENCES 173

LIST OF TABLES

TABLE	PAGE
Table 3.1: Concrete Mix Design (reactive and non-reactive mixes)	54
Table 3.2: Measured concrete slump for each batch	55
Table 3.3: Reactive test specimens	56
Table 3.4: Non-reactive control specimens	57
Table 3.5: Damage Rating Index Weighting Factors	66
Table 4.1: Strains of non-reactive control beams at the end of the experiment	90
Table 4.2: Strains of non-reactive control cylinders and CSA Prisms	90
Table 4.3: Compressive strength of reactive, non-reactive and lime water concrete	108
Table 4.4: Plain Concrete Prism Flexural Strengths for reactive and non-reactive prisms	109
Table 4.5: Static and dynamic moduli of elasticity for reactive and non-reactive cylinders	109
Table 5.1: Unloaded beam overall horizontal expansions	112
Table 5.2: Unloaded beam mid-span horizontal expansions	113
Table 5.3: Unloaded beam vertical expansions	113
Table 5.4: Statically loaded beam overall horizontal expansions	114
Table 5.5: Statically loaded beam mid-span horizontal expansions	114
Table 5.6: Statically loaded beam vertical expansions	115
Table 5.7: Dynamically loaded beam mid-span horizontal expansions	116
Table 5.8: Dynamically loaded beam vertical expansions	116
Table 5.9: Top overall expansions for various beams	117

TABLE PAGE

Table 5.10: Middle overall expansions for various beams 117

Table 5.11: Bottom overall expansions for various beams 118

Table 5.12: Top mid-span expansions for various beams 119

Table 5.13: Middle mid-span expansions for various beams 119

Table 5.14: Bottom mid-span expansions for various beams 120

Table 5.15: Vertical expansions for extreme left hand side of various beams (Set 13) 120

Table 5.16: Vertical expansions for extreme right hand side of various beams (Set 20) 120

Table 5.17: Vertical expansions for mid-span of various beams (Set 16) 121

Table 5.18: Vertical expansions for mid-span of various beams (Set 17) 121

Table 5.19: Vertical and horizontal expansions at the mid span of the unloaded beams 121

Table 5.20: Vertical and horizontal expansions at the mid span of the static beams 122

Table 5.21: Vertical and horizontal expansions at the mid span of the dynamic beams 122

Table 5.22: Reactive cylinder and prism expansions 123

Table 5.23: DRI for the various zones of each beam 127

Table 5.24: Initial stiffness of beams loaded to failure 129

Table 5.25: Concrete properties of the reactive and non-reactive specimens 131

LIST OF FIGURES

FIGURE	PAGE
Figure 1.1: Map cracking of a concrete retaining wall	7
Figure 1.2: Severe map cracking in a bridge pier foundation	8
Figure 1.3: Microcracking in ASR affected concrete	8
Figure 1.4: Aggregate reaction rim	9
Figure 1.5: Aggregate debonding due to ASR	10
Figure 1.6: Microcrack with ASR gel in an aggregate particle	11
Figure 1.7: Concrete air void filled with ASR gel	11
Figure 1.8: Mortar bars used in the CSA accelerated mortar bar test	13
Figure 1.9: Prism used for the CSA concrete prism test	13
Figure 1.10: Typical concrete stiffness degradation curve	15
Figure 3.1: Reinforced concrete beam design	47
Figure 3.2: Beam reinforcing cage	47
Figure 3.3: Typical Demec target	47
Figure 3.4: Demec Target Layout	48
Figure 3.5: Demec target sets used for horizontal expansion measurements	48
Figure 3.6: Demec target sets used for vertical expansion measurements	48
Figure 3.7: Concrete beam mould	49
Figure 3.8: Typical beam specimen	49
Figure 3.9: Cylinder mould with Demec targets	50
Figure 3.10: Cylinder with Demec targets	51
Figure 3.11: Resonant frequency prism	51

FIGURE PAGE

Figure 3.12: CSA expansion test prisms 52

Figure 3.13: Reactive and non-reactive limestone aggregates 53

Figure 3.14: Quartz sand 53

Figure 3.15: Test specimen moulds prior to casting 58

Figure 3.16: Casting of a beam specimen 58

Figure 3.17: Casting of cylinder specimens 59

Figure 3.18: Specimen testing apparatus 60

Figure 3.19: Demec gauges used for expansion measurements 61

Figure 3.20: Huggenberger gauge for beam horizontal overall expansion measurement 62

Figure 3.21: Beam Ultimate Flexural Loading Apparatus 62

Figure 3.22: Forney testing machine, concrete cylinder and modulus of elasticity frame 63

Figure 3.23: Resonant frequency testing apparatus 64

Figure 3.24: Flexural loading of resonant frequency prisms 64

Figure 3.25: CSA Concrete Prism and Comparator 65

Figure 3.26: Zones of DRI measurement 67

Figure 3.27: Demec sets for horizontal expansion measurement 67

Figure 3.28: Polished beam specimen and stereo binocular microscope 68

Figure 3.29: Polished concrete section as viewed through a stereo binocular microscope 68

Figure 4.1: Location of Demec points along the beam specimens 71

Figure 4.2: Location of horizontal beam expansion measurements 71

Figure 4.3: Location of vertical beam expansion measurements 71

Figure 4.4: Beam loading arrangement with bending moment and shear force diagrams 72

Figure 4.5: Unloaded beam overall horizontal expansions (sets 1,2,3) 74

Figure 4.6: Unloaded beams mid span horizontal expansions (sets 7,8,9) 75

Figure 4.7: Unloaded beams top horizontal expansions (sets 1,7) 75

FIGURE PAGE

Figure 4.8: Unloaded beams middle horizontal expansions (sets 2,8) 76

Figure 4.9: Unloaded beams bottom horizontal expansions (sets 3,9) 76

Figure 4.10: Unloaded beams vertical expansions (Sets 13,16,17,20) 77

Figure 4.11: Statically loaded beams overall horizontal expansions (sets 1,2,3) 77

Figure 4.12: Statically loaded beams mid-span horizontal expansions (sets 7,8,9) 78

Figure 4.13: Statically loaded beams top horizontal expansions (sets 1,7) 78

Figure 4.14: Statically loaded beams middle horizontal expansions (sets 2,8) 79

Figure 4.15: Statically loaded beams bottom horizontal expansions (sets 3,9) 79

Figure 4.16: Statically loaded beams vertical expansions (sets 13,16,17,20) 80

Figure 4.17: Dynamically loaded beams overall horizontal expansions (sets 1,2,3) 80

Figure 4.18: Dynamically loaded beams mid span horizontal expansions (sets 7,8,9) 81

Figures 4.19: Dynamically loaded beams top horizontal expansions (sets 1,7) 81

Figures 4.20: Dynamically loaded beams middle horizontal expansions (sets 2,8) 82

Figures 4.21: Dynamically loaded beams bottom horizontal expansions (sets 3,9) 82

Figure 4.22: Dynamically loaded beams vertical expansions (sets 13,16,17,20) 83

Figure 4.23: Overall horizontal expansions for the top of the various beams (set 1) 83

Figure 4.24: Overall horizontal expansions for the middle of the various beams (set 2) 84

Figure 4.25: Overall horizontal expansions for the bottom of the various beams (set 3) 84

Figure 4.26: Mid span horizontal expansions for the top of the various beams (set 7) 85

Figure 4.27: Mid span longitudinal expansions for the middle of the various beams (set 8) 85

Figure 4.28: Mid span horizontal expansions for the bottom of the various beams (set 9) 86

Figure 4.29: Vertical expansions for the various beams (set 13) 86

Figure 4.30: Vertical expansions for the various beams (set 16) 87

FIGURE	PAGE
Figure 4.31: Vertical expansions for the various beams (set 17)	87
Figure 4.32: Vertical expansions for the various beams (set 20)	88
Figure 4.33: Horizontal and vertical expansions for the mid-span of the unloaded beams	88
Figure 4.34: Horizontal and vertical expansions for the mid-span of the static beams	89
Figure 4.35: Horizontal and vertical expansions for the mid-span of the dynamic beams	89
Figure 4.36: Reactive concrete cylinder and CSA prism expansions and reactive prism resonant frequency results vs. time	91
Figure 4.37: Reactive vs. non-reactive resonant frequency results	92
Figure 4.38: Typical unloaded beam macrocracking	93
Figure 4.39: Typical statically loaded beam macrocracking	93
Figure 4.40: Typical dynamically loaded macrocracking	93
Figure 4.41: Zones of damage rating measurements	94
Figure 4.42: Damage rating indices for unloaded beam RB-1	95
Figure 4.43: Damage rating indices for unloaded beam RB-6	95
Figure 4.44: Damage rating indices for statically loaded beam RB-7	96
Figure 4.45: Damage rating indices for statically loaded beam RB-8	96
Figure 4.46: Damage rating indices for dynamically loaded beam RB-3	97
Figure 4.47: Damage rating indices for dynamically loaded beam RB-4	97
Figure 4.48: Damage rating indices for various beams, zone 2	98
Figure 4.49: Damage rating indices for various beams, zone 5	98
Figure 4.50: Damage rating indices for various beams, zone 8	99
Figure 4.51: Load vs. deflection for 28 day and unloaded reactive and non-reactive beams	100
Figure 4.52: Load vs. deflection for 28 day and static reactive and non-reactive beams	100
Figure 4.53: Load vs. deflection for 28 day and dynamic reactive and non-reactive beams	101

FIGURE PAGE

Figure 4.54: Load vs. deflection for all the reactive beams 101

Figure 4.55: Load vs. deflection for all the non-reactive beams 102

Figure 4.56: Typical flexural failure of 28 day reactive beams 103

Figure 4.57: Typical flexural failure of loaded reactive beams 103

Figure 4.58: Flexural failure of 28 day non-reactive beam 103

Figure 4.59: Flexural failure of loaded non-reactive beams 104

Figure 4.60: Shear failure of loaded non-reactive beams 104

Figure 4.61: Stress vs. strain for various reactive cylinders 105

Figure 4.62: Stress vs. strain for various non-reactive cylinders 106

Figure 4.63: Stress vs. strain at 28 days for reactive and non-reactive cylinders 106

Figure 4.64: Stress vs. strain at the end of the testing for reactive, non-reactive and lime water cylinder) 107

Figure 4.65: Stiffness reduction for reactive, non-reactive and lime water cylinders 107

Figure 5.1: Layout of Demec targets used for expansion measurements 110

Figure 5.2: Demec targets used for horizontal expansion measurements 111

Figure 5.3: Demec targets used for vertical expansion measurements 111

Figure 5.4: Beam loading arrangement with bending moment and shear force diagrams 111

Figure 5.5: Zones of damage rating measurements 124

Figure 5.6: Beam Loading Diagrams 125

GLOSSARY

°C	Degree Celsius
AAR	Alkali-aggregate reaction
ACR	Alkali-carbonate reaction
ASR	Alkali-silica reaction
ASTM	American society for testing of materials
CANMET	Canadian Center for Mineral and Energy Technology
CPCA	Canadian Portland Cement Association
CSA	Canadian standards association
DRI	Damage rating index
Ec	Static modulus of elasticity of concrete
Ed	Dynamic modulus of elasticity of concrete
f'c	Concrete cylinder compressive strength
fr	Concrete modulus of rupture
IRC	Institute for Research in Construction
KOH	Potassium Hydroxide
MTO	Ministry of Transportation of Ontario
Na_2O	Sodium Oxide
NaOH	Sodium Hydroxide
NRC	National Research Council of Canada
R/C	Reinforced Concrete
RH	Relative humidity
UPV	Ultrasonic Pulse Velocity

CHAPTER 1

THE ALKALI-SILICA REACTION

1.1 INTRODUCTION

In recent years, alkali-aggregate reactions (AAR) have been of increasing concern to both materials and structural engineers. AAR are chemical reactions occurring between certain unstable mineral phases in susceptible aggregates and alkali hydroxides (alkalis) in concrete pore solution. When severe, these reactions can cause expansive stresses, which usually results in cracking of the affected concrete. This cracking can also contribute to other durability problems such as freeze thaw deterioration and reinforcing steel corrosion. Expansions due to AAR have been known to reach up to 0.2% in field concrete and have reached up to 0.4% in laboratory concrete (CANMET 1993, Monette 1997). The two types of AAR are the alkali silica-reaction (ASR) and the alkali carbonate reaction (ACR). ASR is a reaction between hydroxyl ions associated with sodium and potassium alkalis in the concrete pore solution and certain unstable (usually poorly crystalline, amorphous or fine grained) silica minerals in susceptible aggregates. The reaction may take from 5 to 20 years before the manifestation of visible signs. Similarly, ACR is a reaction between alkali hydroxides in the pore solution and dolomitic limestone aggregates. Signs of ACR usually appear within 5 years following casting of concrete containing reactive aggregate (CANMET 1993). ASR is the most common, most studied, of the alkali-aggregate reactions and is the focus of this thesis.

1.2 HISTORICAL BACKGROUND

As early as the 1920's, researchers noticed cracking in concrete which was not consistent with other durability problems such as freeze thaw and reinforcing steel corrosion (Swamy 1992). However, Stanton in 1940 was the first to recognize that this phenomenon was due to an internal reaction between the constituents of the concrete (Swamy 1992). He discovered that the combination of moisture, elevated concrete pore solution alkalinity and the presence of unstable silica minerals in some aggregates could cause deleterious expansion in concrete. Expansions due to these phenomena could be large enough to cause cracking in the host concrete. Since this development, many structures around the world have been identified as suffering from ASR. The Parker dam (USA), Val de la Mare dam (UK), Beauharnois and Mactaquac dams (eastern Canada), sections of the Johannesburg urban motorway (South Africa) and sections of the Hanshin expressway (Japan) are all examples of structures exhibiting deleterious concrete expansions due to ASR and demonstrate the global extent of the problem (Swamy 1992, CANMET 1993, Blight 1989, Imai 1986).

An increasing awareness of the global problems due to AAR propagated the beginning of a series of international conferences on AAR. The first of these conferences was held in Denmark (1974) and subsequent conferences were in Iceland (1975), the United Kingdom (1976), the United States of America (1978), South Africa (1981), Denmark (1983), Canada (1986), Japan (1989), the United Kingdom (1992) and Australia (1996). The next conference will be held in Québec City, Canada in the year 2000.

An increasing number of structures in central and eastern Canada are being diagnosed with ASR. This is thought to be partly related to an increase in cement alkalinity due to changes in the cement manufacturing process during the past few decades (CANMET 1993). Occurrences of ASR in western Canada have also been reported but are not as frequent as in the central and eastern parts of the country (Swamy 1992). This is thought to be due to lower alkali levels in the cements produced in western Canada compared to the cements produced in the eastern part of the country (Swamy 1992).

The increase in occurrences of ASR in Canada and throughout the world has promoted research into every aspect of the reaction; everything from the reaction

chemistry to the structural effects of the reaction (Swamy 1992, Blight 1989). The effects of the reaction in plain concrete have been extensively studied but there is a lack of knowledge regarding its effects on reinforced concrete members. The following sections of this chapter will briefly introduce current knowledge regarding ASR.

1.3 THE ALKALI-SILICA REACTION

ASR is a chemical reaction associated with pore solution alkalis and unstable (usually poorly crystalline, amorphous or fine grained) silica minerals in susceptible aggregates. The product of this reaction is a gel (called ASR gel) which absorbs water and swells. If present in sufficient amounts the ASR gel causes expansive stresses and cracking in the affected concrete. The severity of, and the damage caused by, the reaction depends on the type of aggregate, the alkalinity of the concrete pore solution, the moisture content of the concrete, the ambient temperature of the concrete and the amount and distribution of the reinforcing steel. To occur, the reaction simultaneously requires a sufficient amount of sodium (Na) and potassium (K) alkalis naturally occurring in Portland cement, susceptible aggregate and sufficient moisture. If one of these elements is missing, the reaction cannot proceed (Swamy 1992).

1.3.1 Type of Aggregate

The level of susceptibility of an aggregate depends on the microstructure of the silica minerals it contains. Reactive aggregates are generally characterized by poorly crystalline, amorphous or fine grained forms of silica minerals. Rates, severity and duration of expansion may vary with different amounts of a same aggregate. With certain reactive aggregates, the maximum expansion in concrete occurs when the aggregate is present in proportions as small as three to ten percent. This amount is known as the pessimum amount (CANMET 1993).

The severity, rate and duration of expansion may also vary with various types of aggregate. Some aggregates are more susceptible to ASR than others depending on the amount and structure of the silica minerals they contain. The amount of expansion and

cracking produced by an aggregate also depends on the amount of reactive gel it produces.

The quality of the concrete also affects ASR. High permeability may allow ingress of moisture contributing to the ASR. However, as with freeze thaw, concrete permeability and air entrainment may help in alleviating expansive gel pressures by providing space for expanding gel (Jensen 1984).

1.3.2 Alkalinity of Pore Solution

A total cement alkali content greater than 0.6 % Na_2O equivalent (NaO_2 equivalent in percent: % Na_2O + 0.658% K_2O) and a total concrete alkali content greater than 3 kg/m^3 are generally considered to constitute an aggressive environment for potentially reactive aggregates. However, these are not magic numbers and there have been cases of expansion at levels below and cases of no expansion at levels above these limits (CANMET 1993).

The alkalinity of concrete not only depends on alkalis derived from Portland cement, but may also depend on alkalis derived from mineral admixtures and chemical additives such as fly ash and superplasticizers (CANMET 1993). It has also been shown that alkalis may be leached from aggregates into the concrete pore solution (Grattan-Bellew 1994).

1.3.3 Moisture Content of Concrete

The moisture content of the concrete must be sufficiently high to allow the transport of hydroxyl ions (associated with the Na and K alkalis in the concrete pore solution) to potentially reactive silica sites. Moisture is also a major component in the expansion mechanism. When present is sufficient amounts, ASR gel expands as it absorbs water and causes expansive pressures.

1.3.4 Ambient Temperature of Concrete

As with many chemical reactions, ASR is accelerated by an increase in ambient temperature. However, ASR can progress in most climatic conditions provided pore water is available to travel to potential reaction sites.

1.3.5 Amount and Distribution of Reinforcement

Concrete reinforcement provides passive restraint to ASR expansion. If isotropic, this reinforcement provides an equal amount of restraint throughout the concrete. Differential expansions may be encountered due to the unequal restraint from reinforcing steel distributed unevenly throughout reinforced concrete members (Swamy 1989). Expansions can also be reduced by applied axial compressive stresses (Jones 1996). Cracking due to ASR in reinforced concrete members and members subjected to applied axial stresses will mostly form in a direction parallel to the primary restraint.

It has also been determined that ASR expansions will be increased in a direction perpendicular to the primary restraint (expansions will occur in a direction of least resistance).

1.3.6 Expansion Mechanisms

The Absorption Swelling Theory and the Osmotic Pressure Theory have been proposed to explain concrete expansion due to ASR, the first of the two being the more widely accepted. The Absorption-Swelling Theory suggests that ASR gel expands when it absorbs water (Struble 1991). Gel can form in aggregate cracks or at the interface of aggregate and cement paste. The swelling of the gel creates pressure on the surrounding medium, which can cause expansive stresses. The Osmotic Pressure Theory proposes that the ASR gel forms a semi-permeable membrane around aggregate particles. This membrane allows various ions to pass through (H_2O, Na and K ions into the silica) but does not let silica ions escape. This results in a build up of pressure within the reacting particle which can rupture and exert pressure on the surrounding concrete.

If moisture is not present in sufficient amounts, ASR gel cannot create expansive stresses in concrete. Thus concrete may be affected by ASR but not expand or crack due to lack of moisture required for the expansion mechanism.

1.4 SIGNS OF THE REACTIONS

The alkali-silica reaction in concrete is characterized by various visible signs such as macrocracks, microcracks, aggregate reaction rims, aggregate debonding and reaction gel. It is important to note that the reaction occurs well before any visible signs become apparent on the surface of affected concrete.

1.4.1 Macro and Microcracks

Macrocracks often appear at the surface of concrete with significant expansions from ASR. This cracking is sometimes referred to as "map cracking" since, from a distance, the cracks often form a pattern that resembles a topographical map. Cracks due to ASR expansions will not always appear as "map cracking" since the direction of the cracks can be influenced by steel reinforcement and restraint due to load. Macrocracks usually occur at a depth equal to steel cover in reinforced concrete. This is due to differential expansions between the cover and core concrete. Cover concrete usually expands less than core concrete due to leaching of alkalis and drying cycles at exposed surfaces (Kobayashi 1989).

Map cracking is often characterized by a staining at the surface of the cracks which makes them appear continuously wet. The source of this staining is calcium carbonate resulting from calcium leaching from the concrete through the cracks. In severe cases, gel may extrude from cracks at the surface of the concrete.

Microcracks can occur at depths greater than steel cover and can usually be observed under microscope in polished sections of affected concrete. Aggregate particles are often cracked during the crushing process. ASR may occur within these cracks, open them further and cause them to extend into the surrounding paste. Similarly, the reaction may also occur at the interior of previously uncracked particles and cause cracking. The

reaction also typically occurs at the interface between aggregate particles and cement paste. Pressures due to the formation of gel at this zone may cause cracking of the paste matrix.

Figures 1.1 and 1.2 show the severe macrocracking of a reinforced concrete retaining wall and a bridge pier foundation. Figure 1.3 shows the typical microcracking of concrete by ASR as seen through a stereo-binocular microscope.

Figure 1.1: Map cracking of a concrete retaining wall

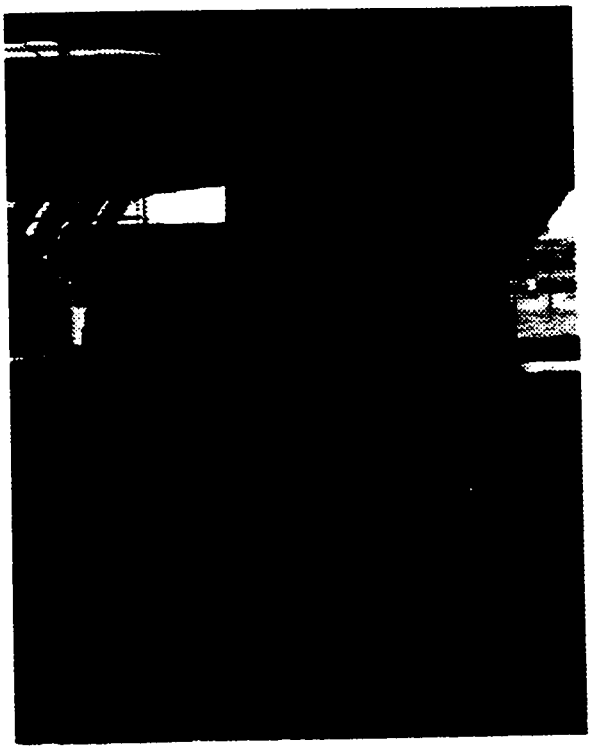

Figure 1.2: Map cracking in a bridge pier foundation

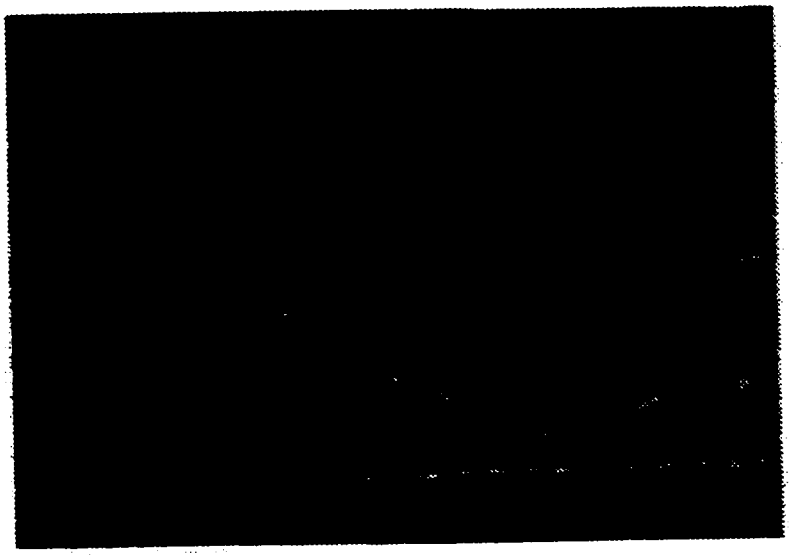

Figure 1.3: Microcracking in ASR affected concrete
(each division on the scale is equal to 0.5mm)

1.4.2 Aggregate Reaction Rims

Reacted aggregate particles commonly exhibit darkened rims at their perimeter. This is typically observed in polished sections of affected concrete through a microscope. However, these rims may be due to other factors such as the weathering of natural gravel. Figure 1.4 shows an aggregate reaction rim as seen through a stereo-binocular microscope.

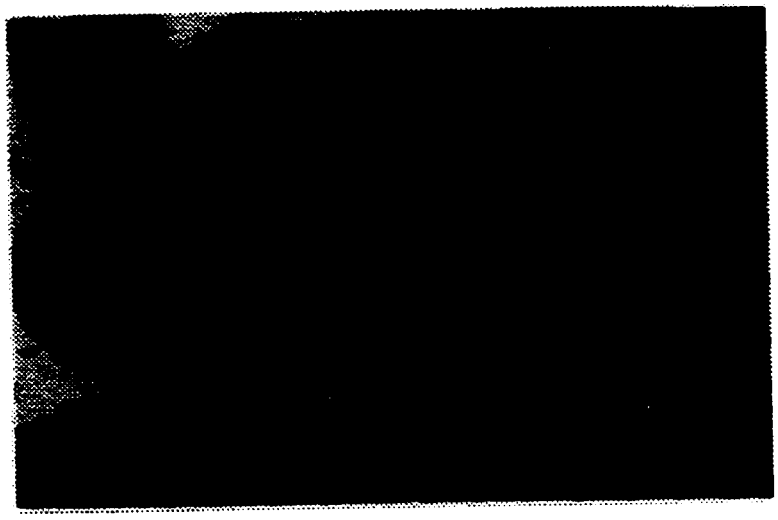

Figure 1.4: Aggregate reaction rim
(each division on the scale is equal to 0.5mm)

1.4.3 Aggregate Debonding

Aggregate debonding occurs when aggregate particles delaminate from the surrounding concrete paste matrix. This can be caused by the formation of gel, causing pressure, at the interface between reactive aggregate particles and cement paste. A typical example of aggregate debonding is shown in Figure 1.5.

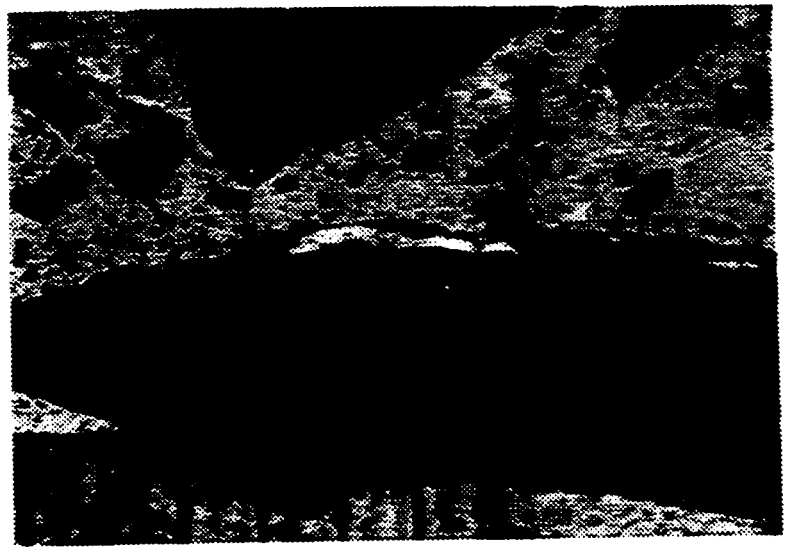

Figure 1.5: Aggregate debonding due to ASR
(each division on the scale is equal to 0.5mm)

1.4.4 Reactive Gel

When present in sufficient amounts, this whitish gel will extrude through cracks at the concrete surface. In most cases, gel can be observed through a microscope when examining polished concrete sections and may be found in aggregate cracks, paste cracks and air voids. This gel is non-crystalline (amorphous) when formed but with time, calcium ions may replace the sodium and potassium ions in the gel and cause it to crystallize. Some research has shown that this may make the gel less absorbent thus less deleterious to the concrete (Thaulow 1996, Swamy 1992). An aggregate microcrack and an air void with ASR gel (as seen through a stereo binocular microscope) are shown in Figures 1.6 and 1.7.

Figure 1.6: Microcrack with ASR gel in an aggregate particle (each division on the scale is equal to 0.5mm)

Figure 1.7: Concrete air void filled with ASR gel (each division on the scale is equal to 0.5mm)

1.5 IDENTIFICATION OF REACTIVE AGGREGATES

Many types of siliceous aggregate have been identified as being susceptible. The following is a brief list of common minerals and rocks which have been known to contain these silica minerals (CSA 1994). Minerals: opal, chalcedony, cristobalite, tridymite,

cryptocrystalline to microcrystalline quartz. Aggregates: chert, flint, shale, sandstone, limestone, greywacke, rhyolite, tuff, gneiss.

Although the only sure way to determine if aggregates will cause expansion in concrete is to conduct long term performance tests, the Canadian Standards Association specifies accelerated standard testing methods for the identification of potentially reactive aggregates (CSA 1994). While all of these tests can determine the potential reactivity of aggregates they cannot determine with absolute certainty whether or not ASR will occur in field concrete since laboratory test conditions differ significantly from field conditions (however, the CSA concrete prism test has proven to be the most reliable of all the tests). The following is a brief description of tests commonly used in Canada for the identification of potentially reactive aggregates.

1.5.1 Petrographic Examination

Petrographic examination is typically used to visually identify the mineral structure and composition of aggregates (ASTM 1997). This visual microscopic inspection can provide information regarding the potential reactivity of aggregates based on the identification of known forms of unstable silica minerals. However, an aggregate should not be rejected for use based on a petrographic examination. All aggregates should be evaluated using the Concrete Prism Test or other accelerated tests.

1.5.2 Accelerated Mortar Bar Test (CSA A23.2-25-1994)

Mortar bars, 25 x 25 x 300 mm, are cast using either the coarse or fine aggregate of interest. The bars are submerged in a 1N NaOH solution at 80°C and their expansions monitored for 14 days. The limit on expansion is set at 0.15% (0.10% for siliceous limestones) at 14 days. If bar expansions are less than 0.15% (or 0.10%) the aggregate is considered non-reactive and acceptable for use in regular concrete. If expansions exceed this limit the aggregate should be further evaluated using the CSA concrete prism test. A typical mortar bar used in the Accelerated Mortar Bar Test is shown in Figure 1.8.

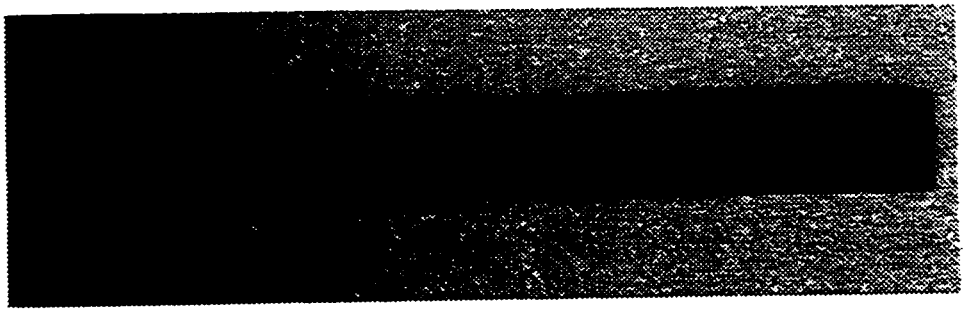

Figure 1.8: Mortar bars used in the CSA accelerated mortar bar test

1.5.3 Concrete Prism Test (CSA A23.2-14A-1994)

Concrete prisms, 75 x 75 x 300 mm, are made from either the coarse or fine aggregate of interest along with control prisms made of non-reactive coarse or fine aggregate. They are tested at 100% relative humidity and 38°C and expansion is monitored for one year. Aggregates causing prism expansion greater than 0.04% at 1 year are considered expansive and should be rejected for use. If expansions are less than 0.04% at one year, aggregates may be accepted for use in regular concrete even though they may have exceeded the allowable two-week expansion limit in the accelerated mortar bar test. Figure 1.9 shows a typical concrete prism used in the CSA Concrete Prism Test.

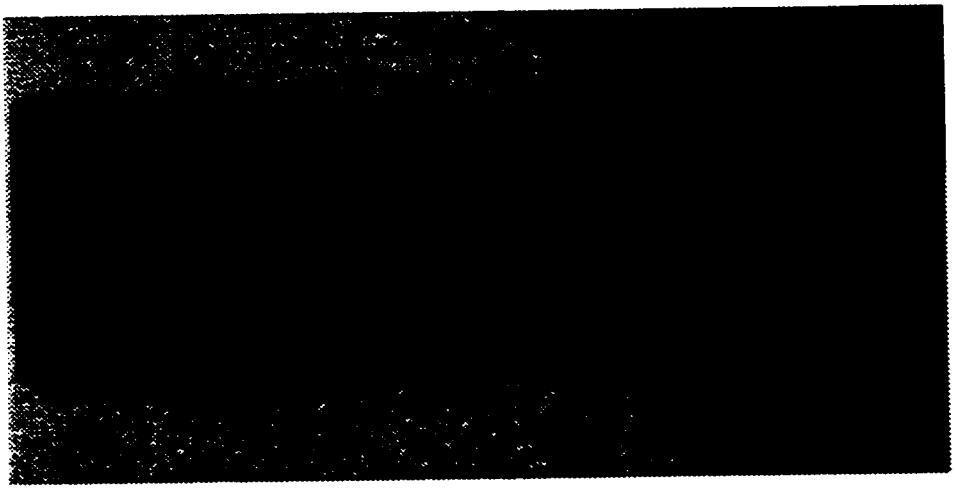

Figure 1.9: Prism used for the CSA concrete prism test

1.5.4 Field Study of Aggregate

Another method of determining the acceptability for use of aggregates is to examine the performance of identical aggregates in existing structures. This is a very useful and reliable method but great care must be taken when it is used. The new aggregate must have similar petrographic characteristics to the aggregate used in the existing concrete under study. Exposure conditions for the new concrete must be nearly identical to those of the existing used for comparison. The total alkali contents of the new and existing concretes must be similar.

In short, a field study can provide valuable information regarding the future performance of aggregates provided the new concrete and aggregates to be used are compared to existing aggregates and concrete with nearly identical compositions, use and exposure conditions.

The first three tests discussed in this section help determine the acceptability of an aggregate for use in regular concrete. Should an aggregate be used in concrete exposed to more severe conditions, such as marine environments, or in concrete with supplementary cementing materials, longer testing periods for CSA concrete prisms would be required to determine the potential reactivity of the aggregate.

The CSA prism and accelerated mortar bar tests provide accelerated results and have been known to accept reactive aggregates and reject some that are not deleteriously reactive. The accelerated conditions of these tests are sometimes much worse than those which may be encountered during the service life of a structure. Conversely, the duration of the accelerated tests may not be sufficient to allow the reaction to occur with slower reacting aggregates. These tests also do not reflect the pessimum effect associated with certain aggregates. Regardless of this, the CSA concrete prism test has proven to be the most reliable test in predicting the reactivity of potential aggregates in concrete.

1.6 EFFECTS OF ASR IN PLAIN CONCRETE

As previously mentioned, ASR can cause expansion and cracking in concrete. But also of interest is the reaction's effects on other concrete properties such as compressive strength, modulus of elasticity, tensile strength and flexural strength.

1.6.1 Compressive Strength

Concrete cylinder compressive strength is generally reduced by ASR. Some studies have shown minimal reductions while others report significant compressive strength losses(Swamy 1988, Abe 1989). Some researchers have reported that while laboratory test cylinders suffered appreciable losses in compressive strength, cores taken from reinforced concrete members tested under similar laboratory conditions exhibited smaller losses (Abe 1989). Reinforcement in these test specimens provided confinement which reduced the damage due to ASR (compared with plain concrete cylinders) thus reducing the loss in concrete compressive strength.

1.6.2 Modulus of Elasticity

The stiffness of ASR affected concrete is significantly less than the stiffness of normal concrete (Hobbs 1988). This is observed by measuring the static modulus of elasticity of ASR damaged concrete cylinders and comparing the results to those of undamaged specimens. A reduction with time of the ultra sonic pulse velocity and resonant frequency of concrete also indicates a loss of concrete stiffness due to ASR.

The stiffness loss in concrete due to ASR cracking can also be observed by repeatedly loading and unloading concrete cylinders to half of the compressive strength and plotting the successive stress-strain curves. The loss in concrete stiffness can be observed by the reduction in the slope of these curves. This phenomenon is referred to as the stiffness degradation of the concrete (caused by the internal cracking of the concrete). Figure 1.10 displays a typical stiffness degradation curve for ASR damaged concrete.

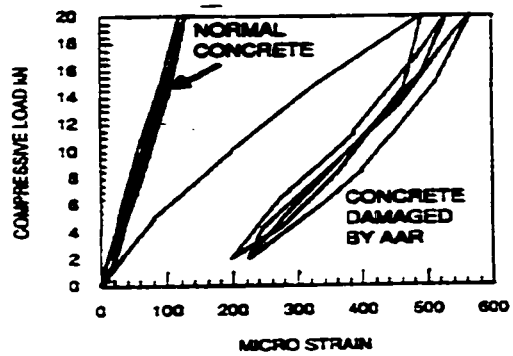

Figure 1.10: Typical concrete stiffness degradation curve (Grattan-Bellew 1993)

1.6.3 Tensile Strength

The tensile strength of plain concrete is greatly reduced by cracking due to ASR (Hobbs 1988). This is not usually significant as the tensile strength of concrete is ignored when designing reinforced concrete members.

1.6.4 Flexural Strength

Flexural strength of plain concrete is directly related to the tensile capacity of concrete at the tension fiber and the stiffness and compressive resistance of concrete in the compression fiber. All of these are reduced by damage due to ASR in turn reducing the flexural resistance of affected concrete (Hobbs 1988).

1.7 EFFECTS OF ASR IN REINFORCED CONCRETE

The effects of ASR in plain concrete are well studied but the majority of affected structures are constructed with reinforced concrete. The following are reinforced concrete structural properties of interest to engineers: flexural strength, effects of restraint due to loading and reinforcement, shear strength and deformations (deflections).

1.7.1 Flexural Strength

Significant decreases in flexural resistance of reinforced concrete members affected with ASR have been observed in experimental studies. Some researchers have reported decreases of up to 26% in ultimate flexural strength of singly reinforced, reduced scale concrete beams (Swamy 1989).

1.7.2 Effect of Restraint (due to loading and reinforcement)

Reinforcing steel has a restraining effect on concrete expansions caused by ASR resulting in a form of prestress of the concrete (Hobbs 1988). This effect, depending on the amount and distribution of reinforcement, can result in differential expansions within reinforced concrete members. These differential expansions can result in member deflections such as camber in singly reinforced concrete beams (Swamy 1989). In some

cases, expansions from ASR have been large enough to cause yielding of longitudinal reinforcement (Hobbs 1988). Applied compressive stresses reduce expansions due to ASR by providing active restraint to expansion (Jones 1996).

1.7.3 Shear Strength

Due to the possible prestressing effects of ASR, the shear capacity of reinforced concrete members may increase (Cope 1992). Again, this depends on the amount and distribution of reinforcement as well as the extent of expansions. Thus, when loaded to failure, reinforced concrete members affected by ASR will usually fail in flexure and not in shear.

1.7.4 Deformations (Deflections)

Laboratory tests have shown that singly reinforced concrete beams affected by ASR may exhibit seemingly brittle failures when loaded to their ultimate flexural capacity (Swamy 1989). During loading, these members had to overcome negative deflections (due to differential ASR expansions between the top and bottom fibers of the beams) prior to deflecting in the positive direction. Thus at failure, positive deflections of these beams were small compared to those of control members, although the total load induced deflection of all the beams were similar. This gave the appearance of less ductile behaviour of these specimens.

1.8 PREVENTION OF ASR

There is a general consensus that the only sure way to avoid ASR is to utilize non-reactive aggregate. However, some regions have a shortage of quality aggregate sources or an abundance of reactive aggregate sources. In instances when potentially reactive aggregates must be used, the suggestions given below may help in avoiding and/or minimizing the effects of ASR.

1.8.1 Concrete Alkali Content

Using cement with an alkali content of no more than 0.6% Na_2O equivalent and/or a total concrete alkali content of 3 kg/m^3 is generally considered sufficient to avoid ASR (CSA 1994). However, this rule of thumb has not always proven successful especially with highly reactive aggregates. In addition, many Canadian cement manufacturers produce cement with alkali levels greater than 0.6% Na_2O equivalent (Swamy 1992).

Minimizing alkalis from other sources such as chemical admixtures and supplementary cementing materials will also help in minimizing the risks of ASR when using potentially reactive aggregate.

1.8.2 Concrete Moisture Content

Concrete moisture content may be reduced by sealing exposed surfaces and properly maintaining these seals (Bérubé 1996). Minimizing moisture will help reduce the effects of ASR. Sealants, however, are not very durable as they do not sufficiently penetrate concrete surfaces and thus are easily worn and weathered. Therefore, preventing the ingress of external moisture is not yet a practical solution for the prevention or control of ASR.

In large concrete members, the control of external moisture may not be effective in controlling or reducing ASR. The internal moisture content of these members may be sufficient to promote the reaction.

1.8.3 Supplementary Cementing Materials

Some supplementary cementing materials decrease the permeability of concrete and thus reduced the ability of alkalis to migrate to potential silica reaction sites. As well, some mineral admixtures can help bind the alkalis present in concrete pore solution (Bérubé 1992). However, the use of some of these admixtures have been known to only delay the onset of ASR (Bérubé 1992). Thus, when testing aggregate for use with mineral admixtures, such as fly ash, ground granulated blast furnace slag and silica fume, concrete prism tests should be conducted for an extended period of time (longer than one year).

1.8.4 Chemical Additives

Lithium salts have been known to reduce or prevent ASR. This element has the capacity to replace the Na and K ions in ASR gel and reduce its capacity to absorb water. Lithium salts have proven effective when used as an additive at the point of concrete mixing (Stokes 1996). The effectiveness of lithium salts as admixtures for the prevention of ASR is dependent on the dosage and type of lithium admixture as well as the nature of the reactive aggregate being used. Tests have been conducted to impregnate existing concrete structures affected by ASR with lithium salt solutions. However, this practice has had little success as the lithium leaches from the concrete with time (Stokes 1996).

1.9 ASSESSMENT OF ASR AFFECTED STRUCTURES

Engineers are often faced with decisions regarding the proper management of structures affected by ASR. The following factors are usually considered when dealing with such structures.

1.9.1 Condition of the Structure

First, the structure must be examined and the serviceability of each of its components must be determined. Residual structural capacities may be estimated by the use of finite element models and measured concrete properties (obtained using non-destructive tests and core samples). A full-scale load test is the best way to determine the residual load carrying capacities of structures and their components. However, this may often be too costly and impractical to perform.

1.9.2 The State of Expansion

The presence of ongoing expansion in ASR affected structures must be assessed prior to performing any repairs. Expansion can be monitored done by installing Demec points in the structure at locations of interest and monitoring the change in distance between these points with time.

1.9.3 Stopping Expansion

If the structure is to be repaired and expansions are ongoing, measures can be taken to stop the reaction and ensure it will not restart after repairs have been completed. The easiest way to stop the ASR would be to remove one of its required phases (reactive aggregate, alkalis or moisture). Concrete aggregate is impossible to replace and there is presently no efficient method of removing alkalis from concrete. The only way to keep structural members dry (reduce moisture) is to seal their surfaces and to ensure the proper maintenance of the sealed areas as these seals have not proven to be very durable (susceptible to weathering). Therefore, there is currently no effective method of stopping the ASR in concrete affected by the reaction.

1.9.4 Method of Repair

Once expansions have ceased, repairs can be effected as required. As different structures may behave differently (depending on their type of construction), and not all cases of ASR are of the same severity, repairs may vary from simple pressure grouting of cracks to the partial or total demolition and re-casting of severely affected members (Hobbs 1988). Sometimes, entire structures may be so severely damaged that total demolition may be the only possible alternative.

It is preferable for expansions to have ceased prior to performing repairs, but to maintain serviceability, some structures may need to be repaired despite ongoing expansion (hydroelectric dams, bridges). In these cases, methods such as steel jacketing and post tensioning of affected members and slot cutting in dams have been used with varying degrees of success depending on the type of structure and the degree of present and future expansion.

1.10 STATEMENT OF THE PROBLEM

Many experiments on ASR have been conducted by constructing reactive reinforced concrete beams and exposing them to environments promoting the reaction. These samples were left to react in an unloaded state. Unfortunately, this work has

limited value in modeling ASR effects on in-service reinforced concrete members such as bridge girders as these structures are subjected to significant live as well as dead loads.

Reinforcement and applied compressive stresses reduce expansions due to ASR, but little is known regarding the effects of flexural loading on the progression of the reaction.

Singly reinforced, simple span concrete beams reacting under unloaded, static service live load and dynamic service live load conditions were tested in an attempt to gain a better understanding of how ASR develops, progresses and affects the structural properties in actual, in-service reinforced concrete members. The following are the three main areas of focus of this thesis.

1.10.1 The Effect of Loading Regime on the Alkali-Silica Reaction

The severity of ASR between the unloaded, statically and dynamically loaded members was examined. Expansions were monitored in various longitudinal locations along the beams as well as vertically between the top fiber and the bottom steel location. These expansions were compared to those of control (non-reactive) specimens to ascertain the presence of other permanent strains due to creep (statically loaded beams) and loss of concrete stiffness (dynamically loaded beams).

1.10.2 The Structural Effects of ASR on the R/C Beams

The structural behaviours of the variously loaded beams were observed and compared. The beams were loaded in flexure to failure while recording their ultimate loads and load deflection behaviour. The behaviour of the reactive beams were compared to those of the non-reactive controls to determine the actual effect of ASR or reinforced concrete beams.

1.10.3 Comparison of the Damage Rating Indices of the Beams

Damage Rating Indices (DRI) were measured on each reactive beam and compared with the expansive and structural behaviours of the beams. The DRI, explained

in detail in Chapter 3, is a method of quantifying concrete damage through petrographic examination.

This was done in an attempt to correlate concrete expansions with measured concrete damage and structural behaviour.

REFERENCES

Abe, M., Kikuta, S., Masuda, Y., Tomozawa, F., 1989, "Experimental Study on Mechanical Behavior of Reinforced Concrete Members Affected by Alkali-Aggregate Reaction", Proceedings of the 8th International Conference on Alkali-Aggregate Reaction, pp. 691-696, The Society for of Materials Science, Japan.

American Society for the Testing of Materials (ASTM), 1997, "ASTM 295", Petrographic Examination of Rocks, ASTM, West Conshocken, Pennsylvania, USA.

Bérubé, M.A., Duchesne, J., 1992, "Does Silica Fume Merely Postpone Expansion Due to Alkali-Aggregate Reactivity?", Proceedings of the 9th International Conference on Alkali Aggregate Reaction, pp. 71-80, Chamelon Press Ltd., London, England.

Bérubé, M.A., Chouinard, D., Boisvert, L., Frénette, J., Pigeon, M., 1996, "Influence of Wetting-Drying and Freezing-Thawing Cycles, and Effectiveness of Sealers on ASR", Proceedings of the 10th International Conference on Alkali-Aggregate Reaction, pp. 1056-1063, Melbourne, Australia.

Blight, G.E., Alexander, M.G., Ralph, T.K., Lewis, B.A., 1989, "Effect of Alkali-Aggregate Reaction on the Performance of a Reinforced Concrete Structure Over a Six Year Period", Magazine of Concrete Research, V. 41, No. 147, June, pp. 69-77, British Cement Association.

Canada Center for Mineral and Energy Technology, Institute for Research in Construction, Groupe de Recherche en Géologie de L'Ingénieur, 1993, "Petrography and Alkali-Aggregate Reactivity, course manual", pp. 576, Ottawa, Ontario, Canada.

Canadian Standards Association, CSA A23.1 Appendix B, 1994, "Alkali-Aggregate Reaction", Concrete Materials and Methods of Concrete Construction, Methods of Testing for Concrete, pp. 112-135, CSA, Rexdale, Ontario

Canadian Standards Association, CSA A23.2-14A-1994, "Potential Expansivety of Aggregates (Procedure for Length change Due to Alkali-Aggregate Reaction in Concrete Prisms)", Concrete Materials and Methods of Concrete Construction, Methods of Testing for Concrete, pp. 205-214, CSA, Rexdale, Ontario

Canadian Standards Association, CSA A23.2-25A-1994, "Test Method for Detection of Alkali-Silica Reactive Aggregate by Accelerated Expansion of Mortar Bars", Concrete Materials and Methods of Concrete Construction, Methods of Testing for Concrete, pp. 236-242, CSA, Rexdale, Ontario.

Cope, R.J., Slade, L., 1992, "Effect of AAR on Shear Capacity of Beams Without Shear Reinforcement", Proceedings of the 9th International Conference on Alkali-Aggregate Reaction, 1992, pp. 184-191, Chamelon Press Ltd., London, England.

Grattan-Bellew, P.E., 1993, "A New Damage Rating System for Evaluation of Condition of Concrete from Structures", Unpublished, National Research Council of Canada.

Grattan-Bellew, P.E., 1994, "Alkali Contribution from Limestone Aggregate to Pore Solution of Old Concrete", ACI Materials Journal, V. 91, No. 2, American Concrete Institute.

Hobbs, D.W., 1988, "Alkali-Silica Reaction in Concrete", pp. 183, Thomas Telford Ltd., London, England.

Imai, H., Yamasaki, T., Maehara, H., Miyagawa, T., 1986, "The Deterioration by Alkali-Silica Reaction of Hanshin Expressway Concrete Structures-Investigation and Repair", Proceedings of the 7th International Conference on Alkali Aggregate Reaction, pp. 131-135, 1986, Noyes Publications, Park Ridge, USA.

Jensen, A.D., Chaterji, S., Christensen, S., Thaulow, N., 1984, "Studies of Alkali-Silica Reaction-Part II: Effect of Air Entrainment on Expansion", Cement and Concrete Research, V. 14, pp. 311-314.

Jones, A.E.K., Clark L.K., 1996, "The Effects of Restraint on ASR Expansion of Reinforced Concrete", Magazine of Concrete Research, V. 48, No. 174, pp. 1-13, British Cement Association.

Kobayashi, K., Shiraki, R., Kawai, K., 1989 "Influence of Alkali Concentration Distribution Occurring in Concrete Members on Expansion and Cracking Due to Alkali-Silica Reaction", Proceedings of the 8th International Conference on Alkali-Aggregate Reaction, pp. 641-646, the Society for of Materials Science, Japan.

Monette, L.J., Gardner, N.J., Grattan-Bellew, P.G., 1997, "The Effects of the Alkali-Reaction on Unloaded, Statically Loaded and Dynamically Loaded Reinforced Concrete Beams", Proceedings of the International Conference on Engineering Materials, Canadian Society for Civil engineering and Japanese Society for Civil Engineering, Ottawa, Canada.

Stokes, D.B., 1996, "Use of Lithium to Combat Alkali-Silica Reactivity", Proceedings of the 10th International Conference on Alkali Aggregate Reaction, pgs. 862-867, Melbourne, Australia.

Struble, L., Diamond, S., 1981, "Unstable Swelling Behaviour of Alkali-Silica Gels". Cement and Concrete Research, V. 11, No. 4, pp. 611-617, Pergamon Press, USA.

Swamy, R.N., Al-Asali, M.M., 1988, "Engineering Properties of Concrete Affected by Alkali-Silica Reaction", ACI Materials Journal, V. 85. No. 5, pp. 367-374, American Concrete Institute.

Swamy, R.N., Al-Asali, M.M., 1989, "Effect of Alkali-Silica Reaction on the Structural behavior of Reinforced Concrete Beams", ACI Structural Journal, V. 84, No. 4, pp. 451-459, American Concrete Institute.

Swamy, R.N., 1992, "The Alkali-Silica Reaction in Concrete", pp. 336, Blackie and Son Ltd., Glasgow, Scotland.

Thaulow, N., Jakobsen, U.H., Clark, B., 1996, "Composition of Alkali-Silica Gel and Ettringite in Concrete Railroad Ties: SEM-EDX and X-Ray Diffraction Analyses", Cement and Concrete Research, V. 26, No. 2, pp. 309-318, Pergamon Press, USA.

CHAPTER 2

LITERATURE REVIEW

There is no work published regarding the effects of flexural loading regime on ASR in reinforced concrete beams. However, there are a numerous publications on subjects related to this research. The following is a review of these works.

This chapter is divided into two sections. The first is a literature review of pertinent works dealing with plain concrete (materials) while the second reviews related work dealing with reinforced concrete members (structural).

2.1 MATERIALS

The following section reviews work by other authors on subjects dealing with plain concrete and related to the research discussed in this thesis. All of the works discussed in the following are presented in chronological order.

2.1.1 Ramachandran, Beaudoin, Sarkar and Aimin 1983

Alkalis react in the cement hydration process and are known to influence the workability, setting, shrinkage, bleeding and strength development of concrete. An investigation was performed into the effects of sodium hydroxide on the strength and hydration of tricalcium silicate (3CaO SiO2).

To study these effects, two sets of cylindrical specimens were prepared. The first set was prepared using laboratory synthesized tricalcium silicate mixed with water at a

water/solid ratio of 0.4. This was the reference paste. The second was mixed similarly but 3% NaOH was added. All samples were cured in a desiccator over distilled water. Periodically, from 1 to 28 days, small cylindrical samples (0.5 inch diameter by 1 inch long) were sliced from the larger specimens and their compressive strengths were determined.

The NaOH greatly affected the hydration of the paste. The total heat of hydration, the calcium hydroxide and the non-evaporable water content of the paste with the added NaOH was greater than in the reference paste.

It was also determined that that the 7 day strength of the paste with added NaOH was similar to the strength of the paste with no NaOH. Subsequently, the paste containing NaOH had consistently lower strength than the reference paste showing a difference of 60% at 28 days.

2.1.2 Akashi, Amasaki, Takagi and Tomita 1986

A study was performed to try to estimate damage to concrete from ASR using ultra sonic pulse velocity (UPV). Two sets of reactive and non-reactive reinforced concrete specimens, 400 x 400 x 540 mm, were made, each set having different reinforcement ratios and configurations. This was done to evaluate the effect of the thickness of concrete cover on the change in concrete properties due to ASR. The reactive and non-reactive concrete mixes were identical in composition except for the use of a reactive coarse aggregate and a total alkali content of 6 kg/m^3 in the reactive mixes.

The first set of specimens was cured for two weeks under a wet blanket while the second was cured for the same period of time immersed in water at 20°C. Each set was then cured at 40 °C and 100% RH for two months. Pulse velocity measurements were periodically taken and at the age of 10 months core samples were obtained from each specimen. Compressive strength and the static modulus of elasticity of the cores were determined. The following are the results of the experiment.

a) ASR damaged both the cover and core concrete of the specimens. The UPV of ASR damaged concrete was reduced to approximately 90% of that of sound concrete. UPV dropped with an increase in concrete damage.

b) The compressive strength of concrete cores was reduced to 70% of the strength of sound concrete at 10 months.

c) The static modulus of elasticity of damaged concrete was reduced to 45% of the sound concrete.

2.1.3 Swamy and Al-Asali 1988

An investigation was conducted into the effects of ASR on the engineering properties of concrete. Specimens were made of concrete containing cement with a total alkali content of 1% Na_2O equivalent and a total cement content of 520 kg/m^3. Two sets of specimens were constructed; the first containing opal as a partial fine aggregate replacement and the second using an amorphous fused silica as the reactive component of the concrete. Expansions of 75 x 75 x 300 mm plain concrete prisms were monitored. The following tests were conducted to determine the engineering properties of ASR affected concrete; compressive strength using 100 x 100 x 100 mm cubes; tensile splitting strength using 100 mm diameter by 200 mm long cylinders; modulus of rupture, dynamic modulus of elasticity and pulse velocity on 100 x 100 x 500 mm prisms. All the test specimens were demoulded after one day and cured at 20°C and 96% RH.

a) The opal concrete suffered a loss in compressive strength, compared to the 28 day and 1 year control concrete, of about 54 and 63% respectively. Similarly, the fused silica concrete displayed a loss in compressive strength of 26 and 39% compared to the 28 day and 1 year control concrete respectively. Thus there is a loss of compressive strength with time due to ASR expansions.

b) The modulus of rupture, flexural strength, and the indirect tensile strength of the fused silica specimens were both reduced by ASR expansions. Due to a lack of availability of opal, these tests were only performed using the fused silica. The modulus of rupture experienced a 13% reduction at 28 days and a 77% loss at one year while the

cylinder splitting strength experienced 16 and 57% losses for the same periods of time. As with the compressive strength, the tensile strengths were reduced by an increase in expansion.

c) The dynamic modulus of elasticity test displayed sensitivity in detecting changes in the concrete microstructure at an early age prior to any significant expansion or visual damage. The loss in concrete dynamic modulus was noticed at a very early age before the indication of any expansion. The losses of dynamic modulus ranged from 42-68% at 12 months. Ultra sonic pulse velocity also was found to be effective in detecting ASR at early ages. The ultra-sonic pulse velocities dropped by 25-42% in a period of twelve months. The dynamic modulus and pulse velocity in the control specimens increased during the first three months and then subsequently leveled off. These same properties in the reactive specimens also increased during the first month before starting to drop for the remaining 11 months.

d) The tensile strength of the concrete is more sensitive in detecting ASR than the compressive strength. In damaged concrete, the ratio of compressive to tensile strength is lower than in sound concrete. For sound concrete, the ratio of tensile to compressive strength varies from 0.11 to 0.07. This ratio decreases with an increase in compressive strength and age. At 0.1% expansion, the ratio decreased to 0.049 and at an expansion of 0.259% the ratio was only 40% of the original. A ratio of less than 0.06 has been recommended as evidence of internal deterioration due to ASR.

2.1.4 Gunatilaka, Machida and Mutsuyoshi 1990

The effects of precracking on the behaviour of concrete under cyclic compressive loading was investigated. Hollow cylindrical reinforced concrete specimens, 150 mm outside diameter, 80 mm inside diameter by 300 mm long, were precracked longitudinally by applying uniform radial pressure to the inside. This was done by pumping water into a rubber tube placed to the interior of the samples. The concrete cylinders were then tested in uniaxial compression. The cracked samples exhibited a lower ultimate compressive strength and static modulus of elasticity. These reductions increased with an increase in specimen cracking.

2.1.5 Habita, Brouxel and Prin 1992

The mechanical behaviour of ASR affected concrete specimens was investigated, with a focus on compressive strength, tensile strength as well as modulus of elasticity. Three concretes were compared; concrete made with 0.917% Na_2O equivalent cement; concrete with an Na_2O equivalent content increased to 1.5% by addition of NaOH; concrete with an Na_2O equivalent content increased to 1.5% by addition of KOH. The reactive aggregate used for every batch was a muscovite gneiss.

Doubly reinforced concrete beams, 150 x 250 x 2300 mm, concrete prisms, 140 x 140 x 560 mm and 70 x 70 x 320 mm, and cylinders, 160 mm diameter by 320 mm long were cast from each batch of concrete. All specimens were cured at 40°C and 100% RH for 1 year.

a) The reinforced concrete specimens exhibited smaller expansions near the locations of longitudinal steel, 0.2-0.3%, and larger expansions, 0.3-0.45%, at their mid-height.

b) The smaller plain concrete prisms exhibited less expansion than the larger ones. 0.6-1% and 1.5-4% respectively. This demonstrates a specimen size effect related to ASR expansions.

c) The concrete specimens with added KOH showed the largest expansions for the first three months. After three months, the concrete containing added NaOH exhibited the larger expansions. The concrete with no added alkalis expanded 50-60% less than the other two batches. This demonstrates the effect of alkalis to the development of ASR.

d) The specimens with added alkalis displayed the smallest compressive strengths at twelve months. The rate of compressive strength gain in these specimens during the first three months was very high compared with the reference concrete. These rates subsequently dropped significantly resulting in strength losses during the next three months and then leveled off during the remainder of the experiment. The control specimens showed an 11% increase in compressive strength during the first three months and a 22% increase at the end of one year. The cylinders from the other two batches (with added alkalis) had an increase in compressive strength of 49-52% during the first three months and a subsequent decrease of 10-22% during the second three months resulting in

a net strength increase of 20-34% after one year. The 28 day strength of the control concrete was 29% higher (45 MPa) compared with the other batches (35 MPa).

e) The concrete specimens with additional alkalis showed a 50-60% decrease in modulus of elasticity compared with the reference concrete.

2.1.6 Le Roux, Massieu and Godart 1992

Core samples were taken from an existing bridge affected by ASR. The structure, located in Paris, France, is a frame bridge with reinforced concrete piers and a prestressed concrete deck. It was proposed to repair the structure by prestressing the piers which warranted the determination of the effect of restraint on ASR. The parts of the structure studied were constructed in 1976. Four 69 mm diameter specimens were prepared from a 150 mm diameter core taken from one of the damaged piers and monitored for expansions under varying levels of applied compressive stress. This core was taken in a direction of the largest expansions observed in the piers. The test was conducted in for 378 days in tap water at a temperature of 20°C and at applied stress levels of 0, 1, 3 and 5 MPa. Applied compressive stresses were found to reduce expansions in concrete. Expansion levels due to different levels of stress were found as follows; free expansion 0.7% at 378 days; 1 MPa applied compressive stress 0.3% at 378 days; 3 MPa applied compressive stress 0.1% at 378 days; 5 MPa applied compressive stress 0% at 200 days and 0.01% at 378 days. This showed the beneficial effects of applied compressive stress on ASR expansions. Swelling pressures due to ASR gel have been previously estimated to be within a range of 3-10 MPa. This coincides well with the 5 MPa active stress which reduced expansions to a negligible level in this study.

2.1.7 Guédon and Le Roux 1993

An investigation into the effects of microcracking on the onset and development of the alkali-silica reaction was conducted. Three sets of 70 x 70 x 280 mm plain concrete prisms were constructed using reactive aggregate and cement with an alkalinity of 0.87% increased to 1.25% Na_2O equivalent by adding NaOH to the mixing water.

The specimens were cured for 28 days at 38 degrees Celsius prior to being loaded to 75% and 100% of ultimate compressive load. Unloaded prisms were used as uncracked references. After cracking, the samples were returned to the curing chamber and periodically measured for expansion and ultrasonic pulse velocity.

The uncracked prisms exhibited expansions of 0.04% at 4 months. The cracked specimens reached this level of expansion in half the time. At 8 months, rates of expansion for the control specimens flattened while for the microcracked prisms, rates continued to grow slightly indicating the availability of additional reaction sites due to precracking. Thus, initial concrete microcracking displayed a significant effect on the onset, progression and duration of ASR.

2.1.8 Jones and Clark 1996

Concrete cylinders were tested to determine the effect of active and passive restraint on expansions due to ASR. One hundred and eighty cylindrical specimens, 100 mm diameter by 200 mm long, were conditioned under applied stresses ranging from 4 MPa in tension to 7 MPa in compression and had reinforcement ratios of 0.125 to 2%. Reinforcement was provided by a single bar passing through the center of each specimen. Applied stresses were not applied until the concrete was 28 days old.

Reinforced concrete beams, 100 x 200 x 2000 mm, with reinforcement of either 1 or 2% were also constructed. They were symmetrically reinforced by placing the bars at an equal distance from the top and bottom faces of the beams. A large reinforced concrete block, 450 x 300 x 600 mm was also tested.

All specimens were cast from the same concrete mix which contained additional alkalis, for a total alkali content of 7 kg/m^3. The coarse aggregate was a limestone and the fine aggregate a chertsey sand. Most specimens were conditioned submerged at 38°C while some others were maintained at 30 and 20°C. Longitudinal and lateral specimen expansions were monitored throughout the experiment. Unrestrained plain concrete specimens were also monitored. Specimens were monitored for a period of approximately 250 days.

a) Unrestrained rates of expansion at 20, 30 and 38°C were 0.01, 0.06 and 0.1% respectively.

b) Applied stress reduced both expansion and the rate of expansion of the unreinforced specimens. An applied stress of 1 MPa reduced expansions by 60-70% at 250 days. However, specimens under an applied stress of 7 MPa still exhibited expansions of 0.05% at 250 days..

c) Expansions of the reinforced specimens with no applied stress varied with the reinforcement ratio. However, this difference increased with a decrease in reinforcement. At a level above 1% reinforcement, an increase in steel provided only a marginal decrease in expansion (0.6-0.25% expansion, unreinforced concrete and concrete with 1% reinforcement respectively and 0.25-0.2% expansion, 1 and 2% reinforcing steel respectively).

d) When compressive stresses were applied to the reinforced specimens the reinforcement ratios made little difference at stresses of 2 MPa and above. Thus at this level the applied stress was sufficient to reduce expansive pressures to negate the effects of the reinforcement.

e) Tensile stresses increased the overall specimen expansions but when non ASR strains such as creep were considered, tensile stresses had little effect on ASR expansions.

f) Reinforcement had a greater restraining effect in the beam specimens than in the cylinder specimens of the same reinforcement ratios. Beam expansions were found to be 50% of the cylinder expansions of the same reinforcement ratios. Expansions in the horizontal direction of the beams were found to be 65% of the vertical beam expansions. Thus showing that restraint does not significantly affect expansion perpendicular to its direction.

g) A comparison was made of the final expansions in the vertical direction of the beams and the unreinforced prisms and cylinders and these specimens' ratio of cross sectional area to surface area. This comparison showed that the specimens with lower cross-sectional area to surface area ratios exhibited lower expansions thus showing a size effect. This is due to the leaching of alkalis which is larger in the smaller specimens .

2.1.9 Shayan and Ivanusec 1996

The influence of NaOH on the mechanical properties of cement paste and mortar made with and without ASR aggregates was investigated. Mortar bars, 25 x 25 x 285 mm, were made using reactive and non-reactive aggregates and cured in 100% RH at 23°C. The cement used in all the specimens had a total alkali content of 0.8% Na_2O equivalent. Two mixes were made. The first was a control mix using non-reactive sand. The second was identical but 5% of the sand was replaced by opal to promote expansion. These bars were monitored for expansion on a weekly basis. Cubes, 25 x 25 x 25 mm, were cast ,using the same mortars as the expansion bars, to monitor compressive strength while bars, 13 x 13 x 100 mm, of the same composition were used to determine the modulus of rupture of each mix. This was determined using a three point loading test. The solutions used for the mixes had an NaOH concentration of 0, 0.5, 1.0, 2.0 and 4.5M. The specimens were cured at 100% RH and 23°C for 7, 28 and 90 days before testing.

a) Control mortar bars (non-reactive sand) showed 0.015% expansion at all alkali levels except for an expansion of 0.038% at an alkali level of 3.8% Na_2O equivalent.

b) The reactive specimens displayed increasing amounts of expansion with increasing levels of alkalinity except at alkali contents of 2.3 and 3.8% Na_2O equivalent where expansions were equal at 14 weeks.

c) NaOH interacts in the cement hydration and weakens the cement paste matrix. The compressive strength of all paste and mortar cubes showed a decrease in strength with increasing alkalinity, at 7, 28 and 90 days. The decrease in compressive strength of the reactive and unreactive mortar specimens (w/c ratio of 0.4) was up to 55%, ranging from 55 MPa to 25 MPa at alkali contents of 0.5% and 4% Na_2O equivalent, respectively, at 28 days.

d) The increase in alkalis also reduced the modulus of rupture of the all the mortar bars. This suggests that the tensile strength of concrete is not only reduced by cracking due to ASR but also by the effect of alkalis on the cement hydration process.

2.1.10 Tawfiq, Armaghani and Vysyaraju 1996

The permeability of concrete is an important factor in concrete durability as an increase in permeability can promote the ingress of water and ionic species. Concrete naturally contains cracks in the form of bond cracks at the aggregate paste interface As load is increased, the existing bond cracks get longer and propagate. The increase in bond cracking does not significantly increase up to applied loads of up to 30% of ultimate. As the load increases, bond cracks are propagated and new cracks are formed. At a level of 70-90% of ultimate load, cracking increased noticeably and bridging occurs between bond cracks forming a continuous crack pattern. At levels of up to 75% of ultimate capacity the transport properties of concrete were not significantly affected. When load increased beyond that point, the concrete became 15 to 20% less resistant to fluid and ion movement. The changes in the transport characteristics of concrete cause by the development and propagation of cracks due to cyclic loading were investigated. Flexural specimens statically and dynamically loaded were tested. Samples were then obtained from these to determine their resulting permeability.

A total of sixty two, 150 x 150 x 500 mm, single edge notch beams and seven un-notched beams were prepared using eight different mixes. The notches were 6 mm wide by 20 mm deep. The permeability of the concretes were obtained by measuring the air permeability at the center of the beam span. Beams were loaded to modulus of rupture to measure the air permeability as the flexural cracks progressed. After flexural testing, core samples were taken from these specimens and tested for water permeability. Dynamic tests were then conducted and varying stress ratios were used on different samples. These stress ratios were based on the modulus of rupture. Permeability readings were taken at different times during the experiment until fatigue of the specimens occurred. The stress ratios used ranged from 40 to 95%. Air permeability was measured by the time taken for a loss from -55 to -50 KPa in induced negative pressure. Similarly to the static beams, cores were taken from the dynamic beams and water permeability tests were taken. The dynamic samples showed a rapid loss in negative pressure indicating an extended channeling of microcracks in the concrete.

2.2 STRUCTURAL

The following section reviews work by authors dealing with the structural behaviour of reinforced concrete members and pertinent to the research described in this thesis.

2.2.1 Koyanagi, Rokugo and Ishida 1986

An investigation into the effects of ASR on the behaviour of reinforced concrete beams was conducted. Reinforced concrete beams, 100 x 180 x 1700 mm, with constant tensile reinforcement ratios (1.66%) and three different compression reinforcement ratios (0, 0.93 and 1.66%) were constructed. The concrete was made with a cement of an alkali content of 0.67% raised to 2.3% by the addition of alkalis. The reactive aggregate used, as a coarse aggregate, was a bronzite andesite. Plain concrete cylinders, 100 mm diameter by 200 mm long, as well as 100 x 100 x 400 mm concrete prisms were also constructed for the monitoring of dynamic modulus. All specimens were cured for 13 days after demoulding at 20°C in moist conditions. A control set of specimens was then placed at room temperature for 27 days. The remainder of the specimens were placed in accelerated conditions of 40°C and 100% RH until 7 days prior to testing. Reinforced concrete beams were tested to failure at 160 and 430 days.

a) The singly reinforced beams experienced random cracking at the top of the specimens where no longitudinal reinforcement was present. The doubly reinforced beams suffered less cracking and most of the cracks occurred in the direction of the reinforcement. The expansions due to ASR were thus restrained by the reinforcement subsequently inducing compressive stresses in the concrete.

b) The dynamic modulus of elasticity in the beams at approximately 120 days stored in accelerating conditions were 50% lower than the control specimens stored at room temperature for the same period of time.

c) The flexural and shear cracking loads of the affected beams were larger than the ones tested at 27 days. The beam with 1.66% compression reinforcement failed in shear at 27 days while the reactive beam of the same reinforcement failed in flexure. This

showed the effect of prestressing due to ASR expansions. The toughness of all the beams were very similar thus showing that even though ASR affected the early behaviour of flexural members, the ultimate behaviours were very similar.

2.2.2 Abe, Kikuta, Masuda and Tomozawa 1989

Reactive and non-reactive small scale reinforced concrete beams and companion concrete cylinders were tested to failure. Three sets of reinforced concrete beams were constructed with reinforcement ratios of 0.75, 1.17 and 1.76% respectively. The longitudinal reinforcement was equal on the top and the bottom of the beams. Shear links were provided to avoid shear failure. The beam specimens were 200 x 200 x 2000 mm. The shear span length ratio of the beams were 2.0. Each set of specimens consisted of reactive and non-reactive beams. The reactive concrete contained crushed andesite as a coarse aggregate. The loading points were placed such that a section of the beam was cantilevered and positive and negative moments in the beams were equal. The total alkali content of the cement used was of 8 kg/m^3 controlled by the addition of alkalis. Specimens were cured at 40°C and at high RH.

Cylinders, 100 mm diameter by 200 mm, were tested to ultimate compressive strength and static modulus of elasticity and compared to cores taken from the beam specimens.

a) Concrete cylinder compressive strengths at 167 and 513 days exhibited a loss from the 28 day strength of 28 and 23% respectively. The concrete cores showed an increase in compressive strength of 9% from the 28 day strength.

b) Beam expansions were monitored and compared with those of unreinforced specimens, 100 x 100 x 400 mm. The beam expansions were reduced with an increase in reinforcement ratio. Expansions in the vertical direction of the beams were significantly larger than the longitudinal ones. Vertical reinforced beam expansions were 18–42% lower than the expansions of the unreinforced prisms over a period of approximately 470 days while, for the same period, the longitudinal reinforced specimen expansions were 82-91% lower than the plain concrete specimens.

c) Unaffected beam specimens failed in diagonal shear tension after flexural yield. Some of the reactive specimens failed by horizontal slip failure along horizontal cracks caused by ASR.

d) During flexural testing, crushing of the concrete at the loading points and the supports occurred. Most specimens from the first two beam series failed by flexural crushing of the compression fiber following flexural yield. The beams from the third series failed mostly by shear.

e) Deflections of beam specimens at yield of longitudinal reinforcement decreased with increasing expansion. The yield deflections of the first two series of specimens were approximately 50% of those of unaffected specimens while the third series deflections were 60% of the unaffected ones.

2.2.3 Inoue, Fujii, Kobayashi and Nakano 1989

Expansion characteristics and structural behaviour of singly reinforced concrete beams were investigated. Singly reinforced, simply supported, concrete beams, 200 x 200 x 1700 mm, complete with shear links were constructed. The total concrete alkali content was increased to 8 kg/m^3 by adding NaCl. Three levels of reinforcement ratios were used, 0.77%, 1.20% and 1.74% in both reactive and control beams. Each specimen was cured for 14 days at 20°C and 80% RH and subsequently placed in a curing condition of 40°C and 100% RH for 178 days. After the accelerated curing the beams were placed at room temperature and 70% RH for two years.

Each beam was statically loaded under four point loading to the design stress and then fully unloaded. They were then loaded to ultimate flexural failure and mid span deflections were measured.

a) The reinforcement ratio has a significant effect on expansions due to ASR. Strains at the upper, non-reinforced fiber of the reinforced concrete beams reached up to 0.7%. The measured strains in reinforcement were 0.14%, 0.10% and 0.085% for reinforcement ratios of 0.77, 1.20 and 1.74% respectively. It is suggested that even after drying for two years, these specimens retained 40% of this prestress.

b) At the time of the loading tests on the beams, plain concrete compressive and tensile strengths as well as static modulus of elasticity were reduced to 64%, 59% and 48% of those of the unreactive concrete.

c) The flexural cracking strength of the ASR beams was larger than those of the non-reactive controls. This was due to the prestressing effect between the longitudinal reinforcement and the ASR expansions.

d) Even though the reinforcing steel in each beam encountered significant ASR induced strains, the measured flexural yield strength of the beams was reduced by less than 10% from that of the control specimens. The unreactive beam with 1.74% longitudinal reinforcement failed in shear while all other specimens failed in flexure. This displayed the potential beneficial effect that ASR induced expansions could have in preventing the premature shear failure of heavily reinforced specimens.

e) The deflection at the failure load of ASR beams was considerably lower than that predicted using the elastic modulus of the damaged cylinders.

2.2.4 Swamy and Al-Asali 1989

The authors studied the structural behaviour of small scale singly reinforced concrete beams affected by ASR. Singly reinforced concrete beams complete with shear reinforcement were constructed of reactive aggregate and stored unloaded. Three sets of beams were constructed. The first was an unreactive control. The second was reactive with beltane opal as the reactive aggregate. The third set was made of reactive fused silica. The beams, 75 x 100 x 800 mm, contained 1.76% reinforcement and were singly reinforced at their center spans. The cement used had a 1% Na_2O equivalent alkali content giving a total concrete alkali content of 5.2 kg/m^3. One day after casting, the beams were demoulded and cured unloaded at 20 degree at 96% RH. They were cured for two years and then loaded to failure. After sufficient ASR expansions had occurred, the beams were monotonically loaded to flexural failure.

a) The control beams showed insignificant expansions during the two year period. Maximum expansions of the reactive beams at the top unrestrained fiber were 1.3% while at the bottom fiber, maximum expansions were approximately 0.12%. The strains were

retained by the beams even after being removed from the curing chamber for several weeks prior to testing. These differential expansions caused up to 6 mm of hogging in the beams and extensive cracking at the top of the beams. Strains in the reinforcing steel due to ASR were measured to be a maximum of 50% of yield strain.

b) Due to a lack of cracking along the reinforcement level, it was concluded that no bond failure had occurred even though large differential expansions had occurred.

c) The ASR affected beams do not appear to lose ductility at ultimate loads. However, due to the hogging deflections, some beams showed little sagging deflections at failure thus giving the appearance of brittle failure.

d) Beams exhibited flexural strength losses of 26 and 15%, for opal and fused silica reactive aggregates respectively, while these same beams exhibited residual steel strains of 80 and 40% respectively. The losses may have been larger if it were not due to the beneficial effects of prestressing at the steel level. This demonstrates the beneficial prestressing effect due to the differential expansions. All beams failed by flexural yielding followed by crushing of concrete. The reactive beams suffered a considerable loss in flexural stiffness.

2.2.5 Ujike, Nagataki, Sato and Ishikawa 1990

The authors investigated the influence of internal cracking of concrete on the permeability of concrete around deformed reinforcing tension bars. Concrete specimens, 150 x 150 mm, with a single reinforcing bar passing through them were cast. The cover concrete thickness varied between 2-6 mm and bar sizes varied from 16-25 mm for deformed bars and plain bars were 22 mm. The specimens were subjected to sustained tensile stresses ranging from 50-200 MPa.

a) The air permeability of the specimens with the 22 mm plain bar was no different than the permeability of plain concrete regardless of the level of applied stress. The air permeability around the deformed bars was similar to that of plain concrete until the application of stress. The difference in air permeability coefficient between the two at 200 MPa applied stress was a factor of 10. The difference in air permeability between the two types of bars is explained by the formation of small cracks by the ribs during loading.

b) The air permeability around the deformed bars increased with an increase in bar diameter. At a stress level of 200 MPa, the air permeability coefficient of the largest bar tested, 25 mm, was larger than that of the smallest bar, 16 mm, by approximately a factor of ten. The size and amount of cracks near reinforcement are affected by the size and spacing of the ribs on bars. The size of ribs on deformed bars are expressed as ratios of their diameters. Thus the larger the diameter, the larger the ribs on the bars.

2.2.6 Cope and Slade 1992

The authors conducted an investigation into the effects of ASR on the shear capacity of reinforced concrete beams without shear reinforcement. All specimens were cast using the same concrete mix with a total alkali content of 7 kg/m^3, raised to this level by adding sodium and potassium sulfates in the mixing water. Beam specimens, 125 x 250 x 2500 mm, were cast and singly reinforced with a 1.48% reinforcement ratio. Larger, 200 x 400 x 4000 mm beams were also constructed with a 1.35% reinforcement ratio. No shear reinforcement was used in any of the beams. It was determined that the restraint to expansion provided by the longitudinal reinforcement resulted in a prestress of the concrete which increased the shear capacity. The increase in shear capacity of the smaller beams was not as high as the increase in shear capacity of the larger beams. ASR cracking occurred at a level of approximately 25 mm from the surface thus indicating a larger cracked surface to volume ratio in the smaller beams thus explaining the reduction in shear capacity. All of the beams suffered shear failures that were above those predicted by code formulae. Thus the ASR affected beams exhibited an increase in shear capacity over the unaffected ones due to a prestressing phenomena caused between the longitudinal reinforcement and the expanding concrete.

2.2.7 Rigden, Majlesi and Burley 1992

An investigation was conducted into the effects of ASR on the bond stress of plain reinforcement. Concrete mixes with sodium oxide equivalents of 7.0 and 12.0 kg/m^3 were used. The two levels of alkali were used to investigate the effect of different levels of

expansion and the direct effect of alkalis on bond stress. This alkalinity was achieved by addition of potassium hydroxide to the mixing water. Longitudinal reinforcement used was 6 mm diameter plain mild steel bars. Fifteen beam specimens, 100 x 145 x 1300 containing three longitudinal bars with 50 mm overlaps at center span were cast using various concrete mixes. Concrete cubes were also tested for each batch to determine concrete compressive strength. All specimens were cured for 4 weeks at 20 degrees Celsius and then the temperature was raised to 38 degrees. The relative humidity in both cases was 100%. All beams were loaded in flexure to failure using four point loading. Non-reactive mixes produced bond stresses of approximately 3 times of those quoted in British standards and four times larger than those of the reactive beams. Reductions in bond stress of 13-21% due to concrete damage by ASR were encountered among the various beams.

2.2.8 Koyanagi, Rokugo, Uchida and Iwase 1996

An examination into the deformation behaviour of reinforced concrete beams affected by ASR was conducted. Singly reinforced concrete beams without shear reinforcement (100 x 180 x 1700 mm) and longitudinal reinforcing steel ratios of 0.92% and 1.66% were cast. The cement used had an alkali content of 0.61% Na_2O equivalent increased to 3% by addition of Na_2SO_3. The beams were wet cloth cured in a thermostatic chamber at 20 degrees Celsius for four weeks after demoulding. The reactive beams were then spray cured at a temperature of 40 degrees Celsius for a period of 4 months while the control beams were left in the laboratory atmosphere for the same period of time. Load tests were performed on the beams at an age of two years. The mechanical properties of plain concrete were measured using cylinders (100 mm diameter by 200 mm long) for compressive strength and static modulus of elasticity, prisms (100 x 100 x 400 mm) for dynamic modulus of elasticity and flexural strength, and cylinders (150 mm diameter by 150 mm long) to determine the splitting tensile strength of the concrete.

a) ASR cracking in the beams was mostly concentrated in the top part of the beams. This cracking was mostly longitudinal near the vertical center while being mostly transverse at the top edge of the beams. There was no significant difference in cracking

between the beams of varying reinforcement ratios. The beams exhibited upward bending attributed to the distribution of the reinforcement.

b) All the beams with the lower reinforcement ratio failed in flexure. However, the beams with the larger reinforcement ratio exhibited shear failure in the unreactive beams and flexural failure in the reactive specimens thus showing the effect of prestressing in ASR affected members.

c) All reactive beams have a higher initial flexural rigidity than the unreactive controls. First flexural cracking occurs at a load 60% higher for the reactive beams than for the controls. This is due to an increase in neutral axis ratio due to reductions in modulus of elasticity of concrete and induced prestress due to reinforcement. The flexural yield point of the reactive beams was approximately 10% lower than that of the unreactive specimens, however, ultimate flexural capacity of both sets of beams were very similar.

REFERENCES

Abe, M., Kikuta, S., Masuda, Y., Tomozawa, F., 1989, "Experimental Study on Mechanical Behavior of Reinforced Concrete Members Affected by Alkali-Aggregate Reaction", Proceedings of the 8th International Conference on Alkali-Aggregate Reaction, pp. 691-696, The Society for of Materials Science, Japan.

Akashi, T., Amasaki, S., Takagi, N., Tomita, M., 1986, "The Estimate for Deterioration Due to Alkali-Aggregate Reaction by Ultrasonic Methods", Proceedings of the 7th International Conference on Alkali-Aggregate Reaction, pp. 183-187, Noyes Publications, Park Ridge, USA.

Cope, R.J., Slade, L., 1992, "Effect of AAR on Shear Capacity of Beams Without Shear Reinforcement", Proceedings of the 9th International Conference on Alkali-Aggregate Reaction, pp. 184-191, Chamelon Press Ltd., London, England.

Guédon, J.S., Le Roux, A., 1993, "Influence of Microcracking on the Onset and Development of the Alkali-Silica Reaction", ACI SP 145-37, pp. 713-723.

Gunatilaka, D., Machida, A., Mutsuyoshi, H., 1990, "Influence of Existing Cracks and Strain Rate on the Behaviour of Concrete Under Cyclic Compressive Loading", Transactions of the Japan Concrete Institute, Vol. 12, pp. 121-126.

Habita, M.F., Brouxel, M., Prin, D., 1992, "Alkali-Aggregate Reaction Structural Effects: An Experimental Study", Proceedings of the 9th International Conference on Alkali-Aggregate Reaction, pp. 403-410, Chamelon Press Ltd., London, England.

Inoue, S., Fujii, M., Kobayashi, K., Nakano, K., 1989, "Structural Behavior of Reinforced Concrete Beams Affected by Alkali-Silica Reaction", Proceedings of the 8th International Conference on Alkali-Aggregate Reaction, pgs. 727-732, The Society for of Materials Science, Japan.

Jones, A.E.K., Clark, L.A., 1996, "A Review of the Institution of Structural Engineers Report, 'Structural effects of Alkali-Silica Reaction (1992)'", Proceedings of the 10th International Conference on Alkali-Aggregate Reaction, pp. 394-401, Melbourne, Australia.

Koyanagi, W., Rokugo, K., Ishida, H., 1986, "Failure Behavior of Reinforced Concrete Beams Deteriorated by Alkali-Silica Reaction", Proceedings of the 7th International Conference on Alkali-Aggregate Reaction, pp.141-145, Noyes Publications, Park Ridge, USA.

Koyanagi, W., Roguko, K., Uchida, Y., Iwase, H., 1996, "Deformation Behavior of Reinforced Concrete Beams Deteriorated by ASR", Proceedings of the 10th International Conference on Alkali-Aggregate Reaction, pp. 458-465, Melbourne, Australia.

Le Roux, A., Massieu, E., Godart, B., 1992, "Evolution Under Stress of Concrete Affected by AAR- Application to the Feasibility of Strengthening a Bridge by Prestressing", Proceedings of the 9th International Conference on Alkali-Aggregate Reaction, pp. 599-606, Chameleon Press Ltd., London, England.

Ramachandran, V.S., Beaudoin, J.J., Sarkar, S.L., Aimin, X., 1993, "Physico-Chemical and Microstructural Investigations of the Effect of NaOH on the Hydration of $3CaO.SIO_2$", Il Cemento, V. 90, pp. 73-84.

Rigden, S.R., Majlesi, Y., Burley, E., 1992, "Bond Stress Failure in Alkali-Silica Reactive Reinforced Concrete Beams", Proceedings of the 9th International Conference on Alkali-Aggregate Reaction, pp. 859-864, Chamelon Press Ltd., London, England.

Shayan, A., Ivanusec, I., 1989, "Influence of NaOH on Mechanical Properties of Cement Paste and Mortar with and without Reactive Aggregates", Proceedings of the 8th International Conference on Alkali-Aggregate Reaction, pp. 715-720, The Society for Materials Science, Japan.

Swamy, R.N., Al-Asali, M.M., 1988, "Engineering Properties of Concrete Affected by Alkali-Silica Reaction", ACI Materials Journal, September-October, pp. 367-374, American Concrete Institute.

Swamy, R.N., Al-Asali, M.M., 1989, "Effect of Alkali-Silica Reaction on the Structural Behavior of Reinforced Concrete Beams", ACI Structural Journal, V. 84, No. 4, pp. 454-459, American Concrete Institute.

Tawfiq, K., Armaghani, J., Vysyaraju, J.R., 1996, "Permeability of Concrete Subjected to Cyclic Loading", Transportation Research Record No. 1532, pp. 51-59, Materials and Construction. Advancements in Concrete Materials Technology, Transportation Research Board, National Research Council, Washington D.C.

Ujike, I., Nagataki, S., Sato, R., Ishikawa, K., 1990, "Influence of Internal Cracking Formed Around Deformed Tension Bars on Air Permeability of Concrete", Transactions of the Japan Concrete Institute, Vol. 12, pp. 207-214.

CHAPTER 3

EXPERIMENTAL PROCEDURE

3.1 THE EXPERIMENT

Most engineering structures affected by ASR are subjected to static load or a combination of static and dynamic loads. An experimental program was developed to examine the effects of ASR on simply supported, singly reinforced concrete beams subjected to three different loading regimes; unloaded, statically loaded and dynamically loaded.

Two sets of concrete specimens were tested. One set of samples was made with ASR susceptible aggregate and a similar set of control specimens was made with non-reactive aggregate.

Singly reinforced concrete beams were tested to determine the effects of beam loading regime on ASR. Eight reactive beams were tested; two were loaded at 28 days to ultimate flexure; six were monitored for expansion for 147 days, two were not loaded, two were loaded statically and two were loaded dynamically.

Seven non-reactive beams were also tested as control specimens. This allowed the determination of non-recoverable, non-ASR strains due to the various loading regimes. These also helped in determining the change in ultimate flexural strength of the ASR beams compared with non-reactive control specimens. One non-reactive beam was tested to ultimate flexural strength at 28 days, and six were tested under the same conditions as the ASR beams, two unloaded, two statically loaded and two dynamically loaded.

Single reinforcement allowed the comparison of expansions and damage rating indices at the unrestrained top fiber and the near bottom fiber (reinforcement level) of each reactive beam. The expansions of each beam were monitored, damage rating indices measured and at the end of the experiment each beam was tested to its ultimate flexural capacity.

Cylinders were tested to determine free concrete expansions as well as ultimate compressive strength and static modulus of elasticity. Resonant frequency prisms were monitored for dynamic modulus as well as modulus of rupture. The expansivity of the concrete mix was measured using the CSA concrete prism test.

All specimens, except the CSA prisms, were tested in accelerating conditions (1N NaOH at 38°C) to promote ASR expansions. Both reactive and non-reactive specimens were tested under similar conditions and the only difference between the specimen sets was the aggregates.

The results obtained from the test specimens were analyzed and comparisons were made to determine the following: whether or not ASR is detrimental to the structural and serviceability behaviour of the reinforced concrete beams; whether or not the loading regime affects the ASR; whether or not a correlation could be made between the expansion, damage rating index and structural results.

3.1.1 Beams

The simple span concrete beam specimens (90 x 120 x 900 mm) were singly reinforced complete with shear stirrups. The effective depth of the beams was 100 mm. They were cast using plywood moulds lined with Plexiglas. Demec targets, 100 mm long and made of 6 mm diameter threaded rod with center holes drilled in each end, were cast into the beams using the Plexiglas mould liners as templates. The Demec targets extended through the beams past 6 mm on each side. This allowed the measurement of horizontal and vertical expansions at various locations throughout the beams on each side. Maximum coarse aggregate size and slump were chosen to allow placement of the concrete in the confined spaces of the moulds. The following six figures display information regarding the reinforced concrete beams and Demec targets.

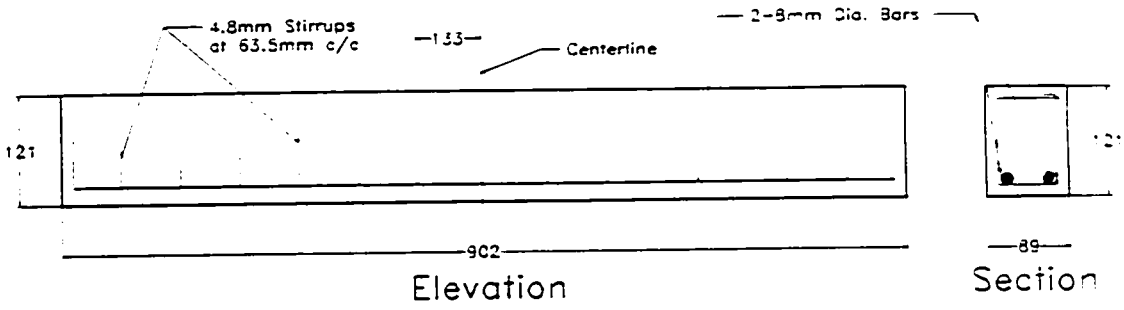

Figure 3.1: Reinforced concrete beam design

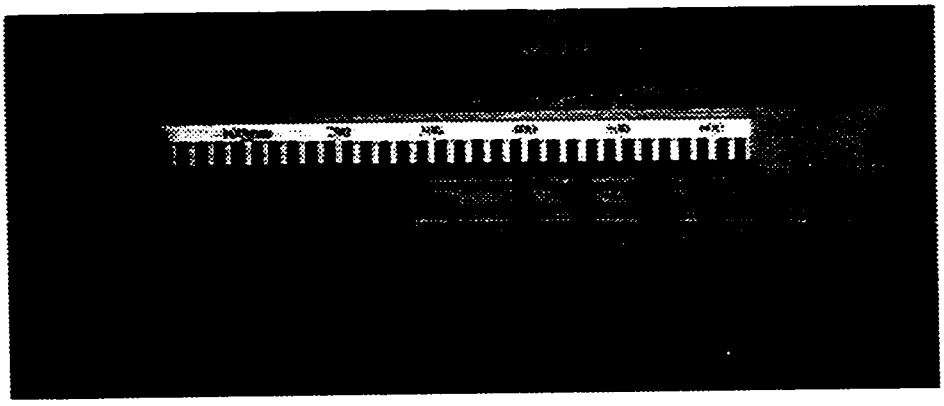

Figure 3.2: Beam reinforcing cage

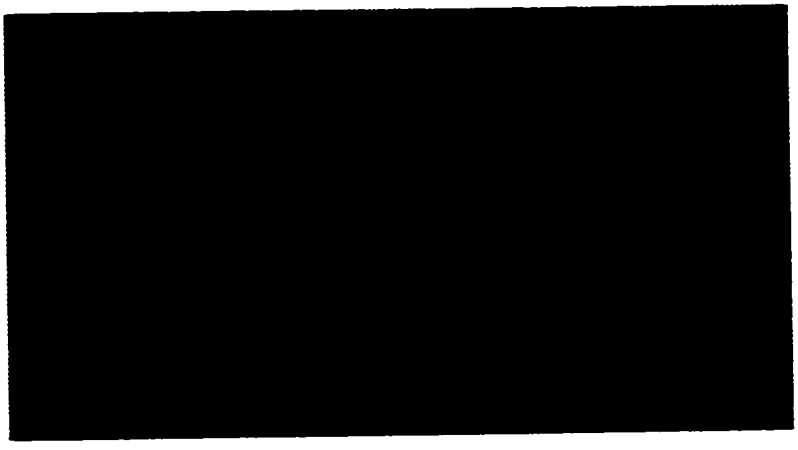

Figure 3.3: Demec targets

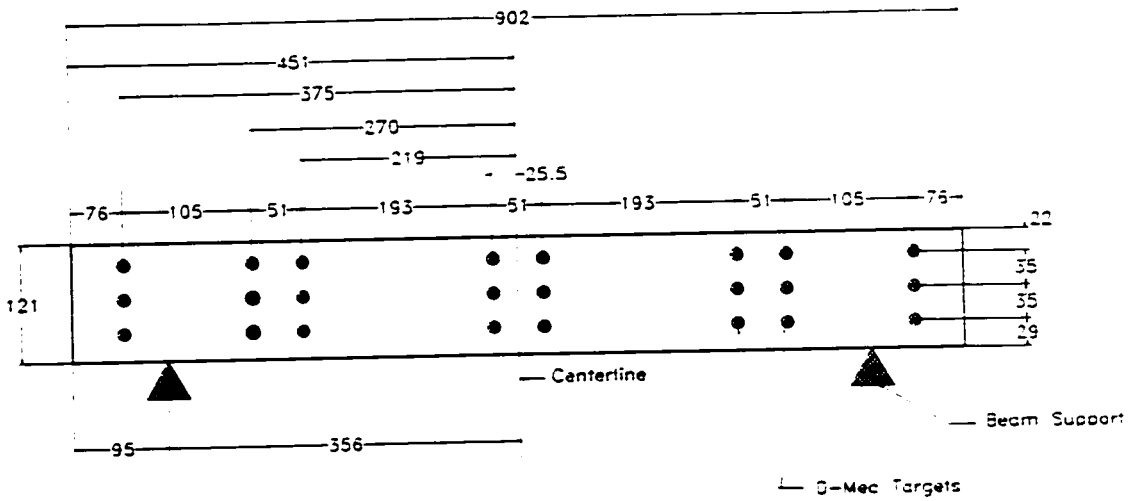

Figure 3.4: Demec Target Layout

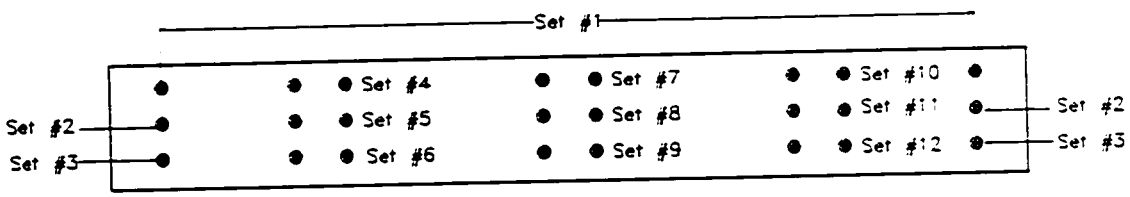

Figure 3.5: Demec target sets used for horizontal expansion measurements

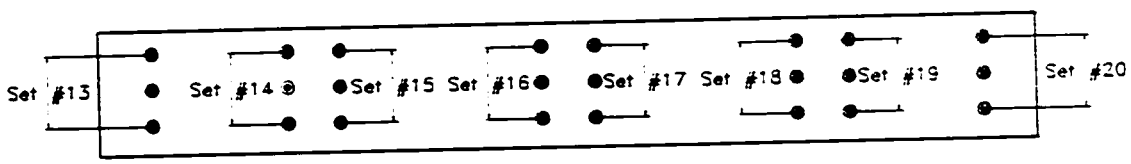

Figure 3.6: Demec target sets used for vertical expansion measurements

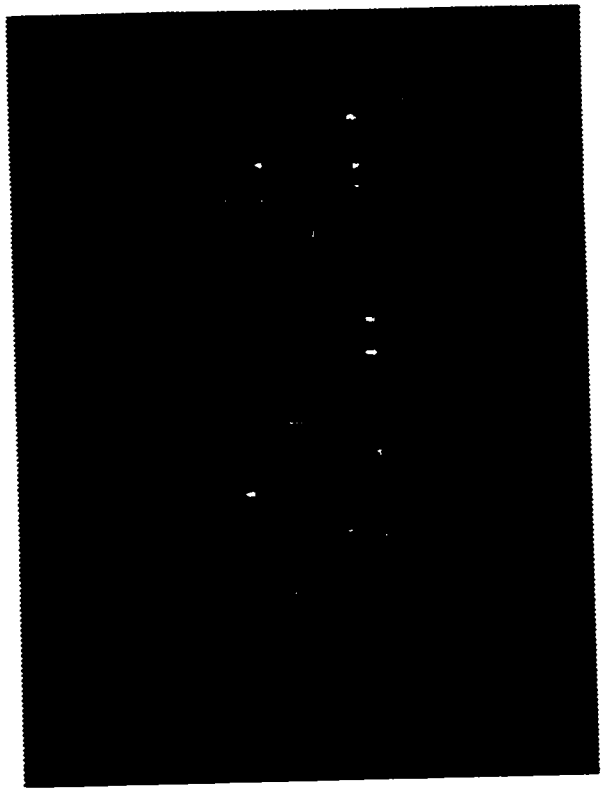

Figure 3.7: Reinforced concrete beam mould

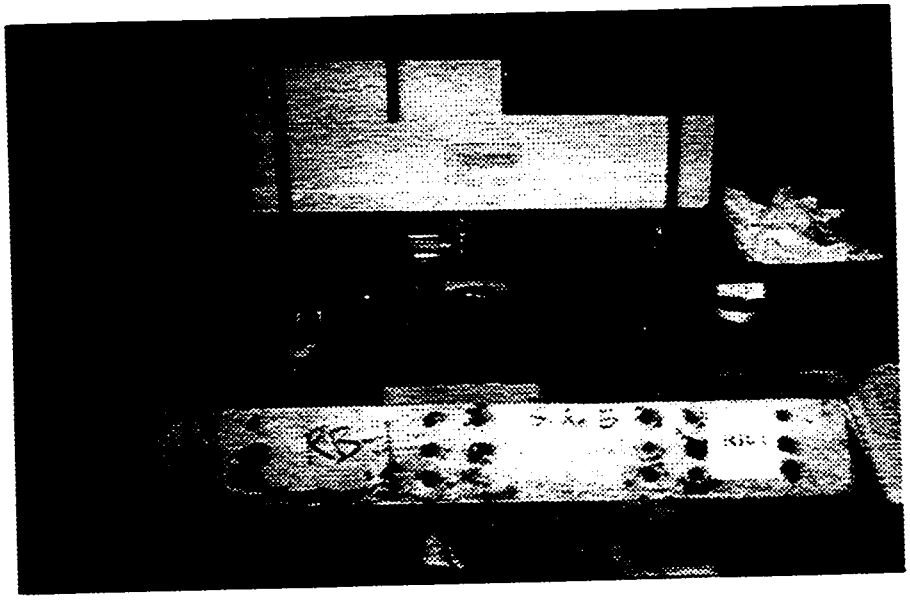

Figure 3.8: Typical beam specimen

3.1.2 Cylinders

Cylinders (100 mm diameter x 200 mm long) were used to determine the free expansion of the concrete, the compressive strength, the static modulus of elasticity and the loss of stiffness of the concrete.

Both the reactive and unreactive cylinders were tested on a similar program to allow direct comparison.

Demec targets, with a gauge length of 50 mm, were cast at the center of the cylinders. The cylinders were stored under the same condition as the beams (1N NaOH at 38°C). Cylinders were loaded at 28 days to obtain their compressive strength.

Figures 3.9 and 3.10 show a cylinder mould with Demec targets and a cast cylinder with the Demec targets.

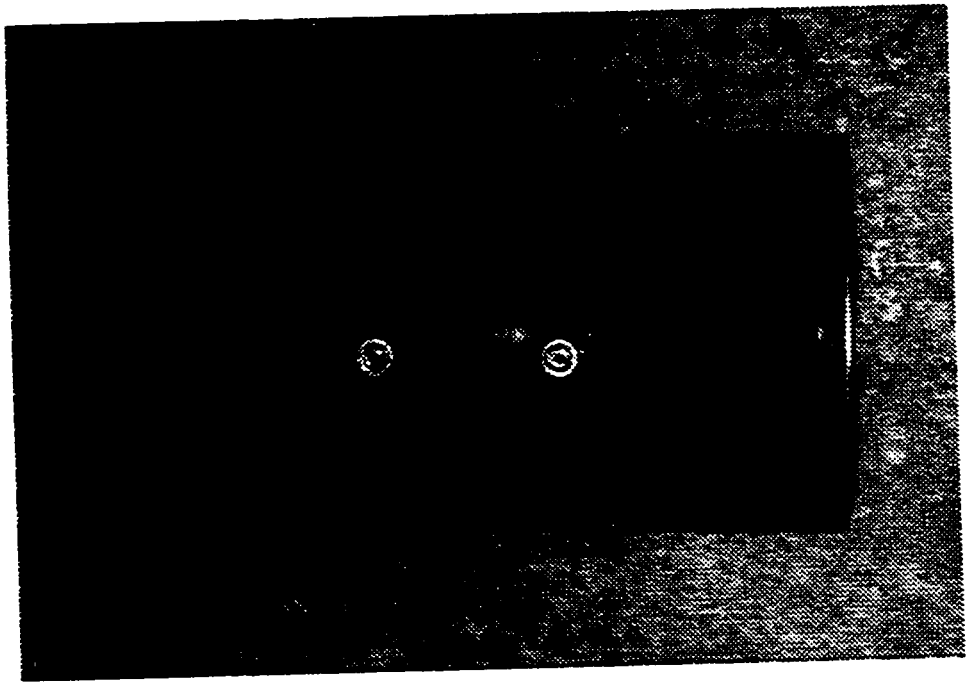

Figure 3.9: Cylinder mould with Demec targets

Figure 3.10: Cylinder with Demec targets

3.1.3 Resonant Frequency Prisms

Prisms, 100 x 75 x 400 mm, were used to monitor the changes in the dynamic modulus of elasticity of the reactive and non-reactive plain concrete. Flexural concrete strengths at 28 and 147 days were also determined using these prisms. These specimens were cured under the same conditions as the beams. Figure 3.11 shows a typical resonant frequency prism.

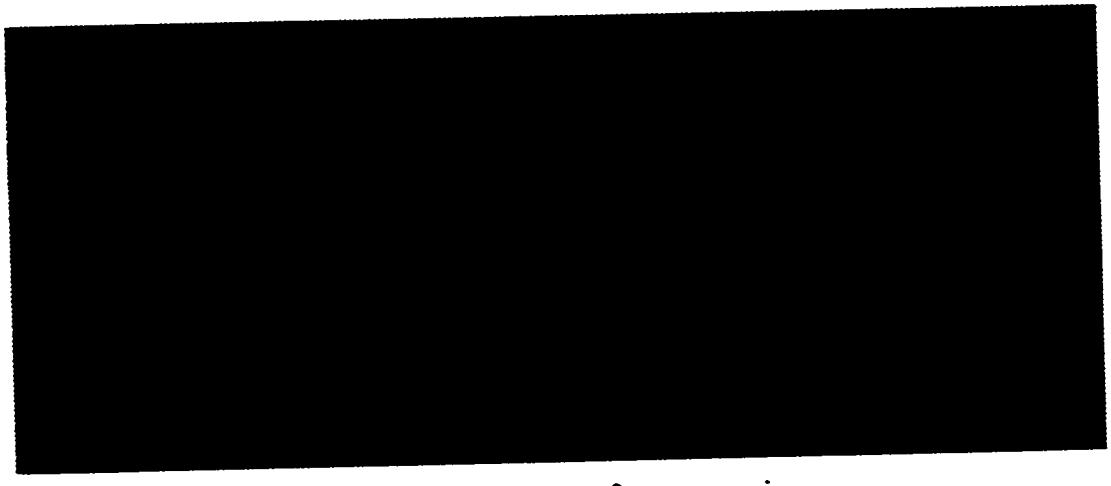

Figure 3.11: Resonant frequency prism

3.1.4 CSA Concrete Prisms

The CSA concrete prism test was used to determine the expansivity of the test concrete mixes. The test was performed per CSA A23.2-14A-1994 with the exception of the following. Figure 3.12 shows a typical CSA concrete prism used for the CSA concrete prism test.

a) The expansion measurements were performed at the same intervals as the measurements taken from the beams, cylinders and resonant frequency prisms. The measurement intervals of the CSA standard were disregarded.

b) Rather than using the code specified concrete mix proportions, the concrete prisms were made with the same mixes as all the other specimens. The prism test is usually used for the determination of potential reactivity of either coarse or fine aggregates. In this experiment, the prism test is used to determine the expansivity of the concrete mixes.

Figure 3.12: CSA expansion test prisms

3.1.5 Coarse Aggregate

The ASR susceptible coarse aggregate was obtained from the MTO in Toronto. It is a very reactive, fine grained and dark grey siliceous limestone originating from Spratt Aggregates' quarry in Stittsville, Ontario. The unreactive coarse aggregate is a fine grained and light grey limestone of high purity originating from the province of

Newfoundland, Canada. The maximum nominal size of aggregate used was 10 mm. Data on the reactive and non-reactive aggregates is given in Appendix A.1 and A.2. Figure 3.13 shows the reactive and non-reactive limestones used as coarse aggregate in the reactive and control test specimens.

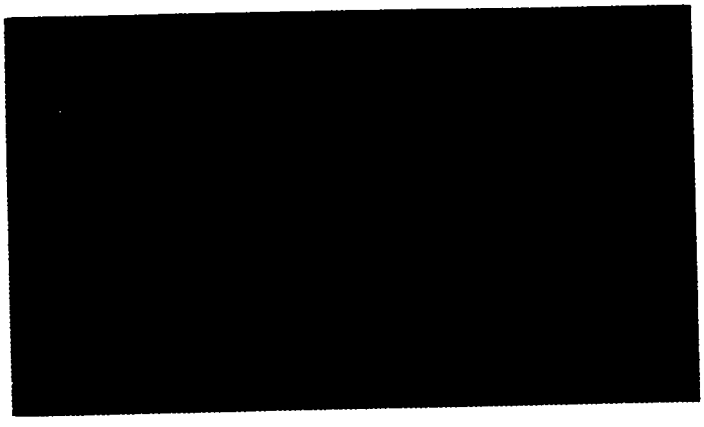

Figure 3.13: Reactive and non-reactive limestone aggregates

3.1.6 Fine Aggregate

The fine reactive aggregate was crusher fines taken from Spratt Aggregates' quarry, mixed with unreactive quartz sand to obtain the required grading for concrete. The non-reactive fine aggregate was crushed Newfoundland limestone mixed with unreactive quartz. Additional data on the fine aggregates are found in Appendix A.1 and A.2. Figure 3.14 shows the non-reactive quartz sand.

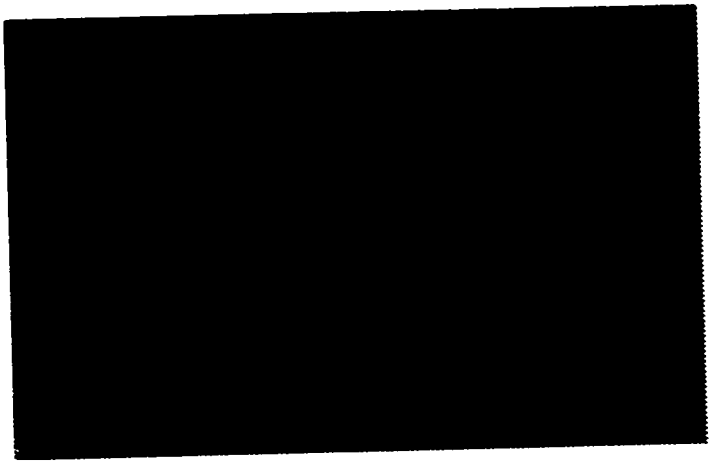

Figure 3.14: Quartz sand

3.1.7 Mix Design

The concrete mixes (reactive and non-reactive) were designed using the CPCA "Design and Control of Concrete Mixes" handbook 1991. The cement used was obtained from St-Lawrence Cement with an alkali content of 0.9% Na_2O equivalent. Sodium hydroxide was added to increase the alkalinity of the cement from 0.9% Na_2O equivalent to 1.25% Na_2O equivalent. This additional alkali increased the total alkali content of the test mixes to 5.3 kg/m^3 (well above the generally accepted threshold of 3 kg/m^3 required to constitute an aggressive environment to potentially reactive aggregate).

Both reactive and non-reactive concrete mixes were identical except for the types (reactive and non-reactive) of coarse and fine aggregates (the gradation of the reactive and non-reactive aggregates varied slightly and are given in Appendix A1).

Because of the concrete mixer size and the number of beam moulds available, the concrete was produced in four batches (two reactive and two non-reactive). The following tables show the mix design used and the slump of each batch of concrete. Table 3.1 shows the concrete mix design and Table 3.2 shows the slumps measured for the four concrete batches mixed.

Table 3.1: Concrete Mix Design (reactive and non-reactive mixes)

Water-Cement Ratio	0.61
Slump	200 mm
Coarse Aggregate Dry Rodded Density	1700 kg/m^3
Coarse Aggregate (nominal size 10 mm)	748 kg/m^3
Fine Aggregate	1000 kg/m^3
Cement (0.9% Na_2O Equivalent)	423 kg/m^3
Water	258.33 kg/m^3
NaOH Added(to 1.25% Na_2O Equivalent)	1.48 kg/m^3

Table 3.2: Measured concrete slump for each batch

Batch No.	Slump (mm)
1. Reactive	200
2. Reactive	210
3. Non-Reactive	230
4. Non-Reactive	235

3.1.8 Preparation of Specimens

All specimens were cast using the same mix design. They were all cured at 23 degrees centigrade and 100% relative humidity for 28 days in a curing room after demoulding and prior to testing. During this time, they were wrapped in plastic to prevent the leaching of alkalis. A high value of slump for the concrete was chosen to increase workability without the use of chemical additives. A vibrating table was used to ensure proper compaction of the concrete and avoid honeycombing. The specimens were left to set at room temperature overnight prior to demoulding and placing in the curing chamber. After 28 days of curing, some specimens were tested to ultimate strength to determine 28 day resistance. The remainder of the specimens was tested for 147 days in accelerating conditions promoting the development of ASR. Tables 3.3 and 3.4 outline the reactive and non-reactive specimens used during the experiment and the tests performed on each of the specimens. Figure 3.15 shows the specimen moulds before casting and figures 3.16 and 3.17 show the casting of beam and cylinder specimens.

Table 3.3: Reactive test specimens

Specimen Designation	Number of Specimens	Type of specimen	Time of Testing	Loading Condition	Measurements
RB-2, RB-5	2	R/C Beam	28 days	—	-Flexural Strength
RB-1, RB-6	2	R/C Beam	147 days	Unloaded	-Expansion -Flexural Strength -Damage Rating Index
RB-7, RB-8	2	R/C Beam	147 days	Static	-Expansion -Flexural Strength -Damage Rating Index
RB-3, RB-4	2	R/C Beam	147 days	Dynamic	-Expansion -Flexural Strength -Damage rating Index
RC-1 to 6	6	Concrete Cylinder	28 days	—	-Compressive Strength -Stiffness
RC-7 to 10	4	Concrete Cylinder	147 days	Unloaded	-Expansion -Compressive Strength -Stiffness
RFP-1 to 4	4	Resonant Frequency Prism	28 days	—	-Flexural Strength
RFP-6 to 8	3	Resonant Frequency Prism	147 days	Unloaded	-Resonant Frequency -Flexural Strength
RFP-5	1	Resonant Frequency Prism	147 days	Unloaded	-Resonant Frequency -Damage Rating Index
RCSA-1 to 4	4	CSA Concrete Prism	147 days	Unloaded	-Expansion

Note: All of the specimens in Table 3.3 were stored in 1N NaOH at 38°C with the exception of the CSA concrete prisms which were stored at 98% RH and 38°C and the 28 day specimens which were stored in a moist curing chamber for 28 days prior to loading to failure.

Table 3.4: Non-reactive control specimens

Specimen Designation	Number of Specimens	Type of specimen	Time of Testing	Loading Condition	Measurements
NB-2	2	R/C Beam	28 days	—	-Flexural Strength
NB-1,7	2	R/C Beam	147 days	Unloaded	-Expansion -Flexural Strength
NB-4, 5	2	R/C Beam	147 days	Static	-Expansion -Flexural Strength
NB-3,6	2	R/C Beam	147 days	Dynamic	-Expansion -Flexural Strength
NC-1,3,4 NC-11,13,15	6	Concrete Cylinder	28 days	—	-Compressive Strength -Stiffness
NC-2,5 NC-12,14	4	Concrete Cylinder Stored in NaOH	147 days	Unloaded	-Expansion -Compressive Strength -Stiffness
NC-6,8,9,10	4	Concrete Cylinder Stored in $Ca(OH)_2$	147 days	Unloaded	-Compressive Strength -Stiffness
NFP-1,2,7,8	4	Resonant Frequency Prism	28 days	—	-Flexural Strength
NFP-3 to 8	4	Resonant Frequency Prism	147 days	Unloaded	-Resonant Frequency -Flexural Strength
NCSA-1 to 4	4	CSA Expansion Test Prism	147 days	Unloaded	-Expansion

Note: All of the specimens in Table 3.4 were stored in 1N NaOH at 38°C with the exception of the CSA concrete prisms which were stored at 98% RH and 38°C and the 28 day specimens which were stored in a moist curing chamber for 28 days prior to loading to failure.

Figure 3.15: Test specimen moulds prior to casting

Figure 3.16: Casting of a beam specimen

Figure 3.17: Casting of cylinder specimens

3.2 TESTING PROGRAM

3.2.1 Specimen Testing Apparatus

Six concrete beam specimens were tested in accelerating conditions for 147 days, two unloaded, two statically loaded and two dynamically loaded to their service loads, (calculation of the service load is given in Appendix A5). The testing apparatus is shown in figures 3.18. The beam specimens were stored in stainless steel baths through which 1N NaOH solution maintained at 38°C was circulated from a reservoir. Cylinder and resonant frequency prisms were stored in the NaOH solution reservoir. The dynamically loaded specimens were loaded using air driven pistons at a frequency of 0.5 cycles per second. The frequency of the dynamic loading was controlled by a signal generator. The statically loaded members were initially loaded using a hydraulic jack. The static load was maintained using a screw jack system. The temperature of the solution was kept constant by an immersed electrical heater in the solution reservoir. Specimen expansions were measured periodically using Demec and Huggenburger gauges (Figures 3.19 and 3.20).

After taking the zero readings; the reactive specimens were removed from the testing apparatus for experimental measurements at 27, 41, 59, 104 and 147 days; the non-

reactive specimens were removed from the testing apparatus for experimental measurement at 66 and 108 days. The loading of the non-reactive controls was discontinued after 161 days because of permanent damage to the dynamically loaded beams caused by abrasion at the loading points.

Original zero measurements of the reactive beams were taken after 28 days of curing in the moist curing chamber, prior to any loading and cracking due to loading of the specimens. The first expansion measurements of the beams were taken two weeks after the start of testing. The first measurements included permanent strains from the cracking of the loaded beams. Therefore, the first expansion readings were taken as the zero readings for the reactive beams to eliminate any strains from the cracking of the beams as ASR expansion strains were of interest.

The testing of the non-reactive specimens began after 28 days in a curing chamber but the expansion measurements did not begin until two months after the beginning of the testing. For this reason, expansion data was measured for 108 days and the beams were tested to failure at 161 days.

Figure 3.18 shows the beam, cylinder and resonant frequency prism testing and storage apparatus.

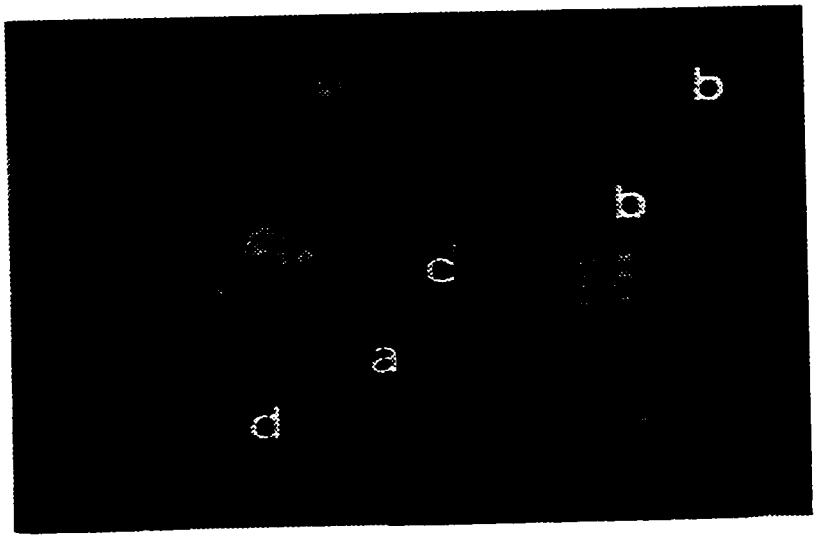

a) Stainless Steel Bath
b) Signal generator
c) Air Piston
d) NaOH Reservoir

Figure 3.18: Specimen testing apparatus

3.2.2 Beams

For periodic measurements, specimens were removed from the testing apparatus, wrapped in plastic to prevent moisture loss and placed in a room at 23°C and 50% relative humidity for 16 ± 4 hours prior to measuring. This is the procedure specified in the CSA concrete prism expansion test. This procedure was adopted to prevent any thermal and drying shrinkage effects from interfering with the expansion measurements. After all readings were taken the specimens were returned to the testing apparatus. Three readings were taken for each expansion measurement and averaged to ensure accuracy.

After the expansion phase of the experimental program had been completed, the exterior faces of the reactive beams were polished to allow measurement of concrete damage rating indices.

At the end of the experiment, the beams were loaded to failure using a hand pumped hydraulic jack loading apparatus and a Tinius Olsen loading apparatus. Beam mid-span deflections were measured using a dial gauge.

Figures 3.19 and 3.20 show the gauges used for the expansion measurements. Figure 3.21 shows the testing apparatus used for the loading to failure of the reactive and non-reactive beams.

Figure 3.19: Demec gauges used for expansion measurements

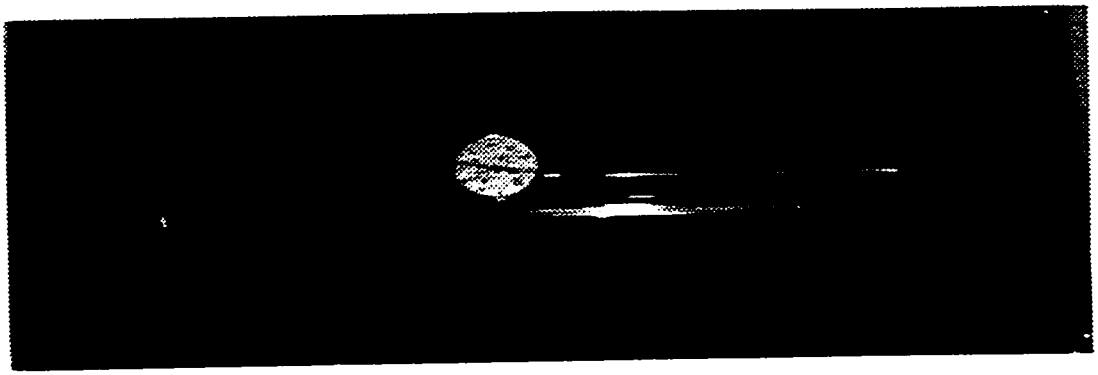

Figure 3.20: Huggenberger gauge for beam horizontal overall expansion measurements

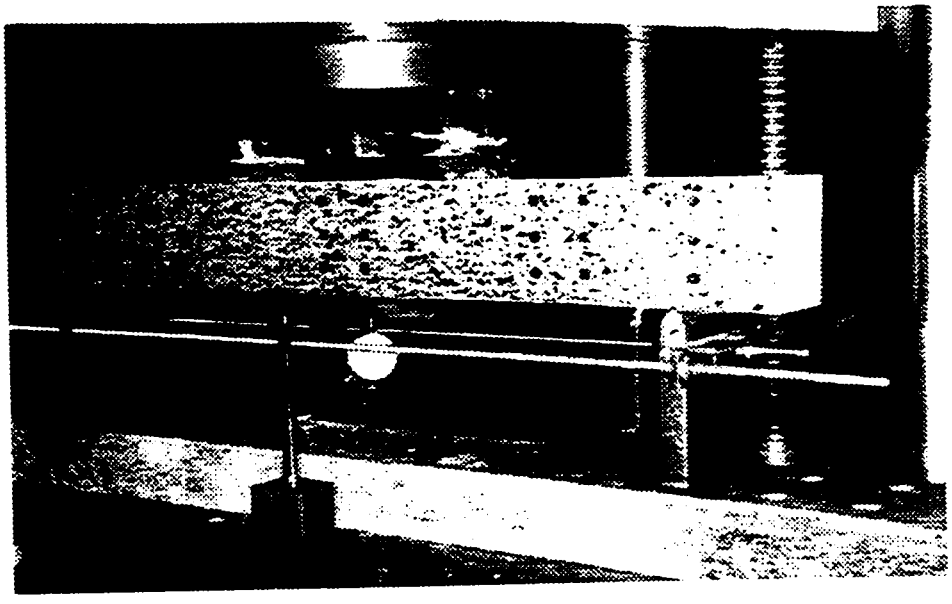

Figure 3.21: Beam Ultimate Flexural Loading Apparatus

3.2.3 Cylinders

Six reactive cylinders and six non-reactive cylinders were failed at 28 days and the rest were monitored for free expansion during the duration of the experiment (147 days). This information was used to compare the free expansion of the cylinders with the top fiber expansions of the reinforced concrete beams. At the end of the experiment these cylinders were failed in compression and their stress-strain curves compared with those

tested at 28 days. Cylinders were loaded to failure using a Forney testing machine. A modulus of elasticity frame was used to collect load-deformation data. Figure 3.22 shows a typical concrete cylinder with a modulus of elasticity frame loaded into the testing machine.

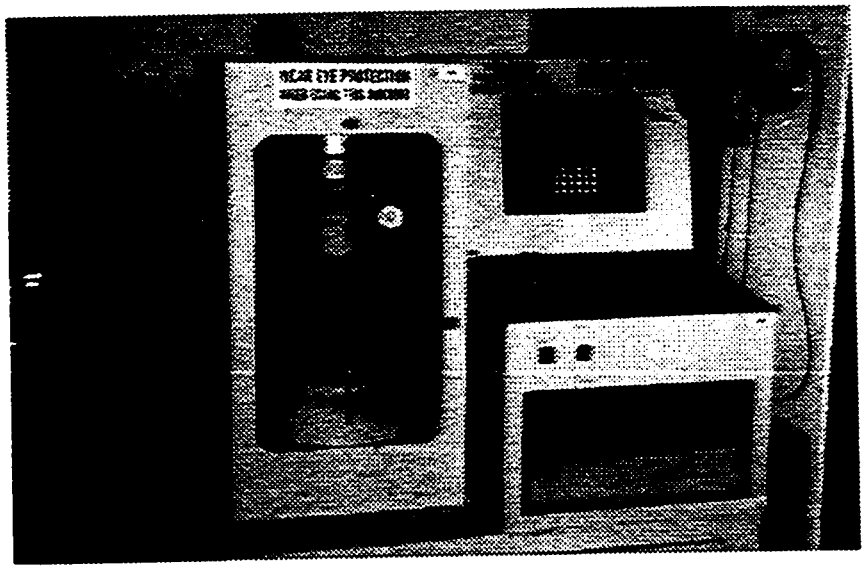

Figure 3.22: Forney testing machine, concrete cylinder and modulus of elasticity frame

3.2.4 Resonant frequency Prisms

Two resonant frequency prisms were failed in flexure at 28 days in a three point bending test and the remaining four were monitored for changes in resonant frequency over the duration of the experiment and then tested in flexure. The dynamic modulus of elasticity was determined using the resonant frequency measurements of these concrete prisms. These tests were performed for both reactive and non-reactive specimens. Figures 3.23 and 3.24 show the resonant frequency measuring apparatus and the apparatus used for the flexural loading to failure of the prisms.

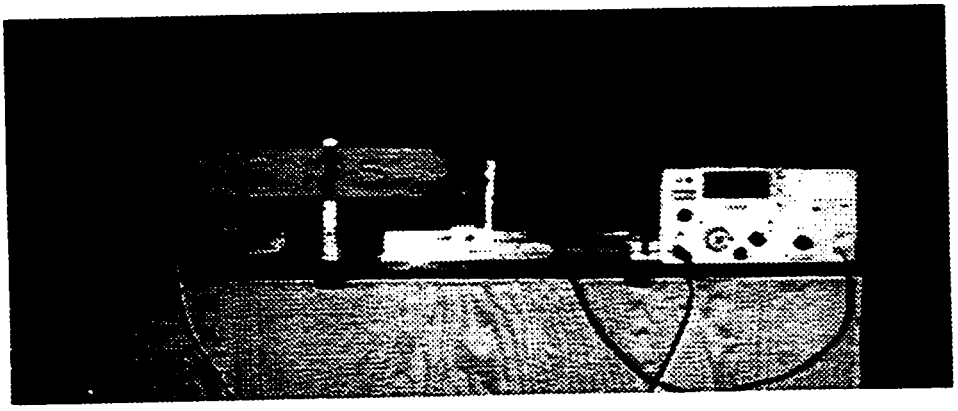

Figure 3.23: Resonant frequency testing apparatus

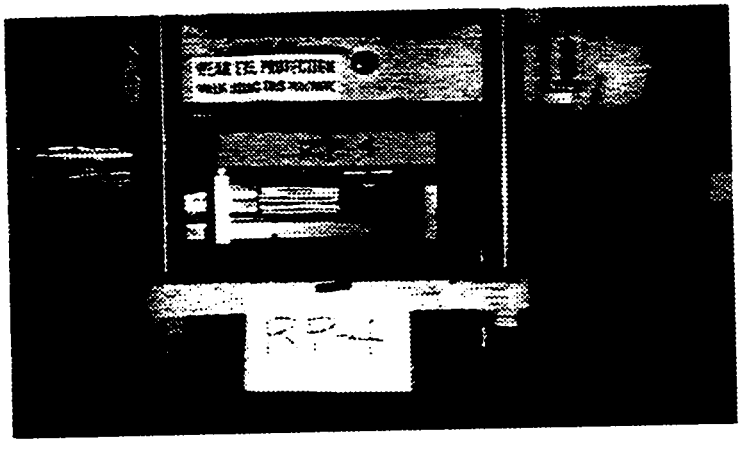

Figure 3.24: Flexural loading of resonant frequency prisms

3.2.5 CSA Concrete Prism Test

These tests were performed per CSA A23.2-14A 1994 with the following modifications.

a) The CSA concrete prism test is usually used to identify the potential for ASR reactivity of either a coarse or fine aggregate, but in this case, the actual mix concrete was used. The mix proportions suggested in the CSA standard were not followed.

b) Prism measurements were taken at the same times as the readings for all the other specimens. The measurement intervals suggested in the standard were not followed.

CSA concrete prism expansions were measured using a comparator as shown in Figure 3.25. This data was collected to compare with unrestrained, accelerated expansions of concrete cylinders.

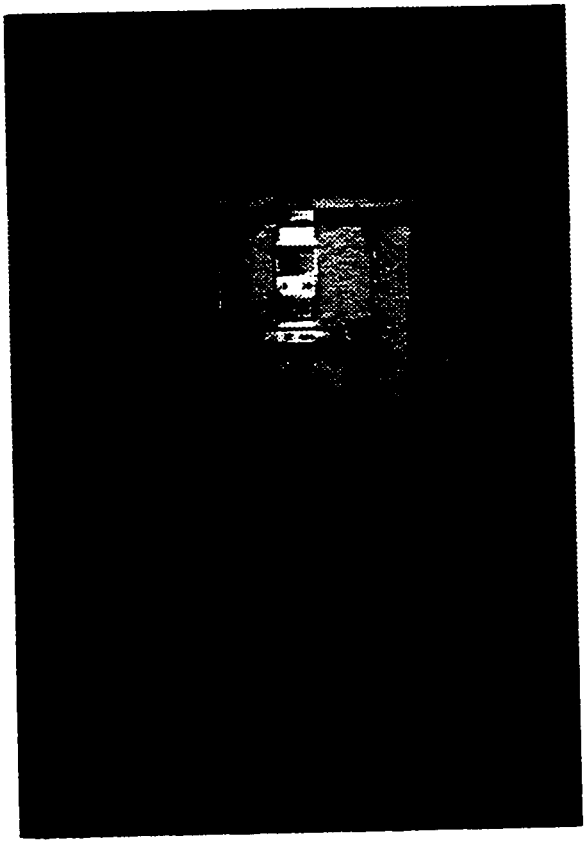

Figure 3.25: CSA Concrete Prism and Comparator

3.3 DAMAGE RATING INDEX

The damage rating index method of quantifying the damage in concrete utilizes polished concrete sections and stereo-binocular microscopy to identify signs of damage due to a given durability problem. Each sign associated with a durability problem is attributed a weighting factor according to its likelihood of having caused damage in a

concrete sample. Table 3.5 lists the weighting factors used in determining the damage rating indices for concrete with ASR.

Polished concrete sections are examined with a stereo-binocular microscope at a magnification factor of 10X and the presence of features associated with ASR are counted for areas of four square centimeters (2 cm x 2 cm). Each occurrence of each sign is summed and multiplied by its respective weighting factor. The sum of all the signs (sum of occurrences x weighting factor) is the damage rating index for a specific two square centimeter area. An average of the damage rating indices for several two square centimeters areas are taken to be the damage rating index of the concrete sample in question.

Table 3.5 contains some weighting factors that are less than one. Although typical signs of ASR damage may be present in a concrete sample, ASR may not have necessarily caused damage to the concrete. For example, cracks in aggregate may originate from crushing and aggregate particles may have reaction rims which were caused by weathering of an aggregate (in the case of natural gravels). Even if gel is present in voids, sufficient amounts of expansive pressure can not occur if the gel is not present in sufficient amounts. All other signs with weighting factors greater than 1.0 indicate not only the presence of ASR but also indicate that ASR is likely the source of the observed damage to the concrete.

Table 3.5: Damage Rating Index Weighting Factors

Feature associated with ASR	**Weighting Factor**
Coarse Aggregate with Cracks	0.25
Coarse aggregate with cracks and gel	2.0
Coarse aggregate debonded from paste	3.0
Reaction rims around aggregate	0.5
Cement paste with cracks	2.0
Cement paste with cracks and gel	4.0
Air voids lined with gel	0.5

Each side of the reactive concrete beams were polished and the DRI were determined using a stereo-binocular microscope. The DRI were determined in nine different zones on each of the six reactive beams corresponding to nine different areas of expansion measurement (80cm^2 per zone). The DRI were determined for each of the nine zones on each side of the six beams. The average of the readings taken for similar zones on each side of the beams was taken as being the DRI for each individual zone. Figures 3.26 and 3.27 show the zones for DRI measurements and the locations of Demec target sets. Figures 3.28 and 3.29 show a typical polished beam and a polished beam as viewed through a stereo binocular microscope.

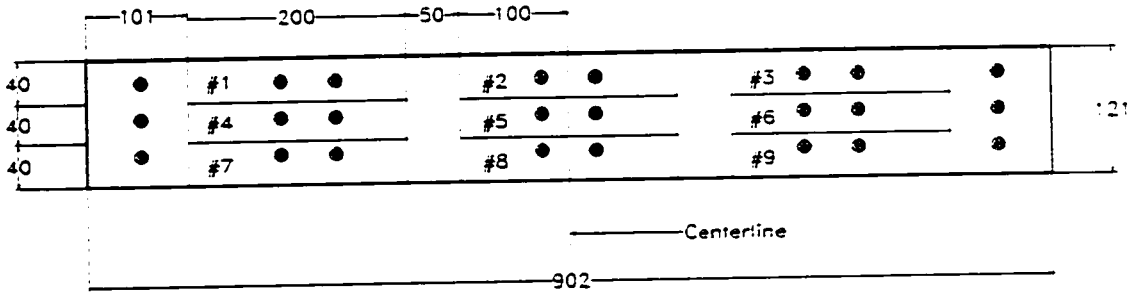

Figure 3.26: Zones of DRI measurement

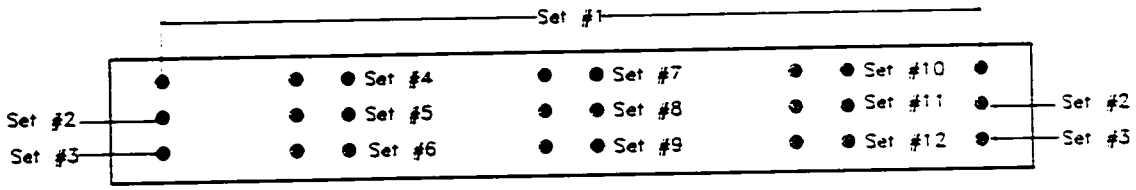

Figure 3.27: Demec sets for horizontal expansion measurement

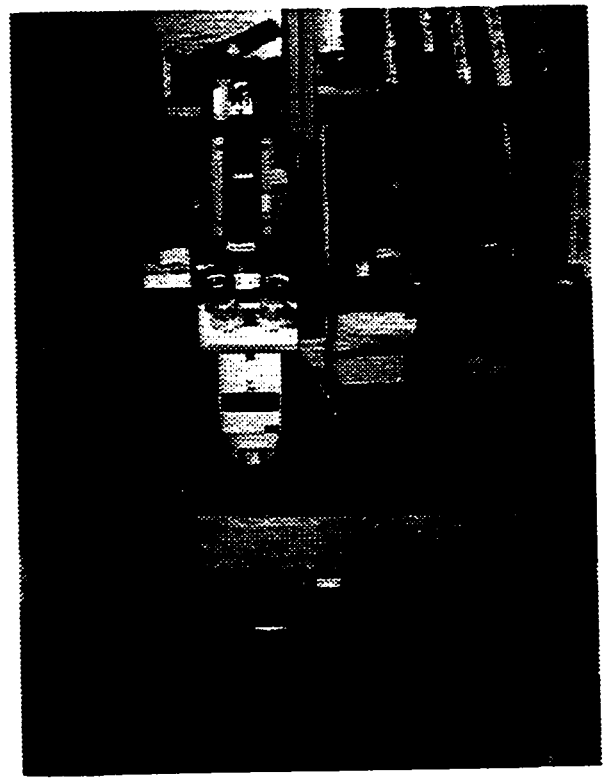

Figure 3.28: Polished prism specimen and stereo binocular microscope

Figure 3.29: Polished concrete section as viewed through a stereo binocular microscope (each division on the scale is equal to 0.5mm)

REFERENCES

Canadian Standards Association, CSA A23.2-14A-1994, "Potential Expansivety of Aggregates (Procedure for Length Change Due to Alkali-Aggregate Reaction in Concrete Prisms), Concrete Materials and Methods of Concrete Construction, Methods of Testing for Concrete, pp. 205-213, CSA, Rexdale, Ontario.

Canadian Standards Association, CSA A23.2-25A-1994, "Test Method for Detection of Alkali-Silica Reactive Aggregate Expansion of Mortar Bars", Concrete Materials and Methods of Concrete Construction, Methods of Testing for Concrete, pp. 236-242, CSA, Rexdale, Ontario.

Canadian Portland Cement Association, 1991, "Design and Control of Concrete Mixtures, CPCA, Ottawa, Ontario, pp. 68-96.

Grattan-Bellew, P.E., 1995 "Laboratory Evaluation of Alkali-Silica Reaction in Concrete from Saunders Generating Station", ACI Materials Journal, V. 92, No. 2, American Concrete Institute.

CHAPTER 4

EXPERIMENTAL RESULTS

4.1 DESCRIPTION OF RESULTS

4.1.1 Beam Expansion Measurement Locations

As discussed in Chapter 3, expansion measurements were taken at the twenty Demec locations illustrated in Figures 4.1 to 4.3. A loading diagram of the beams as well as the bending moment and shear diagrams are shown in figure 4.4 to illustrate the reason for choosing horizontal and vertical expansions at the beam mid-spans and, overall and end locations for comparison. These locations provided the largest stress differences for comparison and allowed the determination of whether or not flexural loading and loading regime affected ASR expansions.

Reactive and non-reactive cylinder expansions were plotted together with those of the beams to compare concrete free expansions with those at the various Demec locations of the reinforced concrete beams.

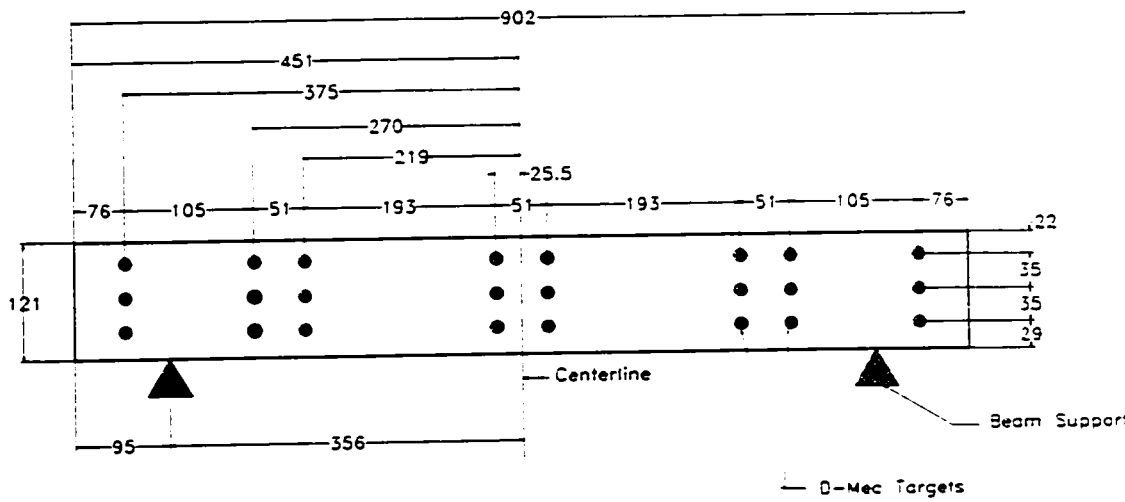

Figure 4.1: Location of Demec points along the beam specimens

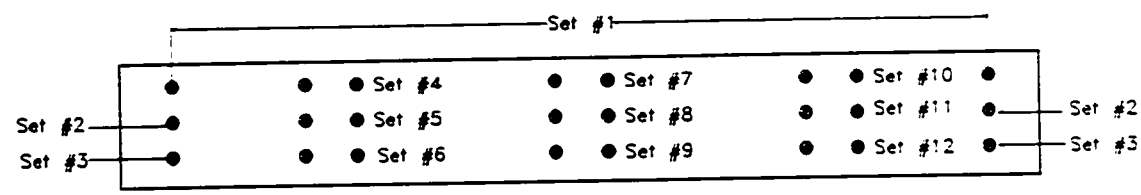

Figure 4.2: Location of horizontal beam expansion measurements

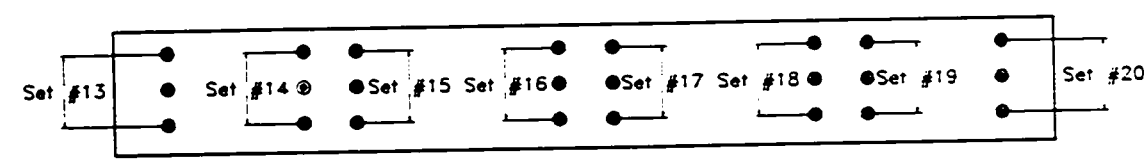

Figure 4.3: Location of vertical beam expansion measurements

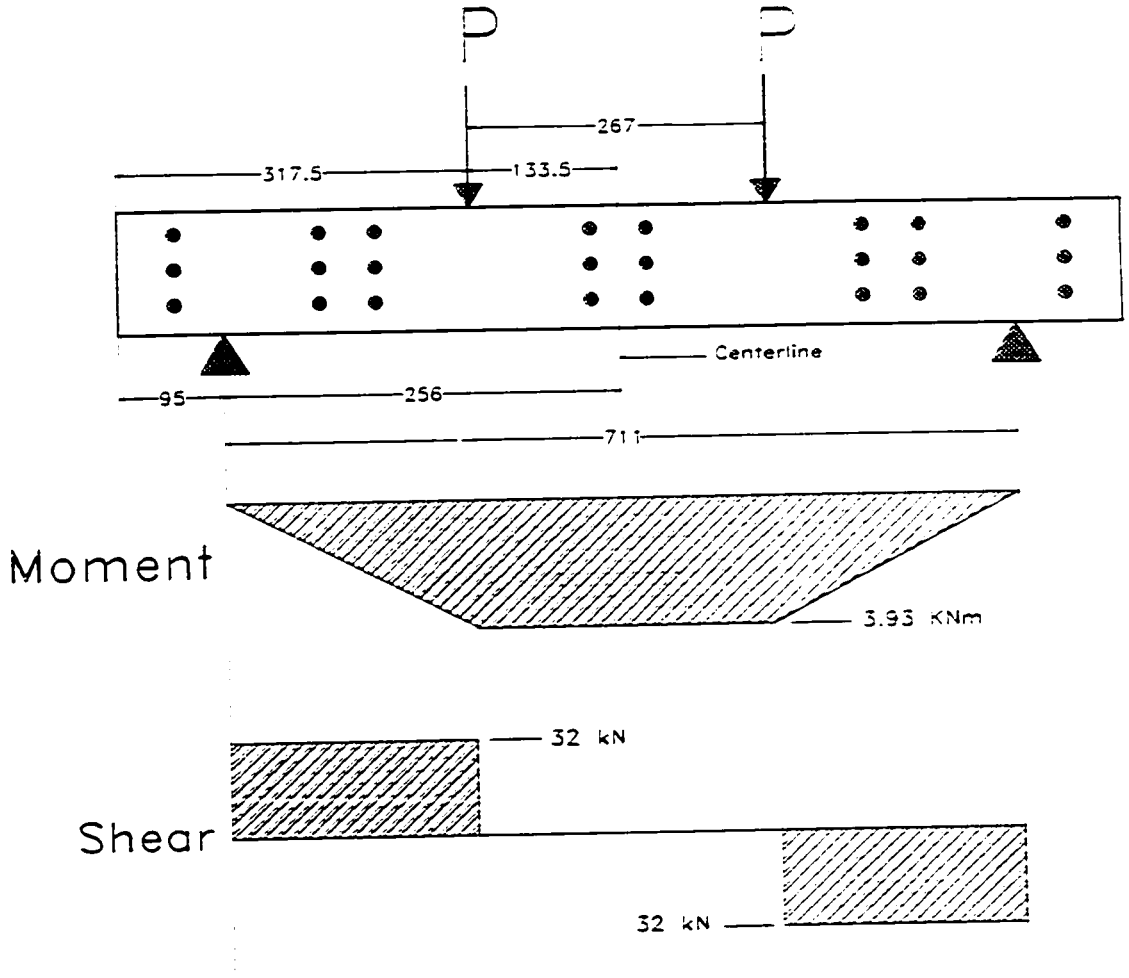

Figure 4.4: Beam loading arrangement with bending moment and shear force diagrams

4.1.2 Results

Most of the experimental results are presented in a graphical form. Because of the large number of expansion and damage rating measurements taken during the experiment, only certain of these results are presented in this chapter for discussion in Chapter 5. The results chosen for discussion are the mid span (sets 7,8,9) and overall (sets 1,2,3) Demec locations in the horizontal direction. In the vertical direction, the mid span (sets 16,17) as well as the ends (sets 13,20) of the beams are of interest. The entirety of the expansion and damage rating results are presented in appendix B.

Expansion results are presented first followed by damage rating, structural and material strength test results.

The reactive beam expansions were monitored for 147 days. Because of this, 147 days is referred to throughout this thesis as the end of the experiment for the reactive specimens. However, the beams were tested to ultimate flexural strength well after the expansion measurements were stopped (±135 days). This occurred because of the time required to have the exterior of the beams polished and time required to perform the DRI measurements and other delays associated with testing equipment. The non-reactive beams were loaded to flexural failure shortly after the end of the testing in sodium hydroxide (161 days of testing).

4.2 SPECIMEN EXPANSIONS

As previously mentioned, only specific expansion and DRI results are presented in this chapter. The loading condition or Demec location is usually identified on the expansion graphs beside the respective curves. However, some graphs have curves which are very close together making it impossible to add text beside them for identification. In these cases, legends are used to identify each curve.

The first three sections (4.2.1, 4.2.2 and 4.2.3) compare expansion results within individual types of beams (unloaded, statically loaded or dynamically loaded). Horizontal expansions are compared vertically and horizontally along the various beams. (i.e., Demec sets #1, 2, 3 or Demec sets #1 and 7).

Vertical expansions are also compared between mid-span locations (Demec sets #16, 17 at the constant bending moment region of the beam) and the ends of the beams (Demec sets #13 and 20, region of no stresses). The fourth section dealing with expansion presents the results compared between the three differently loaded types of beams. Thus the expansions for the Demec locations of interest are compared for the unloaded, statically loaded and dynamically loaded beams (sets #1, 2, 3, 7, 8, 9, 13, 16, 17 and 20 are compared).

With the large amount of data presented and the fact that expansions can be compared in the horizontal and vertical planes, the following chapter may be confusing. The following should help clarify this matter.

The term middle refers to the locations at the vertical center of the beams. The term mid-span refers to the locations at the horizontal center of the beams. Top and bottom expansions were measured as close to the top extreme fiber and steel level as possible. Left and right sides refer to the Demec locations located to each side of the mid span of the beams.

For example, Demec set 2 is at the middle of the beam while sets 9 and 16 are at the mid-span. Set 8 is both at the middle and mid-span of the beams. Sets 4 and 12 are at the left and right sides respectively. The term horizontal refers to expansions measured along the length of the beams while vertical expansions were measured along the height of the beams.

The term unloaded refers to the beams which were left to react under no load while static and dynamic refer to the statically loaded and dynamically loaded beams respectively.

4.2.1 Unloaded Beam Expansions

The expansion results presented in the following sections are for unloaded beams only. Reactive cylinder expansions were plotted with those of the beams to compare concrete free expansions with those at the various Demec locations of the reinforced concrete beams.

The results are compared as per the discussion in Section 4.2. Comparisons of the variously loaded beam expansions are presented in Section 4.2.4.

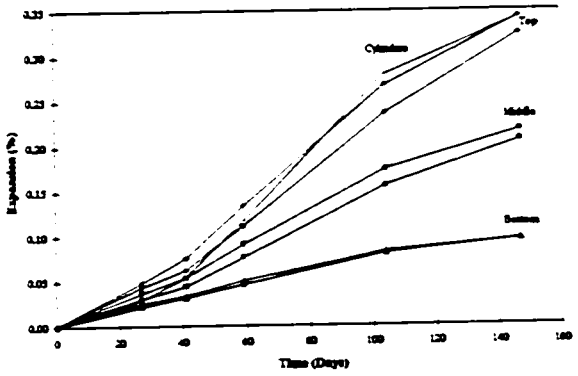

Figure 4.5: Unloaded beam overall horizontal expansions (sets 1,2,3)

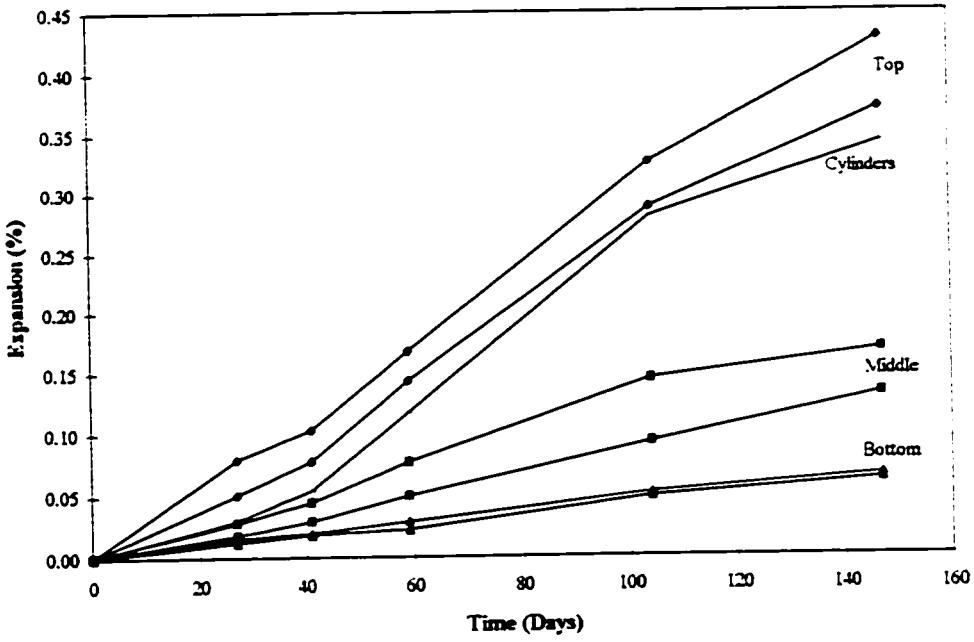

Figure 4.6: Unloaded beams mid span horizontal expansions (sets 7,8,9)

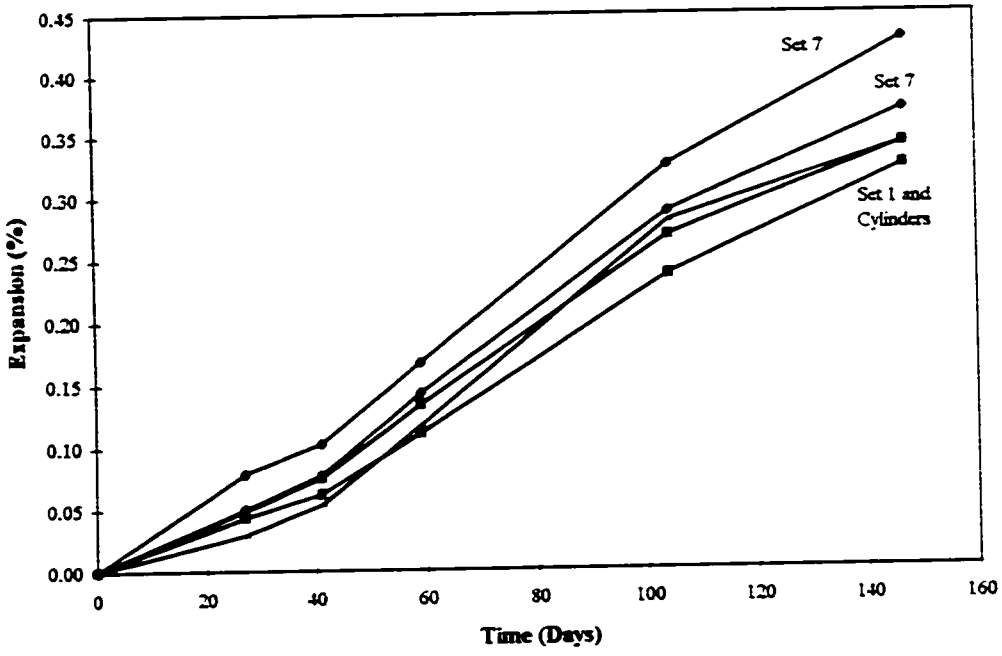

Figure 4.7: Unloaded beams top horizontal expansions (sets 1,7)

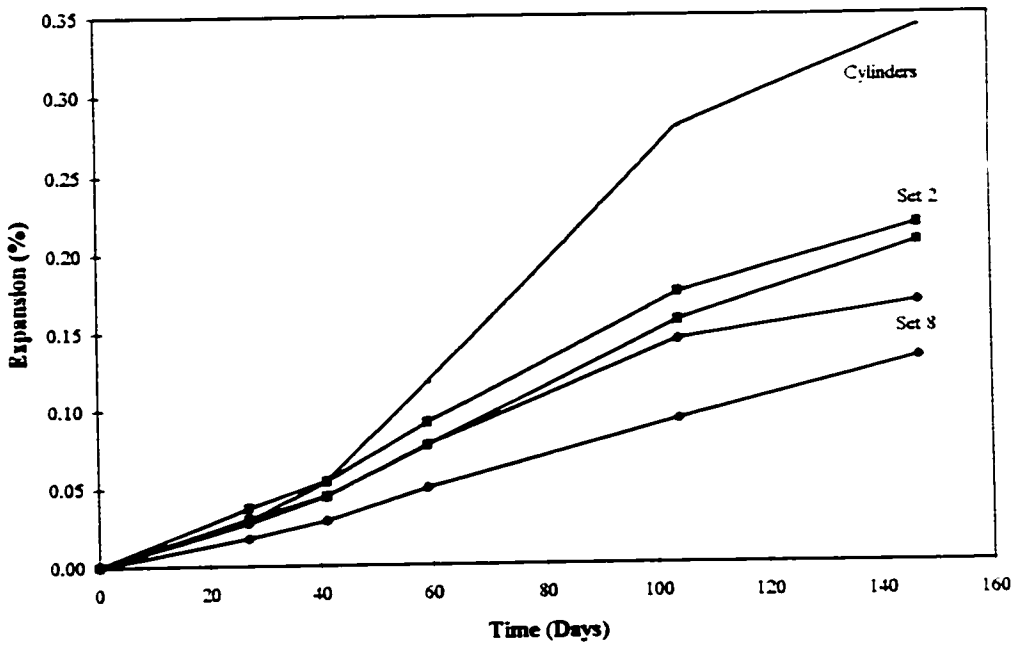

Figure 4.8: Unloaded beams middle horizontal expansions (sets 2,8)

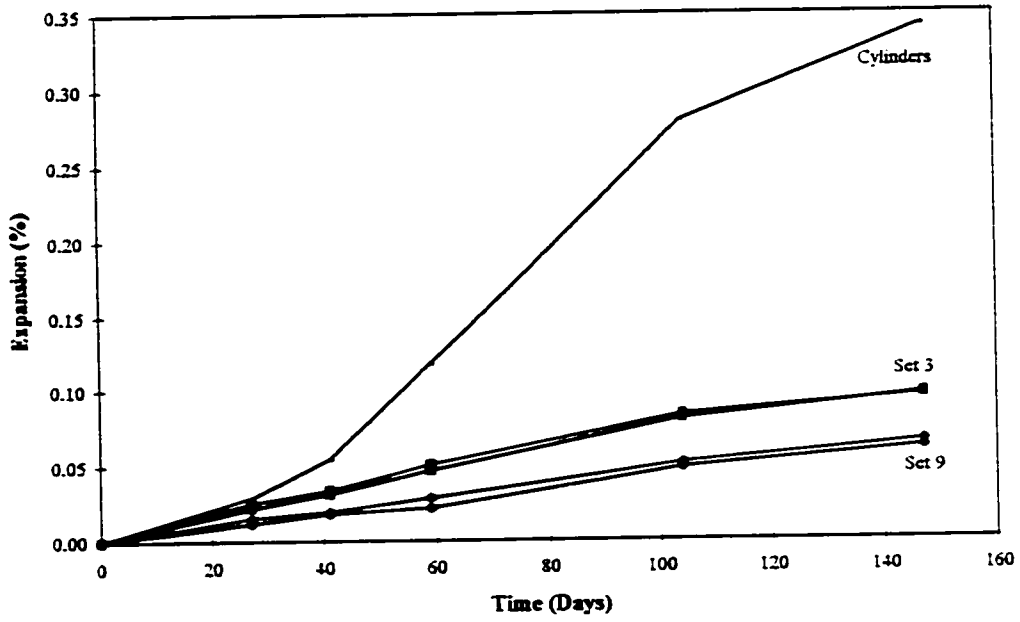

Figure 4.9: Unloaded beams bottom horizontal expansions (sets 3,9)

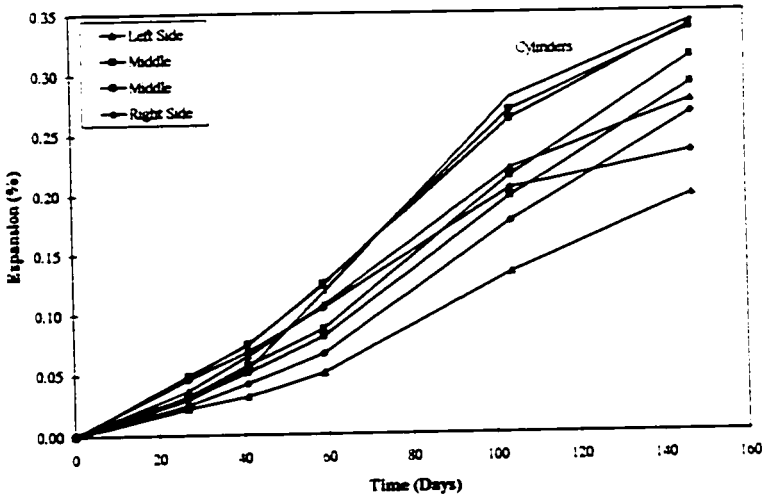

Figure 4.10: Unloaded beams vertical expansions (Sets 13,16,17,20)

4.2.2 Statically Loaded Beam Expansions

The expansion results presented in the following sections are for statically loaded beams. The results are compared per the discussion in Section 4.2. Comparisons of the variously loaded beam expansions are presented in Section 4.2.4. Reactive cylinder expansions were plotted with those of the beams to compare concrete free expansions with those at the various Demec locations of the reinforced concrete beams.

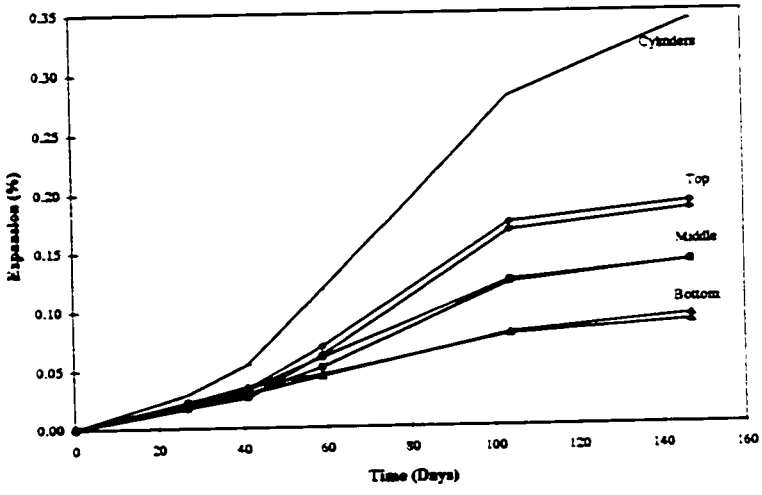

Figure 4.11: Statically loaded beams overall horizontal expansions (sets 1,2,3)

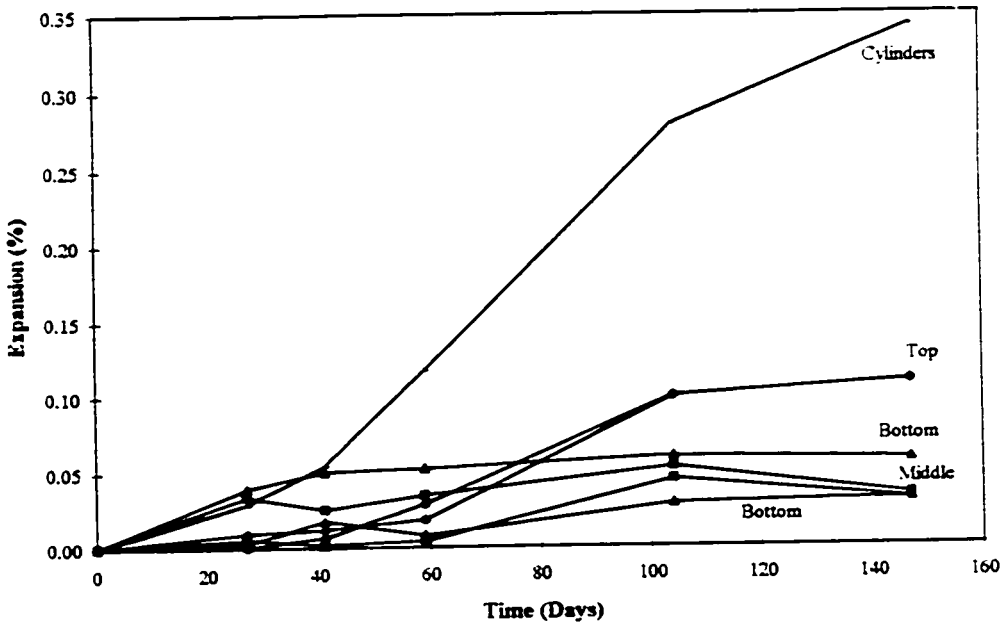

Figure 4.12: Statically loaded beams mid-span horizontal expansions (sets 7,8,9)

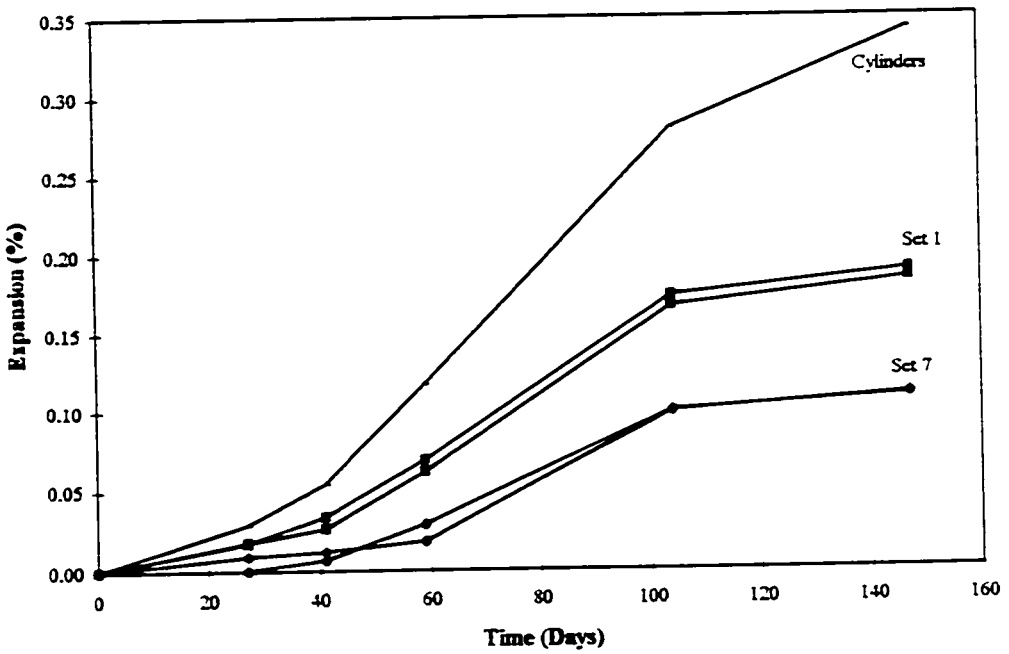

Figures 4.13: Statically loaded beams top horizontal expansions (sets 1,7)

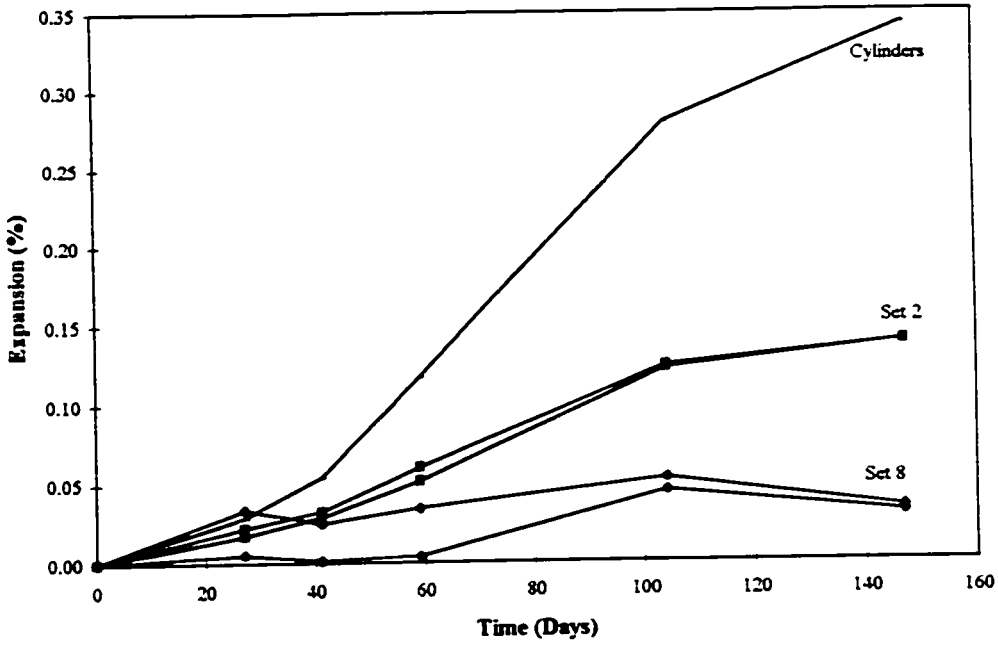

Figures 4.14: Statically loaded beams middle horizontal expansions (sets 2,8)

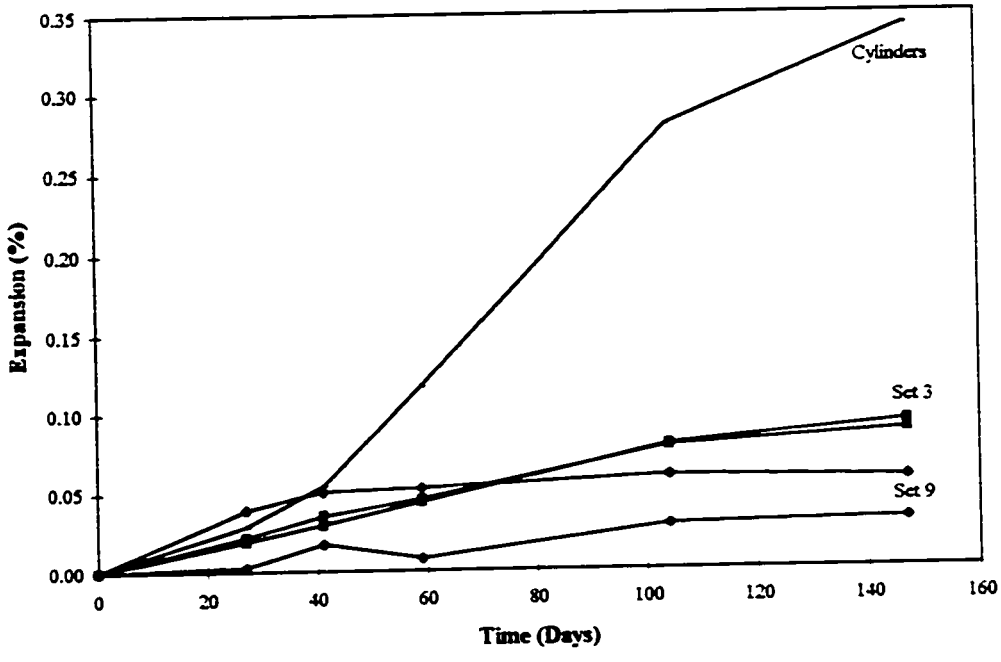

Figures 4.15: Statically loaded beams bottom horizontal expansions (sets 3,9)

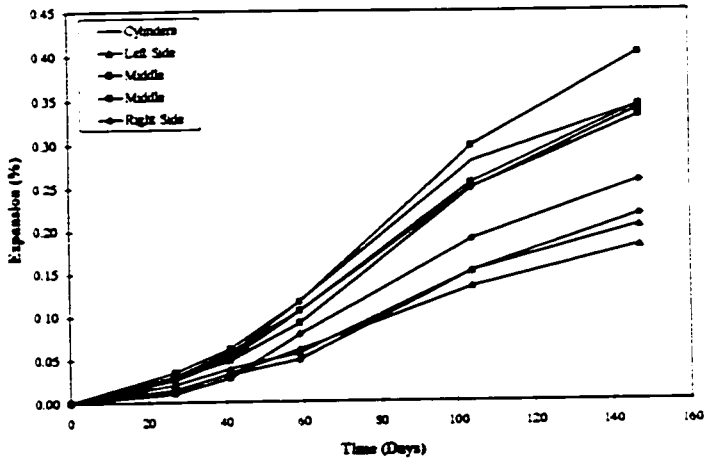

Figure 4.16: Statically loaded beams vertical expansions (sets 13,16,17,20)

4.2.3 Dynamically Loaded Beam Expansions

The expansion results presented in the following sections are for dynamically loaded beams only. The results are compared per the discussion in Section 4.2. Comparisons of the variously loaded beam expansions are presented in Section 4.2.4. Reactive cylinder expansions were plotted along with those of the beams to compare concrete free expansions with those at the various Demec locations of the reinforced concrete beams.

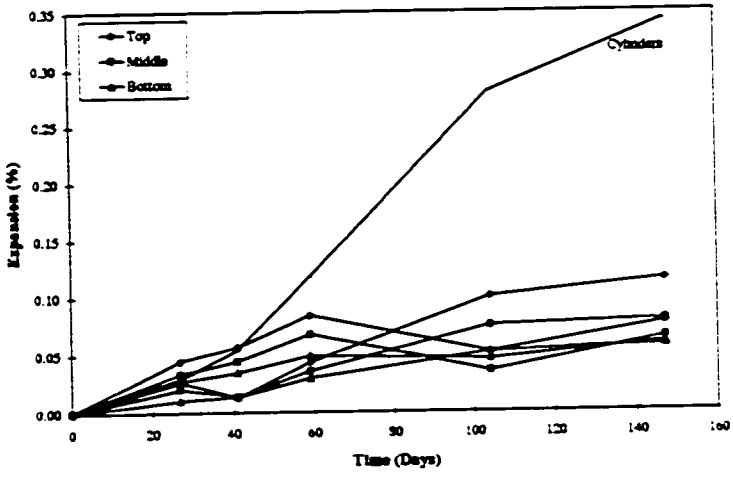

Figure 4.17: Dynamically loaded beams overall horizontal expansions (sets 1,2,3)

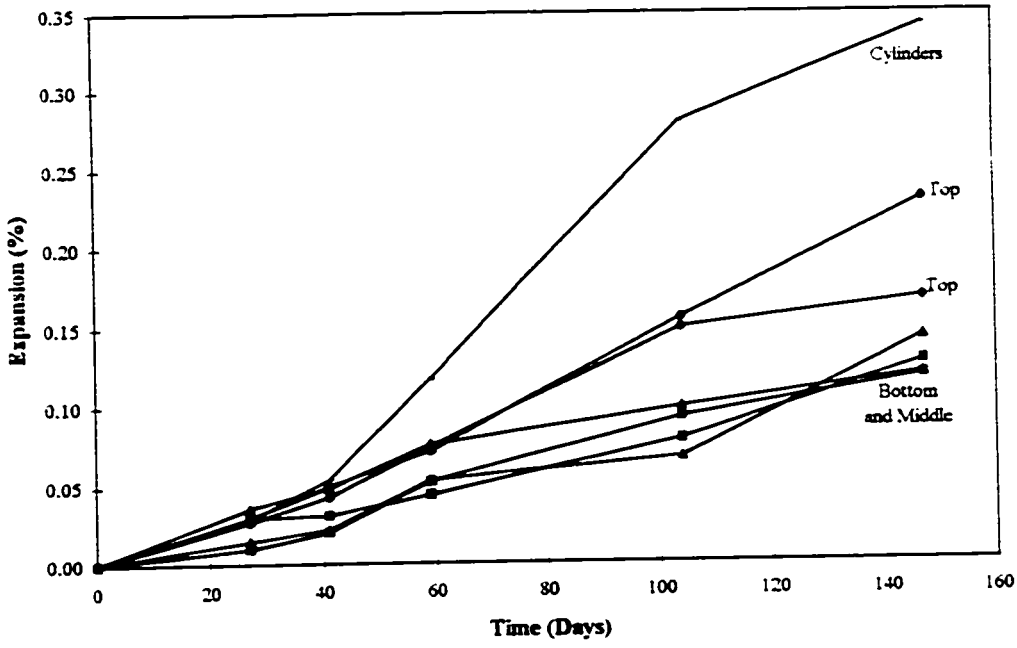

Figure 4.18: Dynamically loaded beams mid span horizontal expansions (sets 7,8,9)

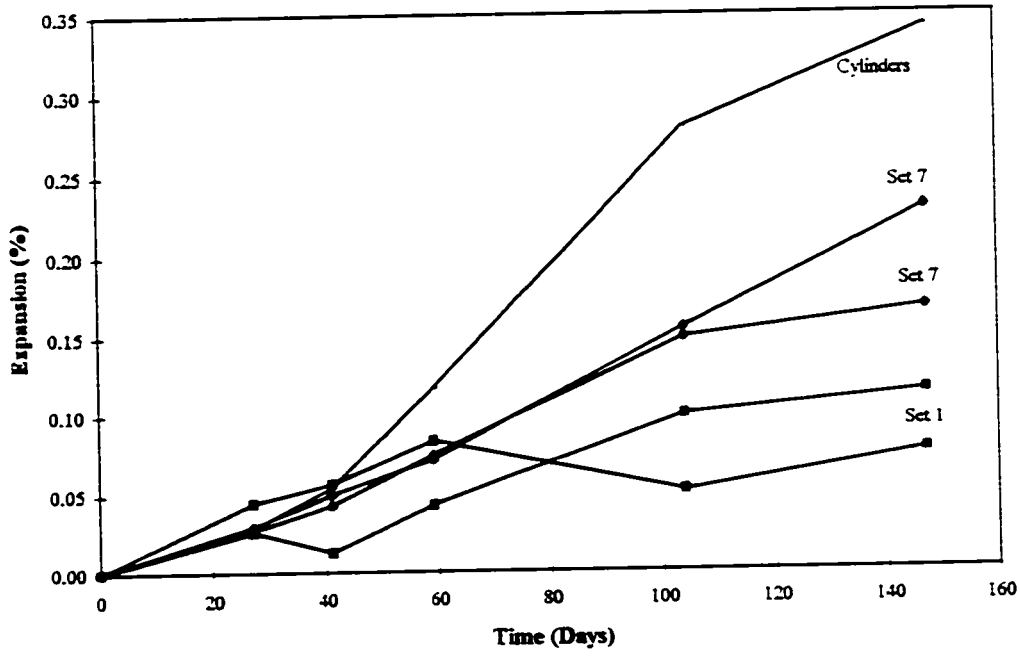

Figures 4.19: Dynamically loaded beams top horizontal expansions (sets 1,7)

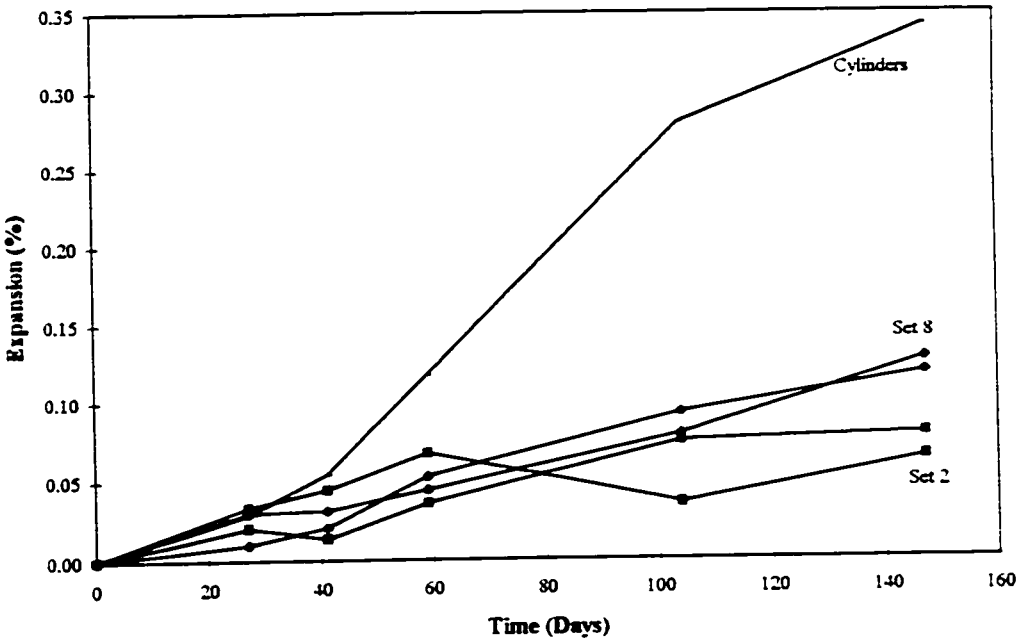

Figures 4.20: Dynamically loaded beams middle horizontal expansions (sets 2,8)

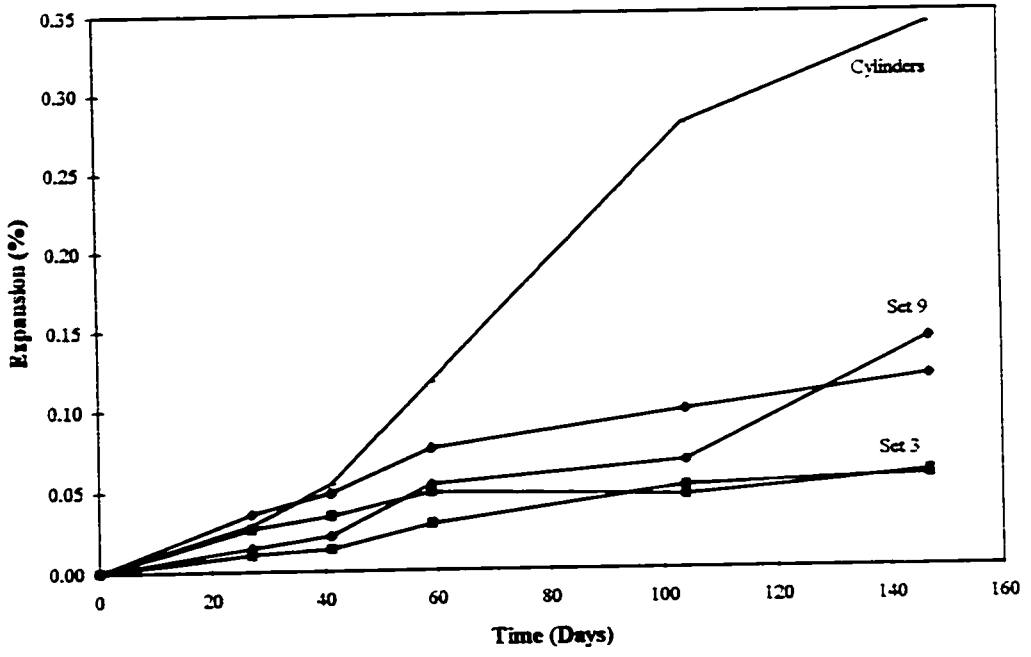

Figures 4.21: Dynamically loaded beams bottom horizontal expansions (sets 3,9)

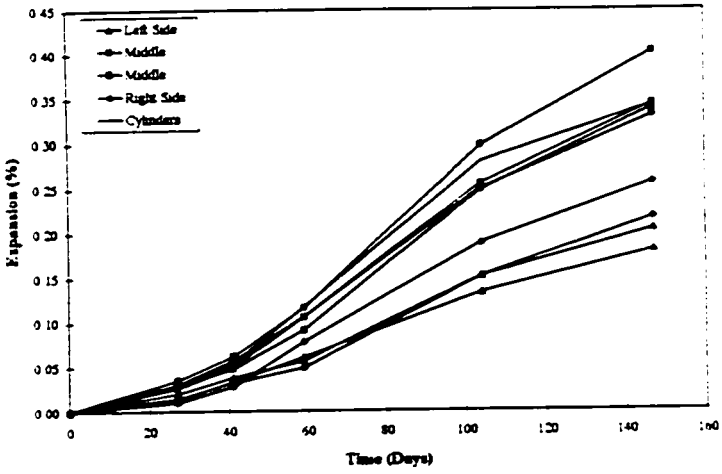

Figure 4.22: Dynamically loaded beams vertical expansions (sets 13,16,17,20)

4.2.4 Expansions for Beams Subjected to Various Loading Regimes

The following section compares expansions for the same locations on the beams which were tested under various loading regimes. These comparisons allowed the determination of the effects of loading conditions on ASR expansion. Once again, only the Demec sets of (#1, 2, 3, 7, 8, 9, 13, 16, 17, 20) are compared. Reactive cylinder expansions were plotted with those of the beams to compare concrete free expansions with those at the various Demec locations of the reinforced concrete beams.

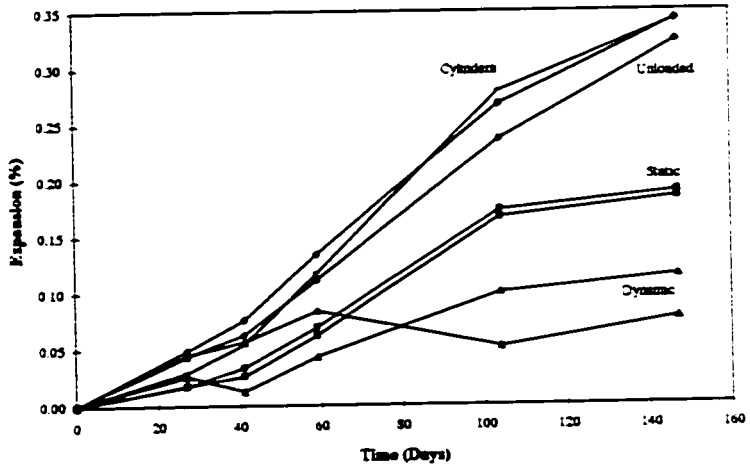

Figure 4.23: Overall horizontal expansions for the top of the various beams (set 1)

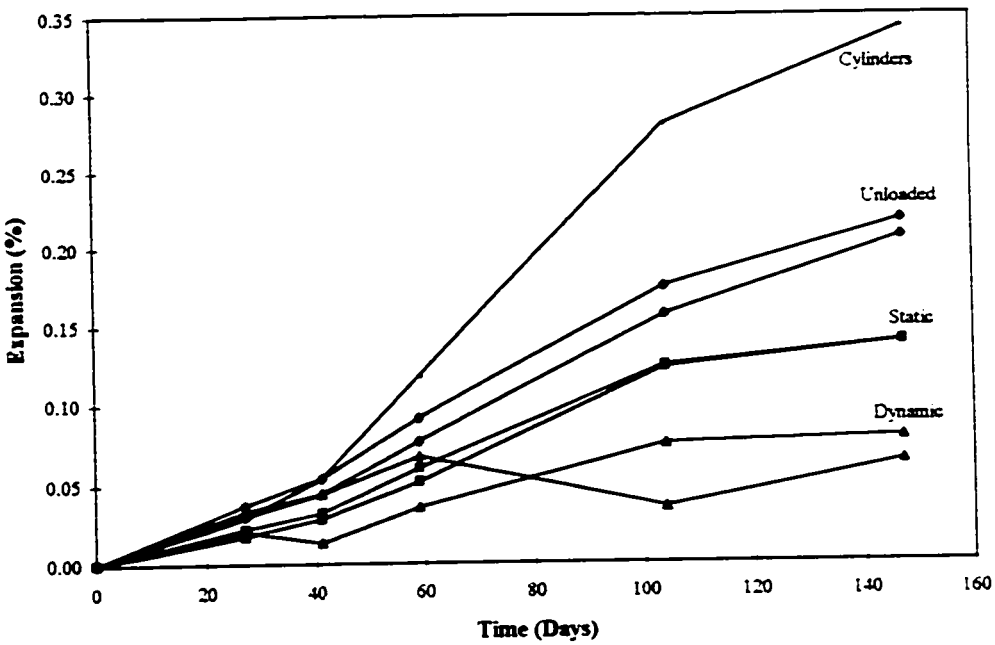

Figure 4.24: Overall horizontal expansions for the middle of the various beams (set 2)

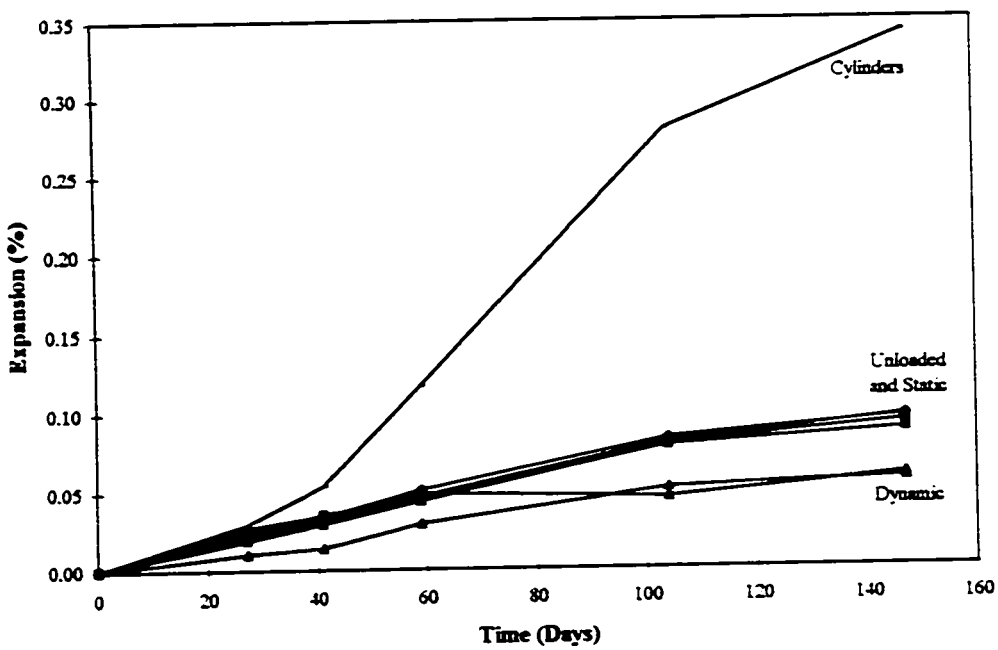

Figure 4.25: Overall horizontal expansions for the bottom of the various beams (set 3)

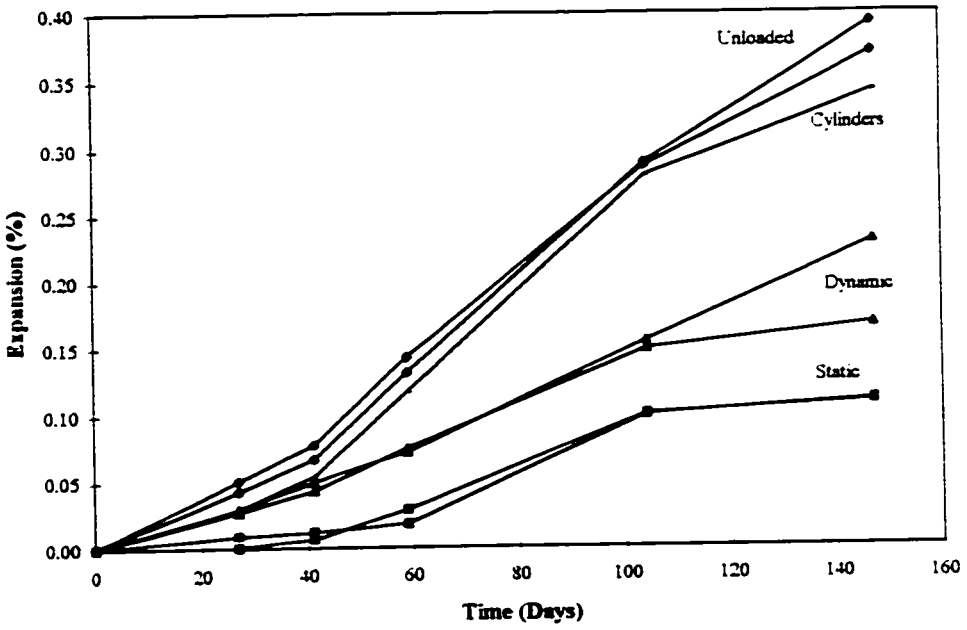

Figure 4.26: Mid span horizontal expansions for the top of the various beams (set 7)

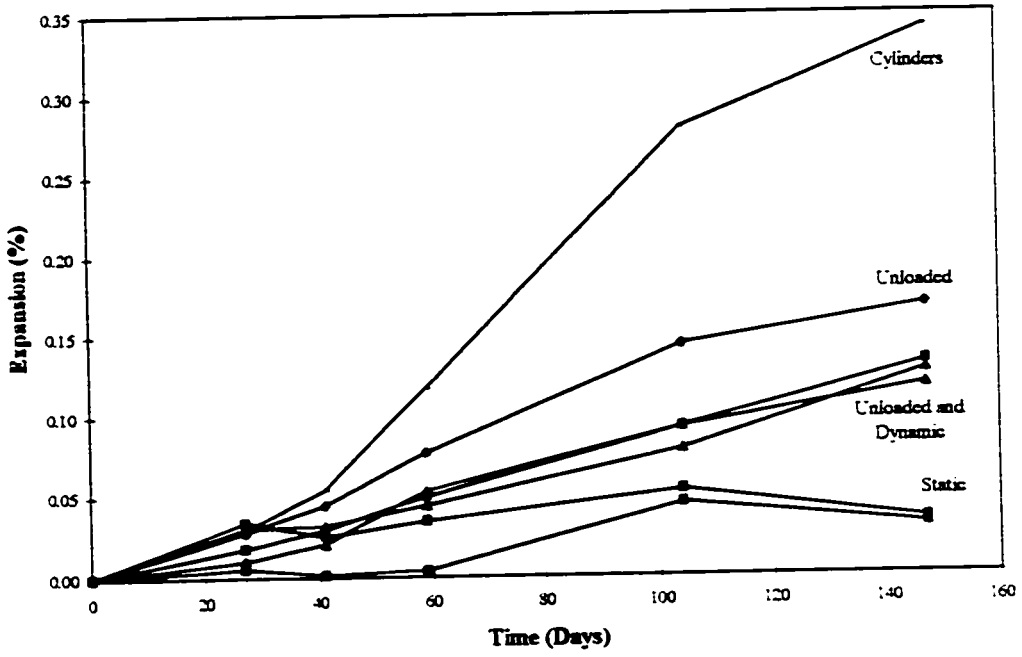

Figure 4.27: Mid span longitudinal expansions for the middle of the various beams (set 8)

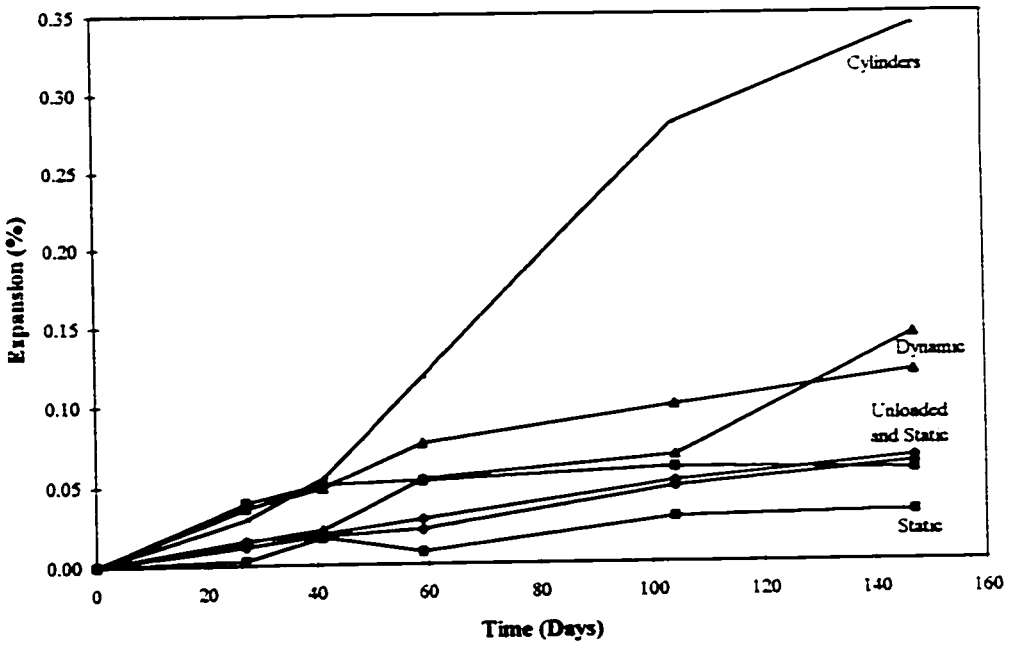

Figure 4.28: Mid span horizontal expansions for the bottom of the various beams (set 9)

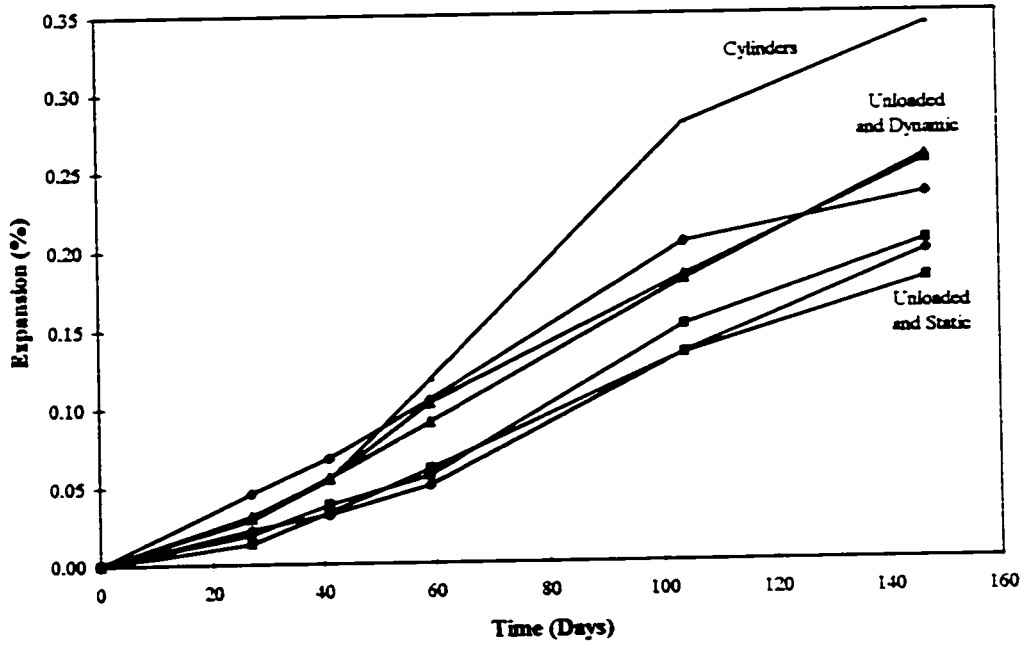

Figure 4.29: Vertical expansions for the various beams (set 13)

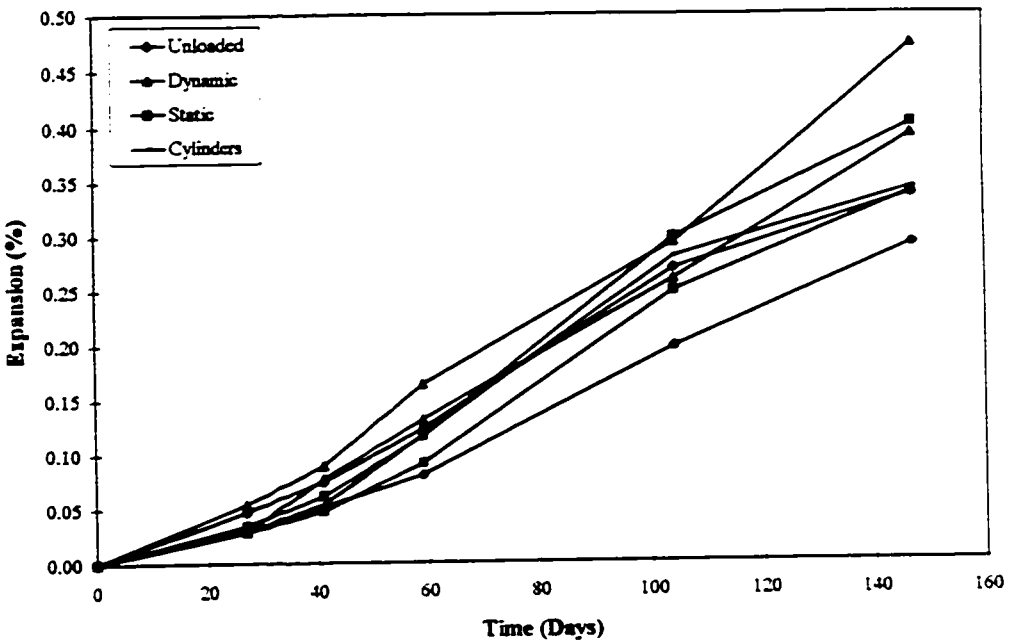

Figure 4.30: Vertical expansions for the various beams (set 16)

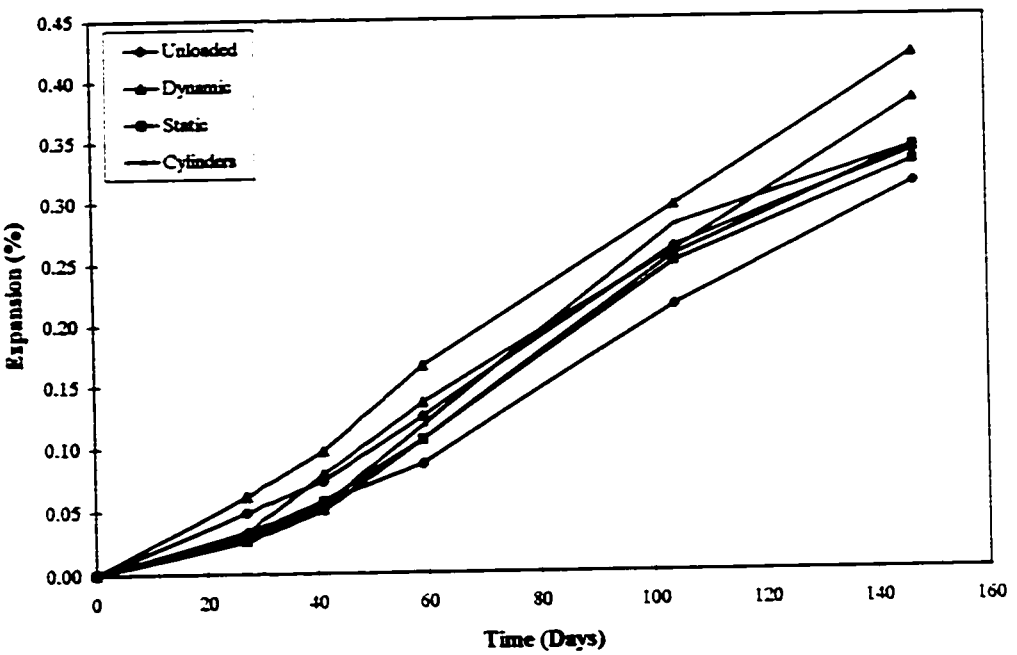

Figure 4.31: Vertical expansions for the various beams (set 17)

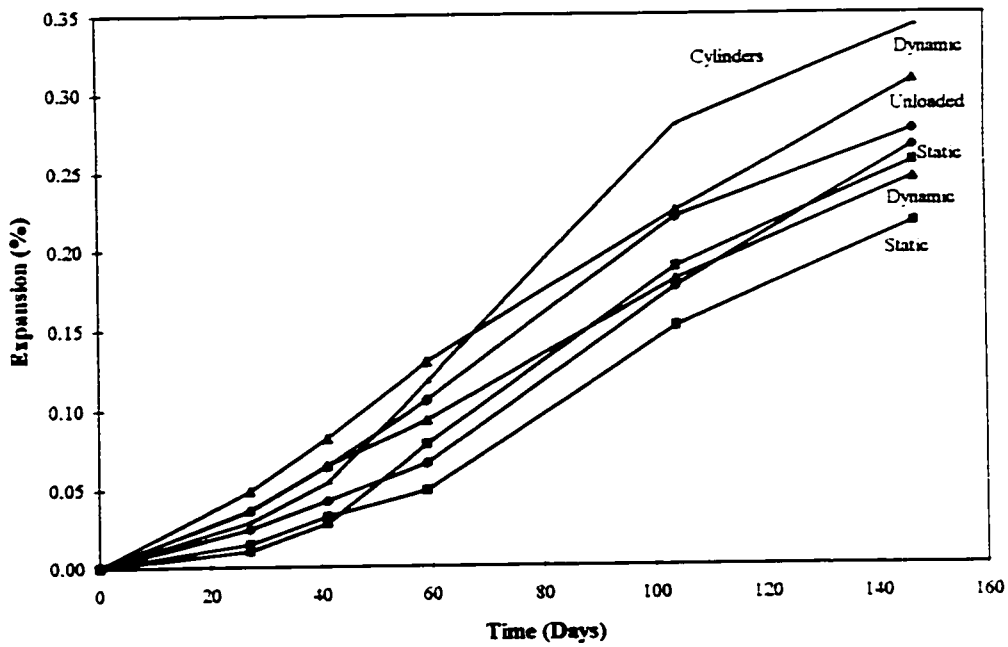

Figure 4.32: Vertical expansions for the various beams (set 20)

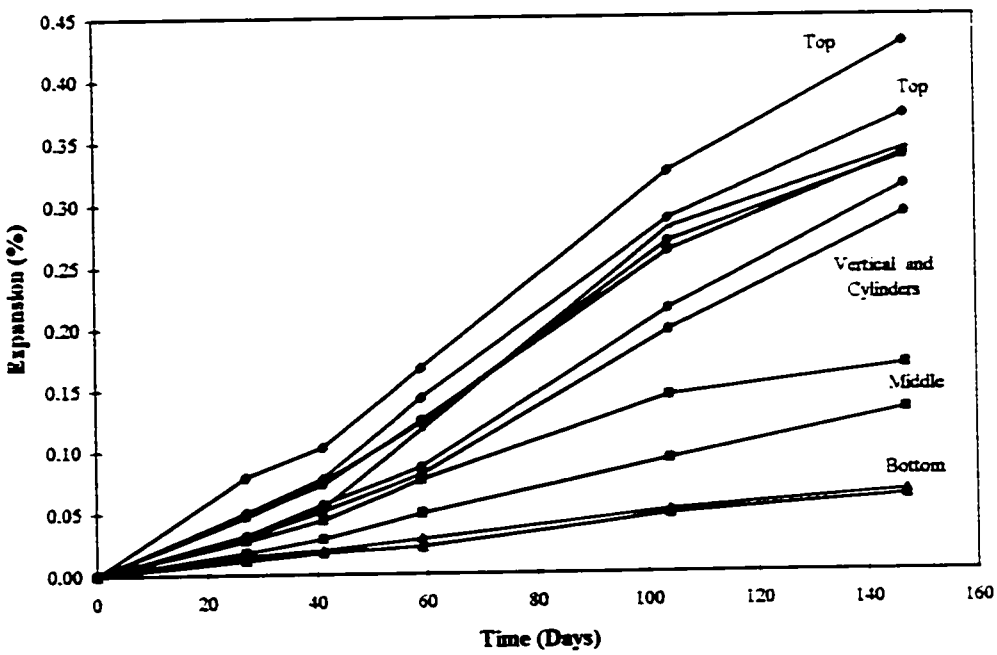

Figure 4.33: Horizontal and vertical expansions for the mid-span of the unloaded beams (sets 7, 8, 9, 16 and 17)

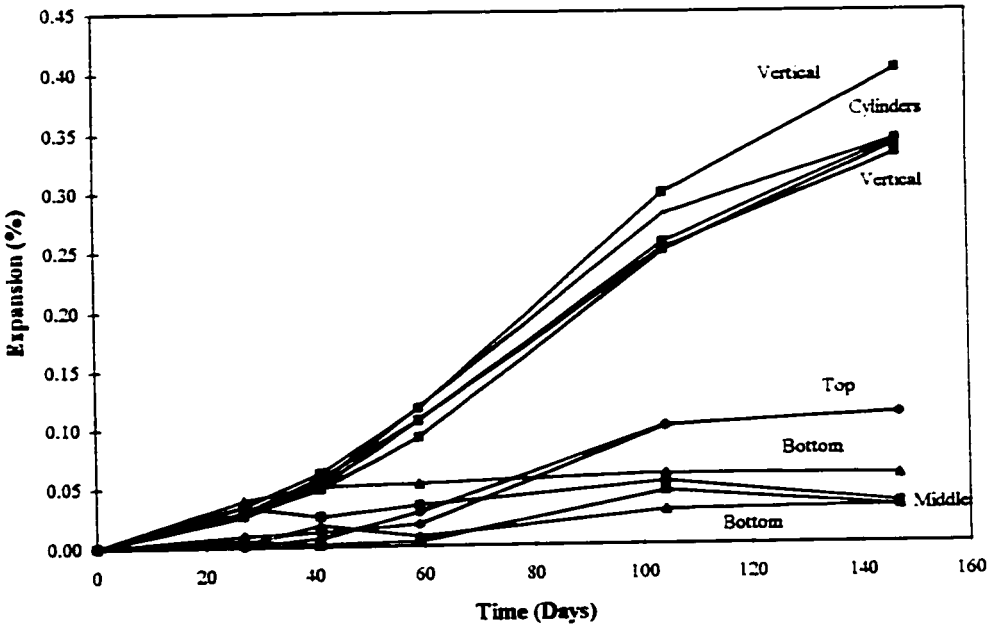

Figure 4.34: Horizontal and vertical expansions for the mid-span of the static beams (sets 7, 8, 9, 16 and 17)

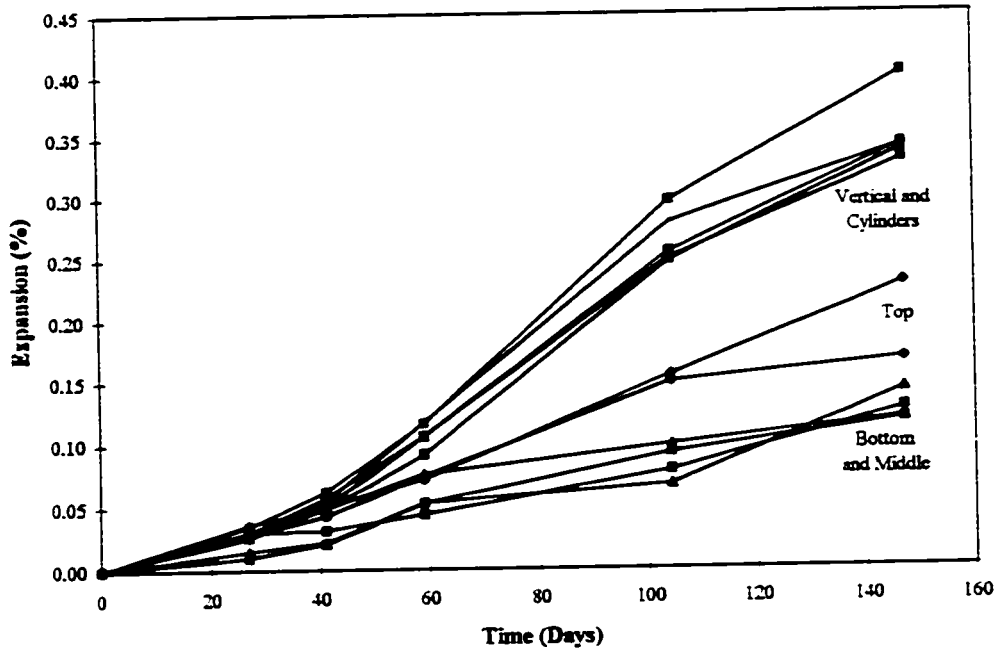

Figure 4.35: Horizontal and vertical expansions for the mid-span of the dynamic beams (sets 7, 8, 9, 16 and 17)

4.2.5 Expansions of Non-Reactive Control Beams

Reinforced concrete beam control specimens made with non-reactive aggregate and tested in similar conditions as the reactive set of specimens were used to determine non-ASR strains in the beams. Table 4.1 shows the percent strain (negative strains denote contractions and positive strains denote expansions) of each of the Demec locations of interest for the non-reactive beams (sets 1,2,3,7,8,9,13,16,17,20). Table 4.2 shows the strain measurements taken for the non-reactive cylinders and CSA concrete prisms.

Table 4.1: Strains of non-reactive control beams at the end of the experiment (at 108 days of strain measurement)

	Strain for various Demec locations (%)									
Specimen	**#1**	**#2**	**#3**	**#7**	**#8**	**#9**	**#13**	**#16**	**#17**	**#20**
Unloaded	0.002	0	0	0	0.01	-0.004	-0.014	-0.007	0.002	-0.004
Unloaded	0	0.002	0.002	0.015	-0.006	0.024	-0.008	0.012	0.005	-0.006
Static	-0.002	0.005	0.008	0.004	0.009	0.024	0.013	0.008	0.022	0.005
Static	0.003	0.007	0.010	-0.006	-0.002	0.005	0.001	0.003	0.009	0.009
Dynamic	—	—	—	-0.009	-0.003	0.004	-0.002	0.009	0.002	0.027
Dynamic	0.024	0.014	0.003	0.005	-0.03	0.006	-0.001	0.002	-0.06	0.008

Table 4.2: Strains of non-reactive cylinders and CSA Prisms (at 108 days of strain measurement)

Specimen	**% Strain**
Cylinder	0.014
Cylinder	0.040
Cylinder	0
Cylinder	0.028
CSA Prism	0.0012
CSA Prism	-0.0024
CSA Prism	0.0016
CSA Prism	-0.0012

4.2.6 Additional Results

The following section presents results dealing with the expansions of the reactive cylinders, CSA concrete prisms and resonant frequency prisms. The resonant frequency results for both the reactive and the non-reactive beams are also presented.

Figure 4.36 displays the resonant frequency results, the CSA concrete prism results and the expansion results for the concrete cylinders stored in sodium hydroxide. Figure 4.37 shows the results for the resonant frequency results of the reactive and non-reactive.

The resonant frequency measurements for the reactive prisms were taken over a period of approximately 160 days. However, when comparing the resonant frequency results of the reactive prisms with reactive specimen expansions, only the last 147 days of the data are used. This was done because the first two weeks of expansion measurements were discarded due to errors in the original zero measurements of the beams (the original zero expansion readings of the reactive beams were taken prior to the loading and cracking of the beams). The entirety of the resonant frequency results for the reactive prisms was used to compare with the resonant frequency results of the non-reactive prisms. This allowed the comparison of the resonant frequencies of reactive and non-reactive prisms in the early stages of the concrete curing as well as at the end of the experiments.

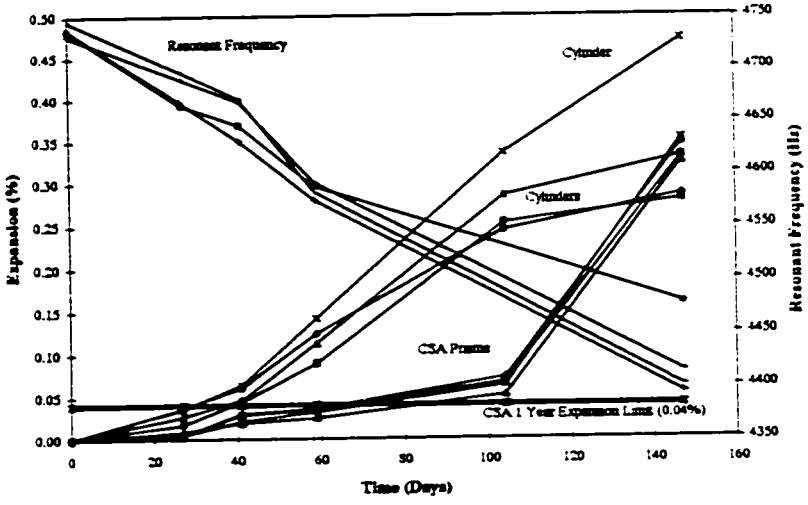

Figure 4.36: Reactive concrete cylinder and CSA prism expansions and reactive prism resonant frequency results vs. time

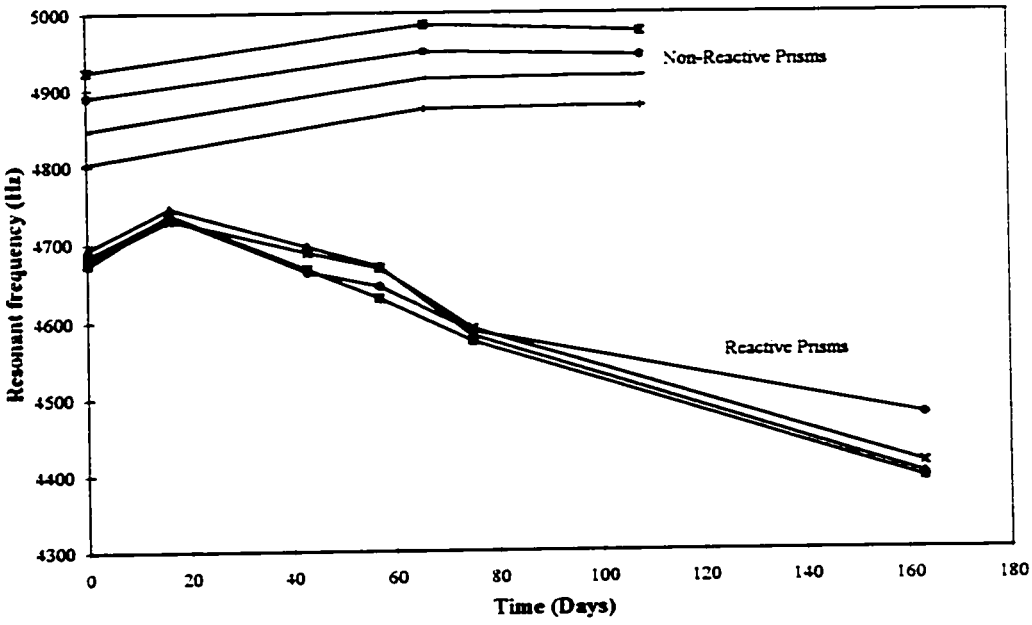

Figure 4.37: Reactive vs. non-reactive resonant frequency results

4.2.7 Reactive Beam Macrocracking at the End of Loading

ASR has been known to cause both microcracking and macrocracking of concrete. The microcracking of concrete is covered in Section 4.3 dealing with Damage Rating Indices (Section 4.3). The following section illustrates the reactive beam macrocracking after 147 days of testing. This allowed the comparison of cracking patterns between the various beams and provided insight into the effect of loading and reinforcement on ASR expansions as expansions are directly related to the cracking of concrete.

The non-reactive specimens displayed little or no surface cracking other than cracks caused by loading.

Figure 4.38: Typical unloaded beam macrocracking after 147 days of loading

Figure 4.39: Typical statically loaded beam macrocracking after 147 days of loading

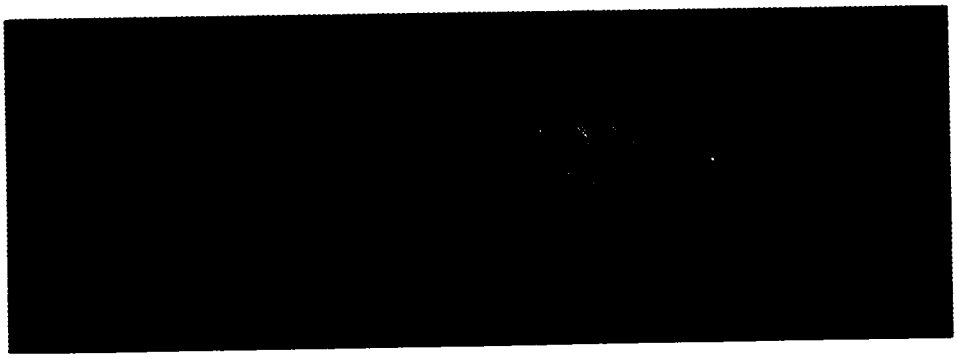

Figure 4.40: Typical dynamically loaded beam macrocracking after 147 days of loading

4.3 DAMAGE RATING INDICES

The damage rating results of the reactive concrete beams are presented in sections 4.3.1 and 4.3.2. The DRI were measured at the nine zones shown in Figure 4.41. Included with the beam results are the DRI for the resonant frequency prism RP-5. These allowed the comparison of unloaded free expansion results with the various beam DRI.

An effort was made to measure Damage Rating Indices in regions which corresponded to the expansion readings presented in Section 4.2.

However, only Demec sets 4 to 12 could be compared with DRI. This is due mainly to the fact that overall DRI results may incorporate DRI from areas of varying damage. This could provide average values which would not be representative of the expansions obtained.

Vertical expansions could not be compared with DRI since the damage readings at the bottom of the beams, near the steel, are significantly lower than those at the top and may not reflect the actual vertical expansion incurred. This is mainly because the DRI is determined over a surface area and takes into account all cracks (occurring horizontally or vertically).

Therefore, the DRI measured are compared to the nine Demec areas shown in Figure 4.41. Overall beam expansions and vertical expansions are not compared to any DRI measurements.

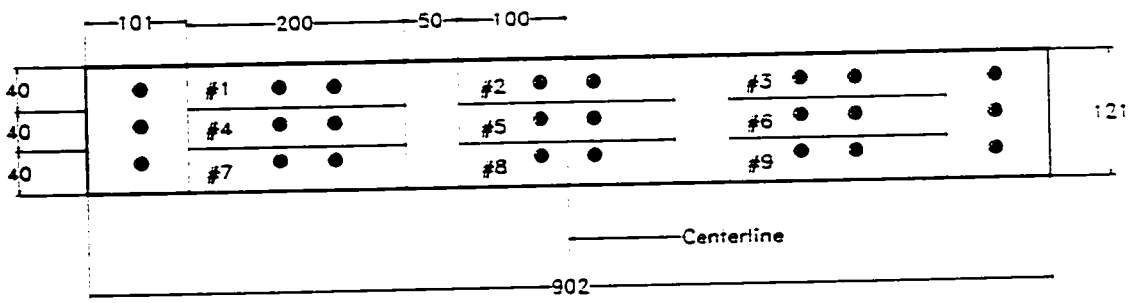

Figure 4.41: Zones of damage rating measurements

4.3.1 Damage Rating Indices for the Individual Beams

The DRI for each individual beam are presented (Figures 4.42 to 4.47). This allows the comparison of these measurements within each beam and demonstrates the varying damage encountered at different locations for each beam. These measurements are also compared to the DRI obtained from an unloaded, unreinforced dynamic frequency prism. This provided insight as to the comparability of unloaded values of DRI in the reinforced and unreinforced prism.

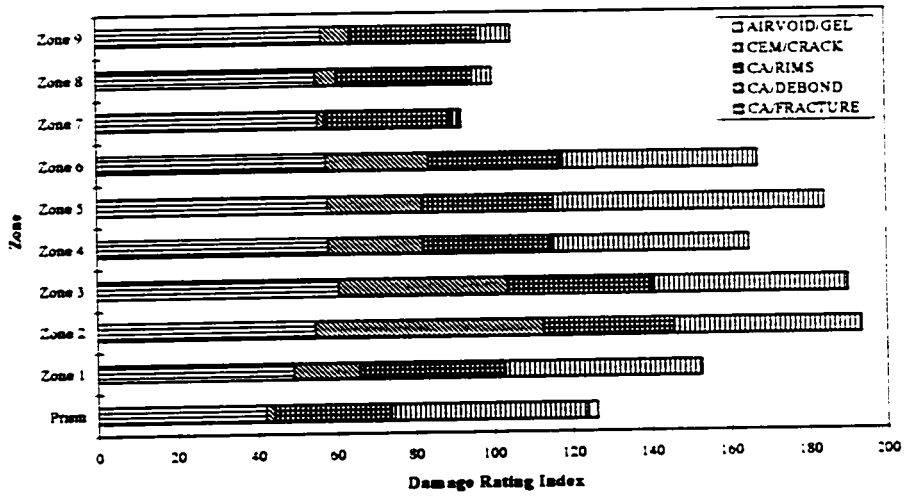

Figure 4.42: Damage rating indices for unloaded beam RB-1

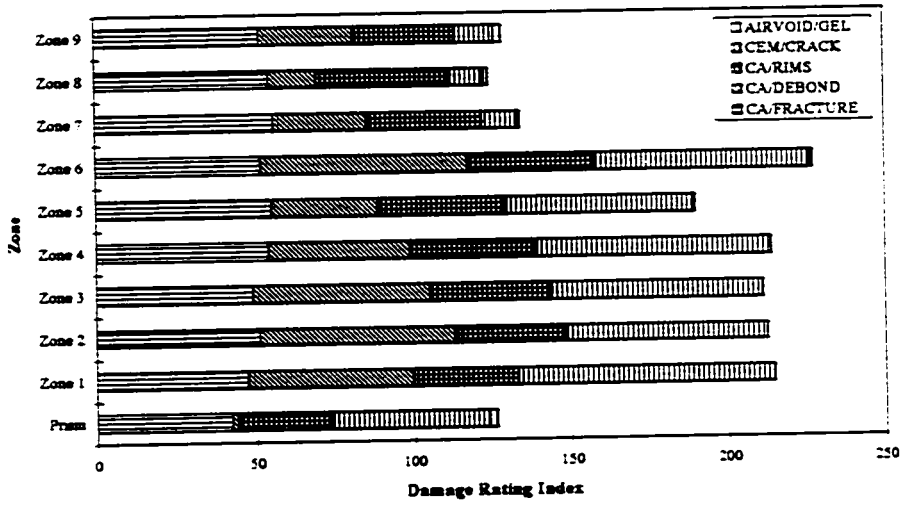

Figure 4.43: Damage rating indices for unloaded beam RB-6

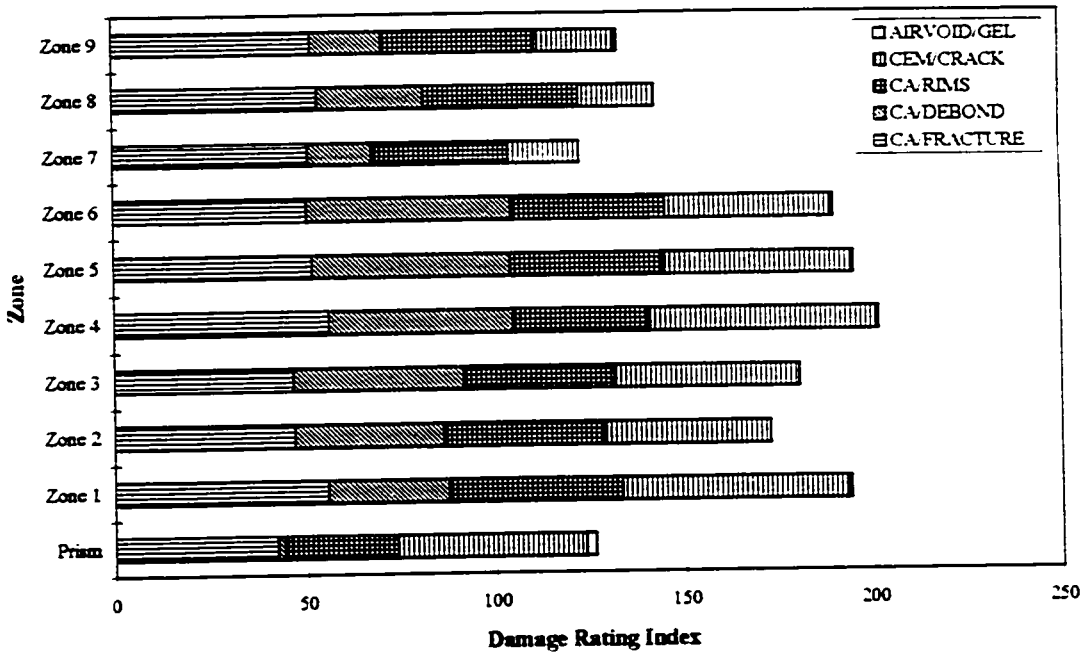

Figure 4.44: Damage rating indices for statically loaded beam RB-7

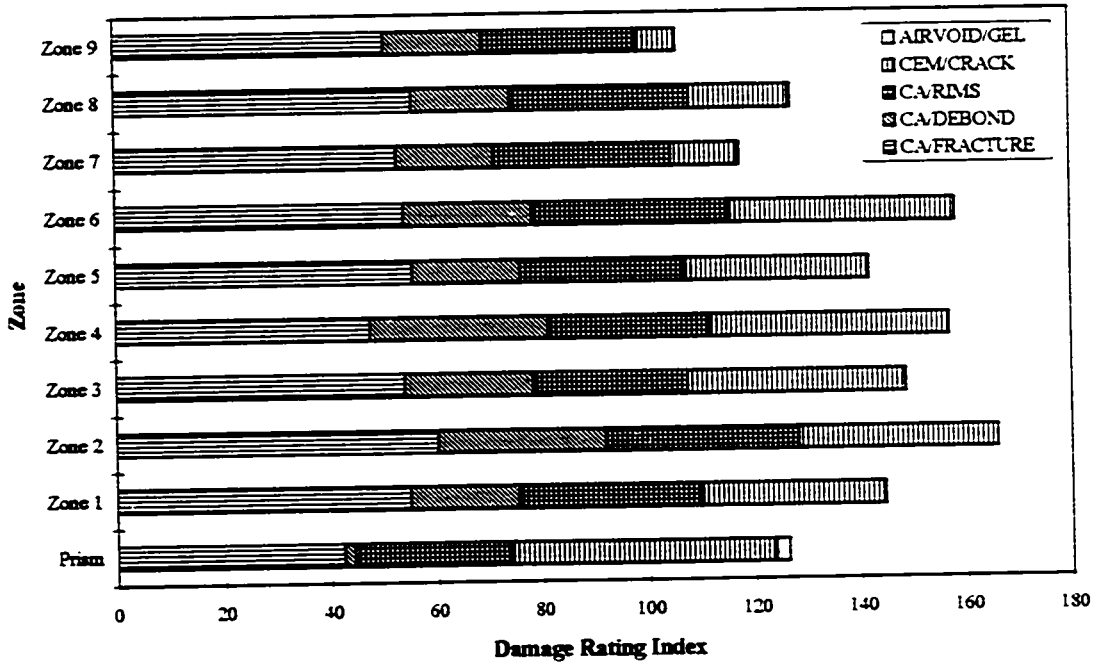

Figure 4.45: Damage rating indices for statically loaded beam RB-8

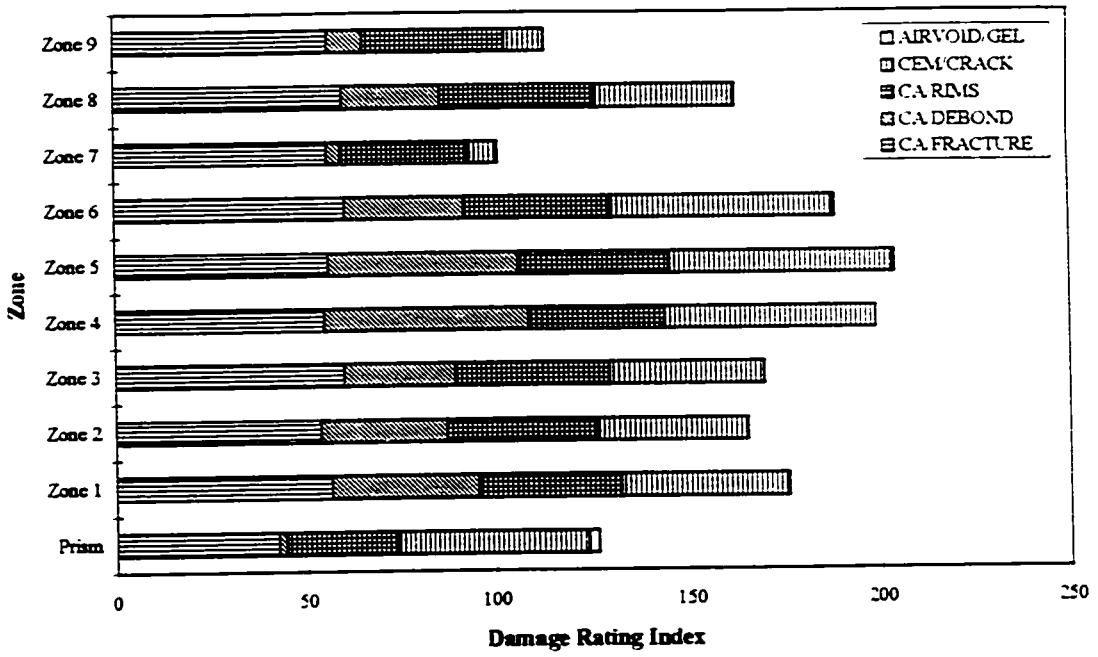

Figure 4.46: Damage rating indices for dynamically loaded beam RB-3

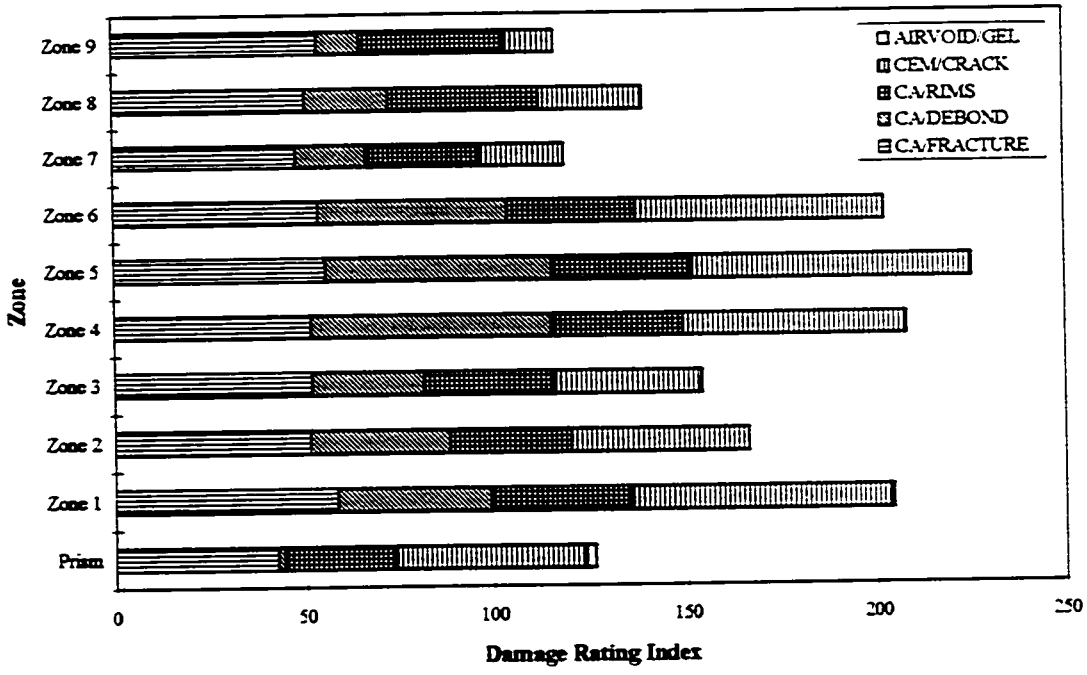

Figure 4.47: Damage rating indices for dynamically loaded beam RB-4

4.3.2 Comparison of Damage Rating Indices for the Various Beams

DRI for each of the nine individual measurement zones are compared for the various reactive beams including the DRI for reactive resonant frequency prism No.5 (Figures 4.48 to 4.50). This allows the comparison of damage due to ASR in beams subjected to various loading regimes.

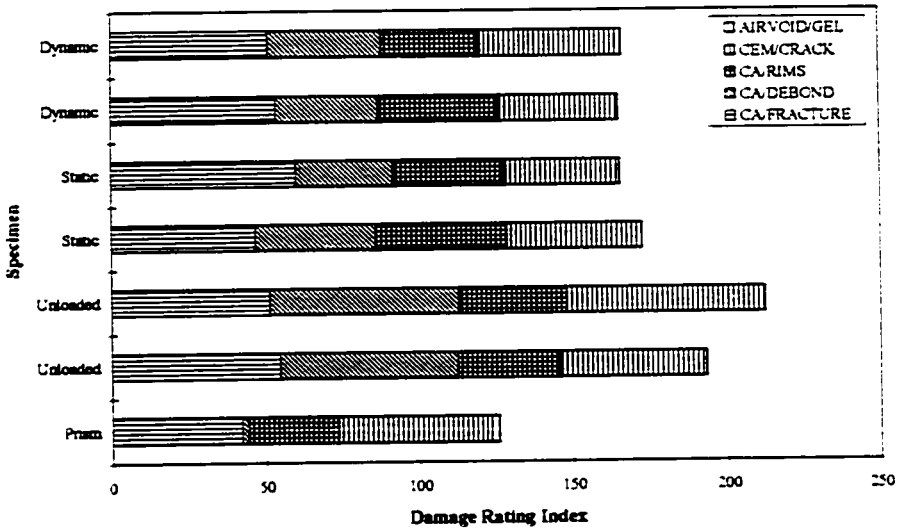

Figure 4.48: Damage rating indices for various beams, zone 2

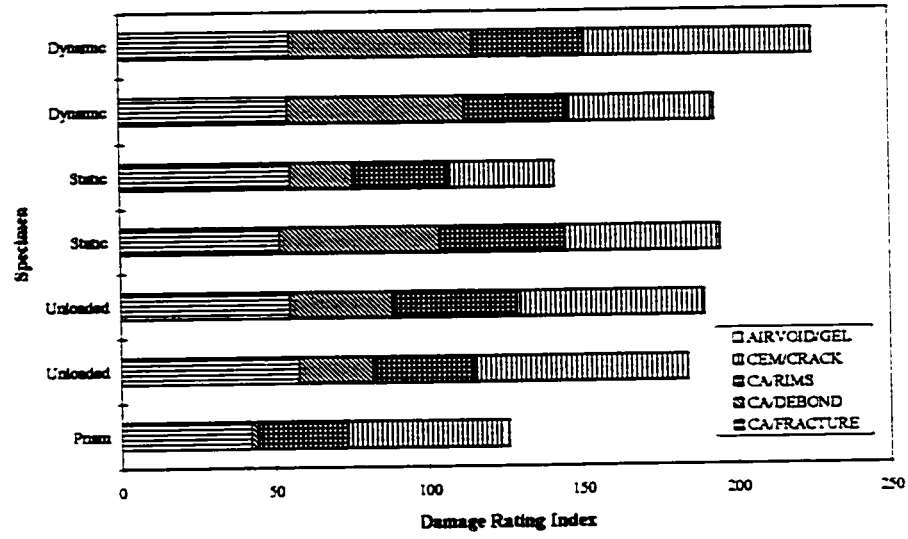

Figure 4.49: Damage rating indices for various beams, zone 5

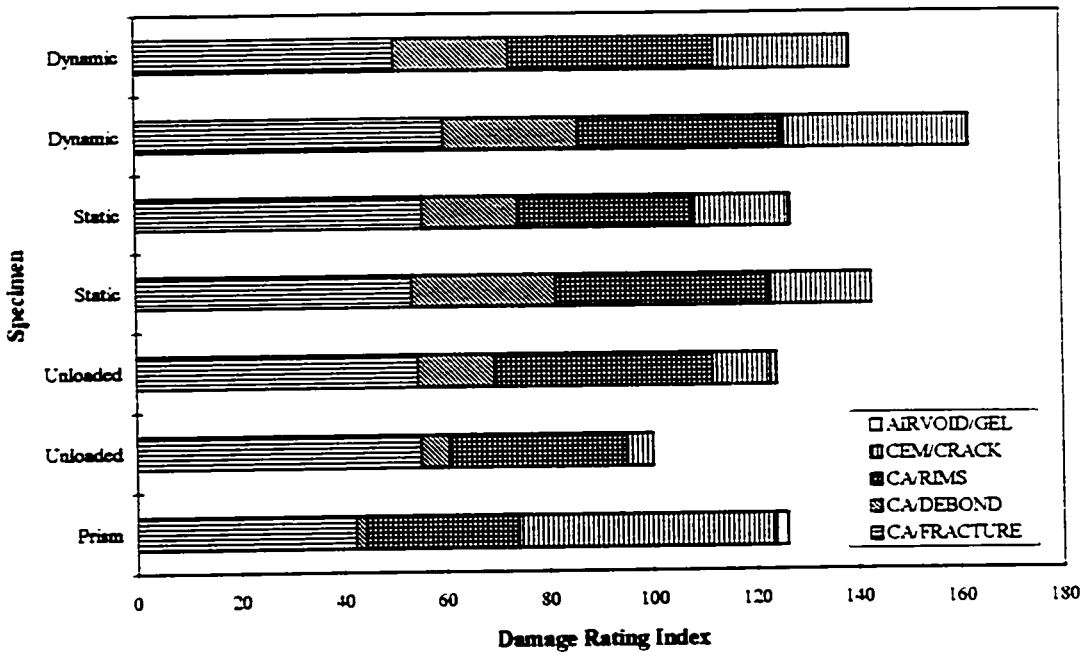

Figure 4.50: Damage rating indices for various beams, zone 8

4.4 STRUCTURAL BEHAVIOUR OF BEAMS

After the various beams were tested, expansions measured and DRI determined, each of the reactive and non-reactive beams were loaded in flexure to failure. The reactive beams were tested for 147 days and loaded to flexural failure ±135 days after the end of testing, during which time they were stored at room temperature. The non-reactive beams were tested for 161 days and loaded to flexural failure shortly thereafter. The following figures display the load-deflection results for all of the beams loaded to failure. Figures 4.51, 4.52 and 4.53 show the load-deflection curves for the reactive and non-reactive beams tested at 28 days along with the unloaded, statically loaded and dynamically loaded (respectively) reactive and non-reactive beams. Figures 4.54 and 4.55 display the load deflection results of all the reactive and non-reactive beams respectively.

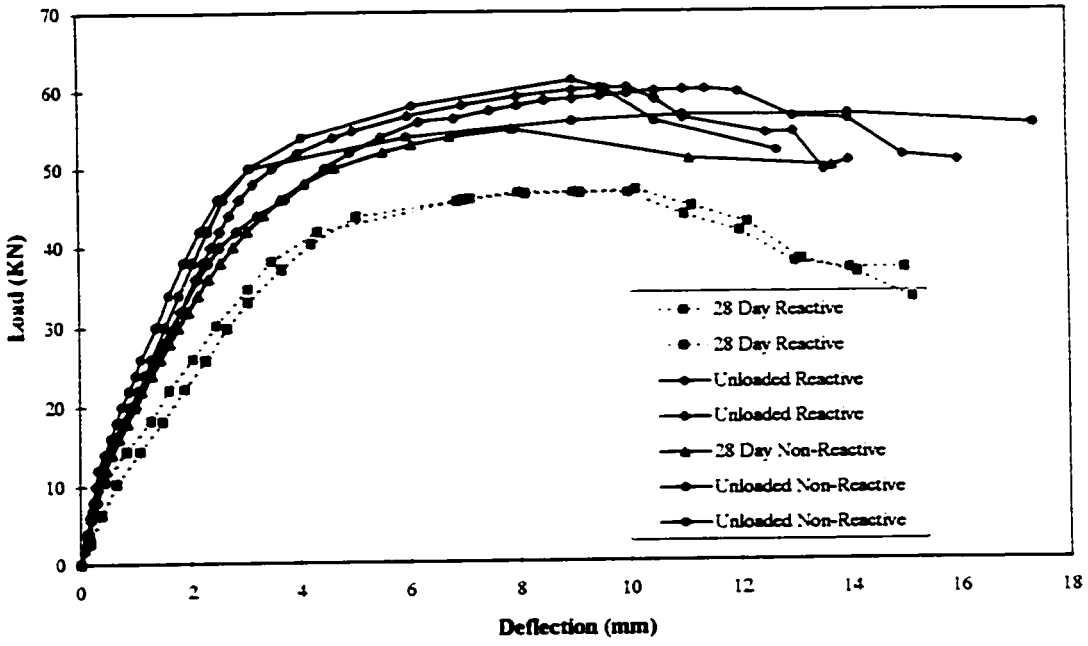

Figure 4.51: Load vs. deflection for 28 day and unloaded reactive and non-reactive beams

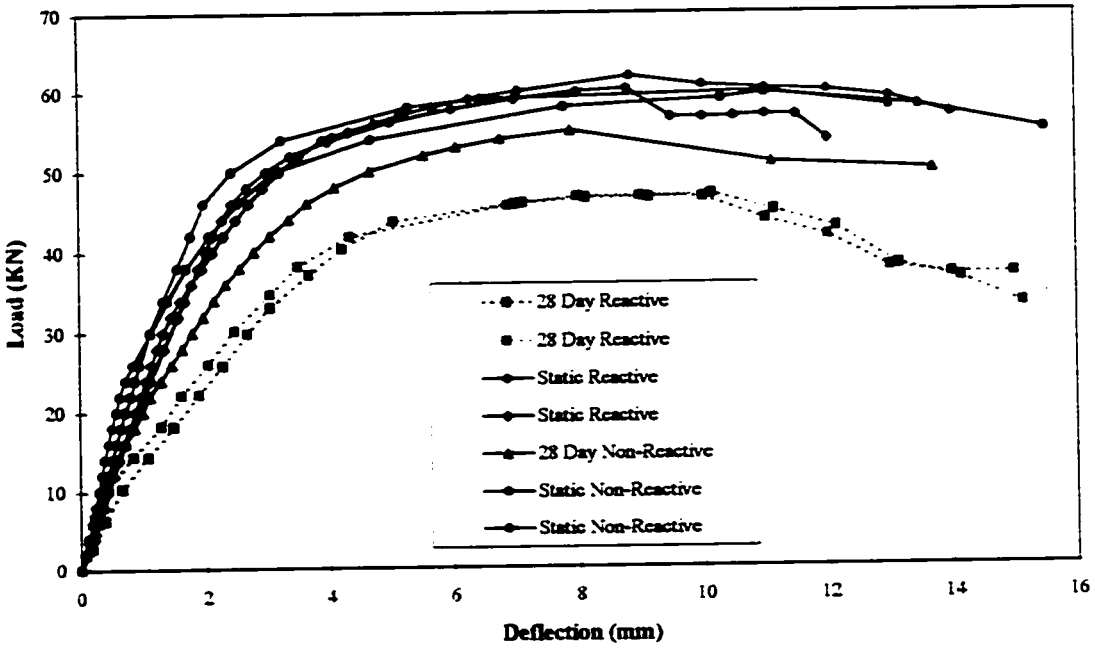

Figure 4.52: Load vs. deflection for 28 day and static reactive and non-reactive beams

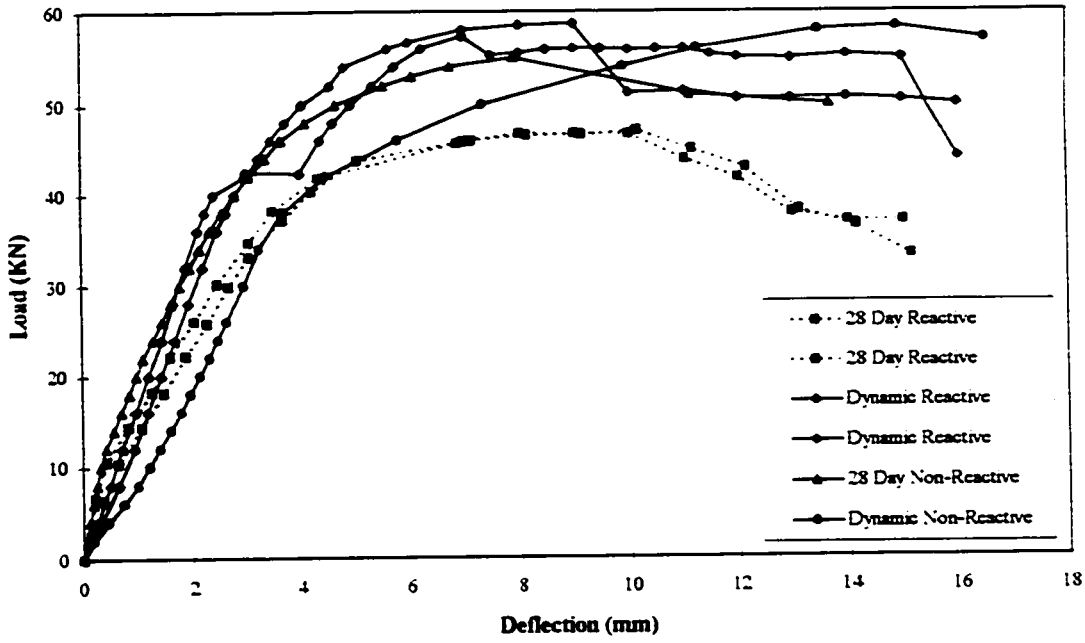

Figure 4.53: Load vs. deflection for 28 day and dynamic reactive and non-reactive beams

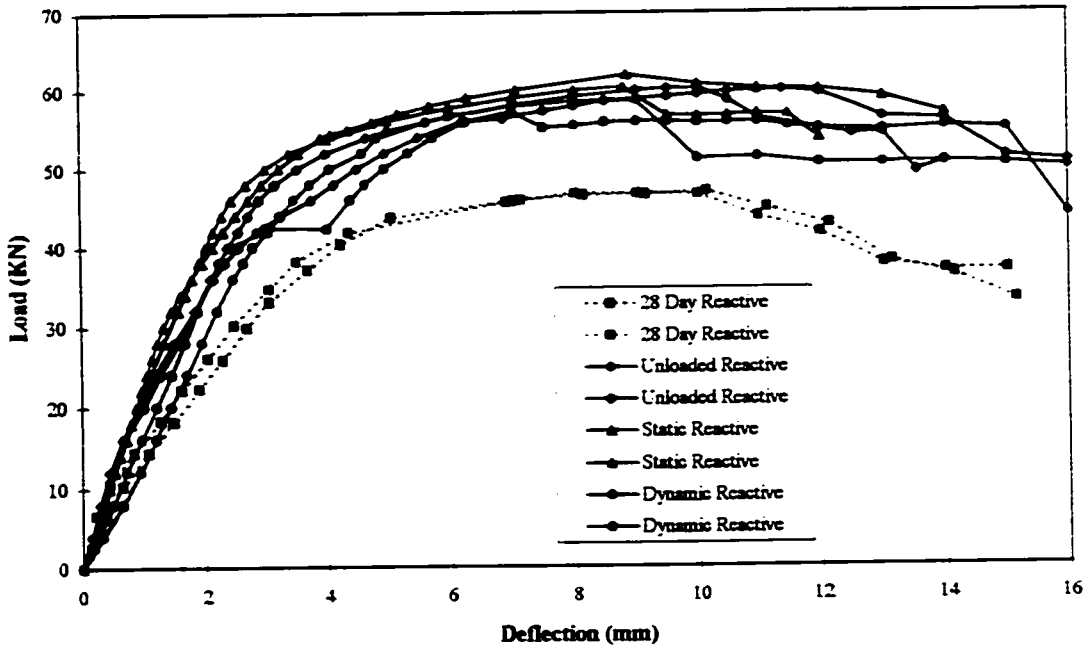

Figure 4.54: Load vs. deflection for all the reactive beams

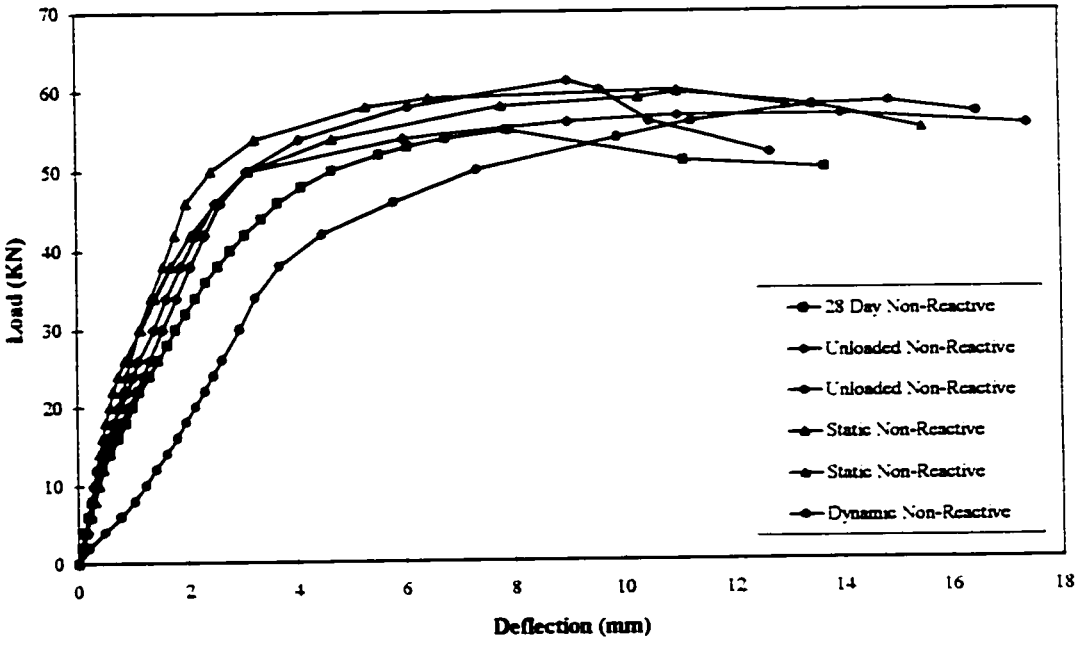

Figure 4.55: Load vs. deflection for all the non-reactive beams

All of the ASR beams failed by crushing of the concrete at the top fiber of the beams between the loading points. Most of the non-reactive beams failed in this same mode except for two beams which failed in shear.

The reactive and non-reactive dynamically loaded beams were damaged by the loading points due to the cyclic nature of the loading regime. Because of this, both reactive dynamic beams suffered a small loss in ultimate flexural strength while one of the non-reactive dynamic beams failed prematurely during the experiment. Figures 4.56 to 4.60 show the typical modes of failure for the reactive and non-reactive beams.

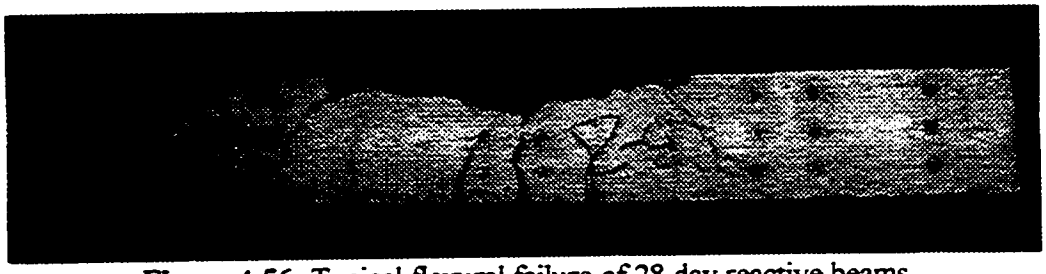

Figure 4.56: Typical flexural failure of 28 day reactive beams

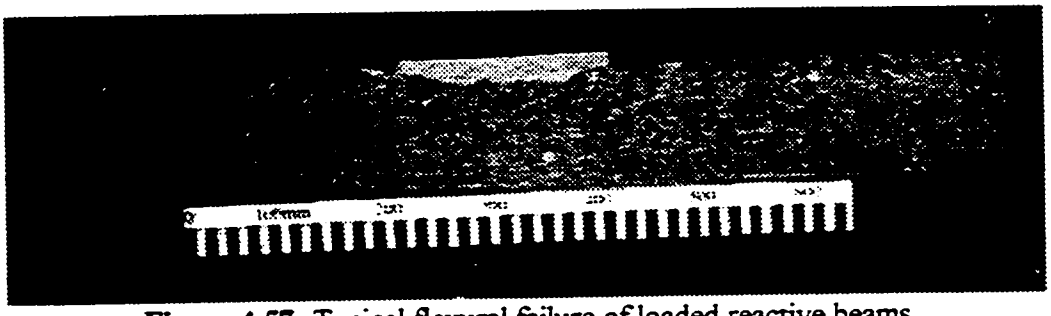

Figure 4.57: Typical flexural failure of loaded reactive beams

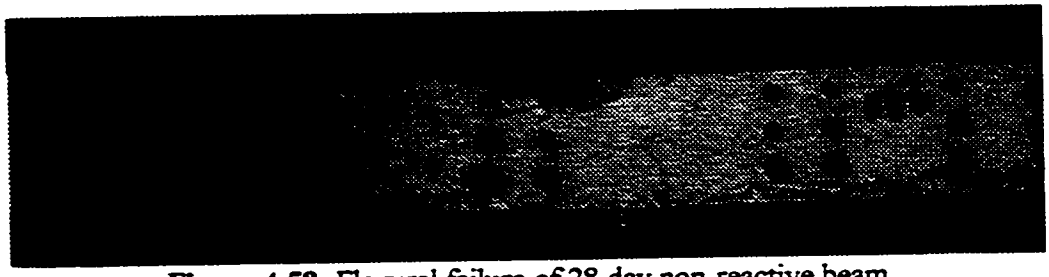

Figure 4.58: Flexural failure of 28 day non-reactive beam

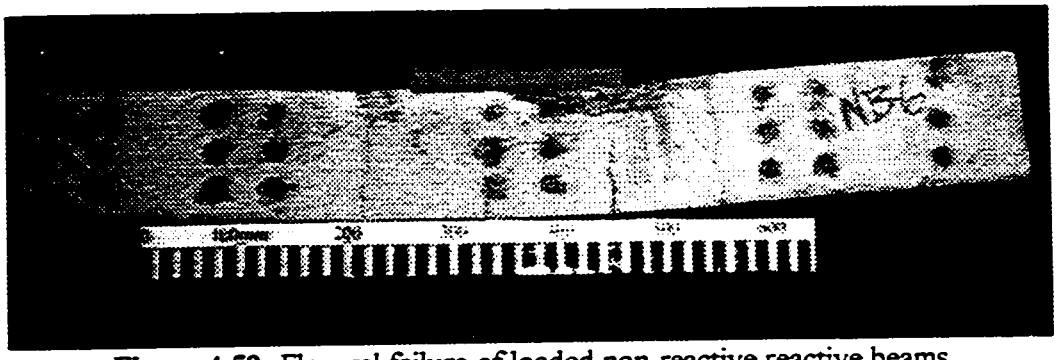

Figure 4.59: Flexural failure of loaded non-reactive reactive beams

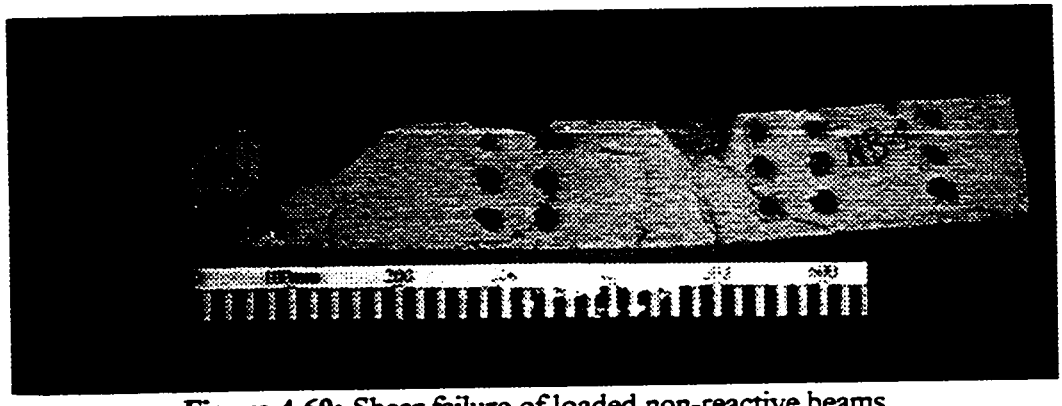

Figure 4.60: Shear failure of loaded non-reactive beams

4.5 BEHAVIOUR OF CONCRETE CYLINDERS AND PRISMS

The stress-strain relationships of the various reactive and non-reactive cylinders were obtained for comparison. Reactive and non-reactive cylinders are compared to determine the effects of the ASR on plain concrete cylinders. Non-reactive cylinders stored in sodium hydroxide are compared with non-reactive cylinders stored in lime water at the same temperature to determine the effect of the alkaline environment on the concrete. Figures 4.61 and 4.62 show the stress-strain results of the reactive and non-reactive concrete cylinders respectively, after being loaded to failure at 28 days and at the

end of testing. Figures 4.63 and 4.64 show the results of stress vs. strain for the reactive and non-reactive cylinders at 28 days and at the end of testing respectively.

Certain reactive and non-reactive cylinders were successively loaded to half of the ultimate load and then unloaded to determine the effects of ASR on the stiffness of plain concrete. Figure 4.65 shows the results of the stiffness degradation tests for various reactive and non-reactive cylinders.

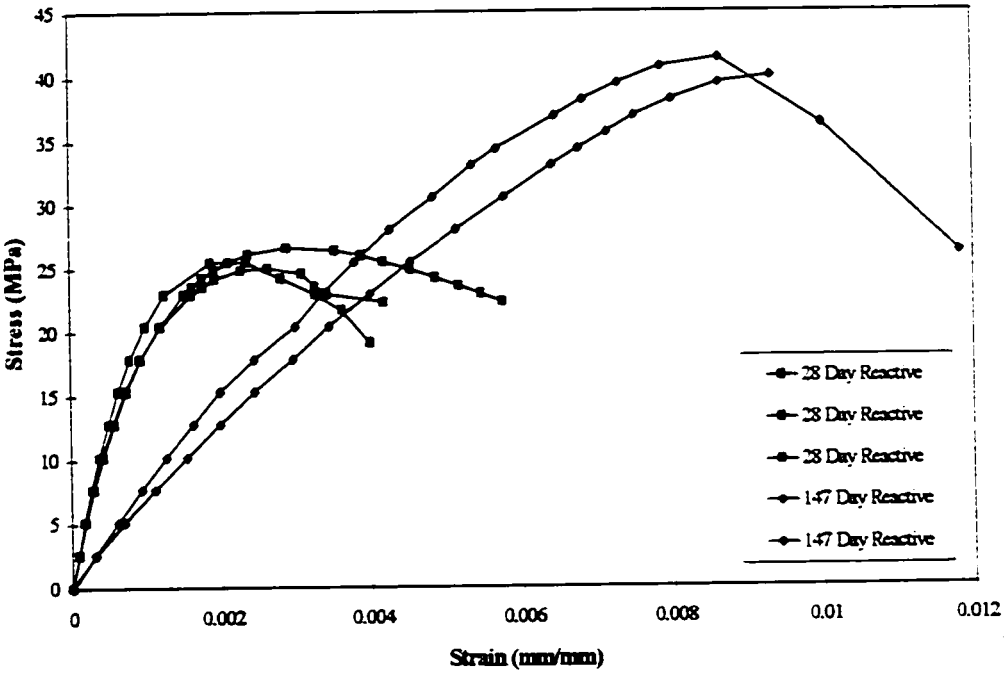

Figure 4.61: Stress vs. strain for various reactive cylinders

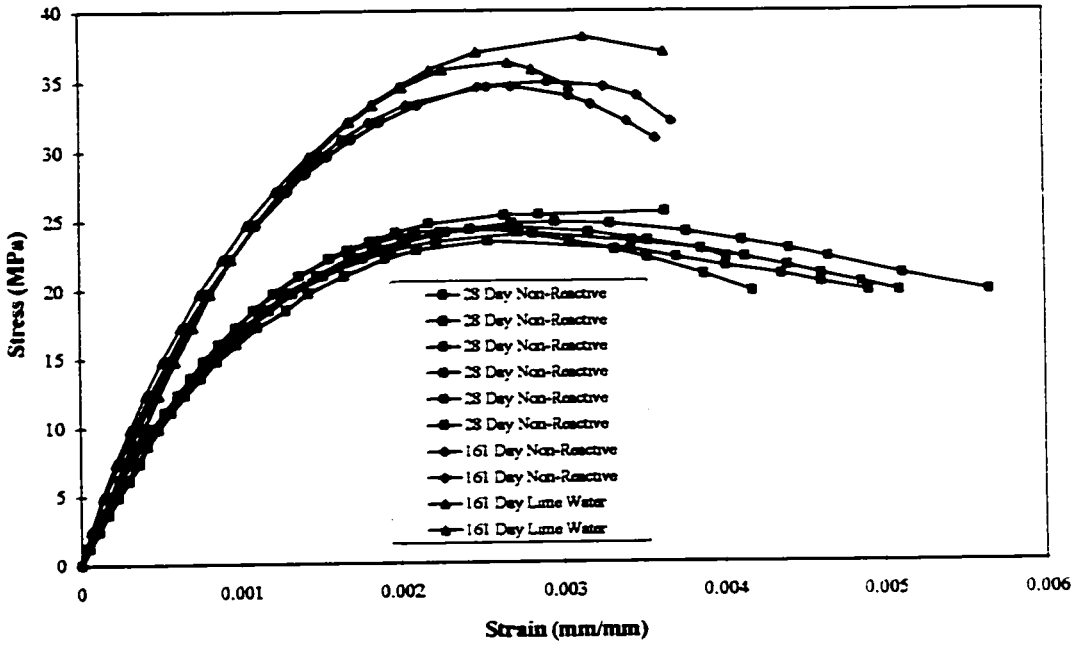

Figure 4.62: Stress vs. strain for various non-reactive cylinders

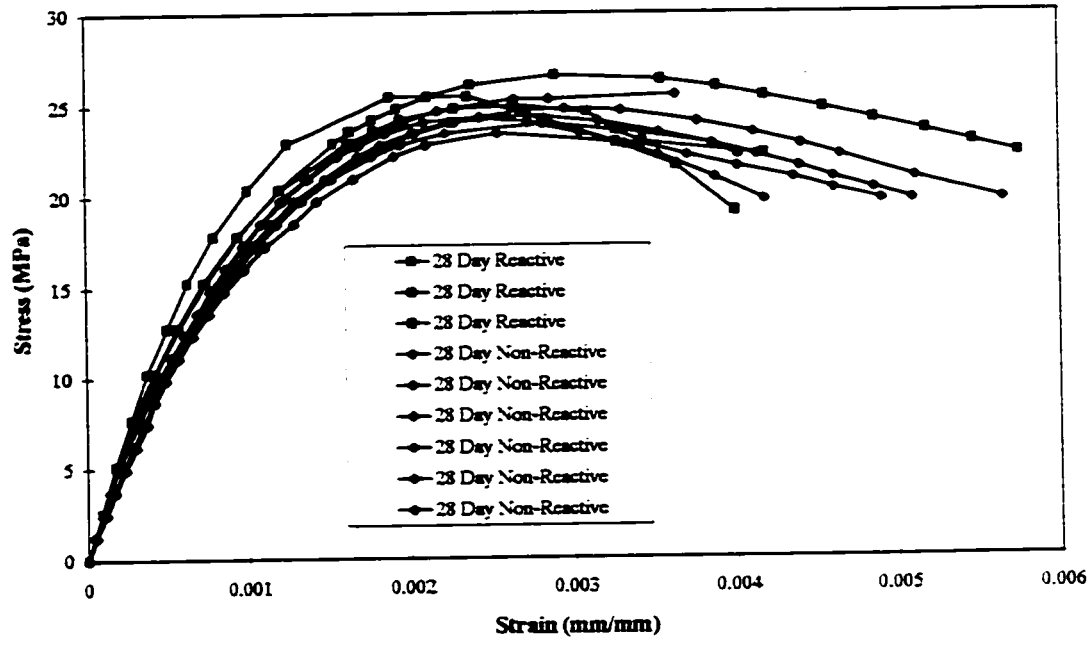

Figure 4.63: Stress vs. strain at 28 days for reactive and non-reactive cylinders

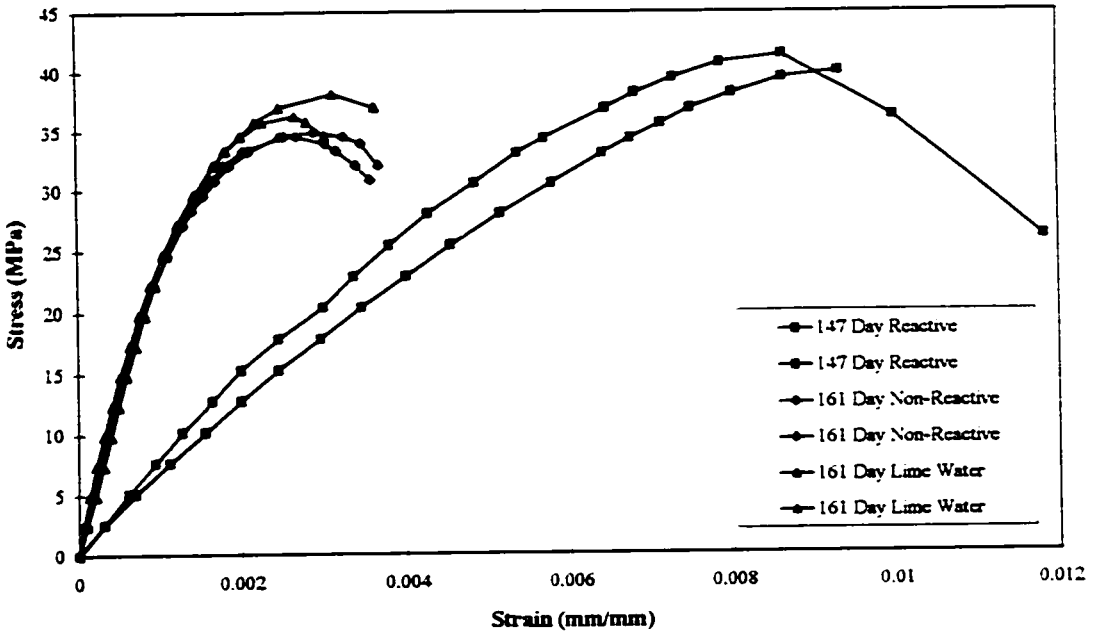

Figure 4.64: Stress vs. strain at the end of the testing for reactive, non-reactive and lime water cylinders

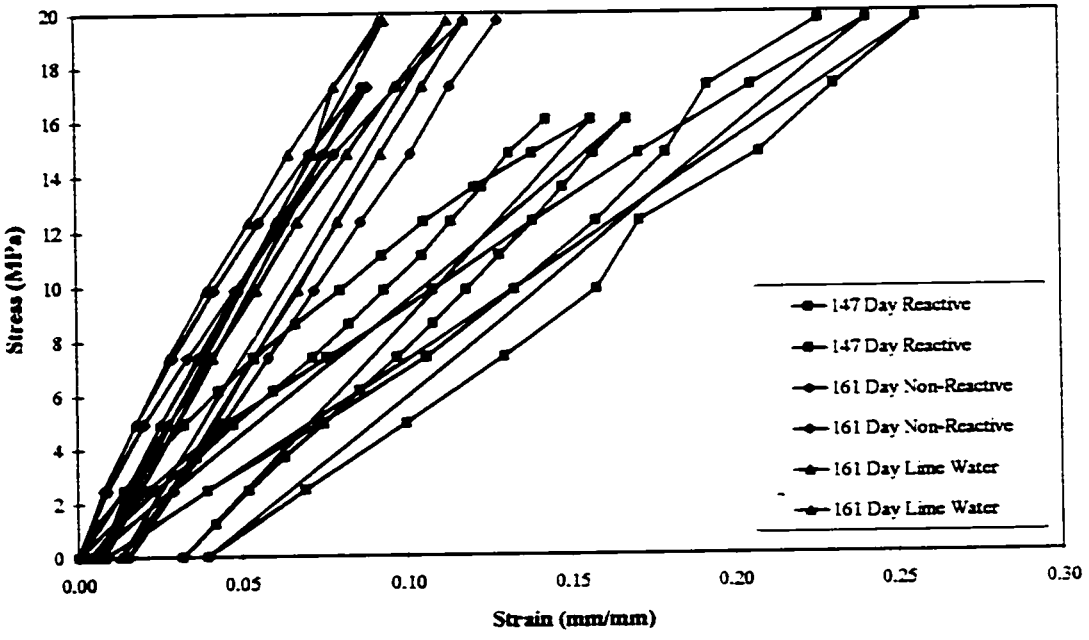

Figure 4.65: Stiffness reduction for reactive, non-reactive and lime water cylinders

The static and dynamic moduli of elasticity, the ultimate compressive strength of the concrete cylinders and the ultimate flexural strength of the resonant frequency prisms were obtained after the completion of testing of all the reactive and non-reactive specimens. Tables 4.3 and 4.4 show the results of ultimate compressive and flexural strengths of the reactive and non-reactive concrete cylinders and resonant frequency prisms. Table 4.5 shows the static and dynamic moduli of elasticity for the reactive and non-reactive concretes.

Table 4.3: Compressive strength of reactive, non-reactive and lime water concrete

Cylinder	Time of Testing	Compressive Strength, f'c (MPa)
RC-1	28 days reactive	25.5
RC-2	28 days reactive	25.8
RC-3	28 days reactive	28.8
RC-4	28 days reactive	26.3
RC-16	28 days reactive	25.0
RC-17	28 days reactive	26.6
RC-7	147 days reactive	40.5
RC-8	147 days reactive	41.4
RC-9	147 days reactive	38.3
RC-10	147 days reactive	40.0
NC-1	28 days non-reactive	24.8
NC-3	28 days non-reactive	24.3
NC-4	28 days non-reactive	25.5
NC-11	28 days non-reactive	24.4
NC-13	28 days non-reactive	23.4
NC-15	28 days non-reactive	24.0
NC-2	161 days non-reactive	32.7
NC-5	161 days non-reactive	34.6
NC-6	161 days non-reactive (stored in lime water)	38.1
NC-8	161 days non-reactive (stored in lime water)	37.9
NC-9	161 days non-reactive (stored in lime water)	36.3
NC-10	161 days non-reactive (stored in lime water)	37.4
NC-12	161 days non-reactive	34.9
NC-14	161 days non-reactive	32.7

Table 4.4: Plain Concrete Prism Flexural Strengths for reactive and non-reactive prisms

Prism	Time of Testing	Ultimate Flexural Strength
RP-1	28 days reactive	5.7
RP-2	28 days reactive	6.6
RP-3	28 days reactive	5.9
RP-4	28 days reactive	5.9
RP-6	147 days reactive	4.4
RP-7	147 days reactive	3.6
RP-8	147 days reactive	4.4
NP-1	28 days non-reactive	5.2
NP-2	28 days non-reactive	5.2
NP-7	28 days non-reactive	4.4
NP-8	28 days non-reactive	4.5
NP-3	161 days non-reactive	7.2
NP-4	161 days non-reactive	6.3
NP-5	161 days non-reactive	5.7
NP-6	161 days non-reactive	6.1

Table 4.5: Static and dynamic moduli of elasticity for reactive and non-reactive cylinders

Type of Cylinder	Static Modulus of Elasticity (MPa)	Dynamic Modulus of Elasticity (MPa)
28 Day Reactive	20 000	38 500
147 Day Reactive	6 450	35 000
28 Day Non-Reactive	20 000	39 000
161 Day Non-Reactive	26 700	43 000
161 Day Lime water	26 700	——

CHAPTER 5

DISCUSSION

The following chapter discusses the results presented in Chapter 4 and is divided into four sections dealing with expansions, damage rating indices, the structural behaviour of beams and the behaviour of plain concrete specimens respectively.

5.1 EXPANSIONS

The following section discusses the expansion results of the reactive and non-reactive specimens presented in Section 4.2.

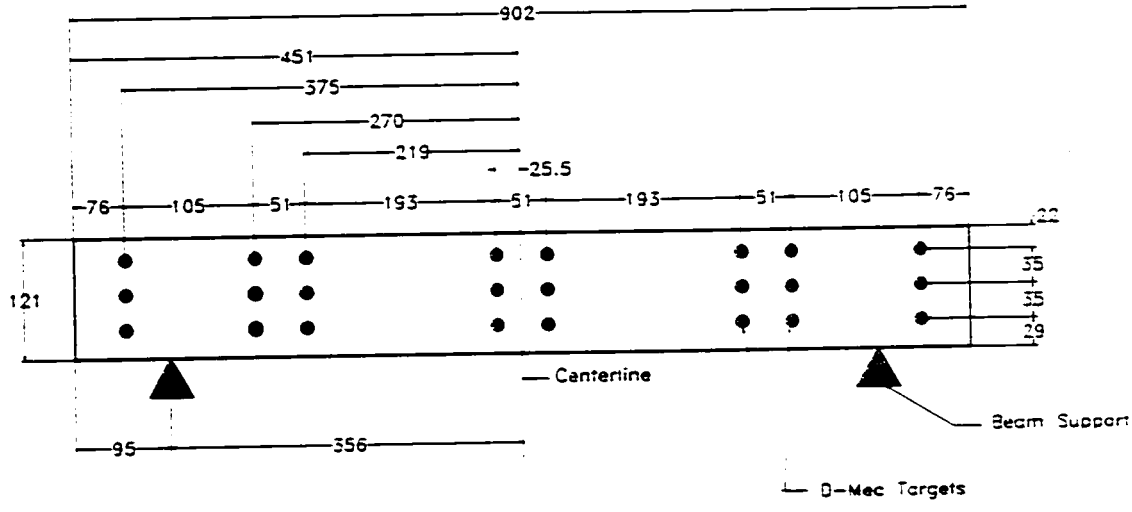

Figure 5.1: Layout of Demec targets used for expansion measurements

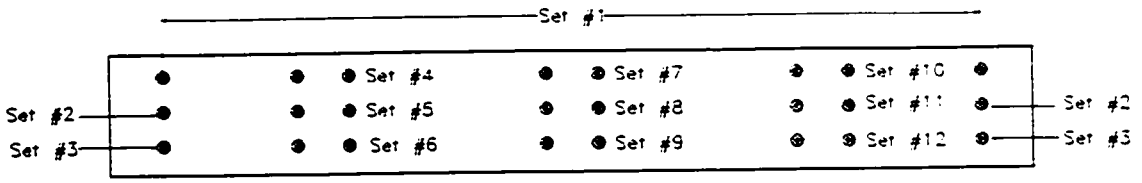

Figure 5.2: Demec targets used for horizontal expansion measurements

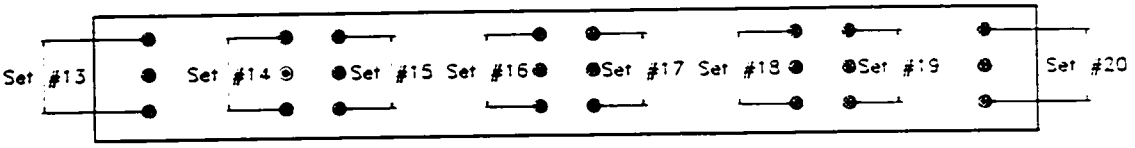

Figure 5.3: Demec targets used for vertical expansion measurements

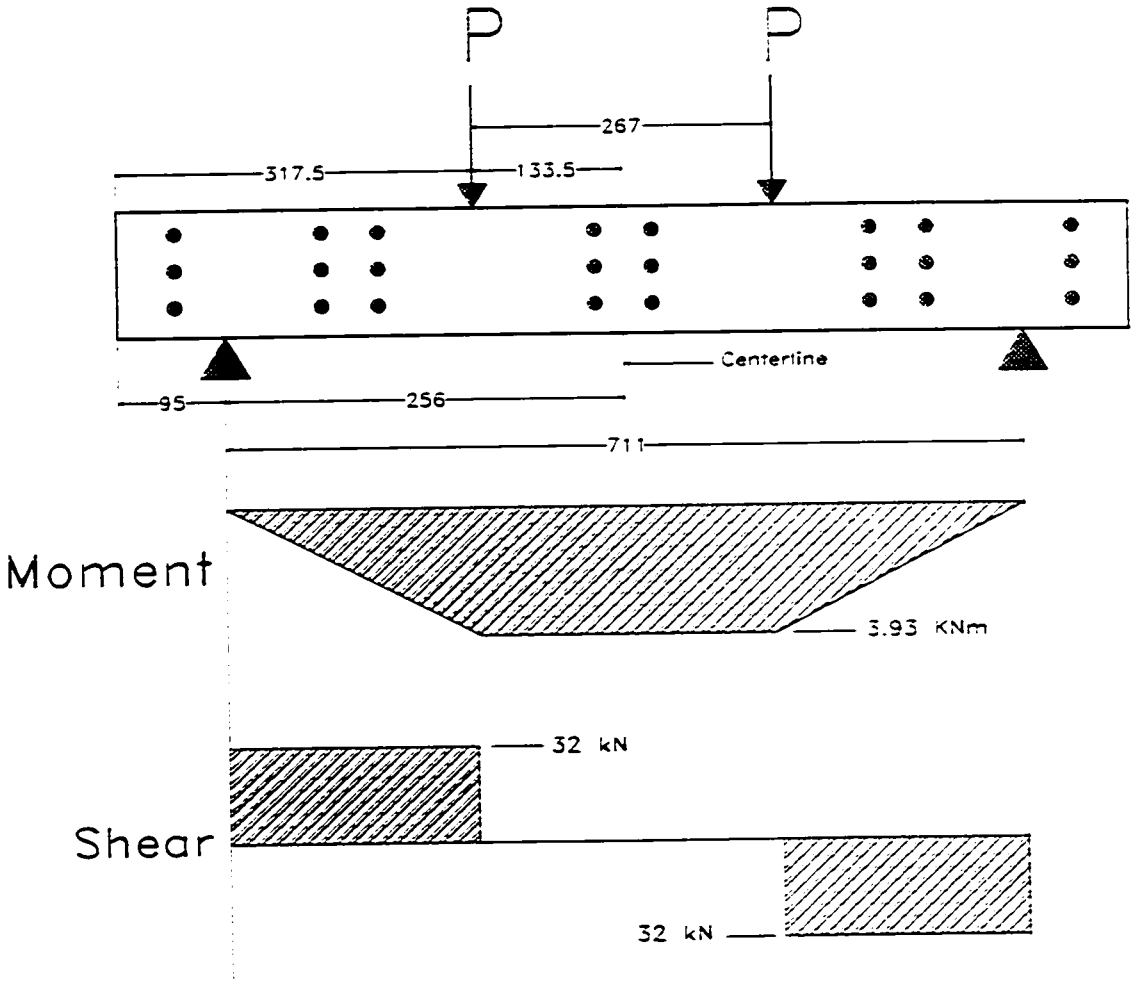

Figure 5.4: Beam loading arrangement with bending moment and shear force diagrams

5.1.1 Unloaded Beam Expansions

The top overall Demec location of the unloaded beams (Figure 4.5, Table 5.1) displayed significantly more expansion than the middle and bottom overall locations. Expansions at the top of the unloaded beams were similar to those of the plain concrete cylinders which suggests that the ASR affected the top of the unloaded beams similarly to unrestrained concrete.

The expansions at the top of the beams are 3.7 times larger than those at the steel level. This behaviour corresponds with previously published results (Swamy et al. 1989).

The difference in expansion between the top and the bottom of the beams caused an upward beam deflection of approximately 5 mm. The variation in expansion from the top to the bottom of the unloaded beams is linear.

Table 5.1: Unloaded beam overall horizontal expansions

Expansion measurement	**Average expansion at 147 days (%)**	**% difference with average cylinder expansion at 147 days**
Cylinders	0.34	----
Top (set 1)	0.33	-2.9
Middle (set 2)	0.21	-38.2
Bottom (set 3)	0.09	-73.5

The expansions at the mid-span Demec locations in the unloaded beams (Figure 4.6, Table 5.2) exhibited a similar behaviour to the overall horizontal expansions. The top mid span expansions are slightly larger than the top overall expansions. The differences in expansion between the top, middle and bottom mid span locations are larger than those of the unloaded overall horizontal beam expansions.

The relationship between the horizontal expansions and the vertical position of the expansion measurements at the mid span of the unloaded beams is not linear as is the case with the overall expansions.

Table 5.2: Unloaded beam mid-span horizontal expansions

Expansion measurement	Average expansion at 147 days (%)	% difference with average cylinder expansion at 147 days
Cylinders	0.34	-----
Top (set 7)	0.39	14.7
Middle (set 8)	0.14	-58.8
Bottom (set 9)	0.05	-85.3

The vertical expansions at the ends of the unloaded beams (Figure 4.10, Table 5.3) were smaller than those at the mid span. The center portion of the beams did not contain shear stirrups while the rest of the beams contained shear reinforcement. This would explain why the vertical expansions at the mid span of the beams where very similar to those of the cylinders. The shear reinforcement provided restraint to expansion where present throughout the beams.

Table 5.3: Unloaded beam vertical expansions

Expansion measurement	Average expansion at 147 days (%)	% difference with average cylinder expansion at 147 days
Cylinders	0.34	-----
Left Side (set 13)	0.26	-23.5
Middle (avg. sets 16, 17)	0.34	0
Right Side (set 20)	0.23	-32.4

5.1.2 Statically loaded Beam Expansions

Similarly to the unloaded beams, the top overall horizontal expansions of the statically loaded beams varied from top to bottom. However, the variation between the top and the bottom expansions is smaller than that of the unloaded beams. This suggests that the compressive stresses from the constant static load applied to the beams during testing had a restraining effect on the ASR expansions at the top of the beams. Figure 4.11 and Table 5.4 show the overall statically loaded beam expansions.

The top expansions of the statically loaded beams are significantly lower than the free expansions (and the unloaded beams) demonstrating a significant reduction in ASR expansions due to compressive top fiber stresses. However, the bottom expansions are similar to those of the unloaded beams suggesting that the tensile stress from the applied load has little effect on expansions due to ASR.

Similarly to the unloaded beams, the rate of change in expansion from the top to the bottom of the statically loaded beams is basically linear.

Table 5.4: Statically loaded beam overall horizontal expansions

Expansion measurement	Average expansion at 147 days (%)	% difference with average cylinder expansion at 147 days
Cylinders	0.34	----
Top (set 1)	0.185	-45.6
Middle (set 2)	0.135	-60.3
Bottom (set 3)	0.085	-75.0

The expansions at the mid span of the statically loaded beams (Figure 4.12, Table 5.5) varied from the top to the bottom of the beams but the variation was less than that of the overall expansions.

Top expansions at the mid span location are significantly less than those of the overall top Demec location expansions. This is explained by the higher level of compressive stress at the mid span of the beams. No explanation could be found for the significant reduction in middle and bottom expansions at the mid span compared with the overall expansions of the statically loaded beams.

Table 5.5: Statically loaded beam mid-span horizontal expansions

Expansion measurement	Average expansion at 147 days (%)	% difference with average cylinder expansion at 147 days
Cylinders	0.34	----
Top (set 7)	0.11	-67.6
Middle (set 8)	0.035	-89.7
Bottom (set 9)	0.045	-86.8

The mid span vertical expansions of the statically loaded beams (Figure 4.16, Table 5.6)) are similar to the cylinder expansions. As with the unloaded beams this demonstrates the restraint provided by the shear stirrups. At the mid span where no stirrups were used, the vertical expansions were very similar to the unrestrained expansions of the reactive cylinders.

Table 5.6: Statically loaded beam vertical expansions

Expansion measurement	Average expansion at 147 days (%)	% difference with average cylinder expansion at 147 days
Cylinders	0.34	-----
Left Side (set 13)	0.25	-26.5
Middle (avg. sets 16, 17)	0.35	2.9
Right Side (set 20)	0.20	-41.2

5.1.3 Dynamically loaded Beam Expansions

Due to the formation of large cracks directly under the loading points of the dynamically loaded beams, the overall expansion measurements could not be compared. These cracks formed due to the crushing of the concrete directly under the loading points. After repeated cycles of loading and unloading, large cracks formed at the damaged areas under the loading points. Once these cracks had formed, some permanent bending deformation occurred at the cracks. For this reason, the overall expansion measurements of the dynamically loaded beams are of no value and will not be discussed any further.

The mid-span horizontal expansions (Figure 4.18, Table 5.7) were measured at Demec points located in between the loading points. Similar to the other loading regimes, the top expansions at the mid span of the beams was larger than the middle and bottom expansions. It appears that the permanent deformation of these beams had little effect on the expansions due to ASR.

In the unloaded and statically loaded beams, the bottom expansions were typically lower than those at the middle Demec locations. The mid-span expansions of the dynamically loaded beams show the middle and bottom expansions to be similar (Figure 4.18, Table 5.7). This suggests that the dynamic load may have promoted additional

expansion at the reinforcing steel level of the beams (bottom). The additional expansions at the steel level may be caused by additional microcracking due to the cyclic nature of the load and a loss of bond between the steel and the concrete (due to a combination of effects from ASR and the dynamic loading).

Table 5.7: Dynamically loaded beam mid-span horizontal expansions

Expansion measurement	Average expansion at 147 days (%)	% difference with average cylinder expansion at 147 days
Cylinders	0.34	----
Top (set 7)	0.19	-44.1
Middle (set 8)	0.125	-63.2
Bottom (set 9)	0.12	-64.7

The vertical expansions of the dynamically loaded beams (Figure 4.22, Table 5.8) are higher in the mid span of the beams than in the end regions. Again this is due to the absence of transverse shear reinforcement in the mid span of the beams. The difference in expansion between the mid span and the ends of the dynamically loaded beams may be partly caused by the restraint due to flexural loading at the mid span. It has been documented that in cases where compressive restraint is provided in one direction, concrete expansions due to ASR may be larger in directions perpendicular to the restraint. This may be occurring in the loaded beams where flexural loading as well as reinforcement is providing restraint to longitudinal expansion. However, the middle portion of the beams did not have shear stirrups which may also explain the larger expansions at the mid span than at the ends.

Table 5.8: Dynamically loaded beam vertical expansions

Expansion measurement	Average expansion at 147 days (%)	% difference with average cylinder expansion at 147 days
Cylinders	0.34	----
Left Side (set 13)	0.26	-23.5
Middle (avg. sets 16, 17)	0.35	2.9
Right Side (set 20)	0.20	-41.2

5.1.4 Comparison of Various Beam Expansions

As expected, the unloaded beams exhibited larger expansions at the top than the loaded beams (Figure 4.23, Table 5.9). The static load provided active restraint to ASR expansions.

The unloaded beams exhibited expansions similar to those of the plain cylinders while the static beam expansions were almost half of the unloaded ones. However the expansions of the statically loaded beams were still significantly large. The dynamic expansions are not discussed due to the permanent deformations of the dynamically loaded beams previously mentioned in this chapter.

Table 5.9: Top overall expansions for various beams (set 1)

Expansion measurement	Average expansion at 147 days (%)	% difference with unloaded beam expansions at 147 days	% difference with average cylinder expansion at 147 days
Cylinders	0.34	-----	-----
Unloaded	0.33	-----	-2.9
Static	0.185	-44.0	-45.6
Dynamic	0.095	-71.2	-72.1

The middle overall expansions of the various beams (Figure 4.24, Table 5.10) exhibited a similar trend to the top overall expansions. The unloaded beam expansions were highest followed by the statically loaded beam expansions which were two thirds those of the unloaded expansions. Once again, the dynamically loaded beam expansions are not discussed due to the permanent bending deformation of these beams which occurred during the testing.

Table 5.10: Middle overall expansions for various beams (set 2)

Expansion measurement	Average expansion at 147 days (%)	% difference with unloaded beam expansions at 147 days	% difference with average cylinder expansion at 147 days
Cylinders	0.34	-----	-----
Unloaded	0.21	-----	-38.2
Static	0.135	-35.7	-60.3
Dynamic	0.07	-66.7	-79.4

The bottom overall expansions (Figure 4.25, Table 5.11) for the unloaded and statically loaded beams are very similar. This suggests that tensile forces in reinforced concrete do not promote ASR. However, many in service reinforced concrete members are cracked at the tension fiber under service load. These cracks may allow the ingress of moisture into the concrete and promote or accelerate the reaction. This did not occur in the experimental specimens as all of the beams were continuously saturated and cracking of the loaded beams did not significantly increase the entry of moisture into the concrete.

As with the previous two Demec locations (top and middle), the overall expansions of the dynamically loaded beams are not discussed because of the inaccuracy of the results caused by the deformation of these beams.

Table 5.11: Bottom overall expansions for various beams (set 3)

Expansion measurement	Average expansion at 147 days (%)	% difference with unloaded beam expansions at 147 days	% difference with average cylinder expansion at 147 days
Cylinders	0.34	-----	-----
Unloaded	0.095	-----	-72.1
Static	0.09	-5.3	-73.5
Dynamic	0.055	-42.1	-83.8

The top mid-span expansions (Figure 4.26, Table 5.12) of the unloaded beams were slightly larger than the cylinder free expansions. This difference (10.3%) may be within a normal error range. However, as previously discussed, the bending moment caused by the differential expansions between the top and the bottom of the unloaded beams is higher at the mid span of the beams. This upward bending moment may have caused some additional expansion at the top of the beams.

The statically and dynamically loaded beams displayed less expansion than the unloaded ones with the statically loaded beams showing the least expansion of all the specimens. This suggests that restraint from the applied flexural loading reduced expansions from ASR. However, the expansions at the top of the statically loaded beams were still large enough to cause the cracking of the concrete.

Table 5.12: Top mid-span expansions for various beams (set 7)

Expansion measurement	Average expansion at 147 days (%)	% difference with unloaded beam expansions at 147 days	% difference with average cylinder expansion at 147 days
Cylinders	0.34	----	----
Unloaded	0.375	----	10.3
Static	0.105	-79.4	-69.1
Dynamic	0.18	-57.4	-47.1

The middle horizontal expansions (Figure 4.27, Table 5.13) at the mid span of the unloaded and dynamically loaded beams are similar. The expansions at this location for the statically loaded beams are lower than the other two loading regimes. The middle Demec locations are situated near the neutral axis of the beams. The compressive force caused by flexural loading at this level is very low. This suggests that the amount of restraint required to significantly reduce ASR is relatively low. The static load provided greater restraint than the dynamic load which is explained by the larger compressive stress with time provided by the static load.

Table 5.13: Middle mid-span expansions for various beams (set 8)

Expansion measurement	Average expansion at 147 days (%)	% difference with unloaded beam expansions at 147 days	% difference with average cylinder expansion at 147 days
Cylinders	0.34	----	----
Unloaded	0.145	----	-57.4
Static	0.03	-79.3	-91.2
Dynamic	0.12	-17.2	-64.7

The bottom mid-span expansions (Figure 4.28, Table 5.14) are not significantly affected by the static loading. The dynamic cycles of load seem to promote ASR expansions. This may partly be caused by bond failure between the concrete and the reinforcing steel occurring during the repeated cycles of loading and unloading.

Table 5.14: Bottom mid-span expansions for various beams (set 9)

Expansion measurement	Average expansion at 147 days (%)	% difference with unloaded beam expansions at 147 days	% difference with average cylinder expansion at 147 days
Cylinders	0.34	----	----
Unloaded	0.06	----	-82.4
Static	0.045	-25	-86.8
Dynamic	0.13	116.7	-61.8

It appears that stresses due to flexural loading may increase the vertical expansions in the beams (Figures 4.29 to 4.32, Tables 5.15 to 5.18). However, the variation between the end and mid-span vertical expansions of the various beams could be explained by the absence of shear stirrups in the beam mid-spans. Thus, the exact effect of the load and loading condition on vertical expansion is not clear.

Table 5.15: Vertical expansions for extreme left hand side of various beams (Set 13)

Expansion measurement	Average expansion at 147 days (%)	% difference with unloaded beam expansions at 147 days	% difference with average cylinder expansion at 147 days
Cylinders	0.34	----	----
Unloaded	0.21	----	-38.2
Static	0.185	-11.9	-45.6
Dynamic	0.25	19.0	-26.5

Table 5.16: Vertical expansions for extreme right hand side of various beams (Set 20)

Expansion measurement	Average expansion at 147 days (%)	% difference with unloaded beam expansions at 147 days	% difference with average cylinder expansion at 147 days
Cylinders	0.34	----	----
Unloaded	0.26	----	-23.5
Static	0.23	-11.5	-32.4
Dynamic	0.27	3.8	-20.6

Table 5.17: Vertical expansions for mid-span of various beams (Set 16)

Expansion measurement	Average expansion at 147 days (%)	% difference with unloaded beam expansions at 147 days	% difference with average cylinder expansion at 147 days
Cylinders	0.34	-----	-----
Unloaded	0.30	-----	-11.8
Static	0.36	20.0	5.9
Dynamic	0.42	40.0	23.5

Table 5.18: Vertical expansions for mid-span of various beams (Set 17)

Expansion measurement	Average expansion at 147 days (%)	% difference with unloaded beam expansions at 147 days	% difference with average cylinder expansion at 147 days
Cylinders	0.34	-----	-----
Unloaded	0.32	-----	-5.9
Static	0.33	3.1	-2.9
Dynamic	0.39	21.9	15.7

The vertical expansions at the mid-span (Figures 4.33 to 4.35, Tables 5.19 to 5.21) of the beams are similar to those of the cylinders. This would suggest free vertical expansions of the concrete at this location. The top horizontal expansions vary from being slightly larger than the vertical and cylinder expansions in the unloaded beams to being smaller in the loaded beams (as expected due to restraint). Vertical expansions were much larger than the middle and bottom horizontal mid-span expansions at the same locations.

Table 5.19: Vertical and horizontal expansions at the mid-span of the unloaded beams

Expansion measurement	Average expansion at 147 days (%)	% difference with average cylinder expansion at 147 days
Cylinders	0.34	-----
Top (set 7)	0.39	14.7
Vertical (avg. sets 16, 17)	0.325	-4.4
Middle (set 8)	0.14	-58.8
Bottom (set 9)	0.06	-82.4

Table 5.20: Vertical and horizontal expansions at the mid-span of the static beams

Expansion measurement	Average expansion at 147 days (%)	% difference with average cylinder expansion at 147 days
Cylinders	0.34	----
Top (set 7)	0.11	-67.6
Vertical (avg. sets 16, 17)	0.325	-4.4
Middle (set 8)	0.03	-91.2
Bottom (set 9)	0.04	-88.2

Table 5.21: Vertical and horizontal expansions at the mid-span of the dynamic beams

Expansion measurement	Average expansion at 147 days (%)	% difference with average cylinder expansion at 147 days
Cylinders	0.34	----
Top (set 7)	0.19	-44.1
Vertical (avg. sets 16, 17)	0.325	-4.4
Middle (set 8)	0.12	-64.7
Bottom (set 9)	0.11	-67.6

5.1.5 Expansion of Non-Reactive Control Specimens

Non-reactive control specimens (Tables 4.1 and 4.2) were tested to help in determining the presence of any non-ASR strains which may have occurred during the loading of the reactive specimens. Tables 4.1 and 4.2 display the strain measurement results obtained from the non-reactive specimens. The non-reactive CSA prisms displayed near zero strains indicating that the concrete used for the non-reactive controls was non-expansive.

All of the non-reactive specimens tested in NaOH at 38°C (the same storage environment as the reactive specimens) displayed negligible permanent strains. This confirmed that the ASR expansions measured in the reactive specimens were not

significantly affected by other strains such as the stiffness loss in the dynamically loaded beams and creep strains in the statically loaded beams.

5.1.6 Cylinder and CSA Prism Expansions and Resonant Frequency Prisms

Referring to Figure 4.36 and Table 5.19, it can be observed that the reactive concrete cylinders cured in NaOH exhibit much more expansion than the reactive CSA prisms during the first 104 days of testing. After this period, the rate of expansion in the CSA prisms increased dramatically while the cylinders' rate of expansion dropped slightly during the same amount of time. The time taken to reach the CSA expansion limit of 0.04% was 72 days in the concrete prisms and 35 days in the cylinders.

There is also a relationship between the reactive cylinder and prism expansions and the resonant frequency of the reactive concrete since the latter dropped as the expansions of the concrete increased. The dynamic modulus of elasticity increased over the first 20 days of the experiment and then decreased significantly during the remainder of the duration (Figure 4.37). In the early stages of the experiment, expansions are more sensitive in detecting ASR than the resonant frequency. This is due to an increase in resonant frequency in the beginning of the experiment due to a gain in concrete strength in the early stages of curing..

Table 5.22: Reactive cylinder and prism expansions

Specimen	Period (days)	Expansion (%)	Rate of Expansion (% per day)
Cylinders	0-104	0.29	0.0028
Prisms	0-104	0.06	0.0006
Cylinders	104-147	0.34	0.0012
Prisms	104-147	0.34	0.0065

5.1.7 Reactive and Non-Reactive Concrete Resonant Frequency Prisms

The resonant frequency of the reactive prisms (Figure 4.37) increased during the first 20 days of storage and subsequently dropped for the remainder of the experiment.

The resonant frequency of the non-reactive prisms increased during the first 60 days of storage and dropped slightly for the remainder of the experiment. These results indicate that while the resonant frequency is affected by damage of concrete by ASR, the curing of the concrete in NaOH also has an effect on the resonant frequency of non-reactive concrete. However, the effect of NaOH on the resonance frequency of the non-reactive concrete was small.

5.1.8 Cracking of Beams

The unloaded reactive beams exhibited cracking visible mostly above the beams' vertical center (Figure 4.38). This cracking was relatively homogeneous throughout the beams. The loaded reactive beams all exhibited cracking above their centroids but the cracking occurred with less frequency than the in unloaded beams (Figures 4.39 and 4.40). The cracks were mostly horizontal, parallel to the direction of stresses due to loading. The statically loaded beams suffered the least cracking (Figure 4.39), suggesting that the nature of the dynamic loading accelerated the ASR and caused additional cracking due to the load cycles.

The non-reactive beams displayed no visible surface cracking other than the shear and flexure cracking caused by loading the specimens.

5.2 DAMAGE RATING INDICES

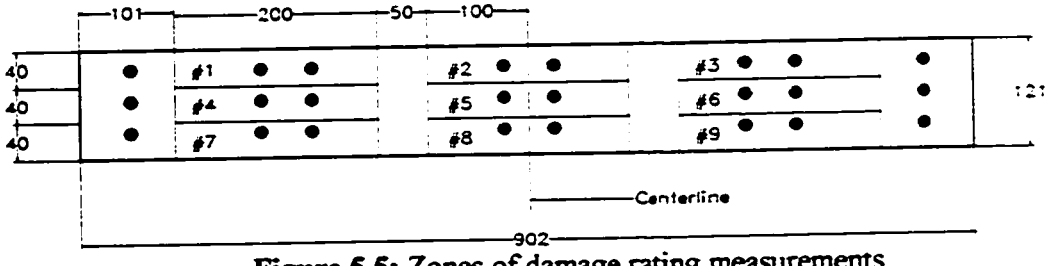

Figure 5.5: Zones of damage rating measurements

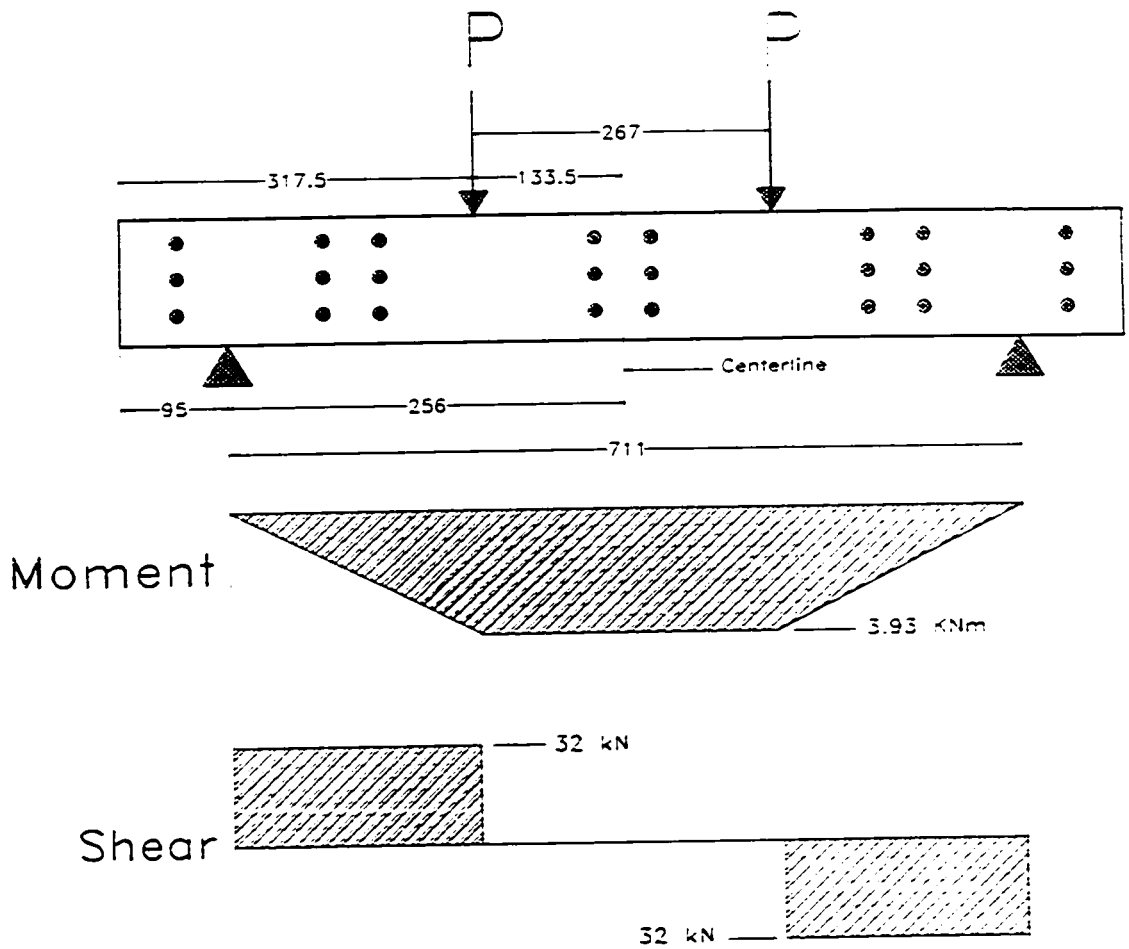

Figure 5.6: Beam Loading Diagrams

The damage rating results shown in Figures 4.42 to 4.47 display a definite difference between the top and middle DRI and the bottom DRI for all of the beams. The top DRI for the unloaded beams are much larger than the DRI for the bottom locations (resulting from larger expansions at the top of the unloaded beams). This difference also exists within the loaded beams with the differences between top and bottom DRI being smaller in the loaded beams than with the unloaded beams. This was caused by the cracking at the bottom fiber from loading of the statically loaded and dynamically loaded beams.

The DRI of the resonant frequency prism corresponds closely with the results obtained at the bottom of each of the beams.

Since the top of the unloaded reactive beams expanded similarly to the reactive plain concrete cylinders, it would be expected that these two regions would have similar DRI. However, the DRI of the reactive resonant frequency prism was lower than the values obtained from the top of the reactive unloaded beams. This strongly suggests that the damage caused by the ASR in the unloaded reinforced concrete beams is not only caused by the reaction but also by the configuration of the longitudinal reinforcement. The differential expansion, caused by the configuration of the reinforcement, in the unloaded beams caused a hogging moment in the unloaded beams. This hogging moment was large enough to cause tension cracking at the top of the reactive unloaded beams. The tension cracking from the hogging moment increased the magnitude of the DRI at the top of the reactive unloaded beams.

The DRI of the various beams for each of the three mid-span zones as shown in Figures 4.48 to 4.50 confirm a weak correlation between the damage in the concrete and expansions at the various zones. The DRI at the top of the unloaded beams are larger than those of the loaded specimens (Figure 4.48). The DRI do not provide a clear conclusion in the middle mid-span zone which is near the neutral axis of the beams (Figure 4.49). The DRI at the bottom of the beams are slightly larger in the dynamically loaded beams and are smallest in the unloaded beams (Figure 4.50). However, the bottom mid-span expansions for the unloaded and statically loaded beams were almost identical. This again shows the effect of the mechanical cracks from loading on the DRI.

There is also generally no significant difference between the DRI at the top and middle in each of the beams with the exception of the dynamically loaded beams which exhibited a slight difference between these two levels. The following table compares the DRI for each zone and each loading case.

Table 5.23: DRI for the various zones of each beam

	Zone 1	Zone 2	Zone 3	Zone 4	Zone 5	Zone 6	Zone 7	Zone 8	Zone 9
	Top			Middle			Bottom		
Unloaded	152	193	190	165	183	167	92	100	105
Unloaded	216	212	210	213	187	227	134	125	128
Static	193	175	180	202	195	190	120	140	130
Static	145	165	148	155	141	157	115	125	105
Dynamic	175	165	170	198	202	185	100	160	112
Dynamic	205	165	155	205	225	202	120	142	117
Prism	127								

5.3 STRUCTURAL BEHAVIOUR OF BEAMS

The load vs. deflection curves for the reactive and non-reactive variously loaded beams (Figures 4.51 to 4.55) show that the ultimate behaviour under load of the various beams is generally similar. The loading condition does not significantly affect the ultimate flexural behaviour of all the beams. However, the dynamically loaded reactive beams did exhibit a slightly lower ultimate flexural capacity than the other two loading cases. This is attributed to fatigue cracks formed directly under the loading points in these beams during testing.

The initial slope of the load vs. deflection curve of the non-reactive dynamically loaded beam is much lower than the slopes of the other curves (Figure 4.53). This is due to the cracking of the beams which occurred directly under the loading points during testing.

There is no significant difference between the ultimate load carrying behaviour of the various reactive and non-reactive beams except for the reactive beams loaded to failure at 28 days (Figure 4.51). This is attributed to an error in the equipment used for the

flexural loading since a different apparatus was used to load the 28 day reactive beams and the rest of the reactive and non-reactive beams. This is not attributed to any increase in strength in the reactive beams tested for 147 days but rather to the different testing apparatus used for the loading of the reactive 28 day beams and all of the other reactive and non-reactive beams.

All of the reactive beams failed in a flexural mode (even the ones with severe cracking under the loading points). The beams failed by the yielding of the reinforcing steel followed (large flexural cracks formed in the concrete) by the crushing of the concrete between the loading points (Figures 4.56 and 4.57).

Five of the non-reactive beams failed in flexure but two failed in shear (Figures 4.58 to 4.60). This showed that a prestressing effect from ASR expansions in the reactive beams may have prevented any shear failure of these beams.

Even though ASR expansions were large, the reaction's effects on the load carrying capacity of the singly reinforced simply supported concrete beams was insignificant.

The slopes of the linear portion of the load-deflection curves are given in Table 5.21. The loading regime and the ASR did have an affect on the initial stiffness of the reinforced concrete beams. This indicates that, although ASR may not be detrimental to the load carrying capacity of well detailed reinforced concrete beams, the reaction may influence the deformation charicteristics of such members.

Table 5.24: Initial stiffness of beams loaded to failure

Loading Regime	Slope of Load-Deflection Curve (KN/mm)
28 day reactive	------
28 day reactive	------
Unloaded reactive	19
Unloaded reactive	19
Statically loaded reactive	23
Statically loaded reactive	23
Dynamically loaded reactive	17
Dynamically loaded reactive	17
28 day non-reactive	17
Unloaded non-reactive	20
Unloaded non-reactive	20
Statically loaded non-reactive	30
Statically loaded non-reactive	30
Dynamically loaded non-reactive	12

Note: The low initial stiffness for the dynamically loaded non-reactive beam may be attributed to the damage of the beam at the loading points during the experiment.

5.4 BEHAVIOUR OF CONCRETE CYLINDERS AND PRISMS

5.4.1 Cylinders

The ultimate cylinder compressive strength (Table 4.2) of the reactive cylinders at the end of the experiment increased by approximately 30% from the 28 day results. Thus even if concrete strength and stiffness are affected by ASR, the increases in strength with time are much larger than the losses due to the reaction.

The strength of the reactive cylinders at the end of the experiment (147 days of testing) was slightly higher than that of the non-reactive cylinders (161 days).

The stiffness of the reactive cylinders at the end of the experiment was significantly lower than the stiffness of the 28 day reactive and all of the non-reactive cylinders (Figures 4.61 to 4.64). This was due to the cracking of the concrete by ASR.

The non-reactive concrete cylinders stored in lime water at 38 degrees Celsius had a higher compressive strength at the end of the experiment than the cylinders stored in NaOH at the same temperature. This shows that the NaOH has an effect on the compressive strength of concrete.

5.4.2 Moduli of Elasticity

Table 4.5 compares the static and dynamic moduli of elasticity of the reactive and non-reactive concretes. The static modulus of elasticity proved to be much more sensitive to the damage in concrete from ASR as the static modulus of elasticity dropped by 68% from the 28 day results while the dynamic modulus for the same concrete only dropped by 9%. Both the static and dynamic moduli of elasticity of the non-reactive concrete increased from 28 days until the end of the experiment.

5.4.3 Concrete Flexural Strength

The concrete flexural strength (Table 4.4) was significantly reduced by ASR and this reduction shows that flexural strength is more sensitive to ASR than compressive strength. However, as mentioned, this reduction is not significant to reinforced concrete as reinforcing steel is used in the tension zones of reinforced concrete members. This loss in flexural strength may affect the cracking load of the beams in turn affecting deflections but does not affect the ultimate load carrying capacity of the reinforced concrete beams.

The flexural strength of the non-reactive concrete prisms increased from 28 days to the end of the experiment.

Table 5.22 summarizes the various plain concrete properties measured from the reactive and non-reactive specimens.

Table 5.25: Concrete properties of the reactive and non-reactive specimens

Specimen	Ec (MPa)	Ed (MPa)	f'c (MPa)	fr (MPa)
28 days reactive	20 000	38 500	26	6
147 days reactive	6 450	35 500	40	4.1
28 days non-reactive	20 000	39 000	24	4.8
161 days non-reactive	26 700	43 000	34	6.3
161 days (lime water)	26 700	——	37	——

REFERENCES

Swamy, R.N., Al-Asali, M.M., 1989, "Effect of Alkali-Silica Reaction on the Structural Behavior of Reinforced Concrete Beams", ACI Structural Journal, V. 84, No. 4, American Concrete Institute.

CHAPTER 6

CONCLUSIONS

Based on the experimental work and discussion presented in the previous chapters the following conclusions can be drawn.

6.1 EXPANSIONS

After monitoring singly reinforced concrete beams, plain concrete cylinders and resonant frequency prisms made with both ASR expansive and non-reactive concretes the following conclusions are made.

a) Flexural loading had a significant effect in reducing expansions due to ASR in the top fibers of the reactive concrete beams. The static load was the most effective in reducing ASR expansions. ASR had little effect on the bottom fiber expansion of the various beams. Differential horizontal expansions between the bottom and the top of the unloaded reactive beams resulted in the hogging of the beams.

b) Steel reinforcement provided significant restraint to ASR expansion in all of the reactive beams.

c) The expansions throughout all of the beams, regardless of the restraint from reinforcing steel and flexural loading, were large enough to cause the cracking of the concrete.

d) Little or no strains from non ASR causes were measured in the non-reactive control specimens. This showed that the strains measured in the reactive specimens were predominantly due to ASR.

e) The plain concrete reactive cylinders exhibited expansions similar to the top fiber expansions of the unloaded beams and of the mid span vertical expansions of all of the reactive beams.

f) The rate of expansion of the reactive CSA prisms was initially lower than that of the reactive plain concrete cylinders but in the later stages of the experiment was significantly larger than that of the cylinders.

6.2 DAMAGE RATING INDICES

After measuring the damage rating indices of the various reactive beams and one plain concrete reactive prism the following can be concluded.

a) The reinforcing steel in the reactive beams was effective in reducing the damage to concrete from ASR as well as expansions.

b) The damage to the top of the unloaded beams was larger in the unloaded beams than in the loaded beams indicating a beneficial effect from the compressive restraint caused by flexural loading.

c) Static flexural load did not significantly increase the damage of the concrete at the bottom of the statically loaded beams. Dynamic load did slightly increase the damage to the concrete at the bottom of the dynamically loaded beams.

d) Although the expansions measured at the top of the unloaded reactive beams correspond well with the expansions of the plain reactive concrete cylinders, the DRI of the reactive resonant frequency prism is lower than those measured at the top of the beams. This indicates that extra cracking of the unloaded reactive beams was caused by the hogging of these beams caused by the differential expansions between the top and the bottom of these beams.

e) The expansion measurements were more sensitive in determining the severity of ASR than the DRI measurements.

f) The resonant frequency prism showed almost no debonding of aggregate particles. Much of the debonding of the coarse aggregate particles in the beams was caused by mechanical cracking of the beams from the loading and the hogging caused by differential expansions.

g) The cracking of concrete by ASR may contribute to other durability problems like reinforcing steel corrosion and freeze thaw of concrete.

6.3 STRUCTURAL BEHAVIOUR OF THE BEAMS

Following the loading of the reactive and non-reactive specimens to their ultimate flexural strength the following conclusions were drawn.

a) The alkali silica reaction does not reduce the ultimate load carrying capacity of simply supported, singly reinforced concrete beams.

b) The alkali silica reaction may reduce the initial stiffness of reactive reinforced concrete beams.

6.4 BEHAVIOUR OF PLAIN CONCRETE SPECIMENS

Comparing the load carrying behaviours of the plain concrete specimens the following conclusions were made.

a) Expansions from the alkali-silica reaction did not prevent the increase of concrete cylinder compressive strength with time.

b) The compressive strength of the reactive cylinders was higher than the non-reactive cylinders stored in NaOH but similar to the cylinders stored in lime water.

c) Concrete cracking caused by ASR expansions significantly reduced the stiffness of the reactive concrete cylinders.

d) The dynamic modulus of elasticity is much less sensitive to the effects of ASR than the static modulus of elasticity.

e) The flexural strength of concrete was reduced by ASR expansions and proved to be more sensitive to ASR than the compressive strength.

f) The compressive strength of the non-reactive concrete cylinders stored in NaOH was lower than that of the cylinders stored in lime water.

APPENDIX A

CHARACTERIZATION OF MATERIALS

Supplementary information regarding aggregates, cement and reinforcing steel used for the construction of all test specimens is presented in the following sections.

A.1 AGGREGATE DATA

A.1.1 Spratt Aggregate Reactivity

Spratt limestone is a well known, highly reactive (ASR) aggregate. It is a hard limestone containing microcrystalline quartz which has proven to be susceptible to alkalis normally found in ordinary Portland cement concretes. The following are the results of an extensive interlaboratory study on the reactivity of Spratt limestone. It should also be noted that the Ministry of Transportation of Ontario stockpiles and specifies Spratt limestone for the control aggregate used in the CSA Concrete Prism Test (CSA A23.2-14A, for the determination of potential ASR susceptibility of aggregates).

Also included in this section (Figures A1 and A2) are the results of preliminary CSA concrete prism and accelerated mortar bar test performed on the coarse and fine Spratt aggregates prior to the beginning of the experimental program. This was done to ensure the reactivity of the aggregates and aggregate mix used in the experiment.

Due to the aggressive nature of the beam specimen testing environment a highly non-reactive aggregate had to be found in order to ensure the success of the non-reactive control specimens.

It was also desirable to use an aggregate of similar composition as the Spratt aggregate used in the reactive specimens. The aggregate chosen was an inert limestone found originally in Newfoundland. This aggregate has previously been used in non-reactive control specimens in the laboratories at CANMET and found to be non-reactive. This limestone was used for both the coarse and fine aggregates in the non-reactive mixes.

A quartz sand was used in both the reactive and non-reactive concrete mixes. The sand was blended with the Spratt and non-reactive crusher fines to produce fine aggregates with a suitable gradation for concrete.

Accelerated mortar bar tests were performed using the quartz sand to determine its potential for ASR reactivity to ensure the sands inertness for use in the non-reactive control specimens.

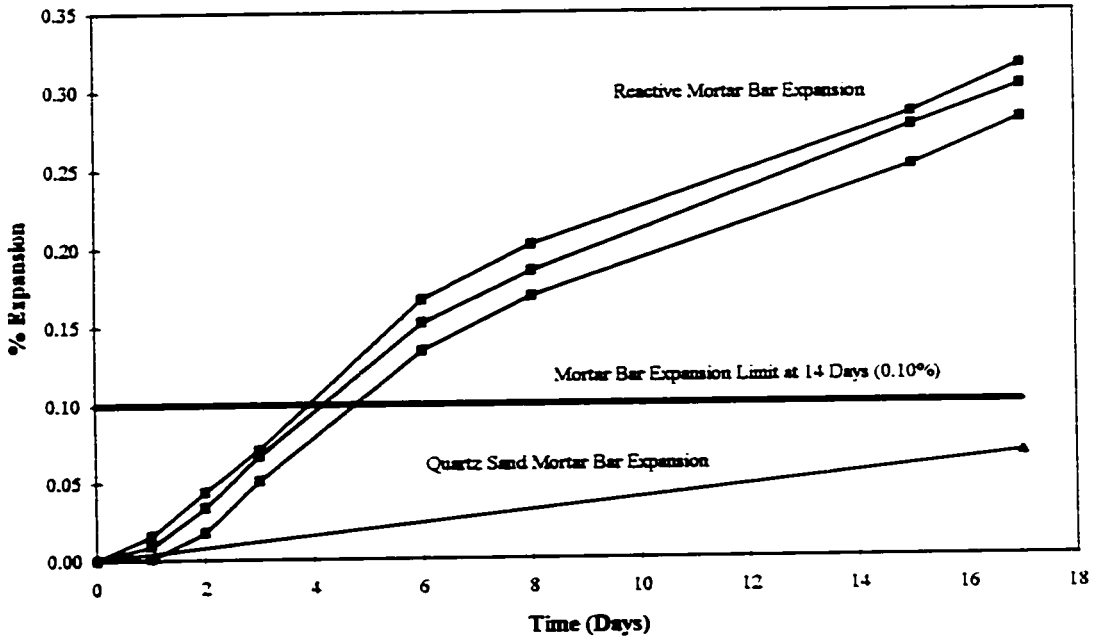

Figure A1: Mortar bar expansion for the reactive and non-reactive aggregates

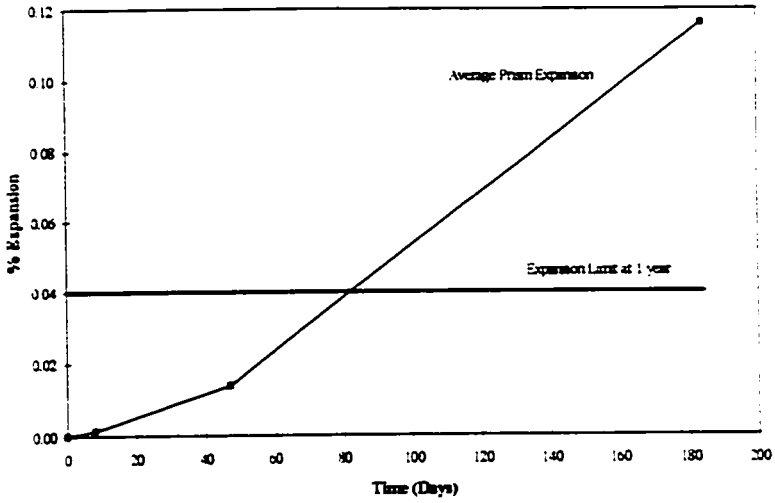

Figure A2: Preliminary concrete prism expansion test for the Spratt limestone

A.2 SIEVE ANALYSIS AND AGGREGATE BLENDING

A.2.1 Coarse Aggregate

The following figures compare the grading of the coarse aggregates (reactive and non-reactive) used for the experimental mixes compared with CSA grading requirements for concrete coarse aggregate.

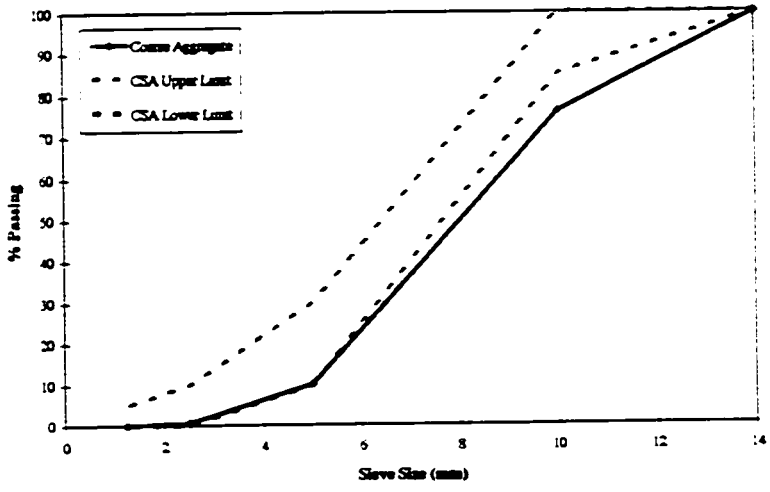

Figure A3: Coarse Aggregate Grading

A2.2 Fine Aggregates

The following figure illustrates the actual grading of the reactive and non-reactive crusher fines and the quartz sand used to produce the blended aggregate for the construction of the experimental mixes. These are compared with CSA grading requirements for concrete fine aggregate.

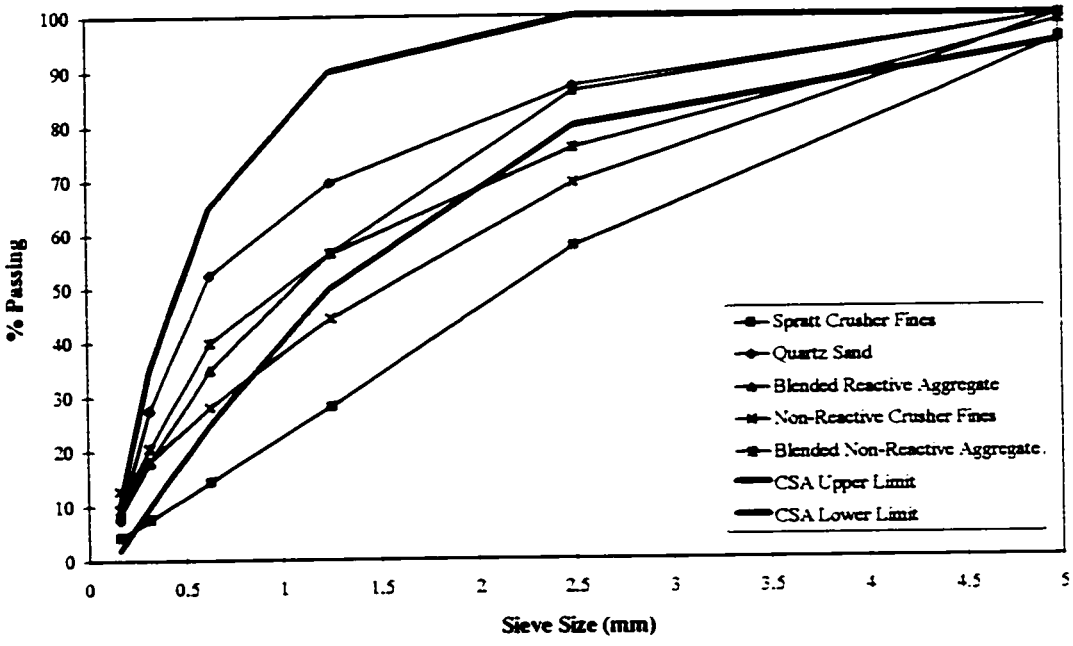

Figure A4: Fine aggregate gradation

A.3 CEMENT

The cement used in both the reactive and non-reactive control concrete mixes was a high alkali (0.9% Na_2O equivalent) ordinary Portland cement (CSA Type 10) obtained from St-Lawrence Cement. This cement has previously been used at the Institute for Research in Construction as a high alkali cement for ASR research.

A.4 LONGITUDINAL AND TRANSVERSE REINFORCEMENT

The yield strength of the reinforcing steel was required for the proper design of the beam specimens. Due to the unavailability of deformed reinforcing bars with a diameter less than 10 mm (in Canada) and the need for smaller bars for construction of small scale specimens, the reinforcing bars (8 mm diameter) were obtained from the United Kingdom. Their yield strength was unknown and therefore a stress-strain test was performed to determine this property as well as the modulus of elasticity.

Shear stirrups were also required to avoid shear failures during the loading of the specimens to ultimate. For this purpose, 4.7 mm diameter cold rolled smooth bars were used as shear ties. A stress-strain test of this steel was performed to obtain the yield stress in order to design the amount of shear reinforcement required in the beams.

The stress-strain curve obtained for the tested sample of shear stirrup material is very linear and does not show a yield point. This occurred because the failure of the specimen occurred outside of the gauge length of the strain measuring device (at the jaws of the testing apparatus). However, a value for the ultimate stress of the material was obtained (600 MPa) and a value of the yield strength was provided by the manufacturer (345 MPa). Therefore, 300 MPa was used for design and determined to be a safe value. All stress-strain data was obtained using a Tinius Olsen testing machine and a dial gauge extensometer with a gauge length of 50 mm.

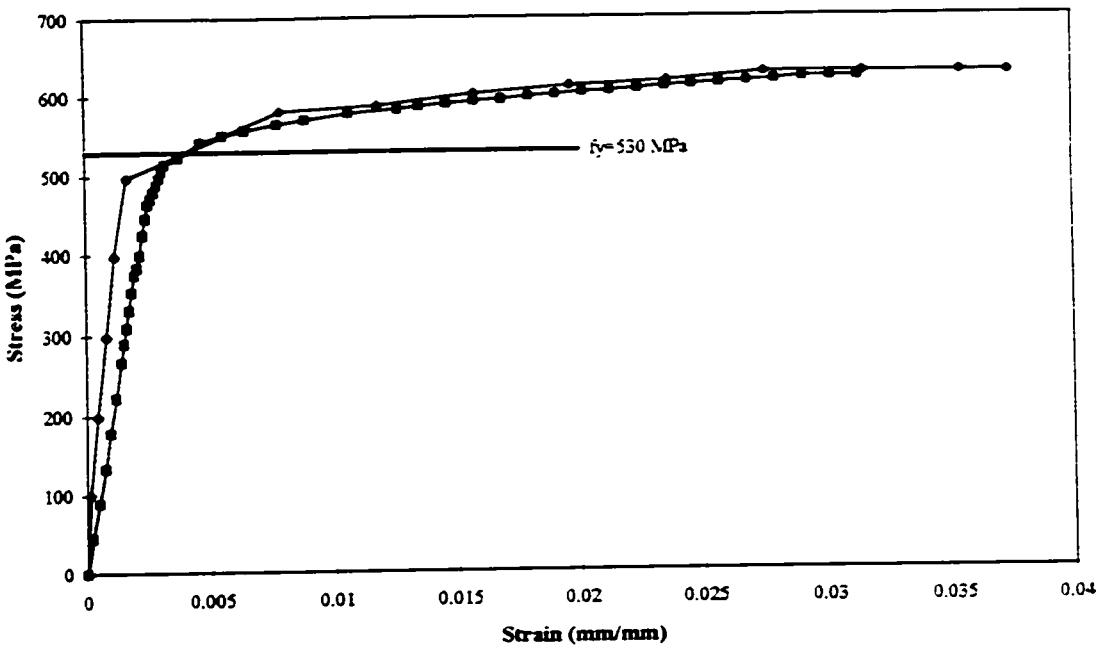

Figure A5: Longitudinal reinforcement stress vs. strain relationship

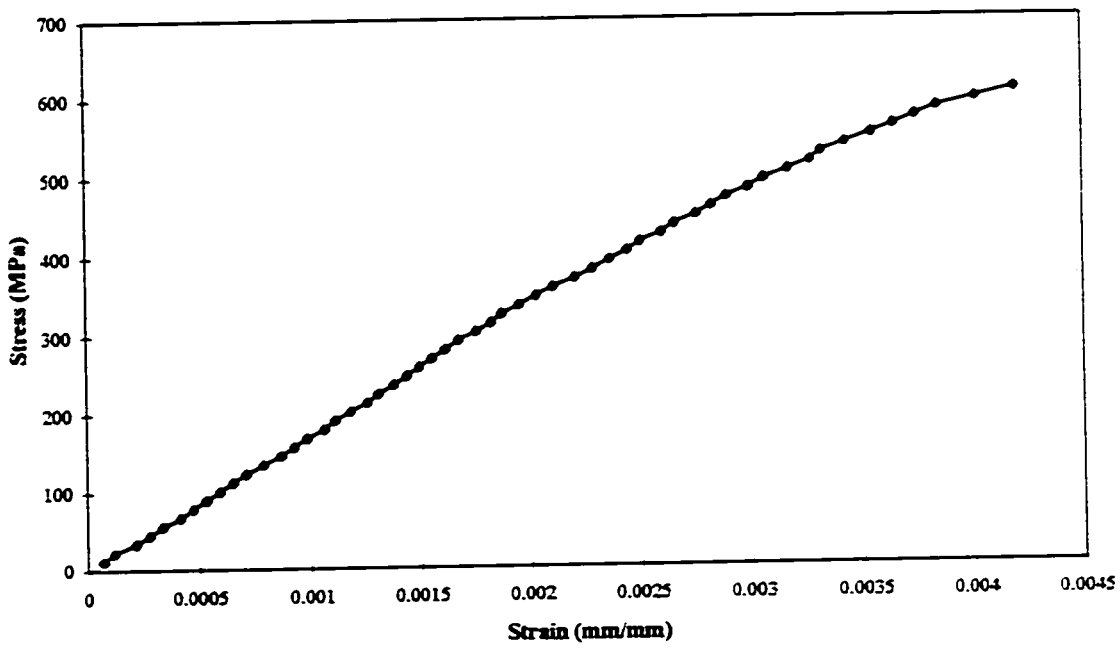

Figure A7: Transverse reinforcement stress vs. strain relationship

APPENDIX B

EXPERIMENTAL DATA

All of the reactive beams expansion and DRI data collected during the experiment is presented in the following appendix. Not all of these results are presented in the body of the thesis but are shown here for reference.

B.1 EXPANSION DATA

The expansions of the reactive beams at the various Demec locations are presented for each type of loading regime (Sections B.1.1, B.1.2 and B.1.3). A comparison of the various horizontal and vertical expansions for the beams subjected to the various loading regimes are presented in Section B.1.4. Figures B.1, B.2, B.3 and B.4 show the Demec positions on the beams, the horizontal Demec sets, vertical Demec sets and the four point loading configuration of the statically and dynamically loaded beams respectively.

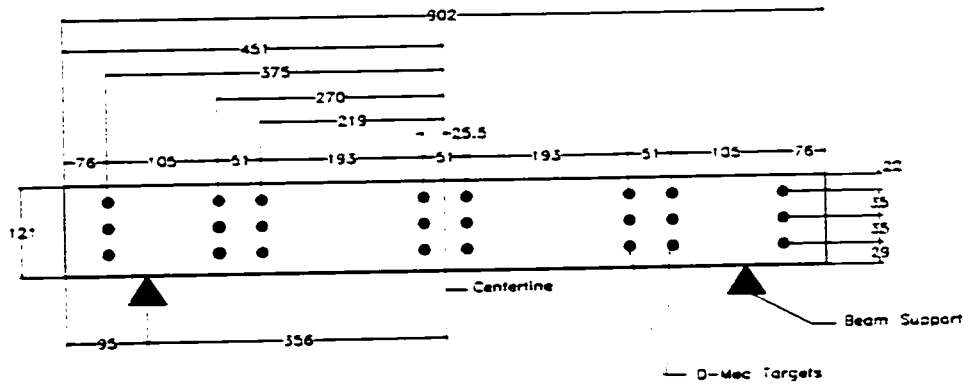

Figure B.1: Demec Target Layout

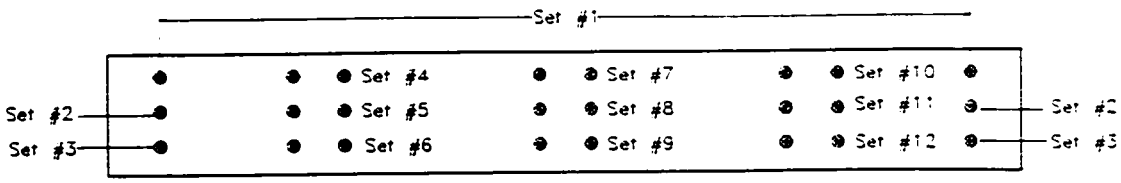

Figure B.2: Demec target sets used for horizontal expansion measurements

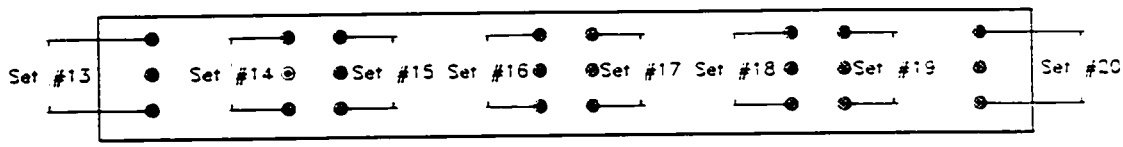

Figure B.3: Demec target sets used for vertical expansion measurements

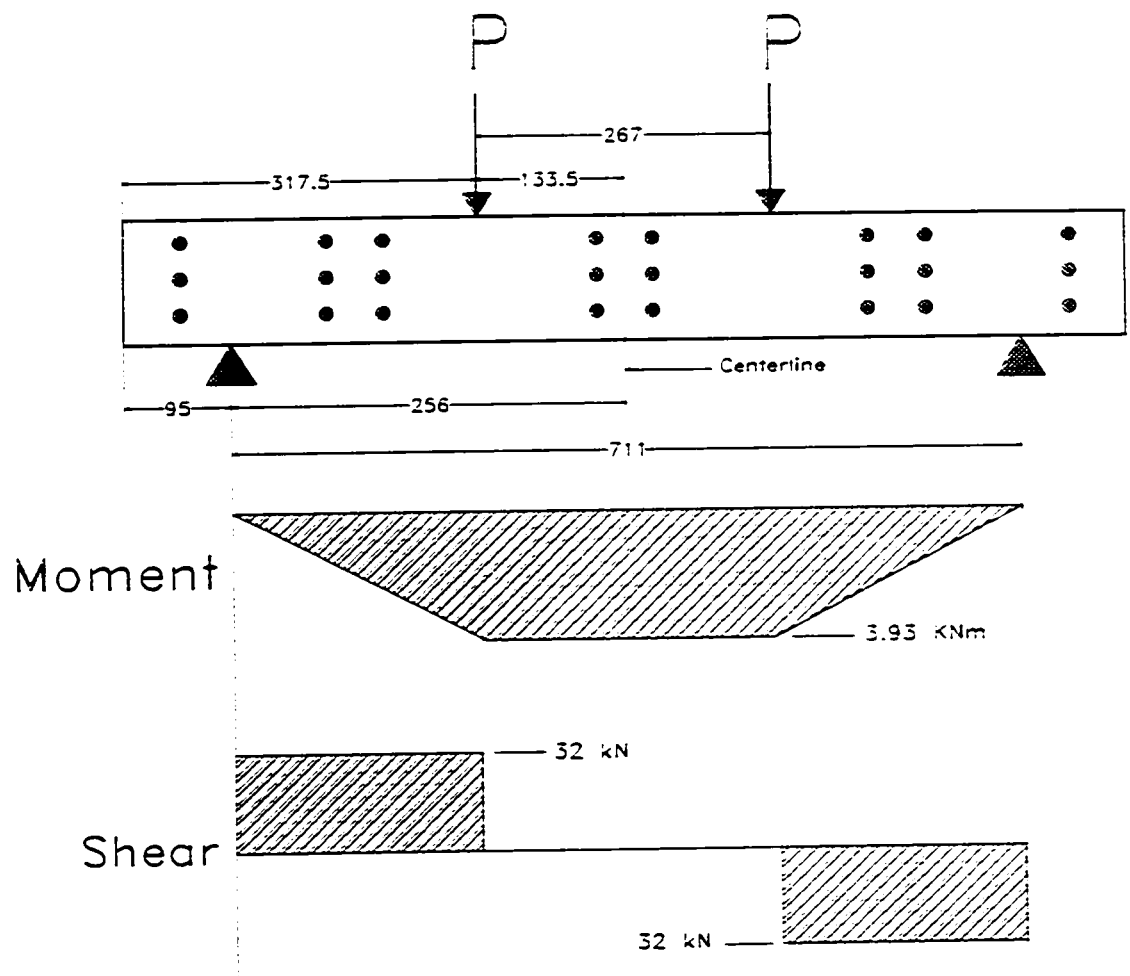

Figure B.4: Beam loading arrangement with bending moment and shear force diagrams

B.1.1 Unloaded Beam Expansions

Horizontal expansions for the overall, left side, mid-span and right side Demec locations shown in Figures B.5 to B.8 display the expansions of each of the three Demec sets at these locations vertically along the unloaded beams. Figures B.9 to B.11 show the horizontal expansion results for each of the Demec locations at the top, middle and bottom of the beams. Figure B.12 shows the vertical expansions of the unloaded beams.

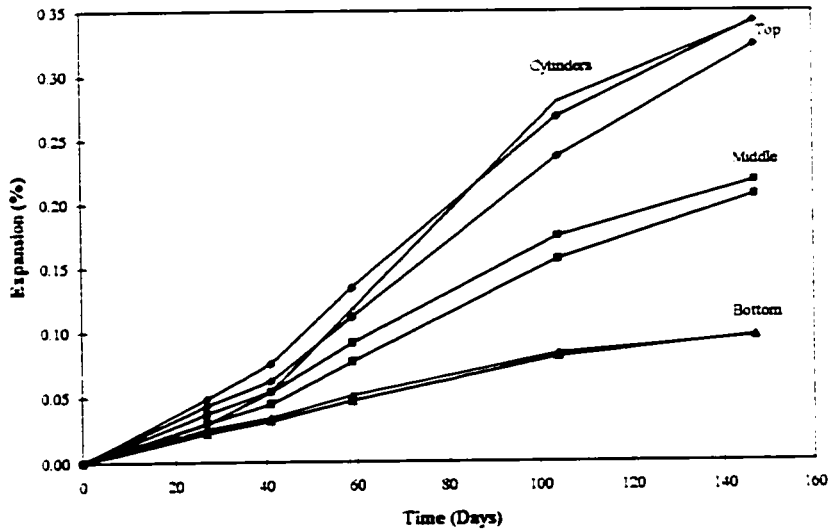

Figure B.5: Unloaded beams overall horizontal expansions (sets 1,2,3)

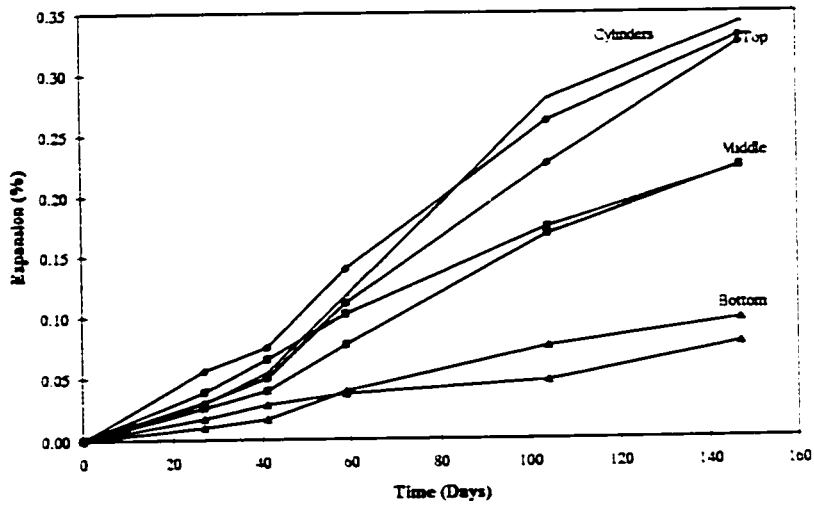

Figure B.6: Unloaded beams left side horizontal expansions (sets 4,5,6)

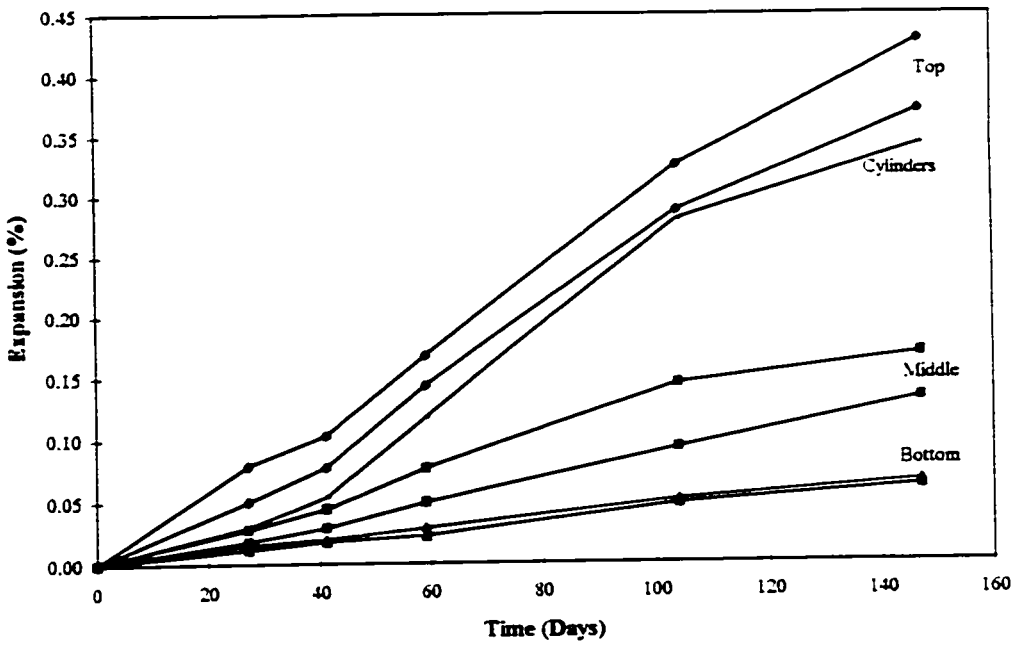

Figure B.7: Unloaded beams mid-span horizontal expansions (sets 7,8,9)

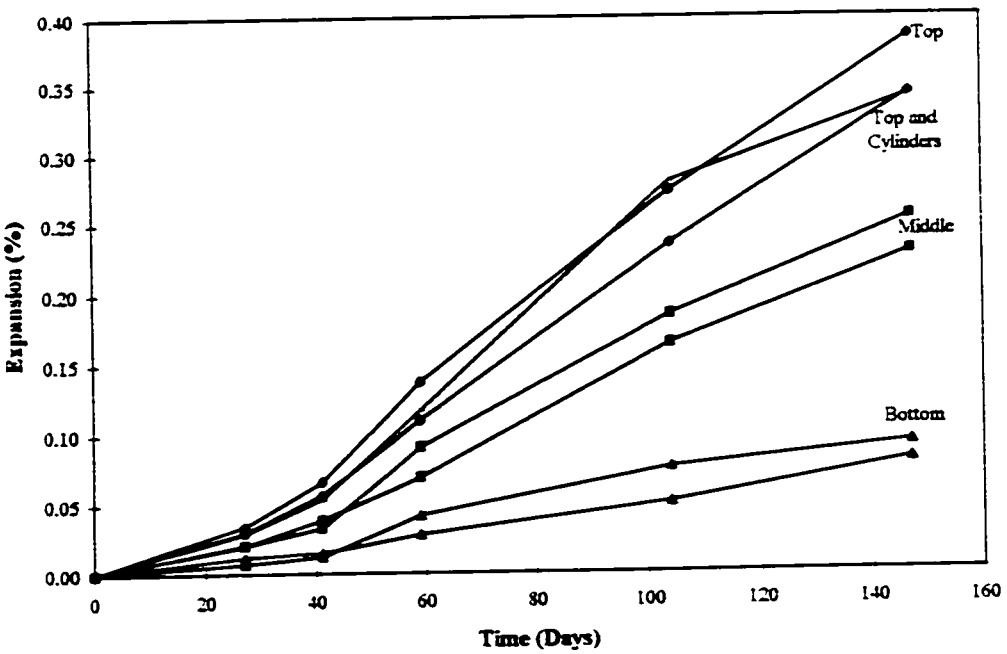

Figure B.8: Unloaded beams right side horizontal expansions (sets 10,11,12)

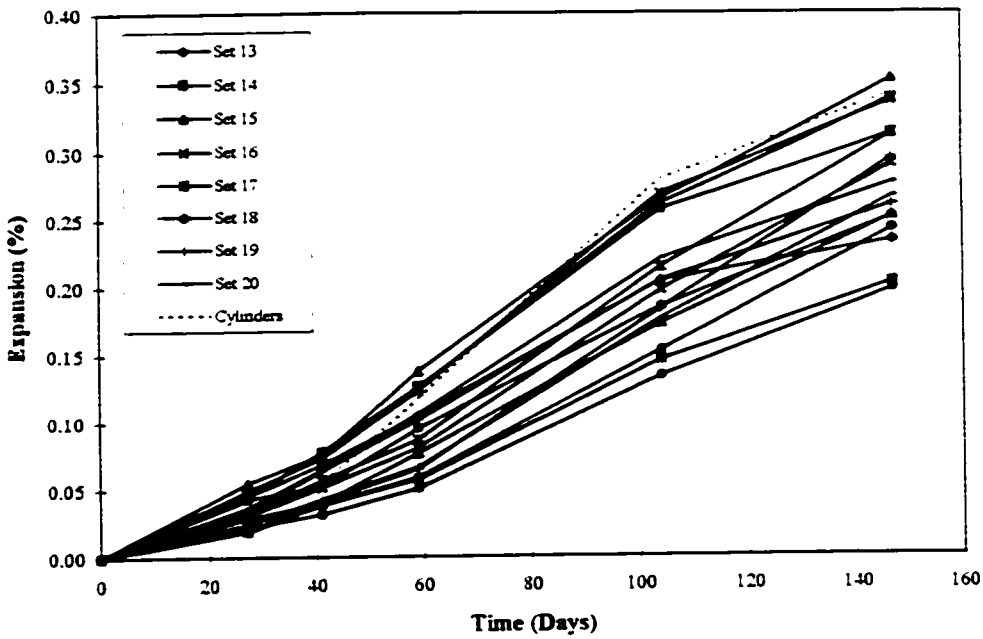

Figure B.9: Unloaded beams vertical expansions (sets 13,14,15,16,17,18,19,20)

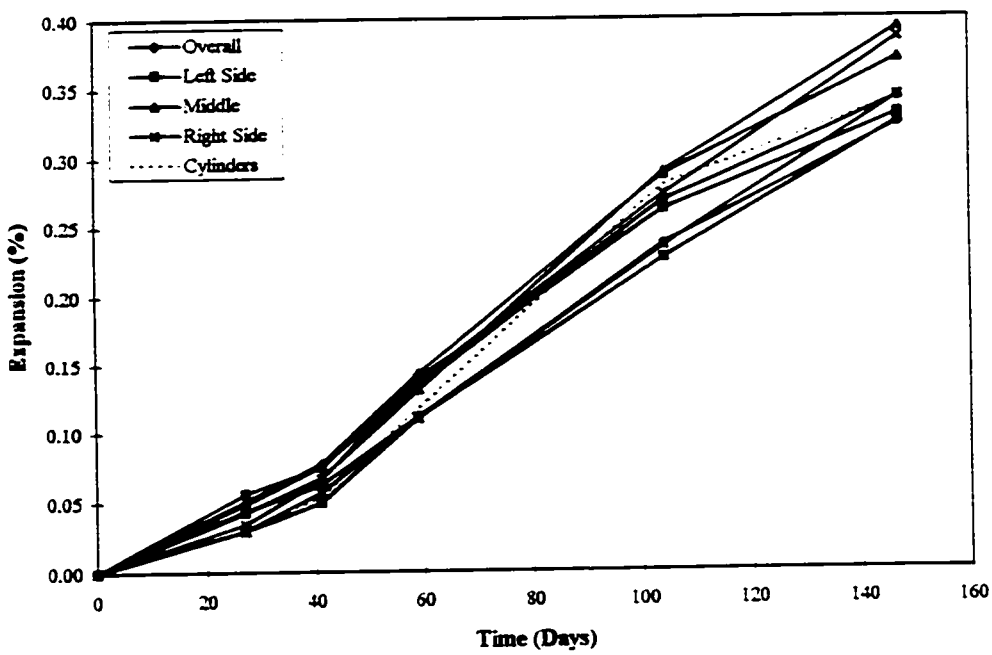

Figure B.10: Unloaded beams top horizontal expansions (sets 1,4,7,10)

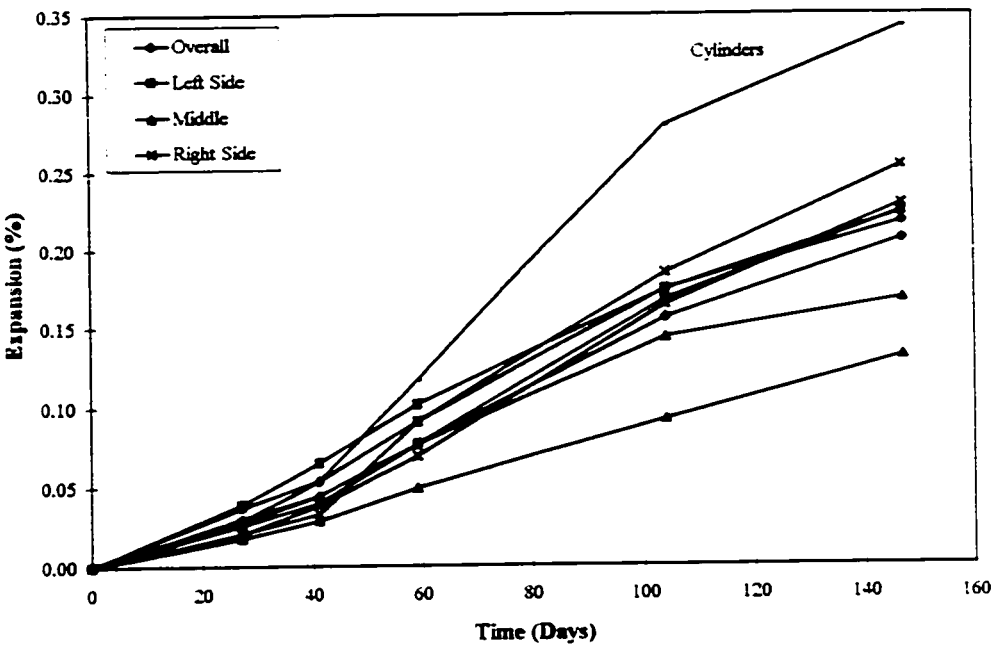

Figure B.11: Unloaded beams middle horizontal expansions (sets 2,5,8,11)

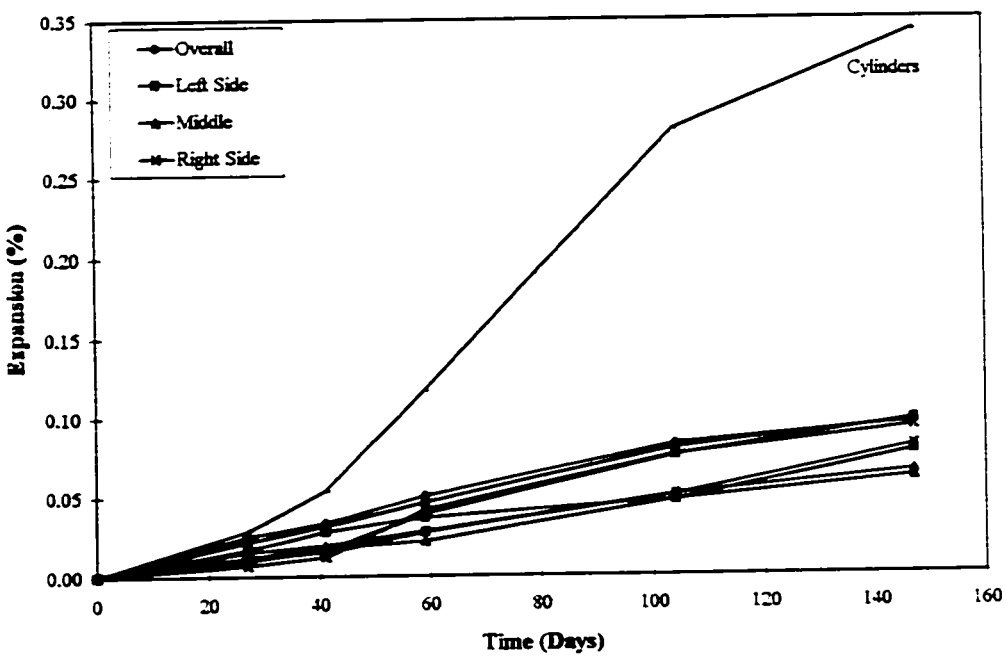

Figure B.12: Unloaded beams bottom horizontal expansions (sets 3,6,9,12)

B.1.2 Statically Loaded Beam Expansions

Horizontal expansions for the overall, left side, mid span and right side Demec locations shown in Figures B.13 to B.16 display the expansions of each of the three Demec sets at these locations vertically along the statically loaded beams. Figures B.17 to B.19 show the horizontal expansion results for each of the Demec locations at the top, middle and bottom of the beams. Figure B.20 shows the vertical expansions of the unloaded beams.

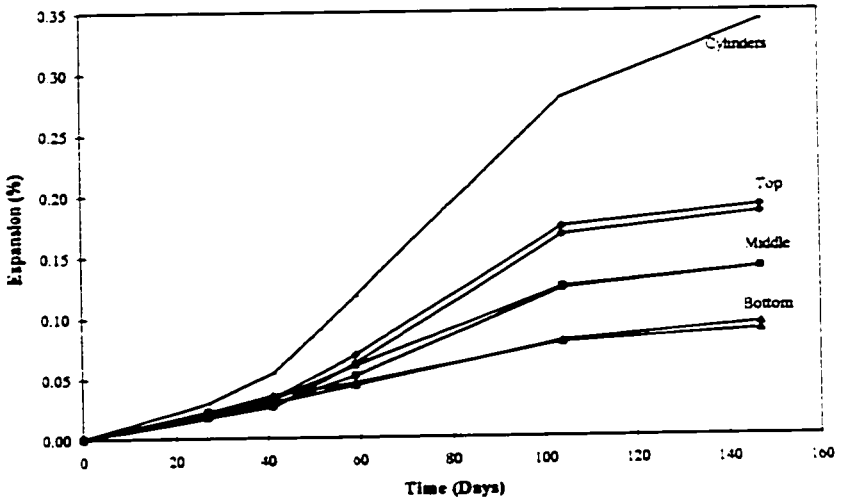

Figure B.13: Statically loaded beams overall horizontal expansions (sets1,2,3)

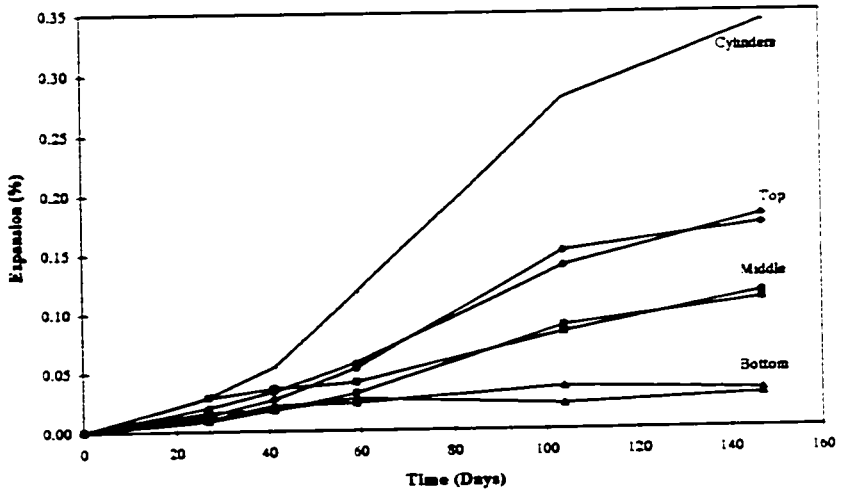

Figure B.14: Statically loaded beams left side horizontal expansions (sets 4,5,6)

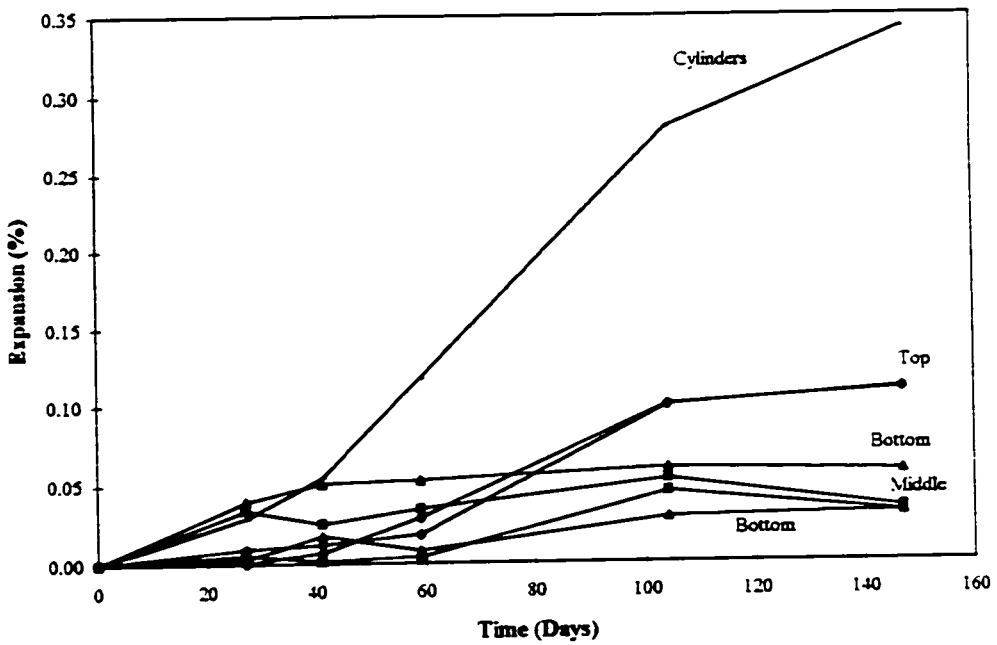

Figure B.15: Statically loaded beams mid-span horizontal expansions (sets 7,8,9)

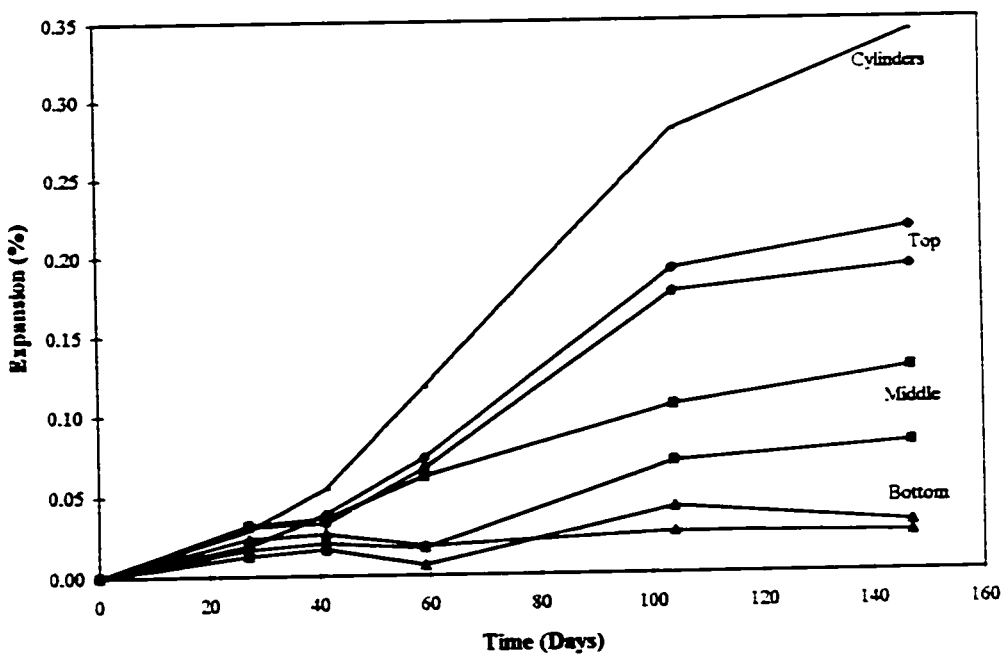

Figure B.16: Statically loaded beams right side horizontal expansions (sets 10,11,12)

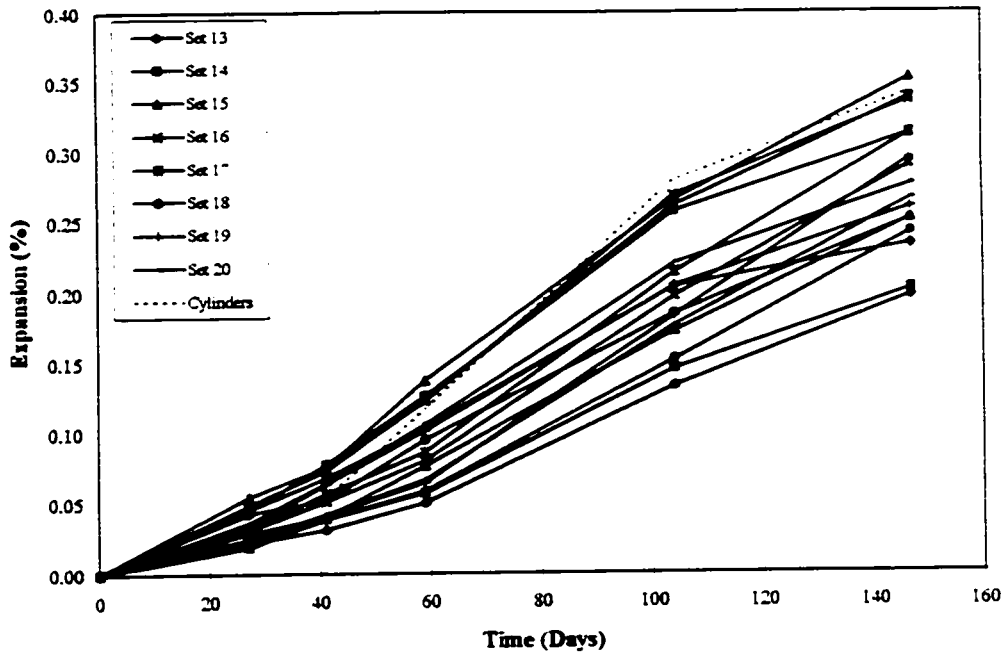

Figure B.17: Statically loaded beams vertical expansions (sets 13,14,15,16,17,18,19,20)

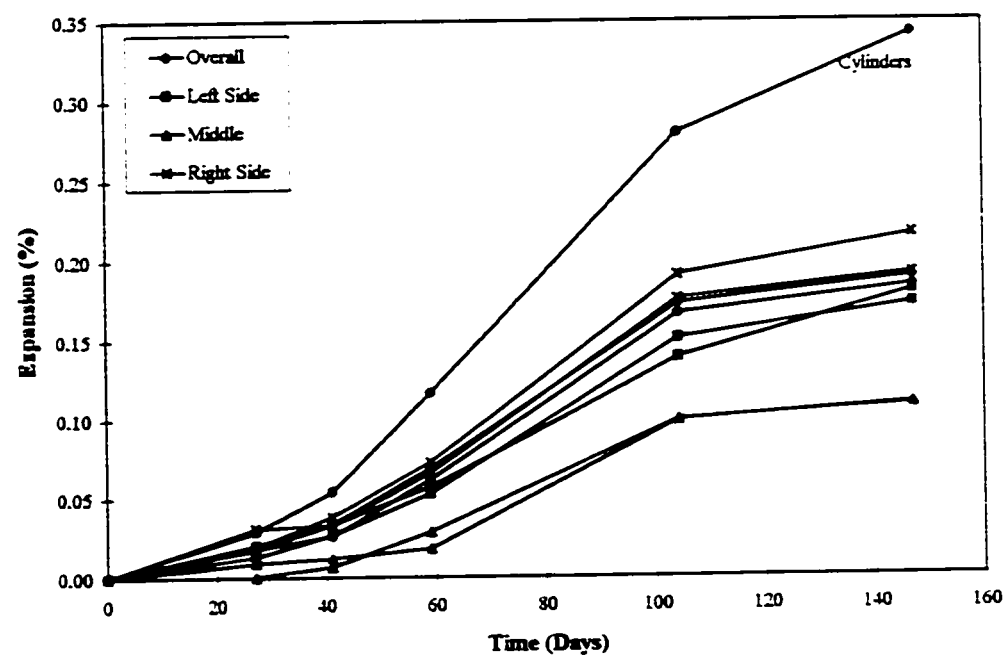

Figure B.18: Statically loaded beams top horizontal expansions (sets 1,4,7,10)

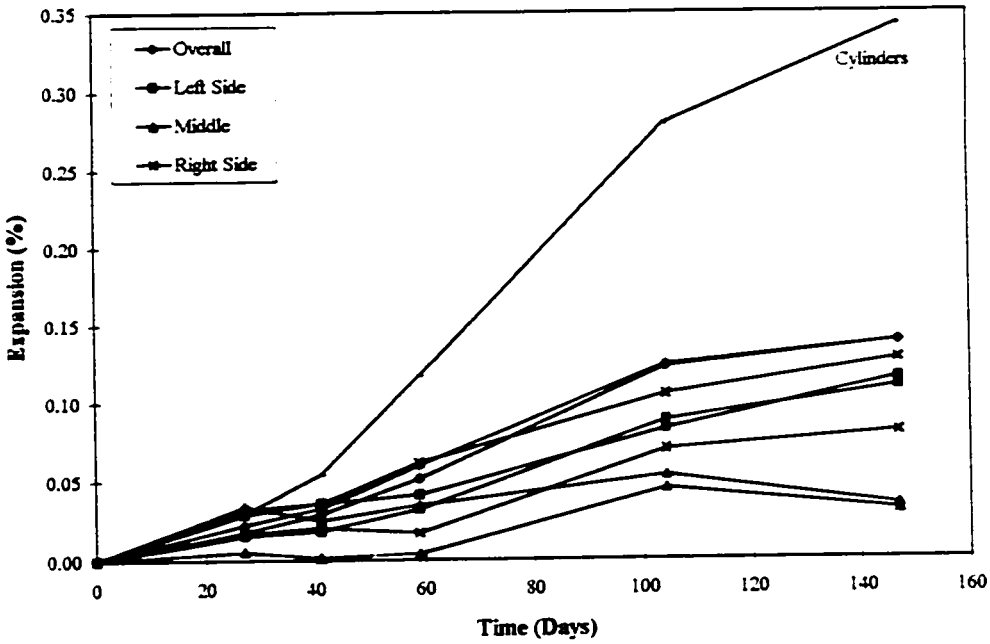

Figure B.19: Statically loaded beams middle horizontal expansions (sets 2,5,8,11)

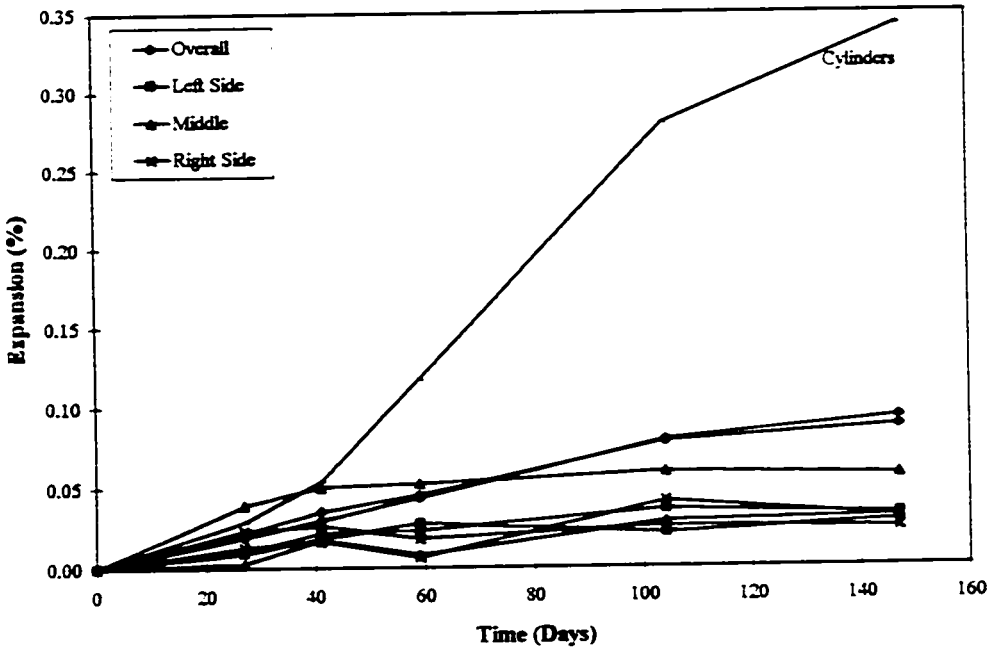

Figure B.20: Statically loaded beams bottom horizontal expansions (sets 3,6,9,12)

B.1.3 Dynamically Loaded Beam Expansions

Horizontal expansions for the overall, left side, mid span and right side Demec locations shown in Figures B.21 to B.24 display the expansions of each of the three Demec sets at these locations vertically along the dynamically loaded beams. Figures B.25 to B.27 show the horizontal expansion results for each of the Demec locations at the top, middle and bottom of the beams. Figure B.28 shows the vertical expansions of the dynamically loaded beams.

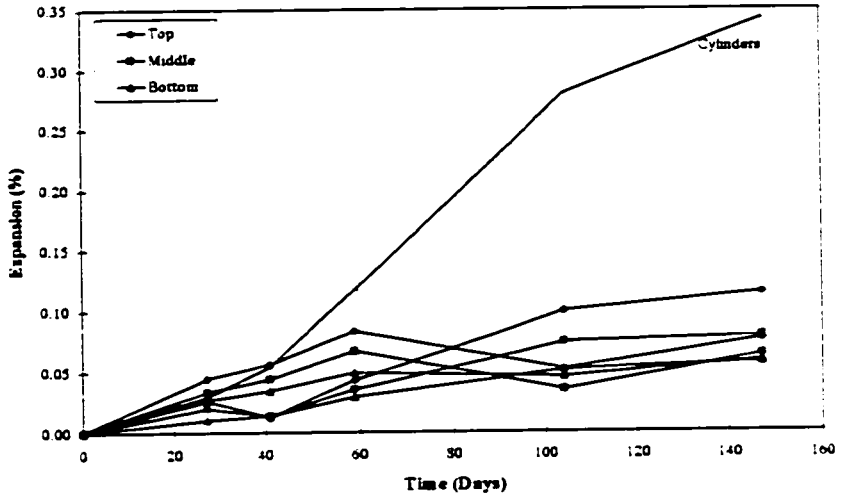

Figure B.21: Dynamically loaded beams overall horizontal expansions (sets 1,2,3)

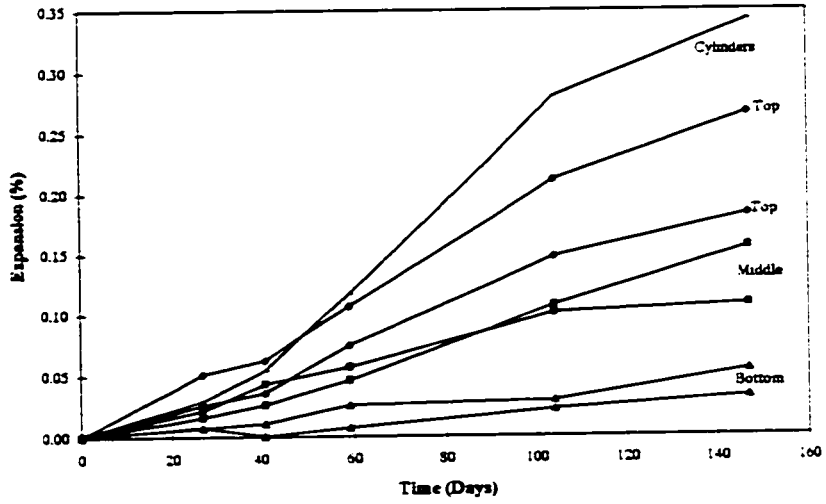

Figure B.22: Dynamically loaded beams left side horizontal expansions (sets 4,5,6)

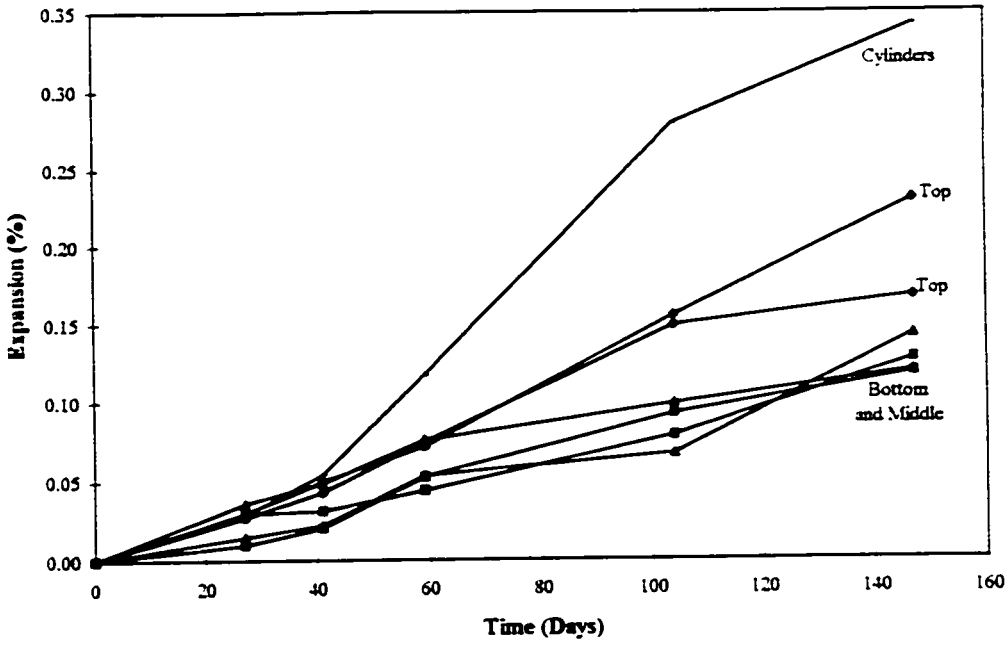

Figure B.23: Dynamically loaded beams mid-span horizontal expansions (sets 7,8,9)

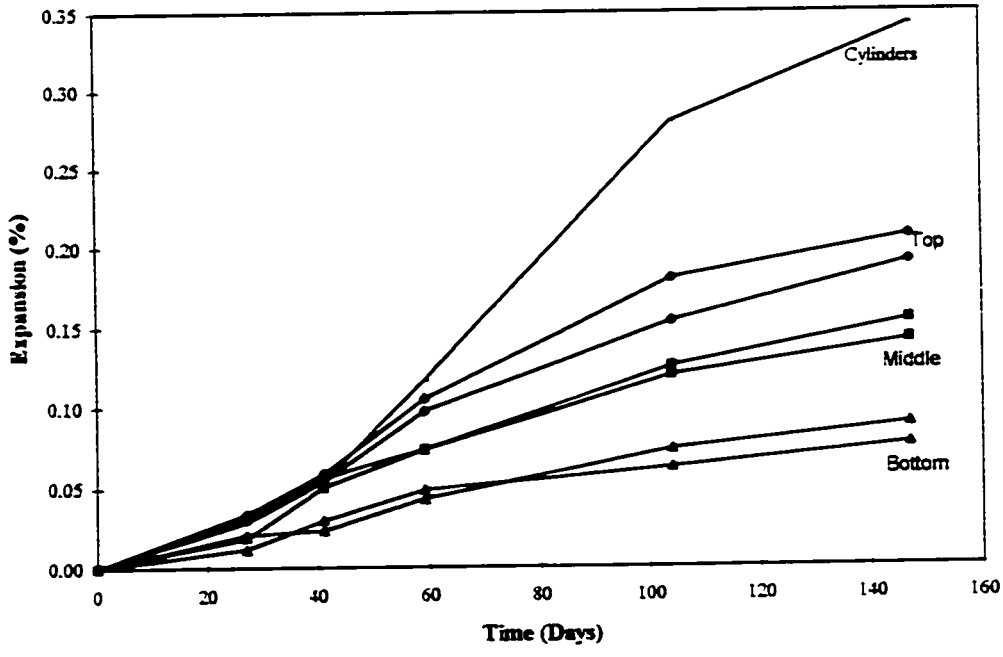

Figure B.24: Dynamically loaded beams right side horizontal expansions (sets 10,11,12)

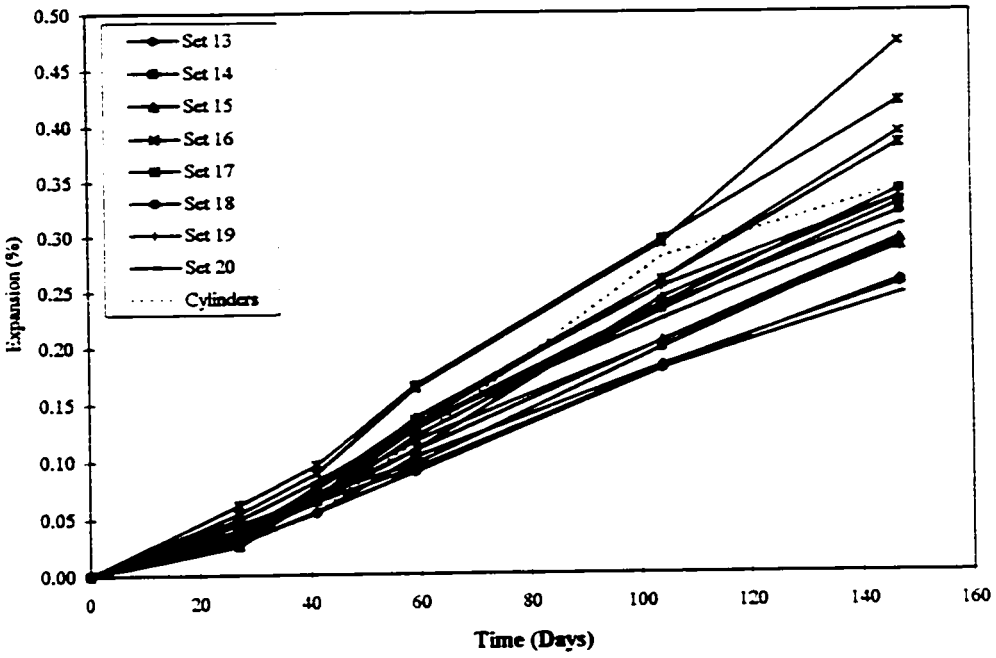

Figure B.25: Dynamically loaded beams vertical expansions (sets 13,14,15,16,17,18,19,20)

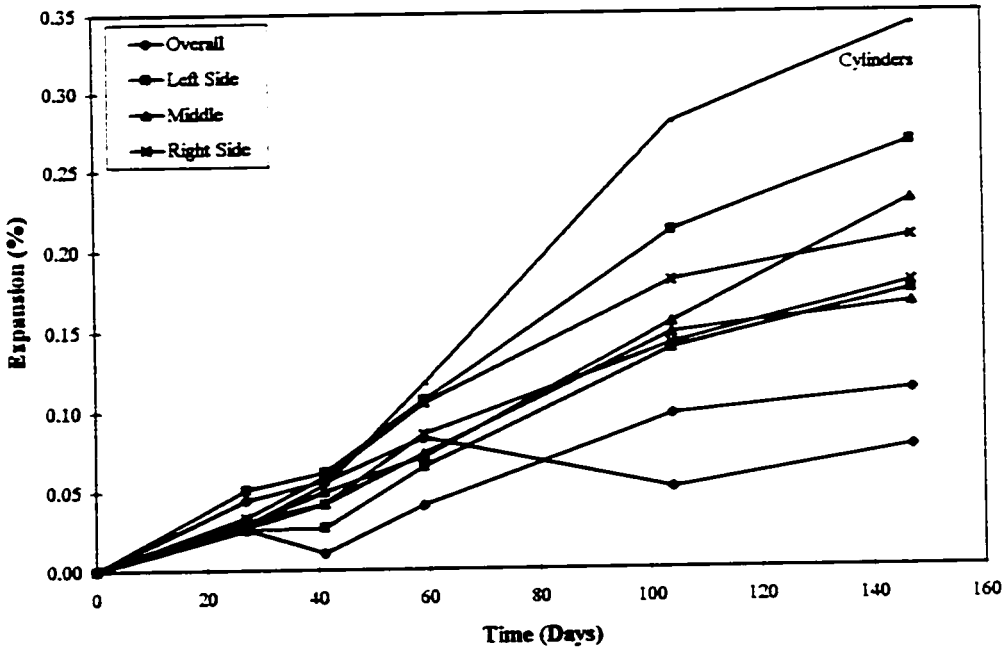

Figure B.26: Dynamically loaded beams top horizontal expansions (sets 1,4,7,10)

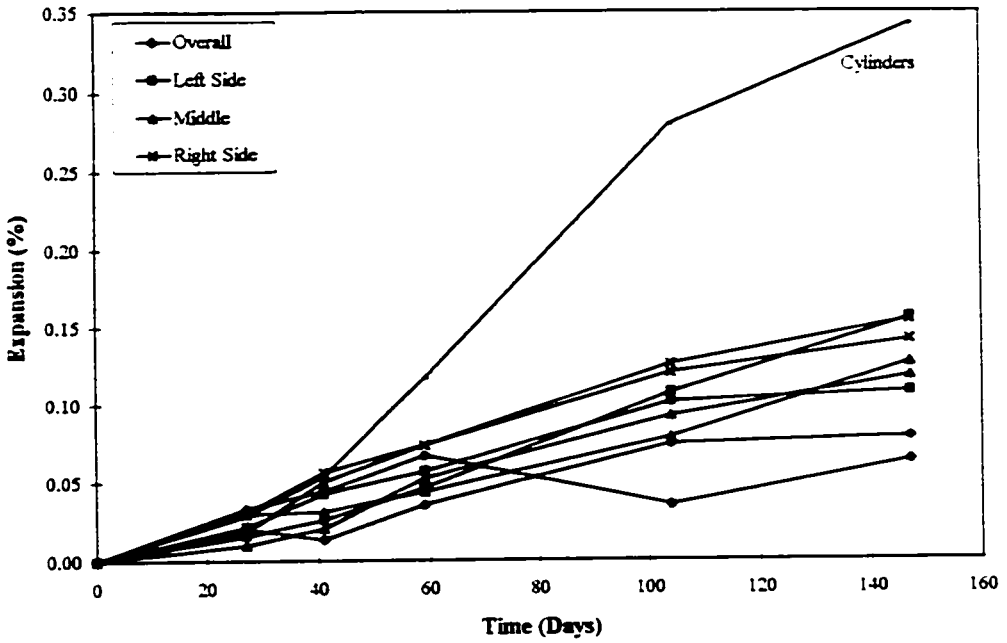

Figure B.27: Dynamically loaded beams middle horizontal expansions (sets 2,5,8,11)

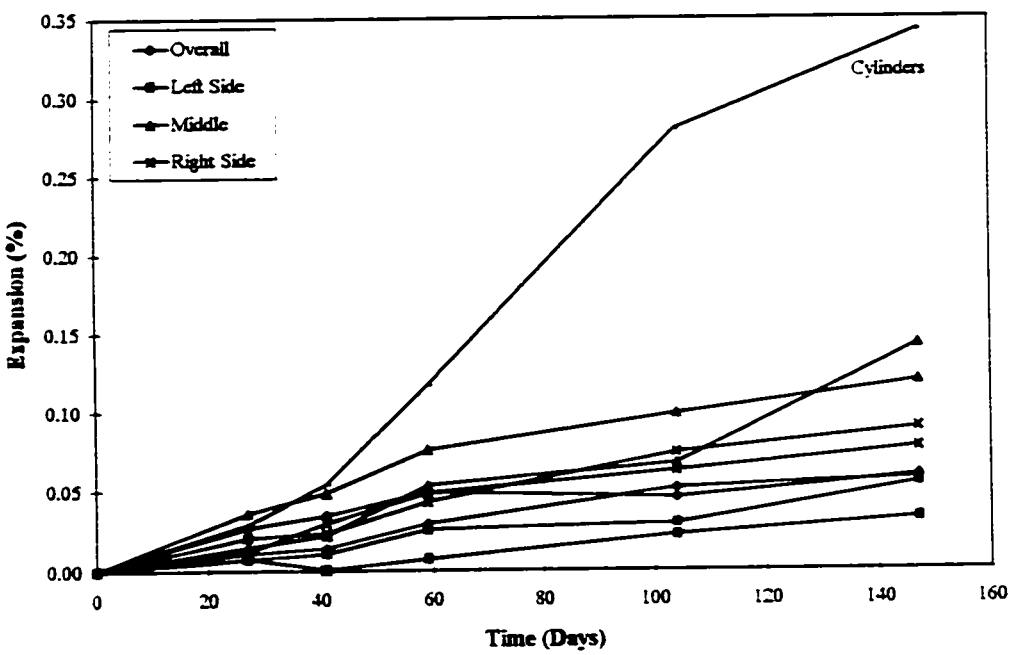

Figure B.28: Dynamically loaded beams bottom horizontal expansions (sets 3,6,9,12)

B.1.4 Expansions of the Beams Subjected to Various Loading Regimes

Figures B.29 to B.48 show the expansions for each the Demec locations of the beams subjected to various loading regimes. The horizontal expansions (Figures B.28 to B. 39) are showed first followed by the vertical expansions (Figures B.40 to B.47) for each of the Demec locations and beams subjected to various loading regimes..

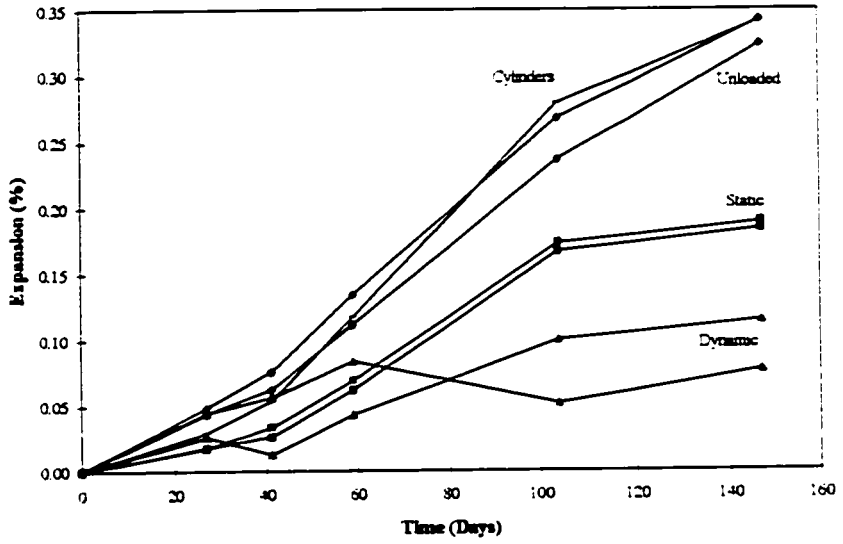

Figure B.29: Overall horizontal expansions for the top of the various beams (set 1)

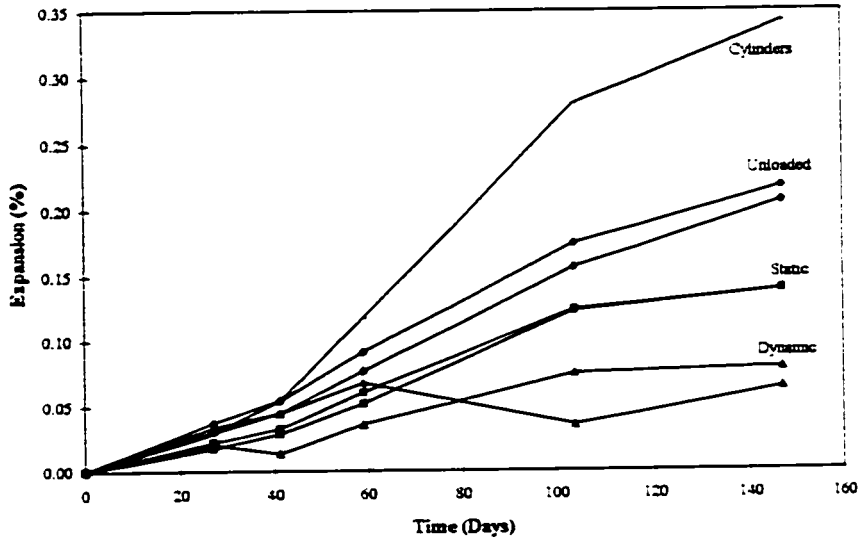

Figure B.30: Overall horizontal expansions for the middle of the various beams (set 2)

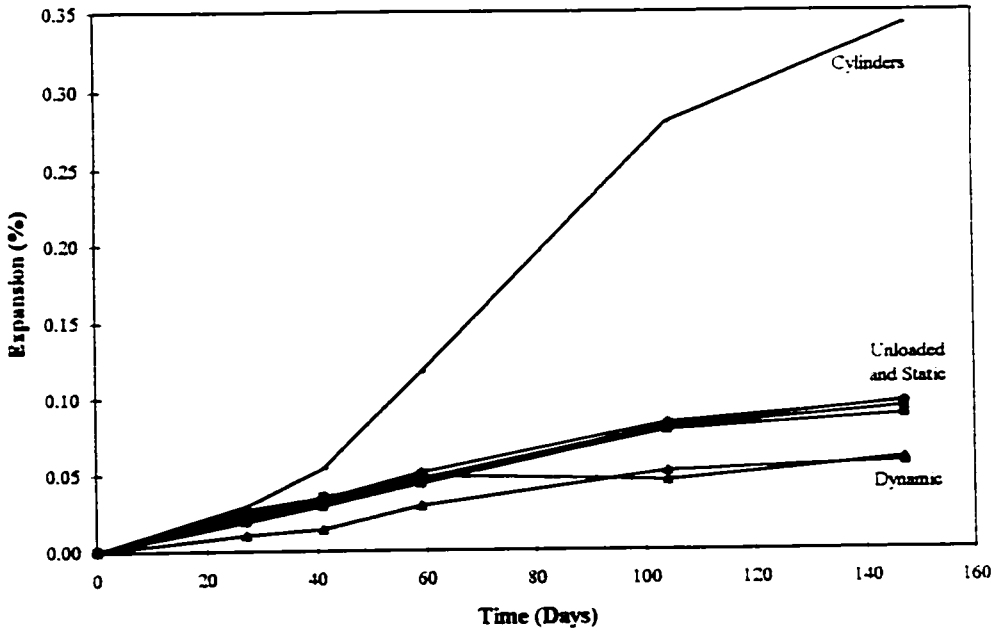

Figure B.31: Overall horizontal expansions for the bottom of the various beams (set 3)

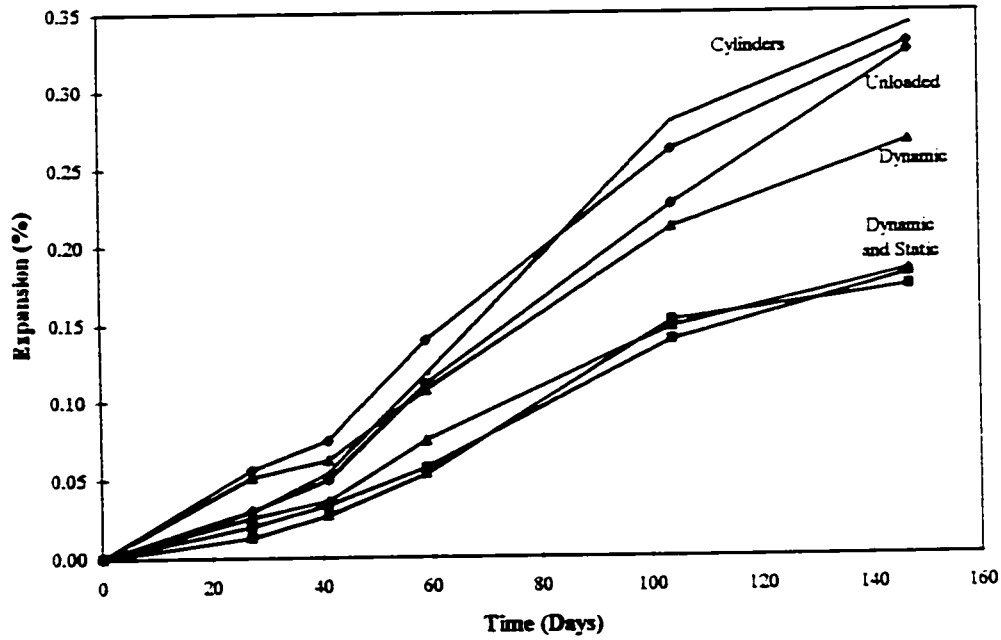

Figure B.32: Left side horizontal expansions for the top of the various beams (set 4)

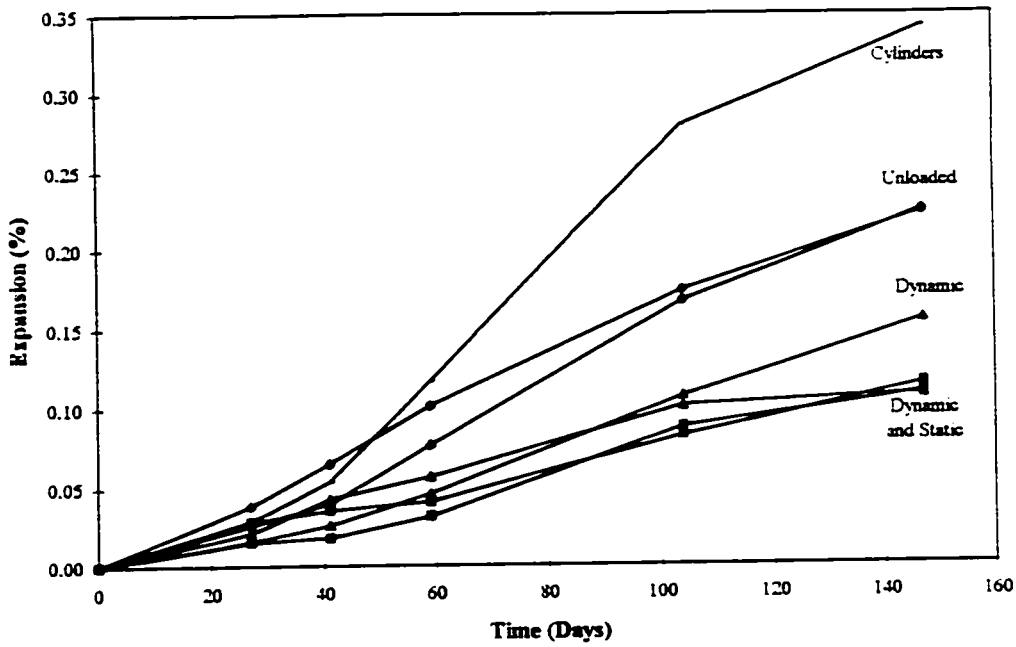

Figure B.33: Left side horizontal expansions for the middle of the various beams (set 5)

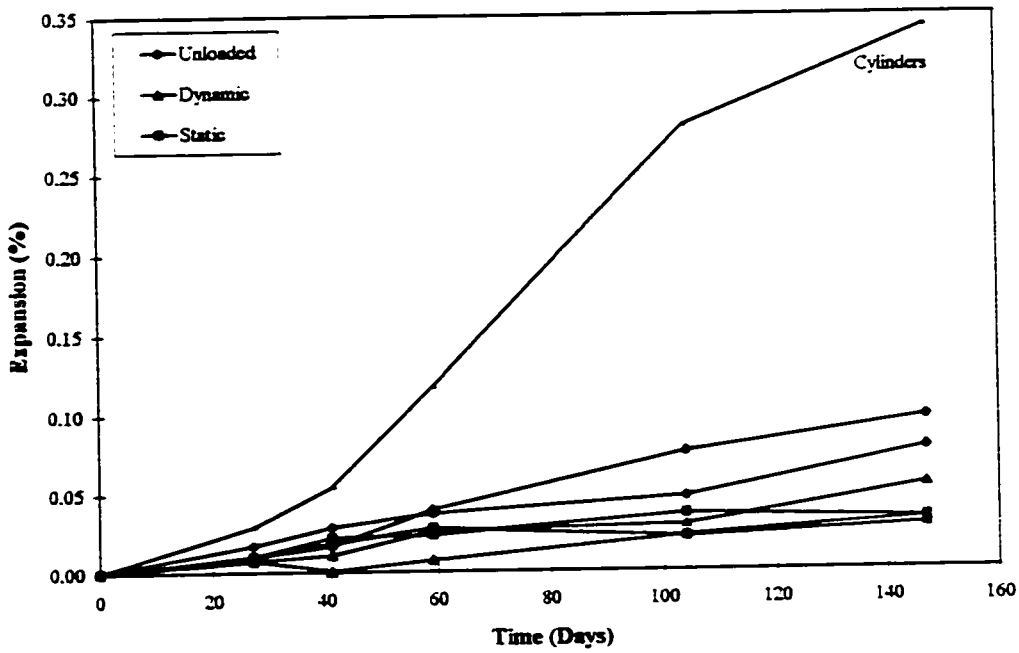

Figure B.34: Left side horizontal expansions for the bottom of the various beams (set 6)

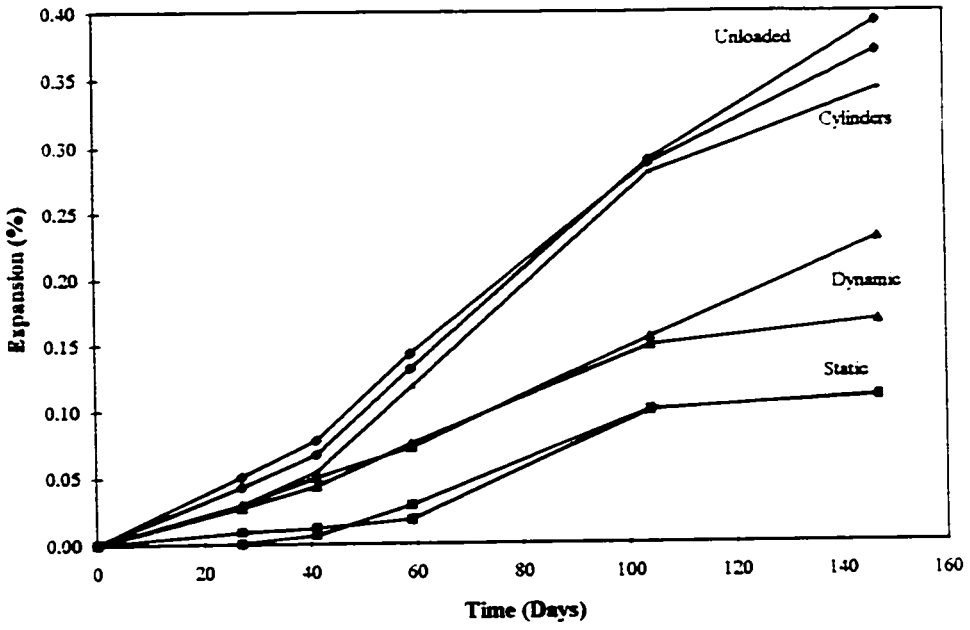

Figure B.35: Mid span horizontal expansions for the top of the various beams (set 7)

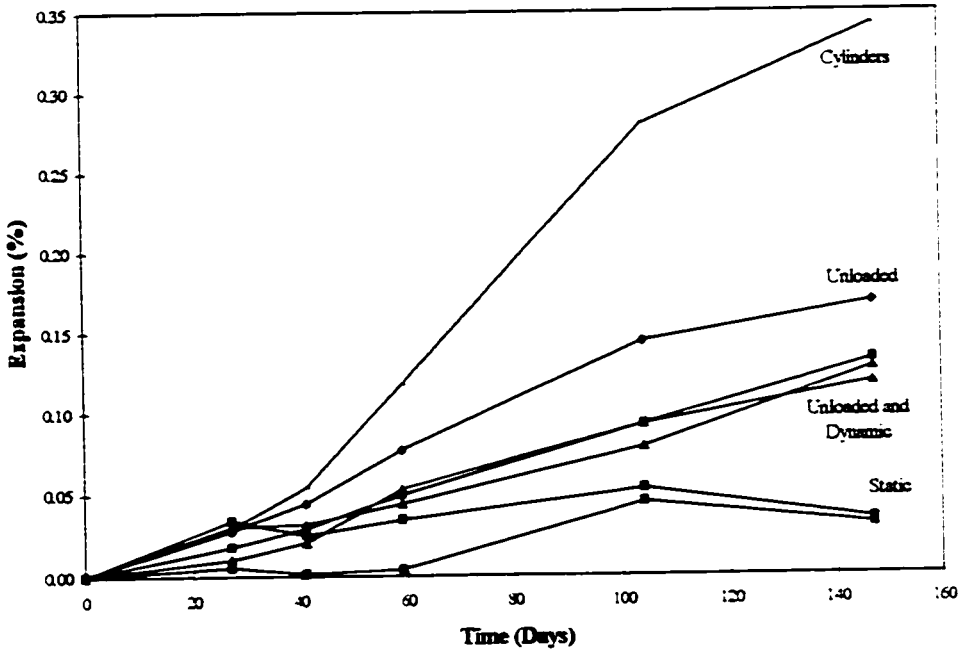

Figure B.36: Mid span horizontal expansions for the middle of the various beams (set 8)

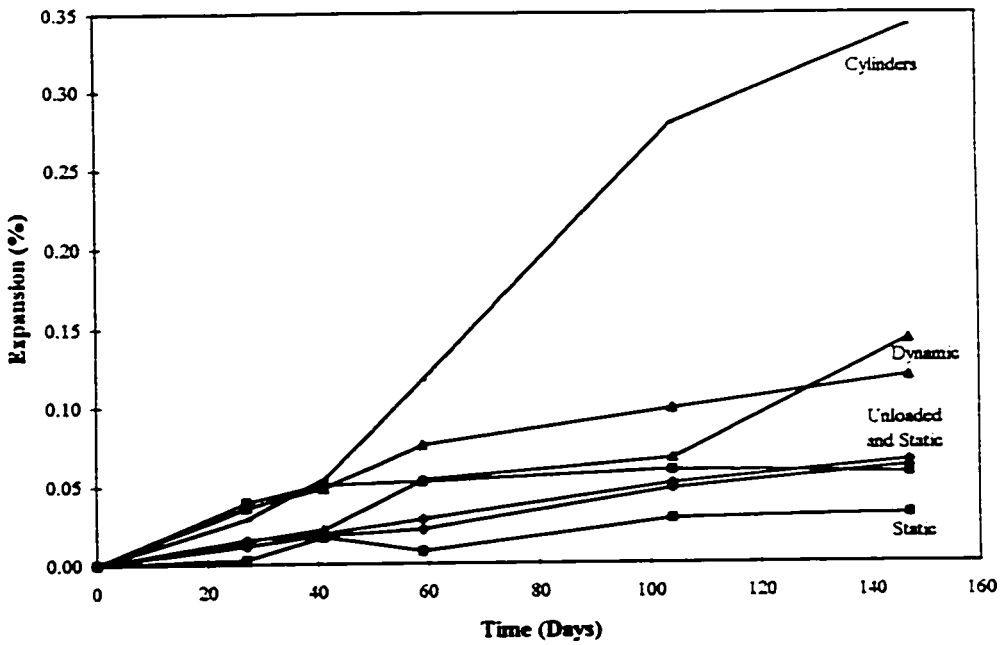

Figure B.37: Mid span horizontal expansions for the bottom of the various beams (set 9)

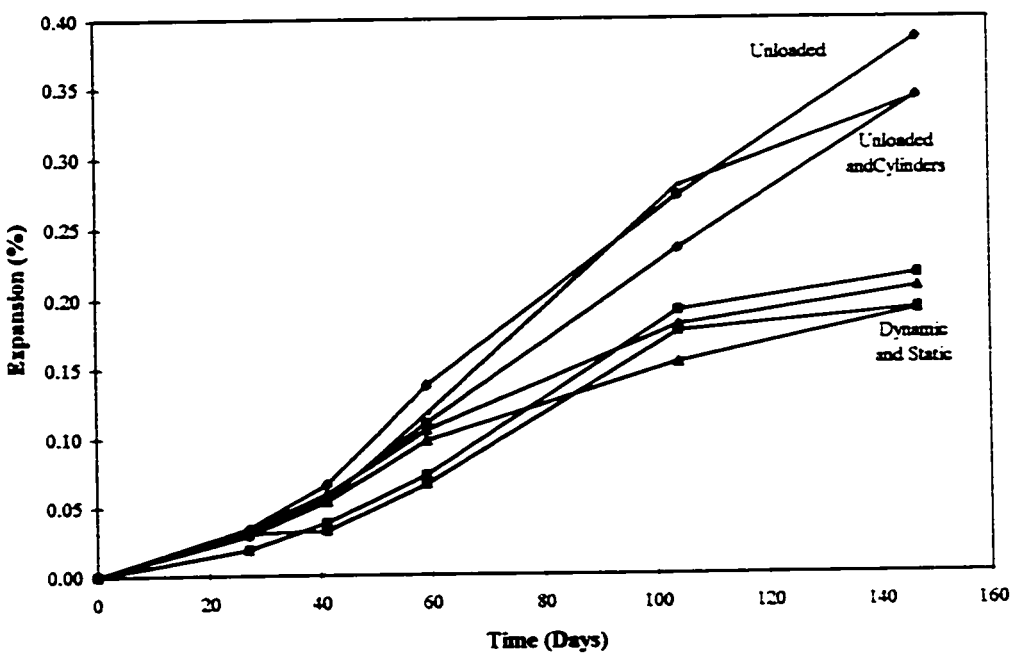

Figure B.38: Right side horizontal expansions for the top of the various beams (set 10)

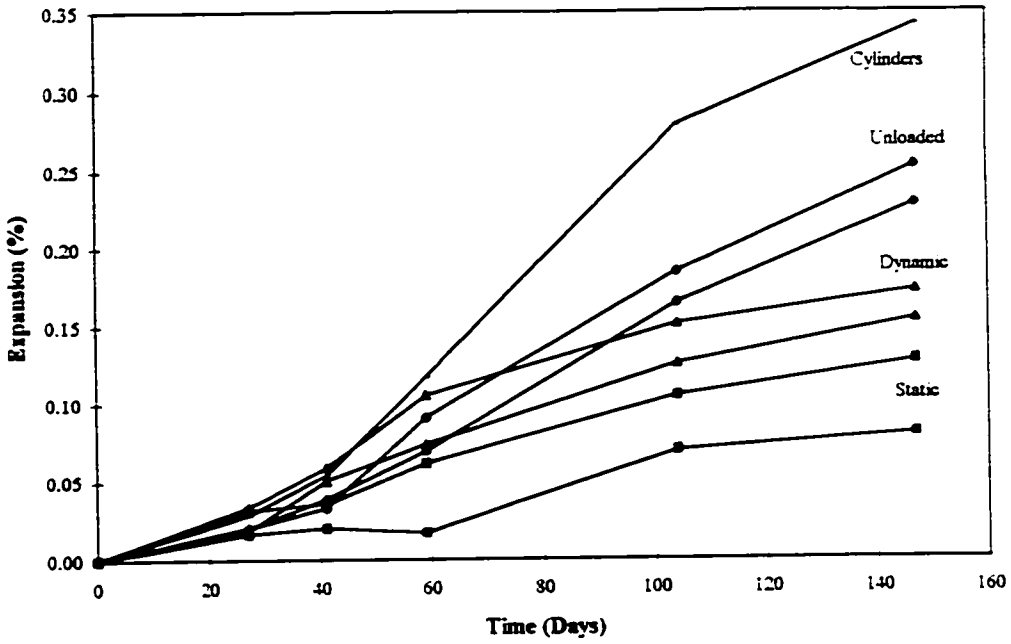

Figure B.39: Right side horizontal expansions for the middle of the various beams (set 11)

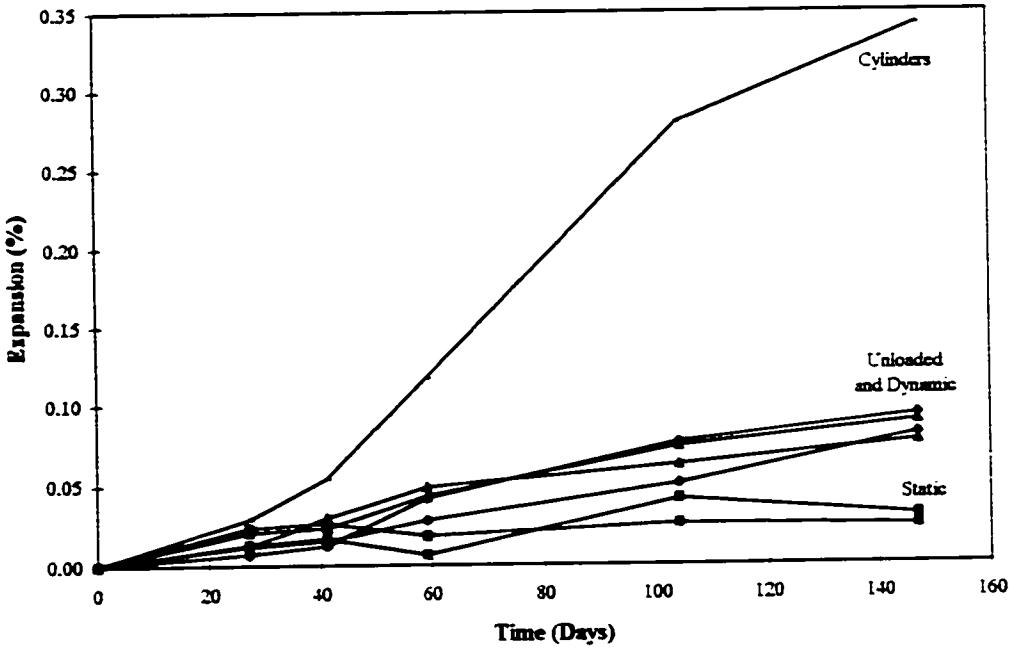

Figure B.40: Right side horizontal expansions for bottom of the various beams (set 12)

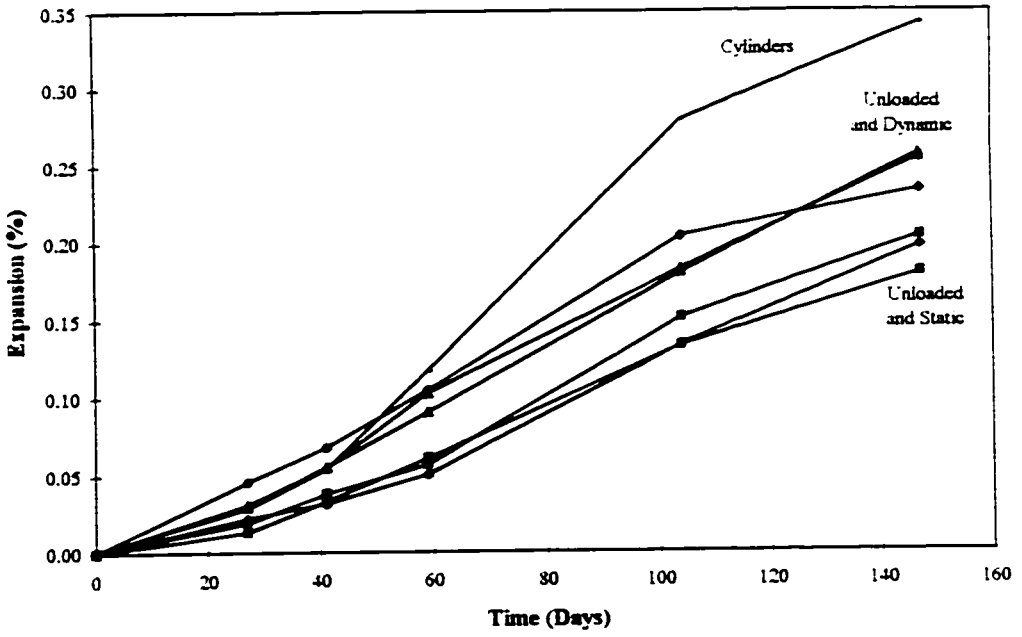

Figure B.41: Vertical expansions for the various beams (set 13)

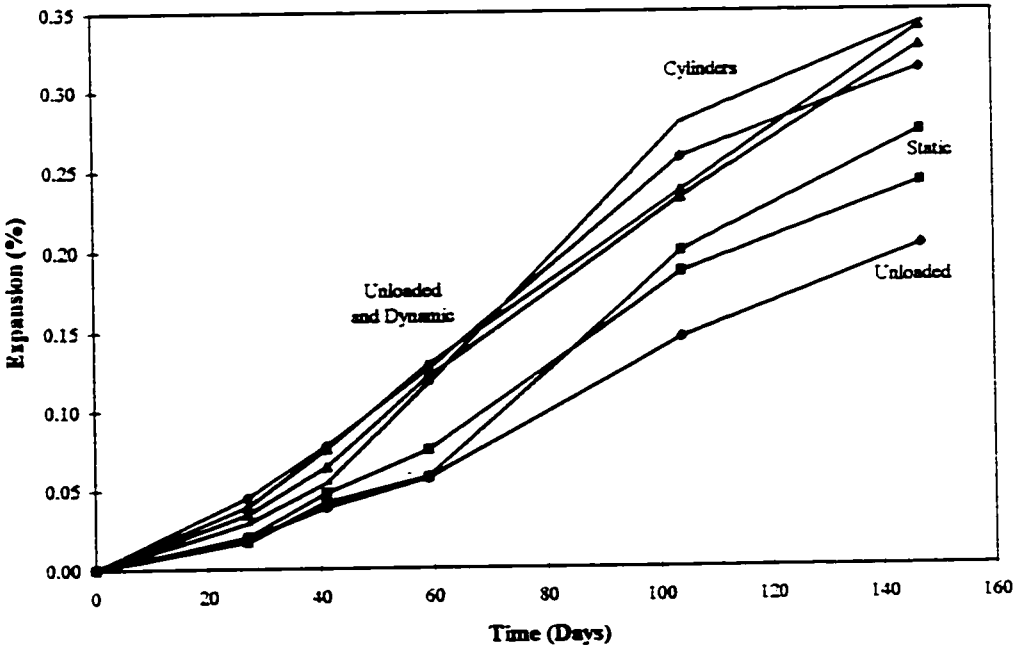

Figure B.42: Vertical expansions for the various beams (set 14)

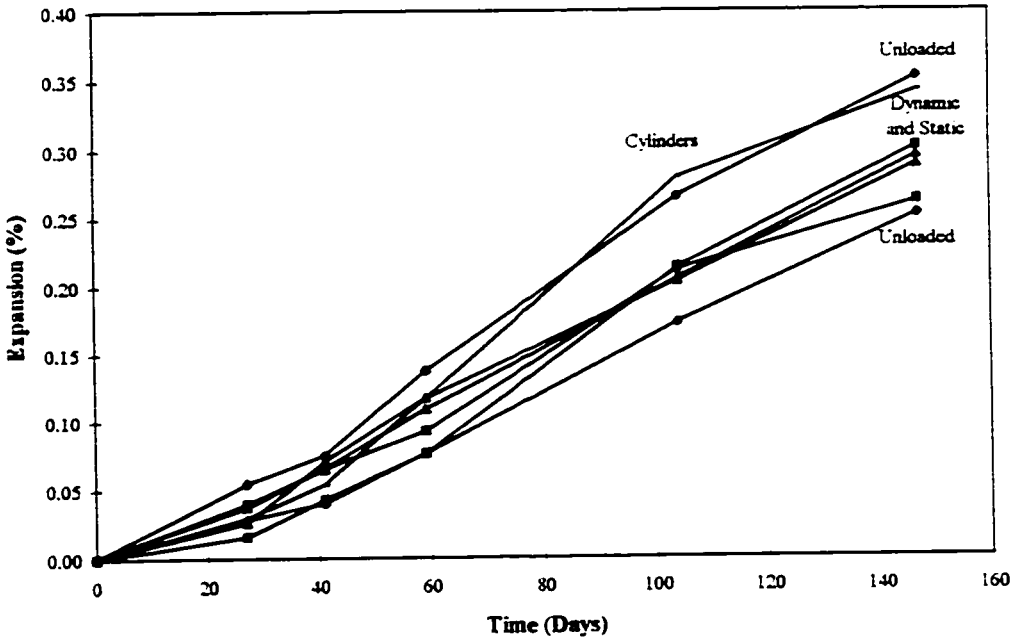

Figure B.43: Vertical expansions for the various beams (set 15)

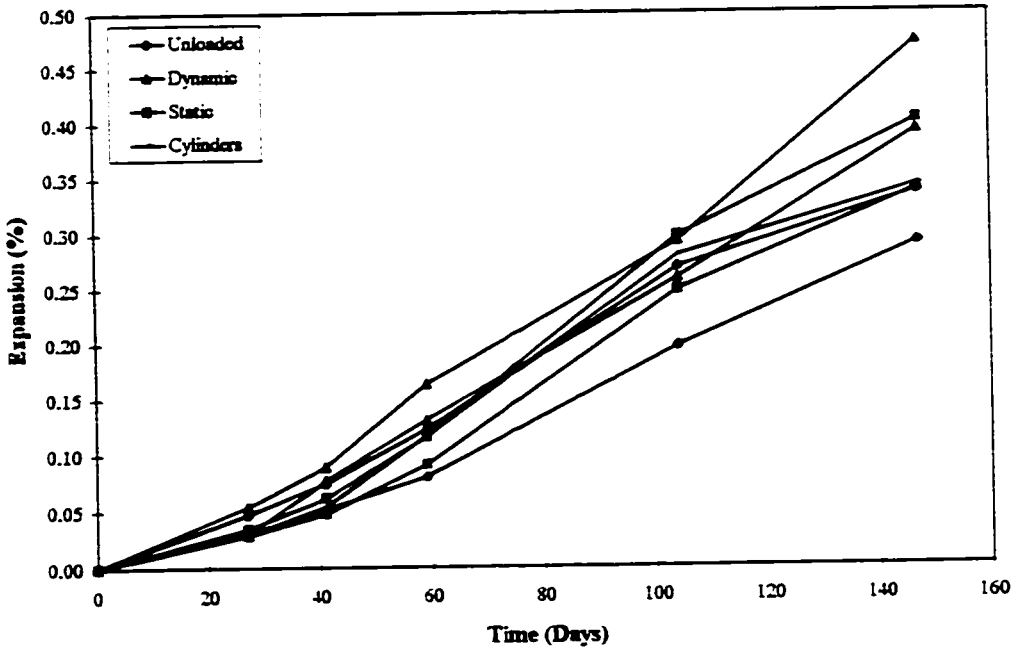

Figure B.44: Vertical expansions for the various beams (set 16)

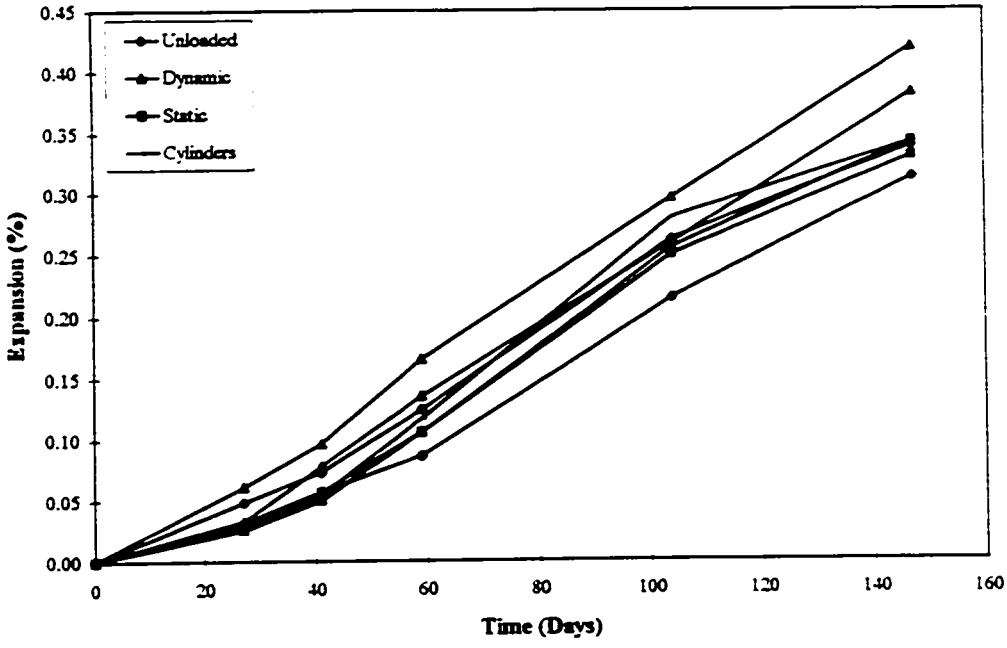

Figure B.45: Vertical expansions for the various beams (set 17)

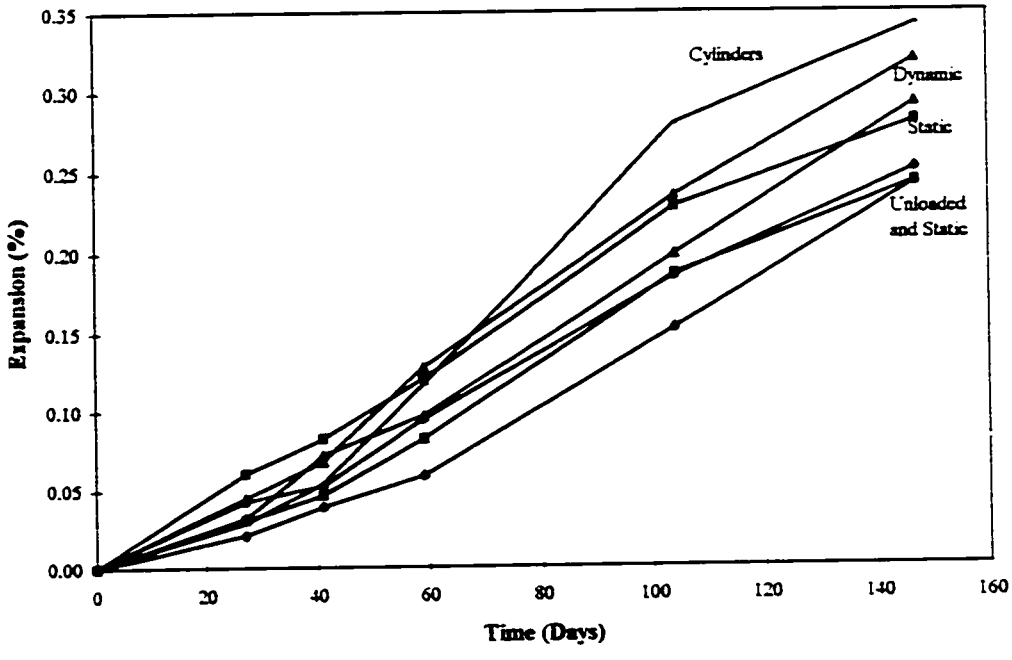

Figure B.46: Vertical expansions for the various beams (set 18)

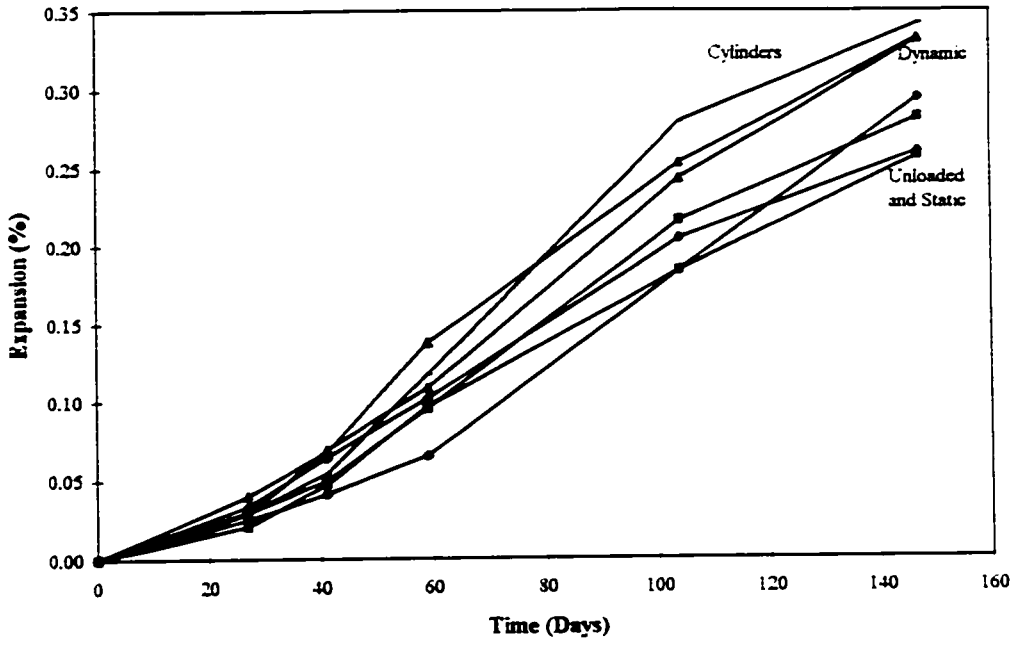

Figure B.47: Vertical expansions for the various beams (set 19)

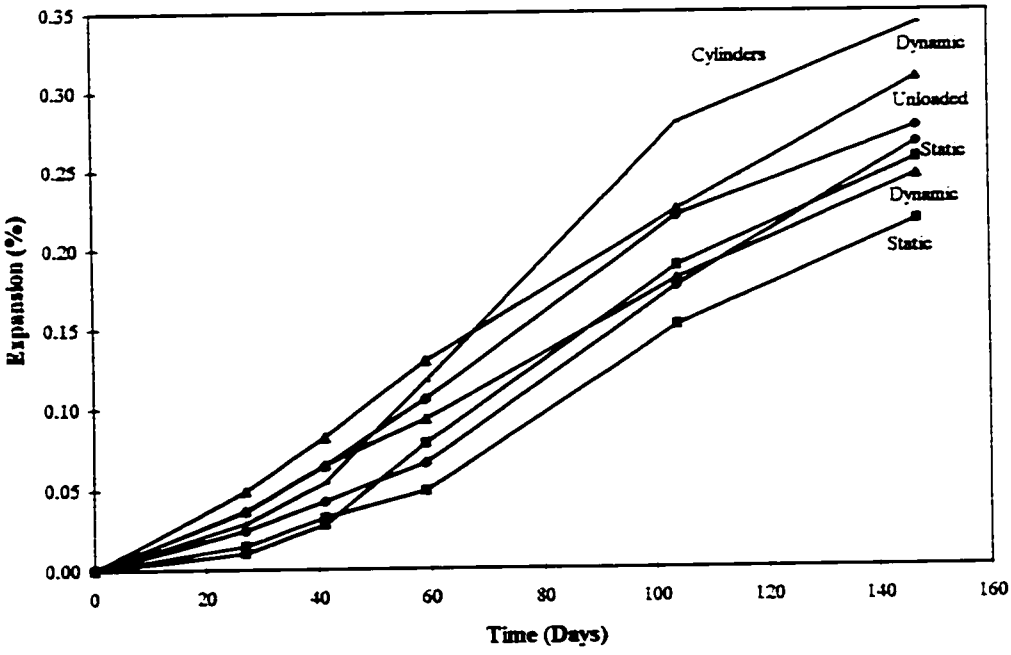

Figure B.48: Vertical expansions for the various beams (set 20)

B.2 DAMAGE RATING INDEX DATA

The damage rating index data for all of the beams are displayed in the following sections. The DRI for each of the beams (Figures B.48 to B.54) subjected to various loading regimes are shown followed by a comparison of the DRI for each measurement zone for the beams (Figures B.55 to B.63) subjected to the various loading regimes. Figure B.49 shows the zones of damage rating measurements for the reactive beams.

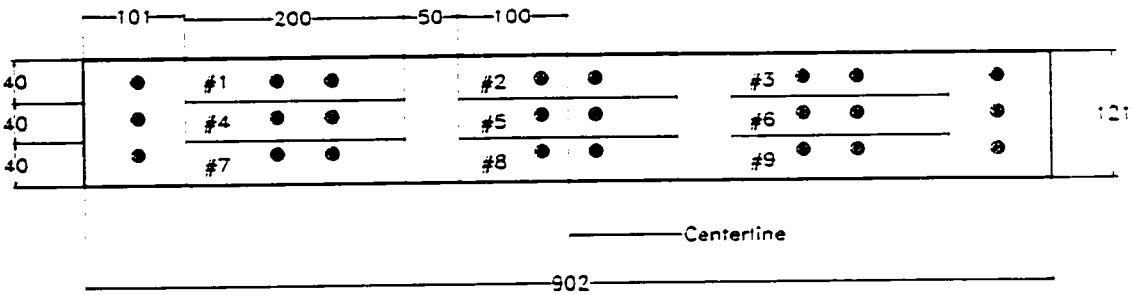

Figure 4.49: Zones of damage rating measurements

B.2.1 Unloaded Beam Indices

Figures B.50 and B.51 show the DRI results for the unloaded beams. The unloaded plain concrete prism DRI results are plotted with those of the beams.

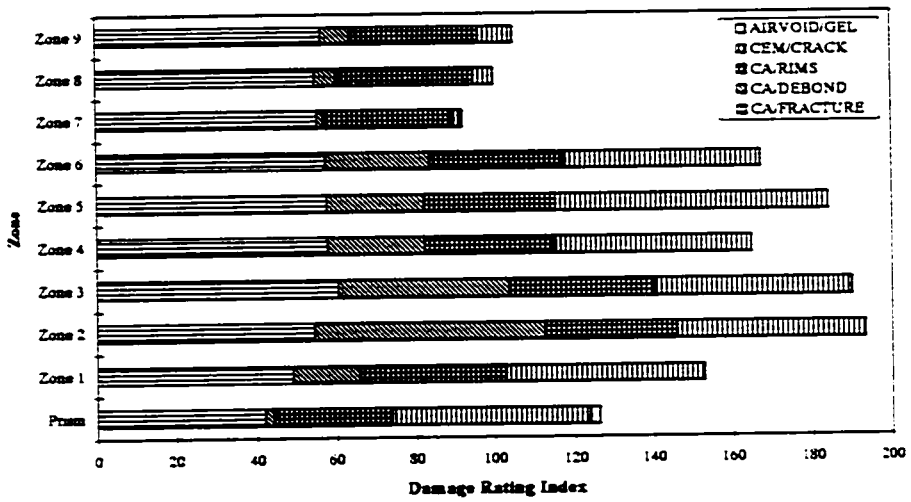

Figure B.50: Damage rating indices for unloaded beam RB-1

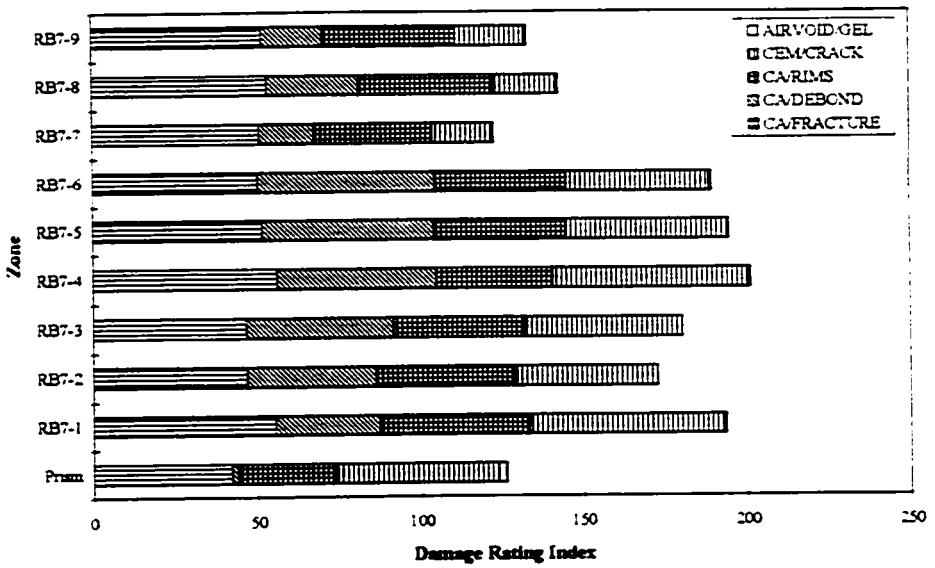

Figure B.51: Damage rating indices for unloaded beam RB-6

B.2.2 Statically Loaded Beam Indices

Figures B.52 and B.53 show the DRI results for the statically loaded beams. The unloaded plain concrete prism DRI results are plotted with those of the beams.

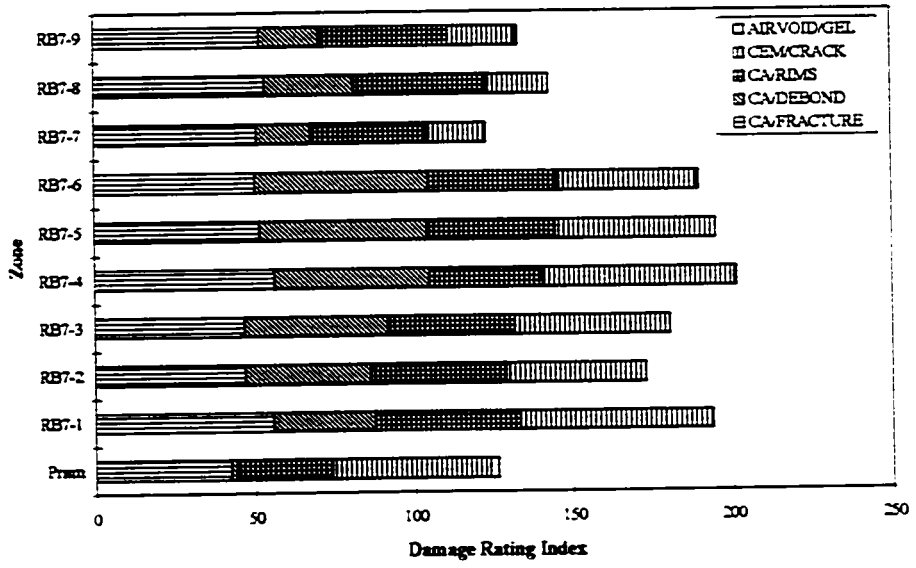

Figure B.52: Damage rating indices for statically loaded beam RB-7

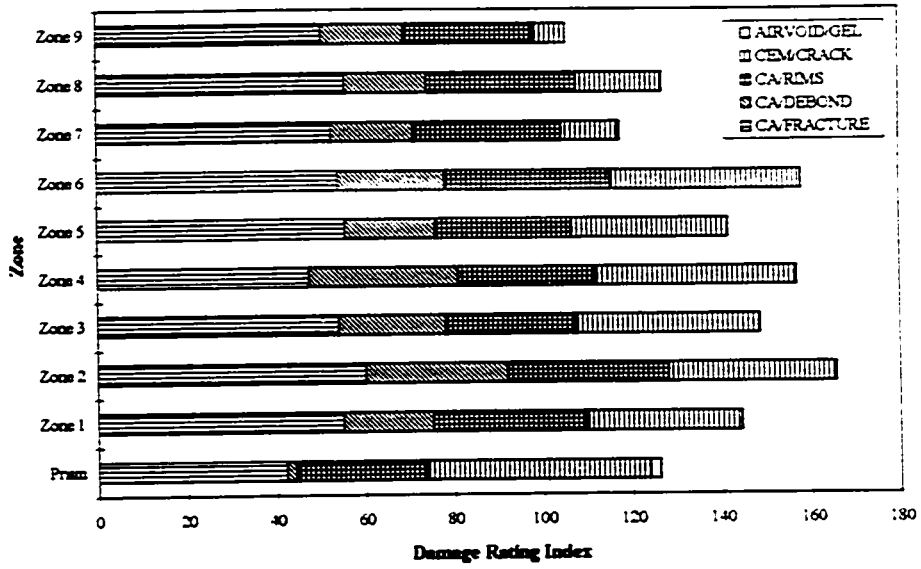

Figure B.53: Damage rating indices for statically loaded beam RB-8

B.2.3 Dynamically Loaded Beam Indices

Figures B.54 and B.55 show the DRI results for the dynamically loaded beams. The unloaded plain concrete prism DRI results are plotted with those of the beams.

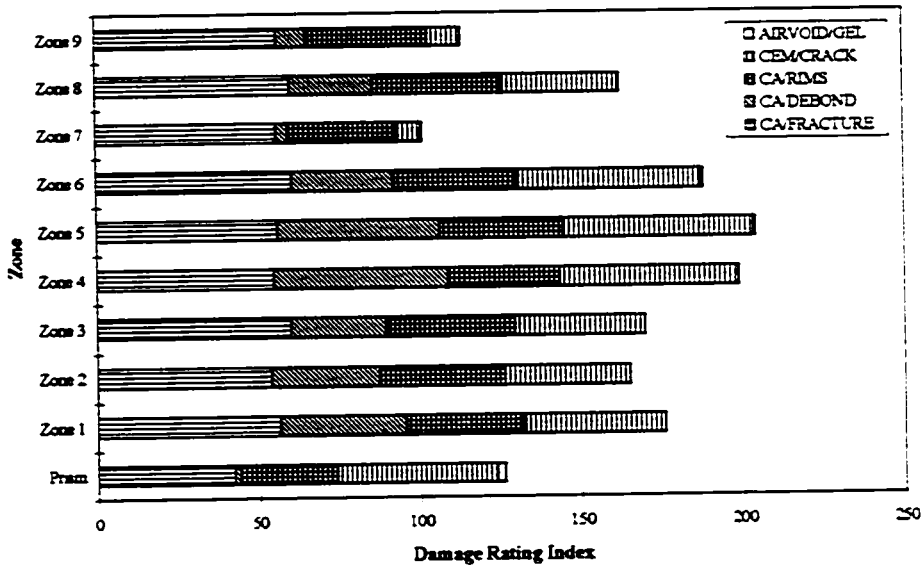

Figure B.54: Damage rating indices for dynamically loaded beam RB-3

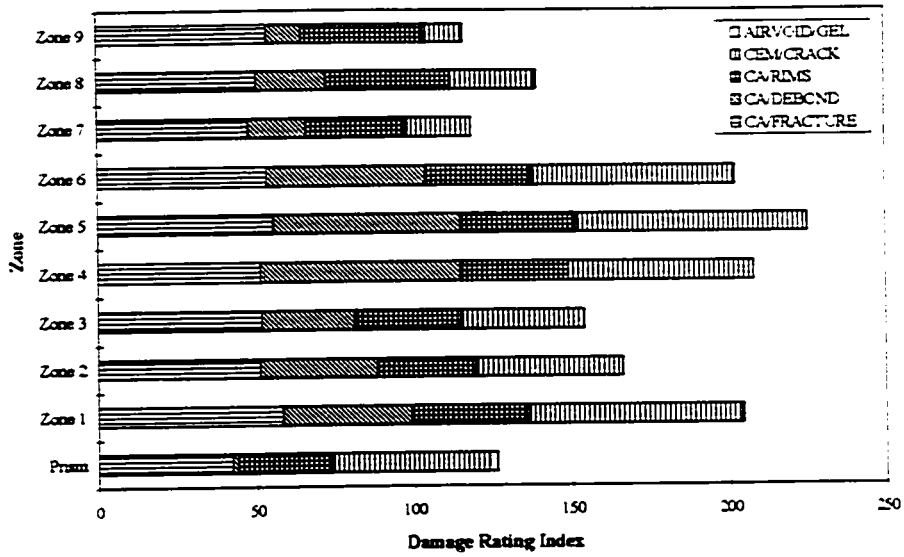

Figure B.55: Damage rating indices for dynamically loaded beam RB-4

B2.4 DRI for the Beams Subjected to Various Loading regimes

The damage rating indices fore each of the measurement zones are compared for the beams subjected to the various loading regimes (Figures B.56 to B.64). The unloaded plain concrete prism DRI results are plotted with those of the beams.

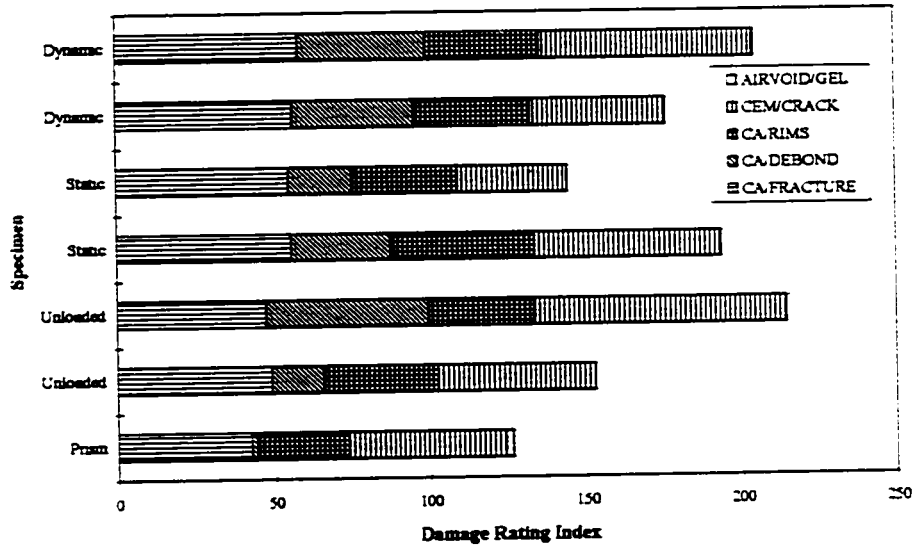

Figure B.59: Damage rating indices for various beams, zone 1

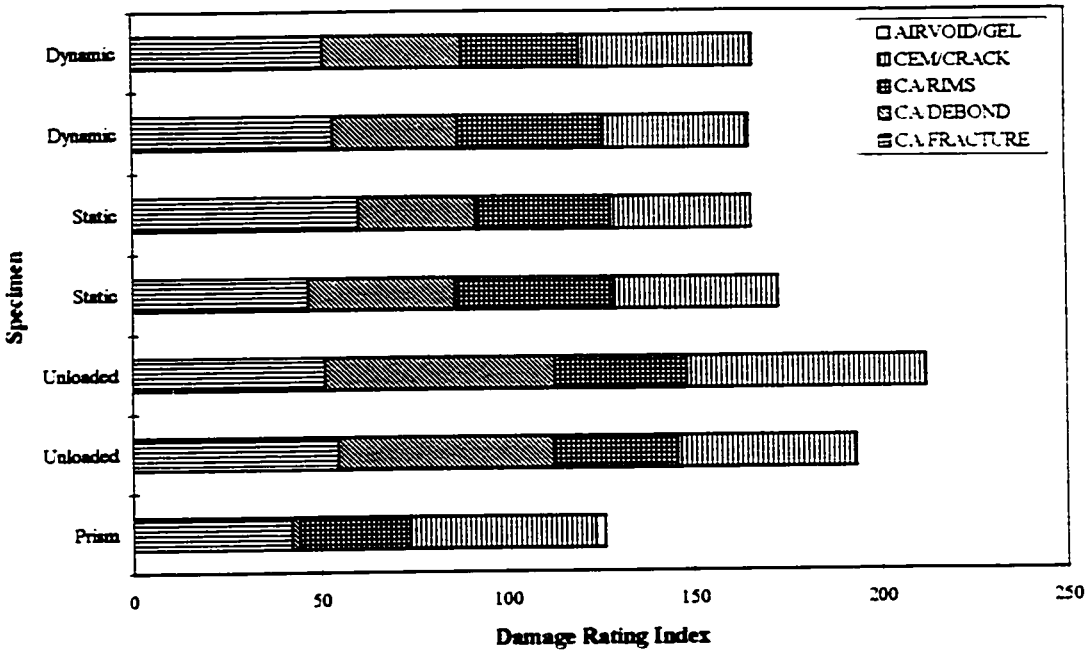

Figure B.60: Damage rating indices for various beams, zone 2

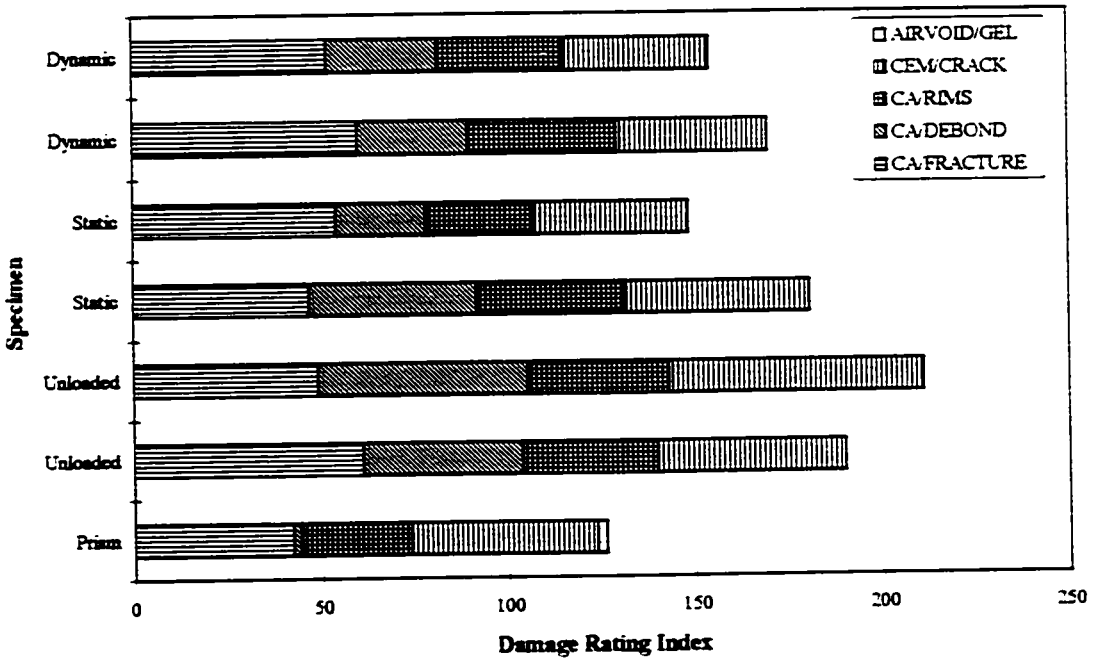

Figure B.61: Damage rating indices for various beams, zone 3

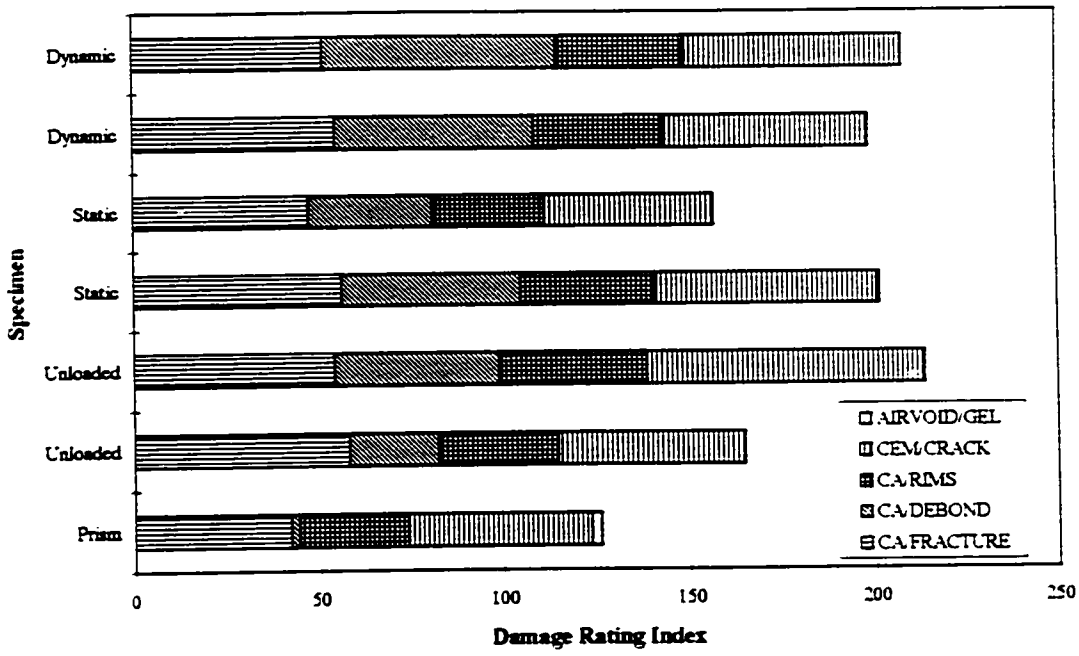

Figure B.62: Damage rating indices for various beams, zone 4

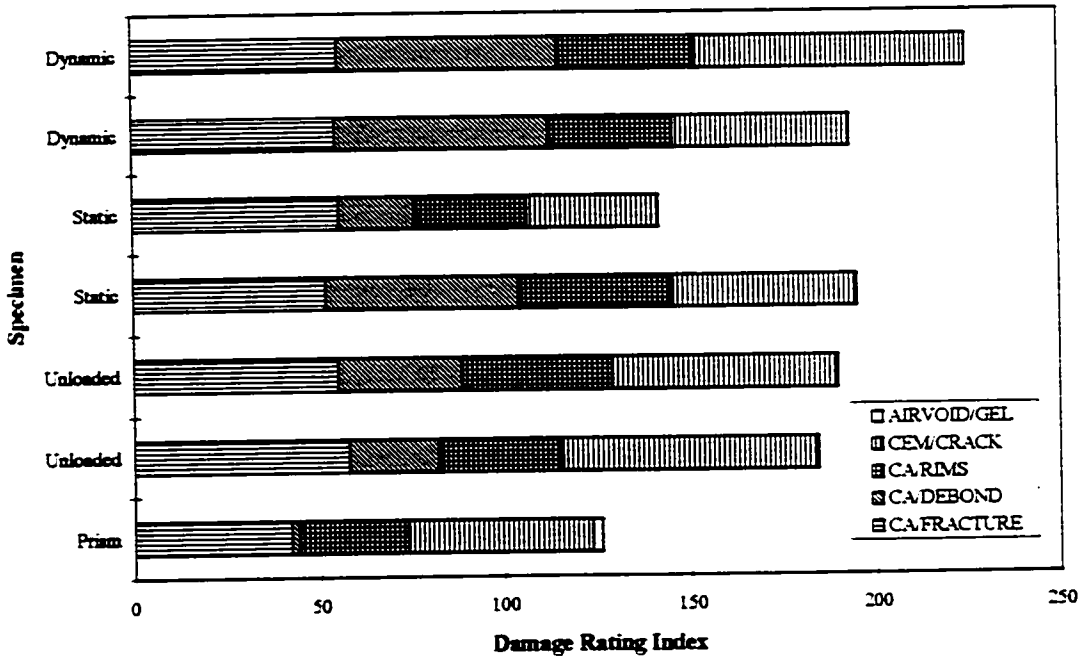

Figure B.63: Damage rating indices for various beams, zone 5

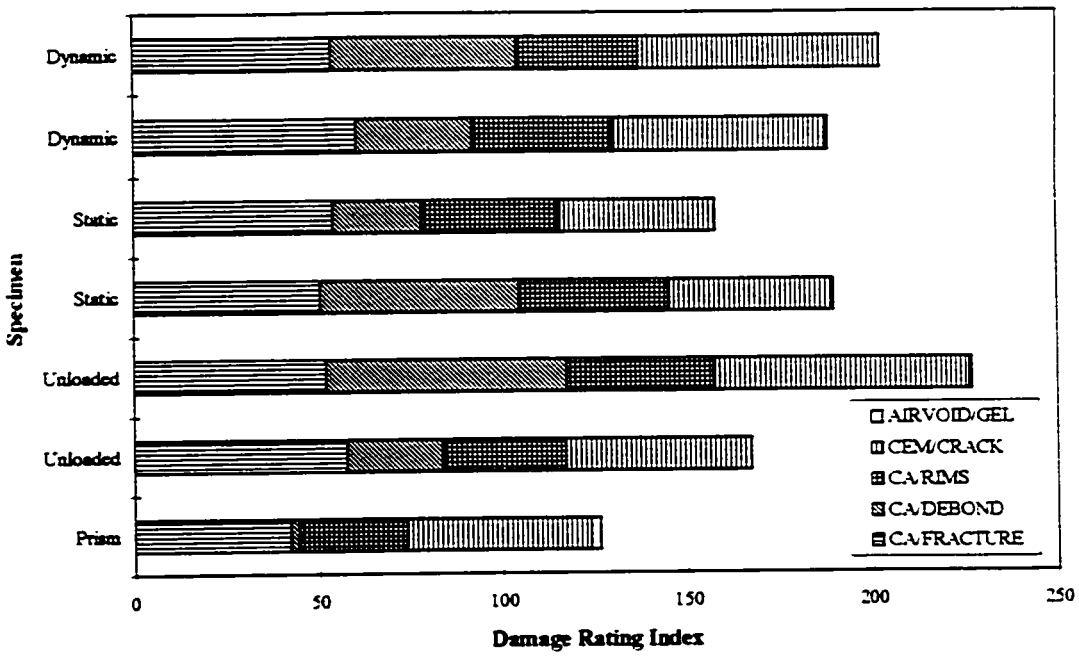

Figure B.64: Damage rating indices for various beams, zone 6

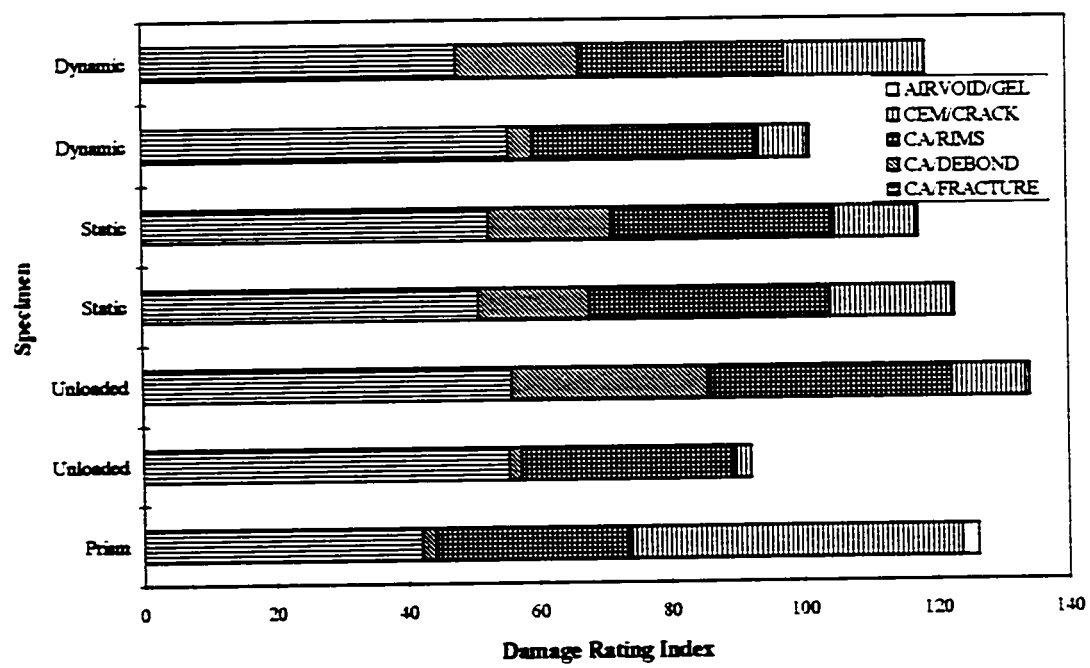

Figure B.65: Damage rating indices for various beams, zone 7

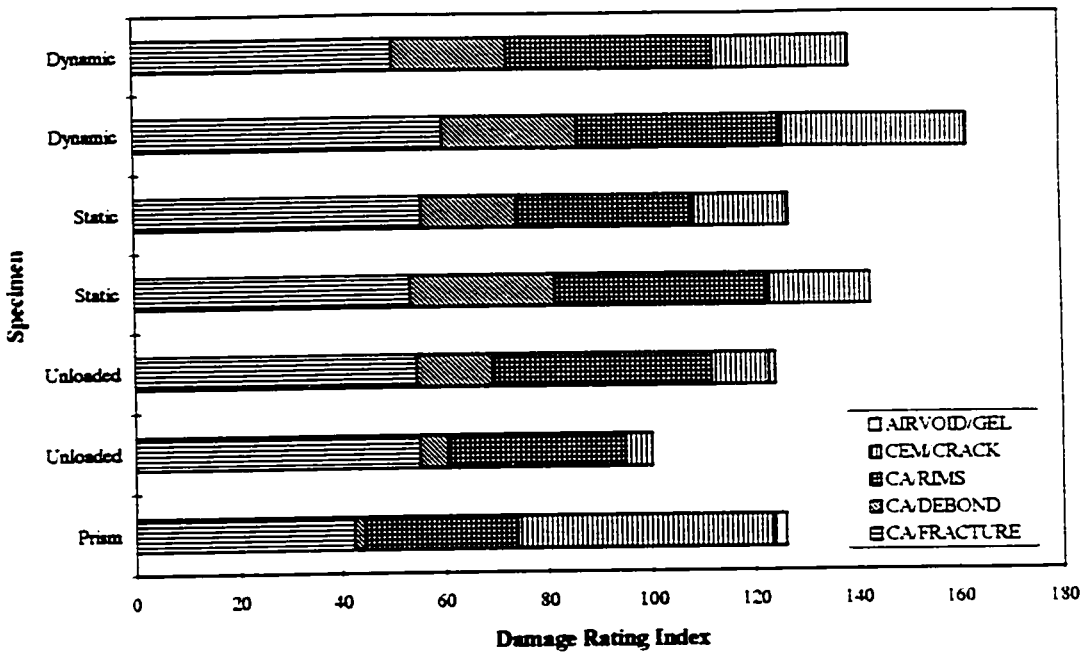

Figure B.66: Damage rating indices for various beams, zone 8

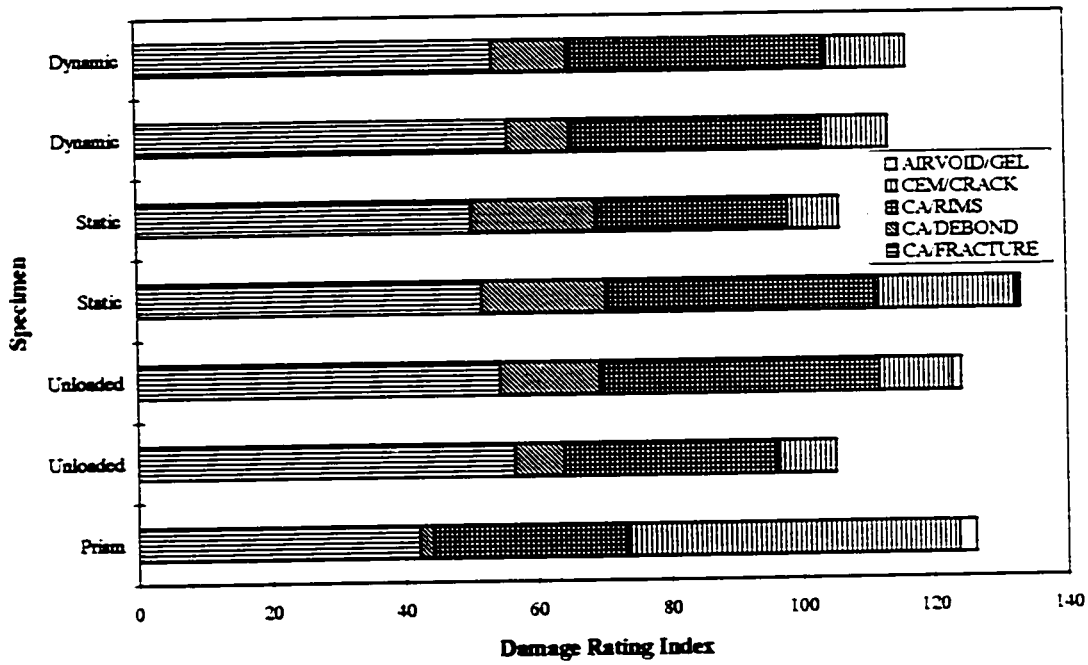

Figure B.67: Damage rating indices for various beams, zone 9

APPENDIX C

ADDITIONAL REFERENCES

Many published paper were read during the preparation of the thesis. Not all of them are used as references but nonetheless provided the author with significant information on various aspects of ASR. All of these works are included in the bibliography as well as the works referenced in the body of the thesis for future reference for the reader.

1. Abe, M., Kikuta, S., Masuda, Y., Tomozawa, F., 1989. "Experimental Study on Mechanical Behavior of Reinforced Concrete Members Affected by Alkali-Aggregate Reaction", Proceedings of the 8th International Conference on Alkali-Aggregate Reaction, The Society for of Materials Science, Japan.

2. Akashi, T., Amasaki, S., Takagi, N., Tomita, M., 1989, "The Estimate for Deterioration Due to Alkali-Aggregate Reaction by Ultrasonic Methods", Proceedings of the 7th International Conference on Alkali Aggregate Reaction, pgs. 183-187, Noyes Publications, Park Ridge, USA.

3. Alexander, M.G., Blight, G.E., Lampacher, B.J., "Pre-Demolition Tests on Structural Concrete Damaged by AAR", Proceedings of the 9th International Conference on Alkali Aggregate Reaction, 1992, pgs. 9-21, Chamelon Press Ltd., London, England.

4. Bach, F., Thorsen, T.S., Nielsen, M.P., "Load Carrying Capacity of Structural Members Subjected to Alkali-Silica Reactions", Proceedings of the 9th International Conference on Alkali Aggregate Reaction, 1992, pgs. 9-21, Chamelon Press Ltd., London, England.

5. Bakker, R.F.M., 1983, "The Influence of Test Specimen Dimensions on the Expansion of Alkali Reactive Aggregate in Concrete", Proceedings of the 6th International Conference on Alkalis in Concrete, June 1983, Technical University of Denmark, Danish Concrete Association, Copenhagen, Denmark.

6. Bérubé, M.A., Chouinard, D., Boisvert, L., Frenette, J., Pigeon, M., "Influence of Wetting-Drying and Freezing-Thawing Cycles, and Effectiveness of Sealers on ASR", Proceedings of the 10th International Conference on Alkali Aggregate Reaction, pgs. 1056-1063, Melbourne, Australia.

7. Blight, G.E., McIver, J.R., Schutte, W.K., Rimmer, R., 1981, "The effects of Alkali-Aggregate Reaction on Reinforced Concrete Structures Made with Witwatersrand Quartzite Aggregate", Conference on Alkali-Aggregate Reaction in Concrete, Proceedings, Capetown, South Africa, s252/15, pp. 1-12.

8. Blight, G.E., Alexander, M.G., "Assessment of AAR Damage to Concrete Structures", Proceedings of the 7th International Conference on Alkali Aggregate Reaction, pgs. 120-125, Noyes Publications, Park Ridge, USA.

9. Blight, G.E., et al., "Effect of Alkali-Silica Reaction on the Performance of a Reinforced Concrete Structure over a Six Year Period", Magazine of Concrete Research, 1989, V. 41, No. 147, June, pp. 69-77.

10. Blight, G.E. et al, "The Effect of Alkali Aggregate Reaction on the Strength and Deformation of a Reinforced Concrete Structure", Proceedings of the 6th International Conference on Alkalis in Concrete, pgs. 401-410, June 1983, Technical University of Denmark, Danish Concrete Association, Copenhagen, Denmark.

11. Blight, G.E., "Engineering Properties of Reinforced Concrete Damaged by AAR", Proceedings of the 10th International Conference on Alkali Aggregate Reaction, pgs. 987-994, Melbourne, Australia.

12. Bolton R.F., Wang, J., "Secondary Effect of ASR on Durability of Concrete: Freeze/Thaw", Proceedings of the 9th International Conference on Alkali Aggregate Reaction,1992, pgs. 117-126, Chamelon Press Ltd., London, England.

13. Bosc, J.L., Chabannet, M., Péra, J., "Comportement au gel interne de bétons sous contraintes mécaniques", Matériaux et constructions, V. 29, August/September 1996, pp. 395-400.

14. British Cement Association, "The Diagnosis of Alkali-Silica Reaction", Working Party, 1988, British Cement Association, UK.

15. Canada Center for Mineral and energy Technology, Institute for Research in Construction, Groupe de Recherche en Geologie de L'Ingenieur, 1991, "Petrography and Alkali Aggregate Reactivity Course Manual", Ottawa, Ontario, Canada.

16. Canadian Standards Association, CSA A23.2-14A-1994, "Potential Expansivety of Aggregates (Procedure for Length Change Due to Alkali-Aggregate Reaction in Concrete Prisms), Concrete Materials and Methods of Concrete Construction, Methods of Testing for Concrete, CSA, Rexdale, Ontario

17. Canadian Standards Association, CSA A23.2-25A-1994, "Test Method for Detection of Alkali-Silica Reactive Aggregate Expansion of Mortar Bars", Concrete Materials and Methods of Concrete Construction, Methods of Testing for Concrete, CSA, Rexdale, Ontario.

18. Capra, B., Bournazel, J.P., "Modelling of Induced Mechanical Effects of Alkali-Aggregate Reactions", Laboratoire de Mecanique et Technologie, ENS Cachan/CNRS/Universite Paris VI, 61 Avenue du President Wilson, 94235 Cachan Cedex France.

19. Capra, B., Bournazel, J.P., Moranville-Regourd, M., "A Mathematical Modelling to Describe the Effects of Alkali-Aggregate Reactions in Concrete Structures", Proceedings of the 10th International Conference on Alkali Aggregate Reaction, pgs. 686-693, Melbourne, Australia.

20. Chana, P.S., Thompson, D.M., "Laboratory Testing and Assessment of Structural Members Affected by Alkali Silica Reaction", Proceedings of the 9th International Conference on Alkali Aggregate Reaction, 1992, pgs. 156-166, Chamelon Press Ltd., London, England.

21. Chrisp, T.M., Waldron, P., Wood, J.G.M., "Development of a Non-destructive Test to Quantify Damage in Deteriorated Concrete", Magazine of Concrete Research, 1993, V. 45, pp. 247-256.

22. Clark, L.A., "Modelling the Structural Effects of Alkali-Aggregate Reactions on Reinforced Concrete", ACI Materials Journal, V. 88, No. 3, May-June 1991, pgs. 271-277, American Concrete Institute.

23. Clark, L.A., Ng, K.E., "Prediction of the Punshing Shear Strength of Reinforced Concrete Slabs with ASR", Proceedings of the 9th International Conference on Alkali Aggregate Reaction, 1992, pgs. 167-174, Chamelon Press Ltd., London, England.

24. Clayton, N., "Structural Performance of ASR Affected Concrete", Proceedings of the 8th International Conference on Alkali Aggregate Reaction, pgs. 671-676, The Society for of Materials Science, Japan.

25. Cohen, M.D., Shah, S.P., Young, J.F., 1993, Chapter 6 of Manual prepared for Faculty Enhancement Workshop obtained from Chapter 6 of "Teaching the Materials Science, Engineering, and Field Aspects of Concrete", NSF-ACBM Center, Northwestern University, Evanston, Illinois.

26. Collins, R.J., Bareham, P.D., "Alkali-Silica Reaction: Suppression of Expansion Using Porous Aggregate", Cement and Concrete Research, V. 17, No. 1, January 1987, pgs. 89-96

27. Cope, R.J., Slade, L., 1992, "Effect of AAR on Shear Capacity of Beams, Without Shear Reinforcement", Proceedings of the 9th International Conference on Alkali Aggregate Reaction, 1992, pgs. 184-191, Chamelon Press Ltd., London, England.

28. Damp, D.E., "The Implications of Producing a Low Alkali Ordinary Portland Cement in the South Western Cape", Proceedings of the Conference on Alkali-Aggregate Reaction in Concrete, 1981, S252/3, pp. 1-3, Cape Town, South Africa.

29. Danay, A., "Structural Mechanics Methodology in Diagnosing and Assessing Long-Term effects of alkali-aggregate Reactivity in reinforced Concrete structures", ACI Materials journal, Vol. 91, No. 1, January-february 1994.

30. Diab, Y., Prin, D., "Alkali-Aggregate Reaction Structural Effects: A Finite Element Model", Proceedings of the 9th International Conference on Alkali-Aggregate Reaction, 1992, pgs. 261-268, Chamelon Press Ltd., London, England.

31. Diamond, S., "Alkali Silica Reactions-Some Paradoxes", Proceedings of the 10th International Conference on Alkali Aggregate Reaction, pgs. 3-14, Melbourne, Australia.

32. Doran, D.K., Moore, J.F.A., "Appraisal of the Structural Effects of Alkali-Silica Reaction", Proceedings of the 8th International Conference on Alkali Aggregate Reaction, pgs. 677-682, The Society for of Materials Science, Japan.

33. Dunbar, P.A., Mukherjee, P.K., Bleszynski, R., Thomas M.D.A., "A Comparison of Damage Rating Index with Long-Term Expansion of Concrete Prisms Due to Alkali-Silica Reaction", Proceedings of the 10th International Conference on Alkali Aggregate Reaction, pgs. 324-331, Melbourne, Australia.

34. Figg, J., "ASR-Inside Phenomena and Outside Effects(crack origin and pattern)", Proceedings of the 7th International Conference on Alkali Aggregate Reaction, pgs. 152-156, 1986,Noyes Publications, Park Ridge, USA.

35. Flanagan, J.C., "Alkali-aggregate reaction: practical, preventive and remedial measures", Proceedings of the Conference on Alkali-Aggregate Reaction in Concrete, 1981, S252/17, pp. 1-4, Cape Town, South Africa.

36. Freitag, S.A., St John, D.A., "Alkali Aggregate Reaction in Existing Structures-What Can it Tell Us?", Proceedings of the 10th International Conference on Alkali Aggregate Reaction, pgs. 183-190, Melbourne, Australia.

37. Fujii, M., Kobayashi, K., Kojima, T., Maehara, H., "The Static and Dynamic Behaviour of Reinforced Concrete Beams with Cracking Due to Alkali-Silica Reaction", Proceedings of the 7th International Conference on Alkali Aggregate Reaction, pgs. 127-130, Noyes Publications, Park Ridge, USA.

38. Gebauer, J., "Alkalis in clinker: influence on cement and concrete properties", Proceedings of the Conference on Alkali-Aggregate Reaction in Concrete, 1981, S252/4, pp. 1-7, Cape Town, South Africa.

39. Dent Glasser, L.S., Kataoka, N., "The chemistry of alkali-aggregate reactions", Proceedings of the Conference on Alkali-Aggregate Reaction in Concrete, 1981, S252/23, pp. 1-6, Cape Town, South Africa.

40. Grattan-Bellew, P.E., "Alkali Contribution from Limestone Aggregate to Pore Solution of Old Concrete", ACI Materials Journal, V. 91, No. 2, March-April 1994, American Concrete Institute.

41. Grattan-Bellew, P.E., "A New Damage Rating System for Evaluation of Condition of Concrete from Structures", 1994, Institute for Research in Construction, National Research Council, Ottawa, Canada.

42. Grattan-Bellew, P.E., "Laboratory Evaluation of Alkali-Silica Reaction in Concrete from Saunders Generating Station", ACI Materials Journal, V. 92, No. 2, March-April 1995, American Concrete Institute.

43. Grattan-Bellew, P.E., "A Critical Review of Accelerated ASR Tests", Proceedings of the 10th International Conference on Alkali Aggregate Reaction, pgs. 27-38, Melbourne, Australia.

44. Guédon, J.S., Le Roux, A., June 1993, "Influence of Microcracking on the Onset and Development of the Alkali-Silica Reaction", ACI SP 145-37, pgs. 713-723.

45. Gunatilaka, D., Machida, A., Mutsuyoshi, H., 1990, "Influence of Existing Cracks and Strain Rate on the Behaviour of Concrete Under Cyclic Compressive Loading", Transactions of the Japan Concrete Institute, Vol. 12, pgs. 121-126.

46. Habita, M.F., Brouxel, M., Prin, D., "Alkali-Aggregate Reaction structural Effects: An Experimental Study", Proceedings of the 9th International Conference on Alkali-Aggregate Reaction, 1992, pgs. 403-410, Chamelon Press Ltd., London, England.

47. Hamada, H., Otsuki, N., Fukute, T., ""Properties of Concrete Specimens Damaged by Alkali-aggregate Reaction, Laumonite Related Reaction and Chloride Attack Under Marine Environments", Proceedings of the 8th International Conference on Alkali Aggregate Reaction, pgs. 603-608, The Society for of Materials Science, Japan.

48. Hobbs, D.W., 1988, "Alkali-Silica Reaction in Concrete", Thomas Telford Ltd., London, England.

49. Hobbs, D.W., "Diagnosis of the Cause of Cracking in Four Structures in Which ASR is Occuring", Proceedings of the 10th International Conference on Alkali Aggregate Reaction, pgs. 209-218, Melbourne, Australia.

50. Inoue, S., Fujii, M., Kobayashi, K., Nakano, K., 1989, "Structural Behavior of Reinforced Concrete Beams Affected by Alkali-Silica Reaction", Proceedings of the 8th International Conference on Alkali-Aggregate Reaction, pgs. 727-732, The Society for of Materials Science, Japan.

51. Jensen, A.D., Chaterji, S., Christensen, S., Thaulow, N., Studies of Alkali-Silica Reaction -part II Effect of Air Entrainment on Expansion", Cement and Concrete Research, V. 14, 311-314, 1984.

52. Jones, A.E.K. et al., "The Suitability of Cores in Predicting the Behaviour of Structural Members Suffering from ASR", Magazine of Concrete Research, 1994, V. 46, No. 167, June, pgs. 145-150.

53. Jones, A.E.K., Discussion on 'Rigden, S.R., Majilesi, Y., Burley, E., 1995, "An Investigation into Factors Influencing the Expansive Behaviour, Compressive Strength and Modulus of Rupture of Alkali Silica Reactive Concrete Using Laboratory concrete mixes", Magazine of Concrete Research, 47, No. 170, pgs. 11-21.', Magazine of Concrete Research, V. 49, No. 178, March 1997, pp. 73-75.

54. Jones, A.E.K., Clark L.K., "The Effects of Restraint on ASR Expansion of Reinforced Concrete", Magazine of Concrete Research, V. 48, No. 174, March 1996, British Cement Association, Crowthorne, UK.

55. Jones, A.E.K., Clark, L.A., "A Review of the Institution of Structural Engineers Report, 'Structural effects of Alkali-Silica Reaction (1992)' ", Proceedings of the 10th International Conference on Alkali Aggregate Reaction, pgs. 394-401, Melbourne, Australia.

56. Kawakami, H., 1988, "Deformation of a Reinforced Concrete Building Due to Alkali Aggregate Reaction and Thermal Expansion", Transactions of the Japan Concrete Institute, Vol. 10, pgs. 99-104.

57. Kawakami, H., "A Reinforced Concrete Building Deformed by Alkali Aggregate Reaction", Proceedings of the 8th International Conference on Alkali Aggregate Reaction, pgs. 597-602, The Society for of Materials Science, Japan.

58. Kawamura, K., Takemoto, K., Ichise, M., "Influences of the Alkali-Silica Reaction on the Corrosion of Steel Reinforcement in Concrete", Proceedings of the 8th International Conference on Alkali Aggregate Reaction, pgs. 115-120, The Society for of Materials Science, Japan.

59. Klink, S.A., "Actual Elastic Modulus of Concrete", ACI Materials Journal, September-October 1985, pp.630-633, American Concrete Institute.

60. Kobayashi, K., Shiraki, R., Kawai, K., "Influence Alkali Concentration Distribution Occuring in Concrete Members on Expansion and Cracking Due to Alkali-Silica Reaction", Proceedings of the 8th International Conference on Alkali Aggregate Reaction, pgs. 641-646, The Society for of Materials Science, Japan.

61. Koyanagi W., et al. "Characteristics and Simulation of Concrete Cracks Caused by AAR", Proceedings of the 8th International Conference on Alkali Aggregate Reaction, pgs. 845-850, The Society for of Materials Science, Japan.

62. Koyanagi, W., Rokugo, K., Ishida, H., 1986, "Failure Behavior of Reinforced Concrete Beams Deteriorated by Alkali-Silica Reactions", Proceedings of the 7th International Conference on Alkali Aggregate Reaction, Noyes Publications, Park Ridge, USA.

63. Koyanagi, W., Rokugo, K., Uchida, Y., "Mechanical properties of Concrete Deteriorated by Alkali Aggregate Reaction Under Various Reinforcement Ratios". Proceedings of the 9th International Conference on Alkali Aggregate Reaction, 1992, pgs. 556-563, Chamelon Press Ltd., London, England.

64. Koyanagi, W., roguko, K., Uchida, Y., Iwase, H., "Deformation Behavior of Reinforced Concrete Beams Deteriorated by ASR", Proceedings of the 10th International Conference on Alkali Aggregate Reaction, pgs. 458-465, Melbourne, Australia.

65. Larive, C., Coussy, O., "Behaviour of AAR-Affected Concrete, Modelling", Proceedings of the 10th International Conference on Alkali Aggregate Reaction, pgs. 662-669, Melbourne, Australia.

66. Larive, C., Laplaud, A., Joly, M., "Behaviour of AAR-Affected Concrete, Experimental Data", Proceedings of the 10th International Conference on Alkali Aggregate Reaction, pgs. 51-67, Melbourne, Australia.

67. Le Roux, A. et al., "Evolution Under Stress of Concrete Affected by AAR-Application to the Feasibility of Strengthening a Bridge by Presstressing", Proceedings of the 9th International Conference on Alkali Aggregate Reaction, 1992, pgs. 599-606, Chamelon Press Ltd., London, England.

68. Le Roux, A., Zelwer, A., Dron, R., Salomon, M., "Ionic Evolution of Pore Solutions Associated with Alkali-Reactivity", Proceedings of the 9th International Conference on Alkali Aggregate Reaction, 1992, pgs. 607-613, Chamelon Press Ltd., London, England.

69. Majlesi, Y., Rigden, S.R., Burley, E., "Restraint Effects on the Performance of Various ASR Structural Elements", Proceedings of the 10th International Conference on Alkali Aggregate Reaction, pgs. 442-449, Melbourne, Australia.

70. Martineau, F., Guédon-Dubied, J.S., Larive, C., "Evaluation of the Relationships Between Swelling, Cracking, Development of Gels", Proceedings of the 10th International Conference on Alkali Aggregate Reaction, pgs. 798-805, Melbourne, Australia.

71. May, I.M., Wen, H.X., Cope, R.J., "Modelling the Effects of AAR Expansion on Reinforced Concrete Members", Proceedings of the 9th International Conference on Alkali-Aggregate Reaction, 1992, Chamelon Press Ltd., London, England.

72. May, I.M., Cope, R.J., Wen H.X., "Modelling of the Structural Behaviour of AAR Affected Reinforced Concrete Members", Proceedings of the 10th International Conference on Alkali Aggregate Reaction, pgs. 434-441, Melbourne, Australia.

73. Meissner, H.S., "Cracking in concrete due to expansive reaction between aggregate and high-alkali cement as evidenced in Parker dam", Proceedings of the American Concrete Institute, V. 37, Jornal of the American Concrete Institute, April 1941, pp. 549-568.

74. Moore, A.E., "An Attempt to Predict the Maximum Forces that Could be Generated by Alkali-Silica Reaction", 4th International Conference on AAR, paper 26, Purdue University, June 1978, p. 363.

75. Moranville-Regourd, M., "Modelling of Expansion Induced by ASR-New Approaches", Proceedings of the 10th International Conference on Alkali Aggregate Reaction, pgs. 51-67, Melbourne, Australia.

76. Nakajima, M., Nomachi, H., Takada, M., Nishibayashi, S., 1990, "Effects of Chemical Admixtures on Expansion Characteristics of Concrete Containing Reactive Aggregate", Transactions of the Japan Concrete Institute, Vol. 12, pgs. 191-198.

77. Nishibayashi, S., Yamura, K., Sakata, K., "Research on Influence of Cyclic Wetting and Drying on Alkali-Aggregate Reaction", Proceedings of the 8th International Conference on Alkali Aggregate Reaction, pgs. 617-622, The Society for of Materials Science, Japan.

78. Nishibayashi, S., Yamura, K., Sakata, K., "Evaluation of Cracking of Concrete Due to Alkali-Aggregate Reaction", Proceedings of the 8th International Conference on Alkali Aggregate Reaction, pgs. 759-764, The Society for of Materials Science, Japan.

79. Norris, P., Wood, J.G.M., Barr, B., "A Torsion Test to Evaluate the Deterioration of Concrete Due to Alkali-Aggregate Reaction", Magazine of Concrete Research, V. 42, No.153, December 1990, pgs. 239-244.

80. Okada, K., sonoda, K., Kojima, T., Seki, K., Murayama, Y., "Deterioration of Reinforced Concrete Slabs with Alkali Aggregate Reaction", Proceedings of the 10th International Conference on Alkali Aggregate Reaction, pgs. 1033-1040, Melbourne, Australia.

81. Ono, K., "Assessment and Repair of Damaged Concrete Structures", Proceedings of the 8th International Conference on Alkali Aggregate Reaction, pgs. 647-658, The Society for of Materials Science, Japan.

82. Pleau, R., Berube, M.A., Pigeon, M., Fournier, B., Raphael, S., "Mechanical Behaviour of Concrete Affected by ASR", Proceedings of the 8th International Conference on Alkali Aggregate Reaction, pgs. 721-726, The Society for of Materials Science, Japan.

83. Ramachandran, V.S., Beaudoin, J.J., Sarkar, S.L., Aimin, X., "Physico-Chemical and Michrostructural Investigations of the Effect of NaOH on the Hydration of $3CaO.SIO_2$", Il Cemento, V. 90, April-June 1993.

84. Rigden, S.R., Majlesi, Y., Burley, E., "Bond Stress Failure in Alkali Silica Reactive Reinforced Concrete Beams", Proceedings of the 9th International Conference on Alkali Aggregate Reaction, 1992, pgs. 859-864, Chamelon Press Ltd., London, England.

85. Rigden, S.R. et al., "The Influence of Stress Intensity and Orientation Upon the Mechanical Properties of ASR Affected Concrete", Proceedings of the 9th International Conference on Alkali Aggregate Reaction, 1992, pgs. 865-876. Chamelon Press Ltd., London, England.

86. Rogers, C.A., Hooton, R.D., "Leaching of Alkalies in Alkali-Aggregate Reaction Testing", Proceedings of the 8th International Conference on Alkali Aggregate Reaction, pgs. 327-332, The Society for of Materials Science, Japan.

87. Rogers, C.A., "Alkali-Aggregate Reactions in Ontario: Occurences, Test Methods, and Solutions", MTO Municipal Materials Update and Concrete Construction Courses, January 1994.

88. Salam, J.M., Rigden, S.R., Burley, E., "The Influence of Stress Intensity and Time of Application on the Mechanical Properties of ASR Affected Concrete", Proceedings of the 10th International Conference on Alkali Aggregate Reaction, pgs. 418-425, Melbourne, Australia.

89. Sellier, A., Bournazel, J.P., Mébarki, A., "modelling the Alkali-Aggregate Reaction Within a Probabilistic Framework", Proceedings of the 10th International Conference on Alkali Aggregate Reaction, pgs. 694-701, Melbourne, Australia.

90. Stark, D., "Alkali-Silica Reactivity in the Rocky Mountain Region", Proceedings of the Fourth International Conference on the Effects of Alkalis in Cement and Concrete, June 4-7, 1978, Purdue University, West Lafayette, Indiana, USA.

91. Shayan, A., Ivanusec, I., "Influence of NaOH on Mechanical Properties of Cement Paste and Mortar with and without Reactive Aggregates", Proceedings of the 8th International Conference on Alkali Aggregate Reaction, pgs. 715-720, The Society for of Materials Science, Japan.

92. Shizawa, M. et al., "Influence of Ionic Species on Alkali-Aggregate Reaction", 8th International Congress on the Chemistry of Cement, September 1986, Rio de Janeiro, Brazil, Secretaria Geral do 8 CIQC 1986, V. V, pgs. 135-140.

93. Skalny, J., Klemm, W.A., "Alkalis in clinker: origin, chemistry, effects", Proceedings of the Conference on Alkali-Aggregate Reaction in Concrete, 1981, S252/1, pp. 1-7, Cape Town, South Africa.

94. Smoak, G., "Lessons learned at deadwood dam", Concrete International, The Magazine of the American concrete Institute, March 1995, pp. 21-25.

95. Spooner D.C., Dougill, J.W., "A Quantitative Assessment of Damage Sustained Concrete During Compressive Loading", Magazine of Concrete Research, 1975, V. 27, No. 92, 151-160.

96. Svendsen, J., "Alkali reduction in cement kilns", Proceedings of the Conference on Alkali-Aggregate Reaction in Concrete, 1981, S252/2, pp. 1-9, Cape Town, South Africa.

97. Swamy, R.N., 1989, "Structural Implications of Alkali Silica Reaction", Proceedings of the 8th International Conference on Alkali-Aggregate Reaction, pgs. 683-689, The Society for of Materials Science, Japan.

98. Swamy, R.N., Al-Asali, M.M., 1990, "Control of Alkali-Silica Reaction in Reinforced Concrete Beams", ACI Materials Journal, V. 87, No. 1, American Concrete Institute.

99. Swamy, R.N., Al-Asali, M.M., 1989, "Effect of Alkali-Silica Reaction on the Structural Behavior of Reinforced Concrete Beams", ACI Structural Journal, V. 84, No. 4, American Concrete Institute.

100. Swamy, R.N., Al-Asali, M.M., 1988, "Engineering Properties of Concrete Affected by Alkali-Silica Reaction", ACI Materials Journal, September-October, American Concrete Institute.

101. Swamy, R.N., Al-Asali, M.M., 1988, "Expansion of Concrete Due to Alkali-Silica Reaction", ACI Materials Journal, January-February, American Concrete Institute.

102. Swamy, R.N., Wan, W.M.R., "Use of dynamic Nondestructive Test Methods to Monitor concrete Deterioration Due to Alkali-Silica Reaction", Cement Concrete and Aggregates, 1993, V. 15, pgs. 39-49.

103. Swamy, R.N., "Assessment and Rehabilitation of AAR-Affected Structures", Proceedings of the 10th International Conference on Alkali Aggregate Reaction, pgs. 68-83, Melbourne, Australia.

104. Takemura, K., Ichitsubo, M., Tazawa, E., yonekura, A., "Mechanical Performance of ASR Affected Nearly Full-Scale Reinforced Concrete Columns", Proceedings of the 10th International Conference on Alkali Aggregate Reaction, pgs. 410-417, Melbourne, Australia.

105. Takeo, K., Matsushita, H., Matsufuji, Y., Sato, T., "Surveys and Repairs of AAR-Damaged Concrete Structures (Bridge Substructure and Water Tank", Proceedings of the 10th International Conference on Alkali Aggregate Reaction, pgs. 1049-1055, Melbourne, Australia.

106. Tawfiq, K., Armaghani, J., Vysyaraju, J.R., 1996, "Permiability of concrete Subjected to Cyclic Loading", Transportation Research Record No. 1532, Materials and Construction, Advancements in Concrete Materials Technology, Transportation Research Board, national Research Council, Washington D.C.

107. The Institution of Structural Engineers, "Structural Effects of Alkali-Silica Reaction", July 1992, Institution of Structural Engineers, UK.

108. Thorsen, T.S., "Alkali-Silica Reactions in Reinforced Concrete Beams with Particular Reference to Bearing Capacity", Proceedings of the 7th International Conference on Alkali Aggregate Reaction, pgs. 146-151, Noyes Publications, Park Ridge, USA.

109. Thorsen, T., Larsen, E.S., "Alkali-Silica Reactions in Damaged Concrete: Static and Dynamic Tests Material Investigations", Proceedings of the 10th International Conference on Alkali Aggregate Reaction, pgs. 402-409, Melbourne, Australia.

110. Tremper, B., "Correlation of laboratory tests with field experience in alkali-aggregate reaction", Proceedings of the American Society for the Testing of Materials, V. 48, pp.1067-1070, 1948.

111. Ujike, I., Nagataki, S., Sato, R., Ishikawa, K., 1990, "Influence of Internal Crackings Formed Around Deformed Tension Bar on air Permiability of Concrete", Transactions of the Japan Concrete Institute, Vol. 12, pgs. 207-214.

112. Vivian, H.E., "Alkalis in concrete", Proceedings of the Conference on Alkali-Aggregate Reaction in Concrete, 1981, S252/5, pp. 1-4, Cape Town, South Africa.

113. Wang, H., Gillot, J.E., 1992, "Effect of Some Chemicals on alkali-Silica Reaction", Proceedings of the 9th International Conference on Alkali Aggregate eaction, 1992, pgs. 1090-1099, Chamelon Press Ltd., London, England.

114. Wen, H.X., Balendran, R.V., "Use of Analytical Methods to Estimate Concrete Deterioration Due to AAR", Proceedings of the 10th International Conference on Alkali Aggregate Reaction, pgs. 678-685, Melbourne, Australia.

115. Wood, J.G.M., Wickens, P.J., "Structural Effects of AAR on Reinforced Concrete and Consideration of Remedial Action", Proceedings of the 6th International Conference on Alkalis in Concrete pgs. 487-494, Technical University of Denmark, Copenhagen 1983, Danish Concrete Association.

116. Wood, J.G.M., Young, J.S., Ward, D.E., "The Structural Effects of Alkali-Aggregate Reaction on Reinforced Concrete", Proceedings of the 7th International Conference on Alkali Aggregate Reaction, pgs. 157-163, Noyes Publications, Park Ridge, USA.

117. Wood, J.G.M., Norris, P., Leek, D., "Physical Behaviour of AAR Damaged Concrete in Structures and in Test Conditions", Proceedings of the 8th International Conference on Alkali Aggregate Reaction, pgs. 765-770, The Society for of Materials Science, Japan.

118. Wood, J.G.M., Nixon, P.J., Lives, P., "Relating ASR Structural Damage to Concrete Composition and Environment", Proceedings of the 10th International Conference on Alkali Aggregate Reaction, pgs. 450–457, Melbourne, Australia.

119. Yamada, K., Kosaka, Y., 1990, "Damping Characteristics of Ultrasonic Pulse Propagating Through Mortar Damaged by Alkali Aggregate Reaction", Transactions of the Japan Concrete Institute, Vol. 12, pgs

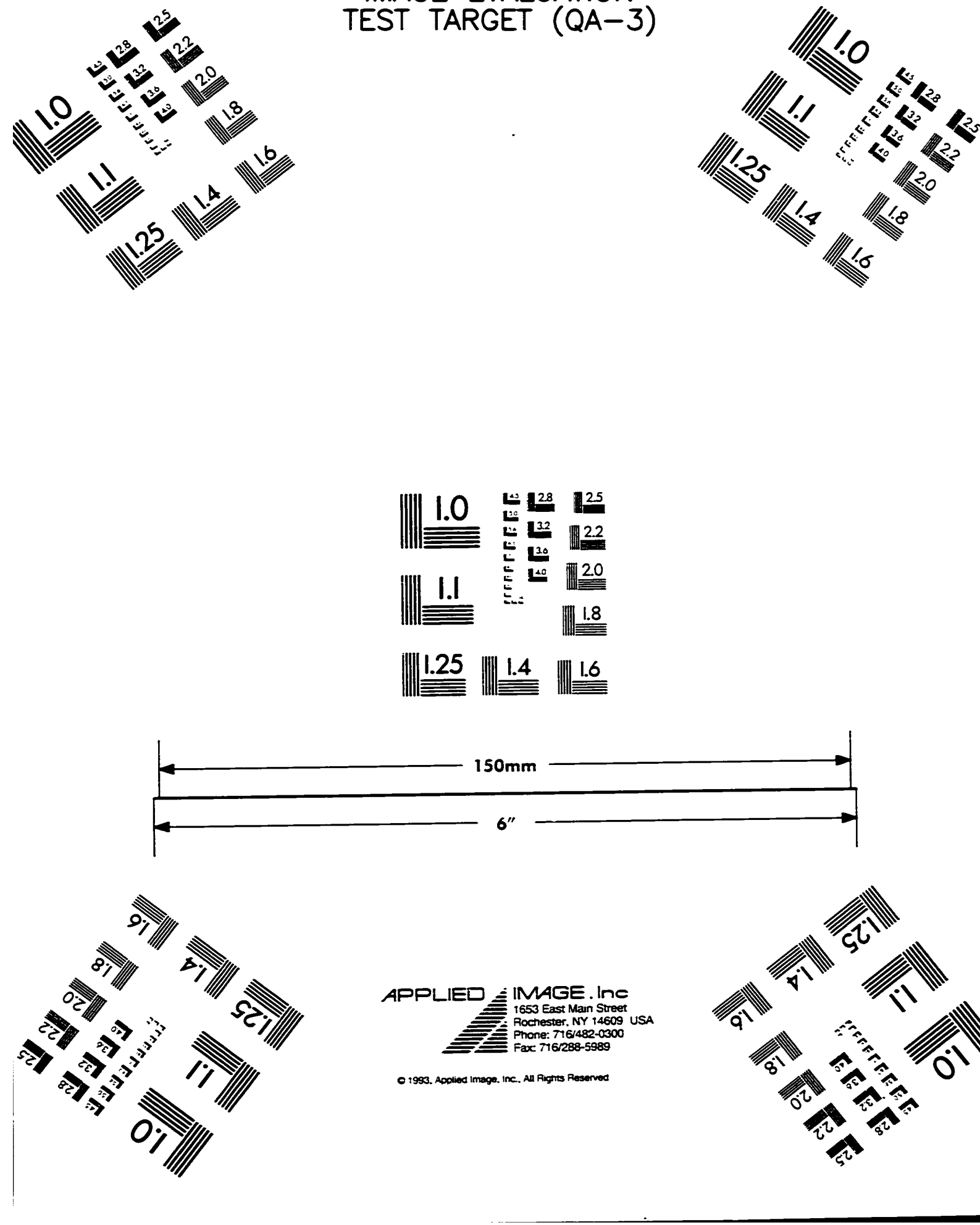
IMAGE EVALUATION
TEST TARGET (QA-3)
1.0
1.1
1.25
1.4
1.6
1.8
2.0
2.2
2.5
2.8
3.2
3.6
4.0
150mm
6"
APPLIED IMAGE, Inc
1653 East Main Street
Rochester, NY 14609 USA
Phone: 716/482-0300
Fax: 716/288-5989
© 1993, Applied Image, Inc., All Rights Reserved